



The Third Gulf

# Water

Conference

Muscat, Sultanate of Oman  
29 Shawwal - 4 Dhol Qada 1417  
8-13 March, 1997

## Towards Efficient Utilization of Water Resources in the Gulf

---

Water Desalination  
Municipal Water Supply Systems  
Domestic Water Quality

---



Water Sciences & Technology Association  
P.O. Box 20018, Manama, Bahrain  
Tel : (0973) 826512, Fax : (0973) 826513

The printing of these proceedings  
have been sponsored by:



**Hitachi Zosen**

HITACHI ZOSEN CORPORATION

International Plant Business Department  
Telefax 081 3 3217 8554

*Under the Patronage of*  
**His Highness Sayyid Haitham Bin Tariq Al Said**  
*Secretary General, Ministry of Foreign Affairs, Sultanate of Oman*

**The Third Gulf Water Conference**  
**Towards Efficient Utilization of Water Resources in the Gulf**  
**Muscat, Sultanate of Oman**  
**29 Shawal-4 Dhol Qada, 1417**  
**8-13 March, 1997**

**Conference Proceedings**

*Organized and Sponsored by*

**Water Science and Technology Association**  
**The Secretariat General of the Cooperation Council (GCC) for the Arab States of the Gulf**  
**Sultan Qaboos University, Sultanate of Oman**

*Co-sponsored by*

**Ministry of Electricity and Water, Sultanate of Oman**  
**Ministry of Agriculture and Fisheries, Sultanate of Oman**  
**Ministry of Water Resources, Sultanate of Oman**  
**Ministry of Regional Municipalities and Environment, Sultanate of Oman**  
**Ministry of Commerce and Industry, Sultanate of Oman**  
**Muscat Municipality, Sultanate of Oman**  
**Arabian Gulf University, Bahrain**  
**Ministry of Electricity and Water, Bahrain**  
**Bahrain Center for Studies and Research, Bahrain**  
**UNESCO Cairo Office (Regional Office for Science and Technology for the Arab States, ROSTAS)**  
**UN Economic and Social Commission for Western Asia, ESCWA**  
**International Desalination Association**  
**European Desalination Society**

*Edited by*

**Dr. WALEED K AL-ZUBARI & Eng. MOHAMMED AK AL-SOFI**

**The Third Gulf Water Conference**  
**Towards Efficient Utilization of Water Resources in the Gulf**  
**Sultanate of Oman, 8-13 March, 1997**

**Conference Executive Committee**

H.E. Shk. Salem Bin Nasser Al-Maskari	Secretary General, Sultan Qaboos University Council	Co-Chairman
Eng. Mohammed AK Al-Sofi	WSTA President, Kingdom of Saudi Arabia	Co-Chairman
Mr. AbdulLateef Al-Mugrin	Director of Agriculture, Water & Trade, Economic Affairs, GCC Secretariat General of the Cooperation Council for the Arab States of the Gulf (GCC)	Representative
Dr. Khalid AlHajri	WSTA Vice-President, Qatar	Member
Eng. Timama Hussain	WSTA Secretary, Kuwait	Repporteur
Eng. AbdulMajeed Al-Awadhi	WSTA Treasurer, Bahrain	Member

**Conference Scientific Committee**

Dr. Waleed K Al-Zubari	Arabian Gulf University, Bahrain	Chairman
Prof. Dr. Mamdouh Nouh	Sultan Qaboos University, Sultanate of Oman	Member
Dr. Shehta O Al-Khateeb	Arabian Gulf University, Bahrain	Member
Dr. Fatima Al-Awadhi	UNDP, Kuwait	Member
Dr. Ahmad R Khater	Bahrain Center for Studies and Research, Bahrain	Member
Eng. Adrian Al-Saati	King Abdulaziz City for Science and Technology, Saudi Arabia	Member

**Conference Organizing Committee**

Mr. Khalid H Al-Bosaeedi	Sultan Qaboos University	Chairman
Eng. Ali Redha Hussain	Ministry of Electricity & Water, State of Bahrain	Coordinator
Dr. Hilal A Al-Hinai	Sultan Qaboos University	Repporteur
Eng. AbdulGhani Khalaf	Ministry of Electricity & Water, State of Bahrain	Member
Dr. Salim K Al-Oraimi	Sultan Qaboos University	Member
Dr. Saleh M Al-Alawi	Sultan Qaboos University	Member
Dr. Amer A Al-Rawas	Sultan Qaboos University	Member

Dr. Ali S Al-Harhi	Sultan Qaboos University	Member
Dr. Salem Al-Rawahi	Sultan Qaboos University	Member
Dr. Taher Ba Omar	Sultan Qaboos University	Member
Prof. John R Flower	Sultan Qaboos University	Member
Dr. Hussein Abdullah	Sultan Qaboos University	Member
Dr. Ali Al-Musawi	Sultan Qaboos University	Member
Eng. Salem S Al-Harbi	Sultan Qaboos University	Member
Mr. Ahmad A Al-Kindi	Sultan Qaboos University	Member
Mr. Amer M Al-Suwaai	Sultan Qaboos University	Member
Mr. Yacoub J Al-Raeesi	Sultan Qaboos University	Member
Mr. Hamood N Al-Hashmi	Sultan Qaboos University	Member
Mr. Salem H Al-Rasheedi	Sultan Qaboos University	Member
Mr. Khamis R Khamis	Sultan Qaboos University	Member
Mr. Khamis R Al-Rasbi	Sultan Qaboos University	Member
Eng. Tahir M Al-Sajwani	Ministry of Electricity & Water, Sultanate of Oman	Member
Eng. Ahmad M Al-Sabahi	Ministry of Regional Municipalities & Environment, Sultanate of Oman	Member
Eng. Saleh Al-Shoukri	Ministry of Water Resources, Sultanate of Oman	Member
Eng. Nabil H. Al-Bahrani	Ministry of Agriculture & Fisheries, Sultanate of Oman	Member
Mr. Mohammed K Al-Kalbani	Ministry of Water Resources, Sultanate of Oman	Member
Eng. Saeed M Al-Qasimi	Muscat Municipality, Sultanate of Oman	Member

### Scientific Papers Reviewers

Prof. Dr. Abdin Saleh	UNESCO, Egypt
Prof. Dr. Ismail H El-Bagoury	Arabian Gulf University, Bahrain
Prof. Dr. Mamdouh Nough	Sultan Qaboos University
Prof. Dr. Mohammed J AbdulRazzak	UNESCWA, Jordan
Prof. Dr. Mohammed Mandil	Emeritus Professor, Alexandria University, Egypt
Dr. A G Dalvi	SWCC, Kingdom of Saudi Arabia
Dr. Ahmad R Khater	Bahrain Center for Studies & Research
Dr. Ali Al-Bahrawi	Qatar University
Dr. Ali Al-Jaloud	King Abdulaziz City for Science and Technology
Dr. Atta Hassan	SWCC, Kingdom of Saudi Arabia
Dr. Fatima Al-Awadhi	UNDP, Kuwait
Dr. Fawzia Al-Ruwaih	Kuwait University
Dr. Hasan Al-Housni	Water and Electricity Department, Abu Dhabi, UAE

Dr. Hilal Al-Hanai	Sultan Qaboos University
Dr. Khalid Al-Hari	Qatar University
Dr. L T Perlash	SWCC, Kingdom of Saudi Arabia
Dr. Mohammed S Osman	SWCC, Kingdom of Saudi Arabia
Dr. Osman A Hamad	SWCC, Kingdom of Saudi Arabia
Dr. Shehta O Al-Khateeb	Arabian Gulf University, Bahrain
Dr. Waleed K Al-Zubari	Arabian Gulf University, Bahrain
Eng. AbdulMajeed Al-Awadhi	Ministry of Electricity and Water, State of Bahrain
Eng. Adnan Al-Saatti	King Abdulaziz City for Science & Technology
Eng. Mohammed AK Al-Sofi	SWCC, Kingdom of Saudi Arabia
Eng. Sadiq Ibrahim	Kuwait Institute for Scientific Research
Eng. Taher Al-Sajwani	Ministry of Electricity and Water, Sultanate of Oman
Eng. Timama Hussain	Ministry of General Works, State of Kuwait
Hyd. Mubarak A. Al-Noaimi	Ministry of Works and Agriculture, State of Bahrain

### **Conclusion and Recommendations Committee**

Prof. Dr. Abdin Saleh	UNESCO, Egypt
Prof. Dr. Hosny Khordagui	UNESCWA, Jordan
Prof. Dr. Ismail El-Bagoury	Arabian Gulf University, Bahrain
Prof. Dr. Mamdouh Nouh	Sultan Qaboos University
Prof. Dr. Mohammed J AbdulRazzak	UNESCWA, Jordan
Prof. Dr. Mohammed Mandil	Emeritus Professor, Alexandria University, Egypt
Dr. Ahmad R Khater	Bahrain Center for Studies and Research
Dr. Ali Al-Jaloud	King Abdulaziz City for Science and Technology
Dr. Fawzia Al-Ruwaih	Kuwait University
Dr. Fatima Al-Awadhi	UNDP, Kuwait
Dr. Hilal Al-Hinai	Sultan Qaboos University
Dr. Khalid Al-Hajri	Qatar University
Dr. Waleed K Al-Zubari	Arabian Gulf University, Bahrain
Eng. AbdulMajeed Al-Awadhi	Ministry of Electricity and Water, State of Bahrain
Eng. Adnan Al-Saati	King Abdulaziz City for Science and Technology
Eng. Mohammed AK Al-Sofi	WSTA, Kingdom of Saudi Arabia
Eng. Sadiq Ebrahim	Kuwait Institute for Scientific Research
Eng. Taher M. Al-Sajwani	Ministry of Electricity and Water, Sultanate of Oman
Eng. Timama Hussain	Ministry of General Works, State of Kuwait
Hyd. Mubarak A. Al-Noaimi	Ministry of Works and Agriculture, State of Bahrain

## Preface

Within the past decade, a considerable research and experiences have been developed and published on water resources assessment and development, water supply augmentation and maximization, and water facilities management in the Arabian Gulf countries. However, very little research was directed towards demand management, conservation, and efficient utilization of water in the different water consuming sectors. Thus the theme of the conference “Towards Efficient Utilization of Water Resources in the Gulf” was chosen to emphasize the role of conservation and demand management as an important and integral part in water resources management in the Arabian Gulf Countries.

As at the previous WSTA conferences (the first was held in Dubai, 1992, and the second was held in Bahrain, 1994), the overall goals of the conference are to encourage scientific studies and research in the different fields of water resources, to create a forum of open discussion, and to exchange experiences among the Arabian Gulf States that the WSTA engendered throughout the two previous conferences.

The objectives of the convening conference are: 1) Assessment of natural water resources and alternative sources in the GCC Countries; 2) Review methods of conservation and efficient utilization of water in different sectors, with emphasize on the agricultural and municipal sectors; 3) Review and exchange of local experiences in the field of water resources and sources planning and management; and 4) Review the latest research and advances in the assessment, development, and management of water resources.

The Third Gulf Water Conference is held under the patronage of His Highness Sayyid Haitham Bin Tariq Al Said, and is organized by the Water Science and Technology Association (WSTA) in cooperation with Sultan Qaboos University and the Secretariat General of the Cooperation Council (GCC) for the Arab States of the Gulf. The Conference is sponsored by the Ministry of Electricity and Water, Ministry of Agriculture and Fisheries, Ministry of Water Resources, Ministry of Regional Municipalities and Environment, Ministry of Commerce and Industry, and Muscat Municipality from the Sultanate of Oman, and the Arabian Gulf University (Bahrain), Ministry of Electricity and Water (State of Bahrain), Bahrain Center for Studies and Research, UNESCO Cairo Office (ROSTAS), UN-ESCWA (Jordan), International Desalination Association (IDA), and European Desalination Society.

This conference proceedings contains 84 papers assembled into 4 volumes, one volume in Arabic and the other three in English. The Arabic Volume contains Fourteen papers with most of them having English Summaries, in addition to

the organizers speeches: The conference papers were selected by the Conference Scientific Committee from over 110 abstracts received from the call of papers. Many of these were modified to meet the standards of the Scientific Committee review. Conference sessions will be held on topics: Water Resources Planning and Management, Groundwater Resources, Water Desalination, Wastewater Treatment and Reuse, Surface Water and Artificial Recharge Experiences, Water Use in Agriculture and Irrigation Efficiency, Municipal Water Supply Systems, Environmental Protection and Public Awareness and Participation, and Domestic Water Quality.

Six papers are invited by the conference organizers. These are from the Secretariat General of the Cooperation Council (GCC) for the Arab States of the Gulf, Ministry of Water Resources, Ministry of Agriculture & Fisheries, Ministry of Electricity & Water, Ministry of Regional Municipalities & Environment, and Muscat Municipality from the Sultanate of Oman. In addition, Eight renowned international and GCC scientists were invited to give scientific presentations in respective technical sessions, and were supported by the WSTA, UNESCO (Cairo Office), and UNESCWA (Jordan).

The Scientific Committee wishes to express its deep appreciation to the Governments of the GCC Countries and the GCC Secretariat General and the sponsoring regional centers and organizations who kindly supported and endorsed this conference.

Organization of these conferences requires considerable time and effort. As in the previous WSTA conferences, individuals from various sectors (industry, Government and academia) have come forth and given generously their time. Special thanks are due to the members of the Organizing Committee, Scientific Committee, and Scientific Papers Coordinators and Reviewers.

Finally, we wish to acknowledge the immeasurable contributions made by the authors and their research associates who were not only willing to rework and modify their abstracts and manuscripts but also had to meet an extremely tight time schedule. Without their efforts this document would not have been possible. We sincerely hope that this conference will be both enjoyable and rewarding for you.

**Dr. Waleed K. Al-Zubari**  
**Head, Conference Scientific Committee**  
*Desert and Arid Zones Sciences Program*  
*Arabian Gulf University, Bahrain*



# TABLE OF CONTENTS

## VOLUME 1

### ***WATER RESOURCES PLANNING AND MANAGEMENT SESSION***

<b>Towards the Establishment of a Total Water Cycle Management and Re-use Program in the GCC Countries</b> <i>Waleed K. Al-Zubari</i>	1
<b>Securing a Blue Transformation Via a Global Freshwater Convention</b> <i>Anthony Milburn</i>	17
<b>Water Security in the Kingdom of Saudi Arabia</b> <i>Mohammed H. Al-Qunaibet</i>	35
<b>The Role of Information Systems in the Management of Urban/Industrial Water Cycle</b> <i>H. Ludwig and K.D. Wolz</i>	37
<b>Specific Privatization Issues Applicable to Water and Electricity Utilities in the Gulf Cooperation Council States</b> <i>Jamil S.K. Al-Alawi</i>	51
<b>The Role of Scientific Research in the Development of Water Resources in Saudi Arabia</b> <i>Ahmed M. Alabdulkader, Abdulrahman I. Alabdulalli and Ali A. Chamman</i>	65
<b>Overview of Water Import by Sea as an Alternative Solution to the Middle East Water Shortages</b> <i>Marwan Haddad, Anan Jayyousi and Numan Mizyed</i>	67
<b>UNESCO's International Hydrological Programme and Sustainable Water Resources Management in the Arab Region</b> <i>A.M.A. Salih</i>	81

## **GROUNDWATER RESOURCES SESSION**

<b>Evaluation of Groundwater Resources of United Arab Emirates</b> <i>Zeinelabidin S. Rizk, Abdulrahman S. AlSharhan and Shizuo Shindo</i>	95
<b>Survey on Groundwater Recharge and Flow in Wadi Wurrayah</b> <i>Mohammed S. Abdulla and Ahmad A. Durabi</i>	123
<b>Hydrogeology of the Geothermal Fractured-Rock Well Field at Jabal Hafit, Abu Dhabi Emirate</b> <i>Mohamed A. Khalifa</i>	125
<b>A New Isotope Water Line for Northern Oman</b> <i>Phillip G. Macumber, J. Mohamed Niwas, Alia Al Abadi and Rohitha Seneviranine</i>	141
<b>Use of Geophysics for Water Resources Assessment in Oman: A Review</b> <i>M.E. Young, Nasser Al-Touqy, Said Al-Hinai and Ali Al-Ismaily</i>	163
<b>Electromagnetic Detection of Underground Water</b> <i>Mostafa S. Afifi</i>	171
<b>Estimating Total Dissolved Solids Concentration of Groundwater Using Borehole Geophysical Logs</b> <i>Daniel J. Bright and Mohamed Al Za'afarani</i>	183
<b>Variable Hydraulic Responses Observed in the Alluvial Aquifer of Eastern Abu Dhabi Emirate</b> <i>Eric Silva</i>	197
<b>Application of the Eden-Hazel Method for Determining Transmissivity from Step-Test Recovery Data</b> <i>Mustafa Al Amin Nasr</i>	209
<b>Numerical Simulation and Experimental Validation of Dual Porosity/Dual Permeability Flow</b> <i>Tariq Cheema and M. Rafiq Islam</i>	219
<b>Advantages of Air-Foam Drilling Methods for Construction of Water Wells in Eastern Abu Dhabi Emirate, UAE</b> <i>Hassan Omer and Gerald Winter</i>	233

***SURFACE WATER AND ARTIFICIAL  
RECHARGE EXPERIENCES SESSION***

- Water Supply Augmentation Through Artificial Groundwater Recharge Techniques** 241  
*Mohamed J. Abdulrazzak*
- Streamflow Records for the Wadis of Oman** 283  
*Aysha Al Khatry and William O'Brien*
- Groundwater Recharge Dam and Hydrogeology of Wadi Al-Fulayj, Wilayat Sur, Sultanate of Oman** 295  
*Majid Bilarab Al Battashi and Syed Rashid Ali*
- Constraints in Traditional Hydrological Frequency Analysis Methods When Applied to Oman** 313  
*Aisha Al Qurashi, Frederiek Kaul and Theodore Calma*
- Investigations for Development of Groundwater Management Strategies in the Eastern Coastal Plain of the United Arab Emirates** 329  
*Mohamed Sager Al-Assam and Wolfgang Wagner*
- Screening of Recharge Dam Sites in Oman** 341  
*Suleiman Al Akhzami, William O'Brien and Ian Cookson*
- Application of One Dimensional Flow Modelling to Estimate Groundwater Recharge—Al Batinah, Sultanate of Oman** 357  
*Richard Lakey and Habiba Al Hina*

# TABLE OF CONTENTS

## VOLUME 2

### ***WATER DESALINATION SESSION***

<b>Roof Structural Damage of Sitra Power and Water Station Phase I Multi-Stage Flash Units</b> <i>Moh'd A. Redha Ghulam Hussain and A. Hussain Al-Jaziri</i>	373
<b>Rehabilitation of Long Tube Parallel Flow Evaporator Al-Ghubrah Power Plant &amp; Desalination</b> <i>A.R. Abu Dayyeh, Ribi Hamdan, P.K. Mukerjee and P.A. Vijay Kumar</i>	391
<b>A Kinetic Model for Scale Formation in MSF Desalination Plants. Effect on Antiscalants</b> <i>A. Mubarak</i>	409
<b>Kinetics of Hydrolysis of Chloroform and Bromoform in Aqueous Solutions</b> <i>A.M. Shams El Din and Rasheed A. Arain</i>	425
<b>The Thermovapor Compression Desalters: Energy and Availability analysis of Single and Multi Effect Systems</b> <i>M.A. Darwish</i>	441
<b>Experience with the Three Different Cogeneration Arrangements at Al-Ghubrah Power and Desalination Station</b> <i>A.R. Abu Dayyeh, Ridhi Hamdan, Wasfi F. Zaki, Salah Abunayib and Joshua Mathew</i>	463
<b>Performance of High Chromium Stainless Steels and Titanium Alloys in Arabian Gulf Seawater</b> <i>Ali Al Odwani, Mohammed Al-Tabtabaei and Ahmed Abdel-Nabi</i>	479
<b>Use of GRP Material in Power and Desalination Plants</b> <i>N.J. Paul, Hasan Ibrahim Al Hasani and Adel El Masri</i>	497

<b>Feed Salinity and Cost-Effectiveness of Energy Recovery in Reverse Osmosis Desalination</b>	509
<i>M.A. Mandil, H.A. Faroq, M.M. Naim and M.K. Attia</i>	
<b>Comparative Performance Analysis of Two Seawater Reverse Osmosis Plants: Twin Hollow Fine Fiber and Spiral Wound Membranes</b>	521
<i>Sameer Bou-Hamad, Mahmoud Abdel-Jawad, Mohammed Al-Tabtabaei and Saud Al-Shammari</i>	
<b>A Case Study of RO Plant Failure Due to Membrane Fouling, Analysis and Diagnosis</b>	537
<i>M. Gamal Khedr</i>	
<b>Performance Evaluation of Ten Years Operation Experience of Brackish Water RO Desalination in Manfouha Plants, Riyadh</b>	551
<i>Raed I.S. Al Mudaiheem, Sami O.A. Al Yousef, A.K.M. Amirul Islam and Tamer Sharif</i>	
<b>Pilot Study of MSF-RO Hybrid Systems</b>	561
<i>Essam El-Sayed, Sadeq Ebrahim, Ahmad Al-Saffar and Mahmoud Abdel-Jawad</i>	
<b>Practical Solutions to Problems Experienced in Open Seawater RO Plants Operating on the Arabian Gulf</b>	573
<i>Mohammed Obaid and Ali Ben Hamida</i>	
<b>The Addur SWRO Desalination Plan, Towards A Full Plant Production</b>	587
<i>Ali Hussain and Ahmed H. Ahmed</i>	
<b>Predictions of Performance of RO Desalination Plants</b>	605
<i>Ibrahim S. Al-Mutaz and Bander A. Al-Sultan</i>	
 <b><i>MUNICIPAL WATER SUPPLY SYSTEMS</i></b>  	
<b>A Computer-Aided Design Program for Water Network Analysis</b>	619
<i>L. Khezzar, S. Harous, M. Benayoune, K. Al-Asmi and TMA Sajwani</i>	

**Conceptual Cost Estimate System for Domestic Water Supply Projects** 635  
*Al-Asfoor, Mashhoor Dawood*

**Computer Analysis of Muscat Pipe Network** 651  
*A. El-Zawahry*

**Water Transportation by Ductile Iron Piping Problems and Prospects** 665  
*N.J. Paul, Murad Seleiman, Abdul Jalil Khoory and Adel El Masri*

### ***DOMESTIC WATER QUALITY SESSION***

**Problems of Operation and Maintenance of Aged Deep Wells** 675  
*Ibrahim M. Abo'Abat, Hasan Thabith Mohamed and Sulaiman Mubarak Abu Alaiwi*

**Microbiological Quality of Bottled Water Sold in Kuwait** 677  
*Al-Nashi B. and Anderson J.G.*

**Experimental Evaluation of Hardness Removal from Buraydah Groundwater Supplies** 693  
*Abdulrahman I. Alabdula'Aly*

**Trace Metals in Groundwater Treatment Plant's Product Water of the Central Region of Saudi Arabia** 705  
*Abdulrahman Alabdula'Aly*

# TABLE OF CONTENTS

## VOLUME 3

### ***WATER USE IN AGRICULTURE AND IRRIGATION EFFICIENCY SESSION***

- A Comparison of Economic and Engineering Efficiencies  
in Modern Irrigation in Oman** 713  
*Lokman Zaibet and Abdulla Omezzine*
- New Technology for Variable-Rate Management  
of Center-Pivot Irrigation** 727  
*Ian R. McCann, B.A. King, W. Ray Norman,  
Walid H. Shayya and Seif Al-Adawi*
- Infiltration Rate reduction Prediction Under Surge  
Irrigation Using Management Variables and Soil Composition** 737  
*Mohammed Al-Saud and Terence H. Podmore*
- Aflaj Irrigation Water Management and Efficiencies:  
A Case Study from Northern Oman** 751  
*W.R. Norman, W.H. Shayya, A.S. Al-Ghafri and I.R. McCann*
- Effect of Soil Amendments and Water Quantity and  
Quality on Cumulative Evaporation and Moisture Distribution** 767  
*Hayden A. Abdel Rahman and Anwar M. Ibrahim*
- Irrigation Water Quality and Frequency Effects on  
Cowpea (*Vigna Unguiculata* L.) and Soybean  
(*Glycine Max* L.) Yields** 781  
*Yahya A. Al-Nabulsi, Awad M. Helalia and Osman A. Al-Tahir*
- Irrigation of Date Palms in Sultanate of Oman** 795  
*Hassan Wahby and Emad Abdul Majeed*
- An Integrated Agriculture System: A Self-Sufficient  
System of Energy and Irrigating Water** 797  
*Hassan E.S. Fath*

<b>Modeling the Sensitivity of Pumped Groundwater Salinity to Irrigated Agriculture in Data Shortage Regions</b> <i>Mahdi Al-Sayed and George Fleming</i>	807
<b>A Remote Sensing Approach for Monitoring Salt-Affected Soils: A Case Study in Saudi Arabia</b> <i>Saleh A. Al-Hassoun and Saud A. Taher</i>	823
<b>Comparison Study Between Native and Soil Irrigated by Brackish Groundwater, Southern Kuwait</b> <i>Muhammad F. Al-Rashid</i>	837
<b>Field Estimation of Unsaturated Hydraulic Parameters Using Point Source and Disc Tension Infiltrometer</b> <i>Salem A. Al-jabri and A.W. Warrick</i>	847
<b>WASTEWATER TREATMENT AND REUSE</b>	
<b>Wastewater Treatment and Reuse in the Sultanate of Oman</b> <i>Ahmed bin Mohammed Al-Sabahi</i>	859
<b>Performance of Wastewater Treatment Plants in Riyadh</b> <i>Abdullah El-Rahaili and Mohammed Misbahuddin</i>	889
<b>Slow Sand Filtration of Secondary Effluent - with and Without Chlorination</b> <i>Shaukat Farooq and Syed A.V. Imran</i>	905
<b>“Nanofiltration/bioreactor” and “Nanonfiltration/ Crystallization” - Two Examples for the Potential of Nanofiltration in Wastewater Treatment</b> <i>Robert Rautenbach and Thomas Linn</i>	919
<b>Water Reclamation in Salalah, Sultanate of Oman</b> <i>Michael J. Walsh and Mohamed Alamin Ahmed Younis</i>	935
<b>Preliminary Selection of Suitable Sites for Sewage-Based Irrigation in Egypt</b> <i>Akram Fekry and Fatma A.R. Attia</i>	945



**ENVIRONMENTAL PROTECTION AND PUBLIC  
AWARENESS AND PARTICIPATION**

- Environmental consideration of Brine-Water Disposal  
from Desalination Plants** 957  
*Hosny Khordagui*
- The Gulf Sea Basin: A Clean Water Supply Intake  
or A Dumping Sink?** 977  
*Khalid AlHajri and Hassan Darwish Ahmed*
- Measurement of Low Level Emitting Nuclides  
of Uranium and Thorium in Groundwater by  
High Resolution Alpha-Spectrometry** 999  
*E.I. Shabana, A.S. Al-Hobaib and A.A. Al-Yousef*
- Community Participation-A Mean for Improving  
Rural Environment—A Case Study** 1009  
*Madiha Mustafa Darwish and Fatma Abdel Rahman Attia*
- Effect of Wastewater on Soil and Plant** 1021  
*Ali Abdulla Al-Jaloud*
- The Ecology of Wastewater in the Open Sections  
of a Sewage Treatment Continuum under Arid Conditions** 1023  
*Reginald Victor and Salma M. Al-Harassi*



# **Roof Structural Damage of Sitra Power and Water Station Phase I Multi-Stage Flash Units**

*Moh'd A. Redha Ghulam Hussain and A. Hussain Al-Jaziri*

# **ROOF STRUCTURAL DAMAGE OF SITRA POWER AND WATER STATION PHASE I MULTI STAGE FLASH UNITS**

**Moh'd A. Redha Ghulam Hussain  
A. Hussain Yousif Al-Jaziri**

## **ABSTRACT**

Phase I Multi Stage Flash (M.S.F.) units roofs have recently experienced major structural damage, specially at heat reject section. Excessive corrosion of the roof structural supporting beams and plates were not detected at earlier stages because of the thermal insulation material covering the entire roof area of these units.

Preliminary investigations revealed that the corrosion of the roof supporting beams and plates was mainly caused by:

1. Trapping of water (rain and or sea water) between the structure support beams & roof plates, causing corrosion of the structural roof beams and hence leading to weak structure and roof partial sagging.
2. Trapping of rain water under the insulation material for prolonged period of time.
3. An overlooked area.
4. Insulation material absorbed the water provided good corrosion cell.

Temporary corrective repair work was carried out to bring the unit back into service by welding in new supporting beams. Proper repair work is planned for the station rehabilitation works.

## INTRODUCTION

Desalination units 1A-1B are cross tube Multistage Flash evaporation distillers of brine recycle type, consisting of 15 stages with a capacity of 11,500 M<sup>3</sup>/d each when operated at 90°C top brine temperature (T.B.T.) and sea water temperature of 32°C. The distillate has a total dissolved solid content of 15 parts per million (ppm) and pH range of 6.2 - 7.00. The main distiller shell is fabricated from 20.0 mm carbon steel plates except the first two recovery stages, where the plates thickness is 40.0 mm.

Sitra Power and Water Station is a co-generation plant, where passout steam is used to heat brine water to a maximum temperature of 90°C. The desalination units were designed and constructed by Societa Italiana Resine (SIR) - Italy and commissioned in 1976. Each distiller consists mainly of :

1. Evaporator
2. Brine heater
3. Associated ancillary equipment i.e. chemical dosing and acid cleaning system
4. Rotating equipment, such as pumps & compressors.

## DISTILLER OPERATING HISTORY

The distillers were commissioned in 1976 and have been under continuous service with the exception of annual overhaul, maintenance and forced outages. These units were operated under normal condition up to 1990 and produced maximum production up to 433 M<sup>3</sup>/h against the design figure which is 479 M<sup>3</sup>/h even though the corrosion was a major factor in the distillers. During recent years, they had experienced excessive corrosion mainly on the outer surface due to the plant ageing and certain design factors. For example, structural I- beams supports and roofing catchment area were designed without consideration of roof drainage.

## MECHANICAL REHABILITATION & LIFE ASSESSMENT

Since excessive corrosion rate was experienced on the flash chamber walls especially at the vapour spaces, rehabilitation work had to be undertaken to protect these areas. This rehabilitation work was executed by M/S Sasakura Engineering Co., Ltd., Japan during 1987 {1}.

The following remedial and protection works were carried out during the rehabilitation:

1. Welding stainless steel - type 316L, protective lining above the demisters on the upstream vapour side of stages nos. 2 to 9.
2. Ankiol paint was applied to the inside of all surfaces of distillate channel in all stages and upstream vapour space walls and roof in stages 10 up to 15.
3. Restoration of heavily corroded structural parts through patch welding / replacing.
4. Replacing tube support hangers in selected stages and renewing the demister supports by stainless steel material.

As the rate of corrosion had increased by 20 to 30% beyond design life, the Directorate had commissioned M/s Ewbank Preece Limited (EPL) to study the problem during 1990 and assess the remaining life of the distillers. It was recommended that rehabilitation work has to be undertaken so as to extend the life of the distillers up to year 2010 {2}. Refer to figures 1A and 1B.

## **MAINTENANCE PHILOSOPHY**

The station adopted up to date methodology and approaches for plant maintenance to improve plant availability and reliability. A well organized effective maintenance programme on Planned Preventative Maintenance (P.P. M) technique was developed and implemented based on the information gained from the condition monitoring techniques.

Although there were shortcomings in the maintenance criteria at the initial stages from 1976, the maintenance approach was further developed utilizing the expertise gained on the installed plants. Annual overhaul of 6 to 8 weeks were initially adopted depending upon plant performance and defects. This is normally carried out during winter tune when the water demand is minimum.

Prior to annual outage, pre-shutdown checks were conducted to ascertain the condition of the distiller so as to identify any defects. Normally during distiller annual outages, the following major activities are carried out:

1. Distiller stages partition walls in vapour spaces and brine areas cleaned to remove scale.
2. Cleaning of tubes in reject and recovery stages by means of high pressure water jetting.

3. Thickness measurement and monitoring of walls in flash chambers, vapour spaces and distillate channels to analyze the rate of corrosion.
4. Eddy current test for assessing tube condition as required.
5. Monitor the condition of equipment and overhaul as required.
6. Painting of non-protected structures to reduce external corrosion.

### **CORROSION IMPACT ON PLANT AVAILABILITY**

Station inspection revealed evidence of severe corrosion on thermally insulated areas of the distillers roof. This corrosion is attributed to stagnant sea water leaks from ejector condensers as well as accumulated rain water. Due to design deficiency, water seepage was not catered for during the initial design stages. This stagnant water induced corrosion of the supporting I- beams and roof plates. Refer to Photo nos. 1&2.

As these areas are covered by thermal insulation they were overlooked during inspections. Had these insulated areas were left undetected for longer time, then it would have eventually had catastrophic failure.

Severe corrosion on the roof I-beam supports, roof plates (including structures), and pipe works has raised concern for plant integrity and personnel safety. A recent corrosion survey together with 1993 survey on distiller-1A stages are graphically illustrated in Figures 2A & 2B. Distiller 1B corrosion survey showed similar phenomenon as that of distiller 1A.

Impact of corrosion on distiller's structures affected the plant availability even though the station had taken interim corrective measures. The average rate of corrosion exceeded the corrosion allowance by 20 to 30% in the inter-stage walls of the hottest stages. As shown in figure 2B, one can suggest that these are of uniform corrosion mode. In other words, the most serious problems are those of localized corrosion mode of lower temperature stages.

### **PERFORMANCE DETERIORATION**

During recent years, the production and the plant availability dropped beyond the targets. Production of each distiller dropped from 3.60 million cubic meters to 1.27 million cubic meters, i.e. around 65% less than earlier production figures. Simultaneously distiller reliability went down to 65% and 76% for distillers 1A

& 1B respectively. The forced outage rate had gone up to 46% and 33% for distillers 1A & 1B respectively. Refer to Tables 1. An analysis of annual production illustrates the distiller performance since commissioning in 1976 and up to 1996 as shown in Table 2.

A comprehensive plan was envisaged to identify the source of performance deterioration and to enable corrective action during annual overhaul of distillers.

## **PROBLEM INVESTIGATION**

During annual overhaul of 1994, major inspection for both the distillers was carried out. Analysis of vacuum decay test during previous years indicated poor vacuum condition due to air ingress into tile system. Refer to Figures 3 & 4.

However, the severity of the roof corrosion was not obvious at the initial inspection but when hydrostatic test was carried out, it revealed major leaks from the roof plates. Roof plates deflection ranging from 12 to 100 mm at stages 9 to 15 was noticed.

As the distiller roof areas, have always been neglected during surveys over the years, the middle part of the I-beam section decayed completely and hung over the roof plates. Further inspection showed holes and cracks on the roof plates which allowed air ingress into the stages. The stages roof corrosion was evident for almost all the I-beams from stage 9 to 15.

The following are the attributing factors to the supporting I-beams' corrosion:

1. As the distiller roof is inclined towards the deaerator, it maintained stagnant rain/sea water on the roof from stages 9 to stage 15.
2. No provision was contemplated for catchment area drain from the distiller roof, therefore rain, sea water and condensate drain from ejectors seeped through the insulation, thus contributed to corrosion.
3. The roof is completely insulated for maintaining the stages temperature. This prevented natural evaporation of the stagnant water.

## **CORRECTIVE ACTIONS**

After investigating corrosion problems and identifying their causes, the following remedial steps were considered on short and long term basis.



## **1. SHORT TERM SOLUTION**

In order to maintain plant availability, a decision was taken to replace the badly corroded I-beams with new structural steel beams.

The existing corroded I-beams were cut and the beam seating areas were ground for proper contact with the roof plate. Sagged roof plates were lifted by fabricating a special jig suitably welded to the roof plates and jacked up by using two hydraulic jacks of a 100 ton capacity each so as to make skip welding on the I-beams. Refer to Photo no. 3

There are 11 rows of beams across the flash chamber, each 12 meters long equally spaced over the roof plates. Among them, 6 rows were replaced by new I-beam sections. Cracked areas of the roof plates were repaired by patch welding.

The above task was done within a short duration as an interim solution to commission the distillers as quickly as possible. After completion of work, vacuum decay test was conducted during commissioning which showed significant improvement. Refer to Figures 3 & 4.

## **2 LONG TERM SOLUTION (LIFE EXPECTANCY ASSESSMENT)**

As discussed in the Mechanical Rehabilitation/Life Assessment earlier, the Ministry of Electricity and Water had commissioned the consultants M/S Ewbank Preece Limited (EPL) to conduct a survey for assessing the remaining life of the plant. Accordingly, rehabilitation survey was carried out by them during distiller outage cycle in September / October 1990.

Their rehabilitation survey included the existing condition of the plant, assessment of remaining life and recommendation for rehabilitation for extending the plant life up to the year 2010.

Since the advanced rate of corrosion exceeds the life prediction of Ewbank Preece Limited (EPL) survey, the Ministry of Electricity and Water is in the process of studying the different options available to rehabilitate these two units. The study also includes cost/benefit analysis for these options.

## **CONCLUSIONS & RECOMMENDATIONS**

By virtue of expertise gained with the distillers 1A and 1B, Phase II distiller roof was inspected and similar phenomenon was found but to a lesser extent. Corrective action was taken at an early stage. Phase III (Dist. 2, 3 & 4) roofs were inspected and found to be in good condition.

As a consequence of the above, roof maintenance P.P.M. was introduced for all distillers.

Advanced rate of corrosion affects the overall plant safety. Desalination plant designers should review the factors of catchment area drainage and other operating environmental conditions.

Distiller roof should be free from stagnation of rain or other drain water underneath the thermal insulation.

Vacuum system heat exchangers sea water leak contributed to distillers 1A & 1B roof corrosion. Therefore considerations should be given to shifting them away from distillers roof.

Rehabilitation work should include 100% removal of insulation and external coating to protect the structures.

Roof and other areas insulation should include access panels for routine maintenance inspection.





## **REFERENCES**

- { 1 } Khalid Borashid -Forth World Congress on Desalination and Water Reuse (IDA), Proceedings, Kuwait-November, 1989, p 283-288
- { 2 } Ewbank Preece Limited (EPL) Final Report and Recommendations on Distillers 1A and 1B Rehabilitation Study - August 1993, Fig. 4.1 and Fig. 4.2

Sl No.	PLANT	91	92	93	94	95	96	97	98	99	00	01	02	03	04	05	06	07	08	09	10
1	VAPOUR SPACE INTERSTAGE WALLS	Dependant on Oxygen Reduction to Reduce Corrosion										[Hatched]									
		Lined wall conditions remain unchanged										[Hatched]									
2	BRINE SPACE INTERSTAGE WALLS	Corrosion rates have increased marginally from 0.07 mm/yr to 0.1 mm/yr.										Dependant on Oxygen Reduction									
		[Hatched]										[Hatched]									
3	FLOOR PLATE SIDE PLATE ROOF PLATE	Roof plates Sided floor										ROOF Plates are in advanced state of Corrosion in Heat reject stages									
		[Hatched]										[Hatched]									
4	DEAERATOR & VENT COND.	Vent Cond. are in poor condition										[Hatched]									
5	BRINE HEATER TUBES	[Hatched]										Do not exceed TBT over 90 Deg C (Use Belgrad)									
		Full Evaluation after Eddy Current SURVEY										[Hatched]									
6	RECOVERY & REJECT TUBES	[Hatched]										Do not exceed TBT over 90 Deg C (Use Belgrad)									
		Full Evaluation after Eddy Current Survey										Recovery									
7	WATER BOXES	[Hatched]										[Hatched]									
8	BRINE HEATER	[Hatched]										[Hatched]									
		Heaters Successfully completed stat. Inspections										[Hatched]									
9	SEA WATER PUMP TURBINE	Aux. pipe work failures & E/B limiting factors										Spare Turbine to be provided Comprehensive pump spares required									
		Gears to be Refurbished										[Hatched]									
10	BRINE RECIRCULATING PUMP/TURBINE	[Hatched]										[Hatched]									
11	MISC. PUMPS	Replace SW Sump Drainage pumps										[Hatched]									
12	ACID CLEANING SYSTEM	[Hatched]										[Hatched]									
13	ANTI FOAM SYSTEM	[Hatched]										[Hatched]									
14	ANTI SCALE SYSTEM	[Hatched]										[Hatched]									
15	SODIUM SULPHITE	[Hatched]										[Hatched]									

**FIGURE 1A - SITRA POWER & DESALINATION PLANT**  
**Distillers No's 1A & 1B**  
**Life Expectancy Prediction Chart**

LEGEND :-

-  E.P. PREDICTION
-  E.P. OPERATIONAL CONDITIONS PREDICTION No. 1
-  REVISED PREDICTIONS
-  E.P. OPERATIONAL CONDITIONS PREDICTION No. 2

Sl No.	PLANT	91	92	93	94	95	96	97	98	99	00	01	02	03	04	05	06	07	08	09	10		
16	BRINE PIPEWORK	Reduce Output to prolong to life: 4 YEAR Refurbishment to achieve 2010																					
17	SEA WATER PIPEWORK	Avoid Stagnation Zones: 4 YEAR Refurbishment to achieve 2010																					
18	VENT PIPEWORK	Examine over next years all joints, valves & Inlet branches																					
19	STEAM PIPEWORK	Check Thickness of Bands										Overhaul all joints and branches											
20	DRAIN PIPEWORK	Programme 2 year Refurbishment to prolong to 2010										Subject to MD											
21	MANUAL VALVES	Update Stores Holding & PROGRAMME Replacement / Refurbishment																					
22	ACTUATOR OPERATED VALVES	Update Stores Holding & Programme Replacement / Refurbishment																					
23	BRINE FILTER	Consider Replacement with Duplex or Fit Case Baffle seal																					
24	SEA WATER FILTER	Consider Replacement with Duplex or Fit Case Baffle seal																					
25	COMPRESSORS																						
26	PNEUMATIC LINES & VESSELS																						
27	LAGGING & CLADDING	Remove Lagging up to stage 13, cut out lagging at DRAINS.																					
28	TRENCHES & TRENCH COVERS	Renewal required in areas										Remove lagging up to Stage 13, cut out lagging at drains											
29	ROOF BEAMS	Prediction not given in EW Bank Preca. Survey										Covered under Civil Rehab.											
		Items repairs carried out																					

**FIGURE 1B - SITRA POWER & DESALINATION PLANT**  
**Distillers No's 1A & 1B**  
**Life Expectancy Prediction Chart**

LEGEND :-

- E.P. PREDICTION
- E.P. OPERATIONAL CONDITIONS PREDICTION No. 1
- REVISED PREDICTIONS
- E.P. OPERATIONAL CONDITIONS PREDICTION No. 2

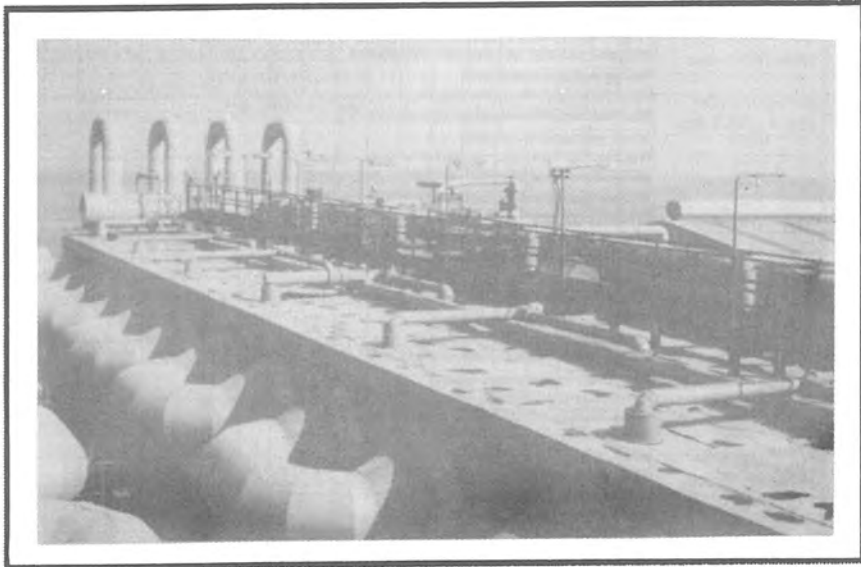


PHOTO NO. 1- DISTILLER 1A ROOF

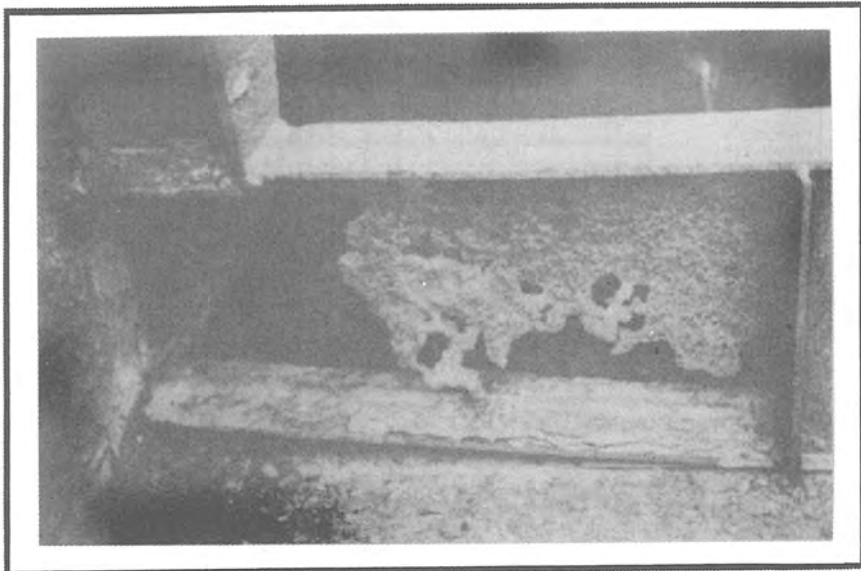


PHOTO NO. 2- DISTILLER 1B CORRODED ROOF I- BEAM

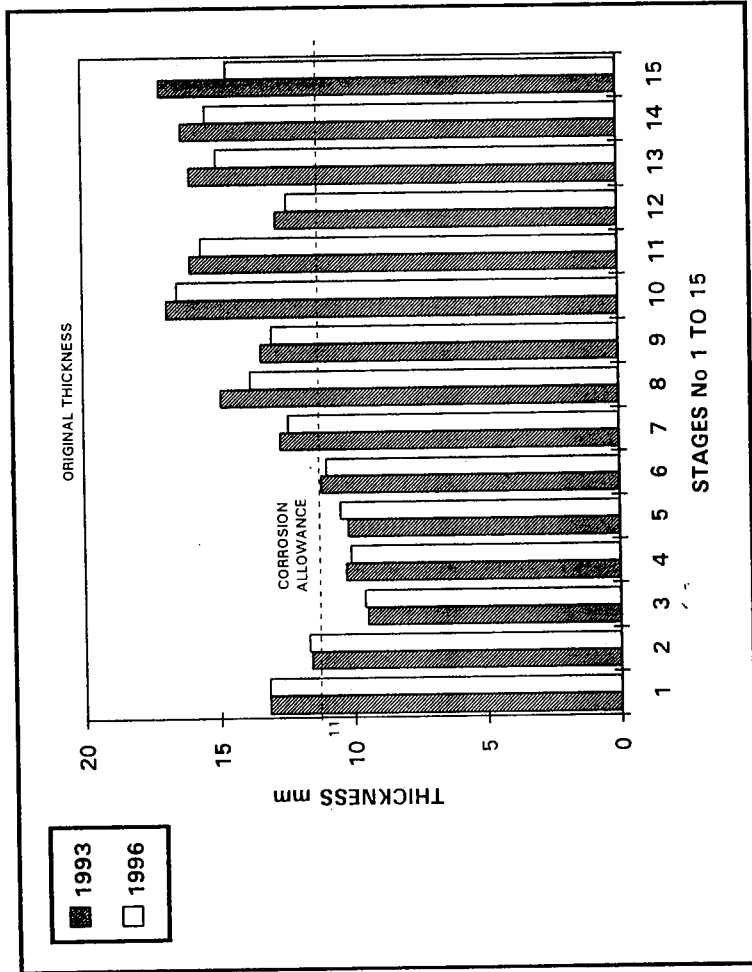
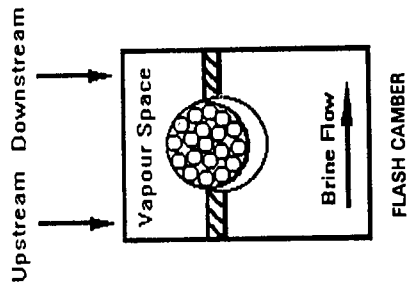


FIGURE 2A - DISTILLER 1A DOWNSTREAM WALLS THICKNESS 1993 & 1996 VAPOUR SIDE

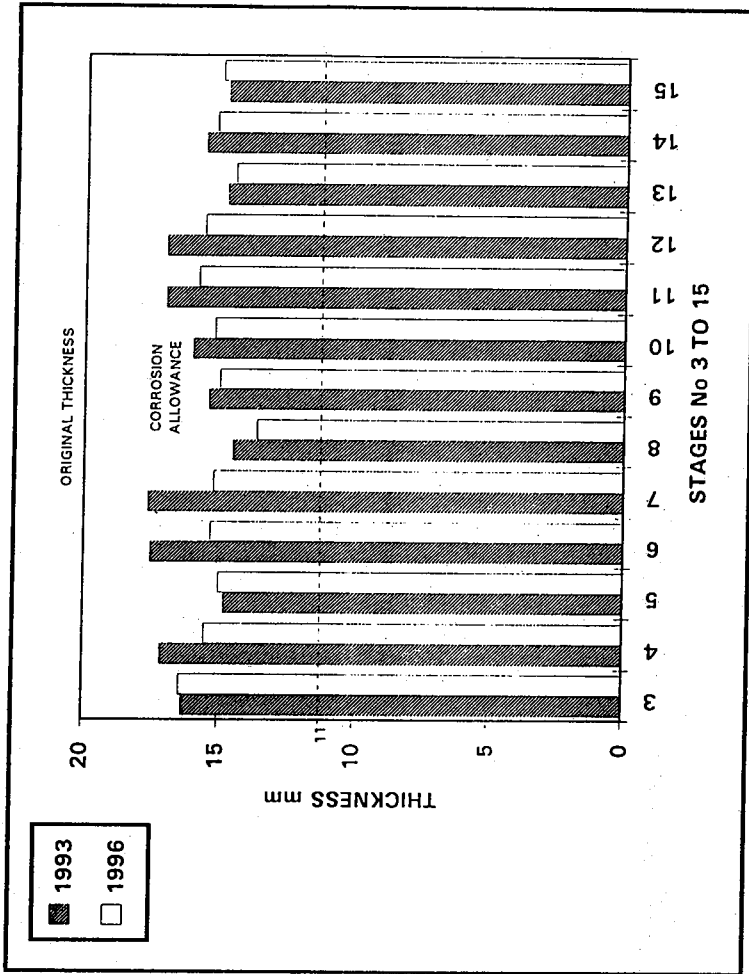
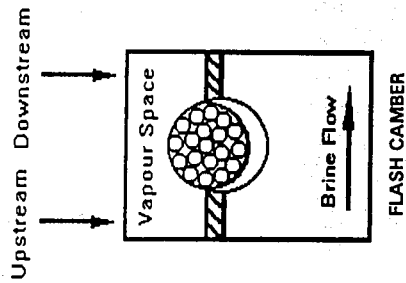


FIGURE 28 - DISTILLER 1A DOWNSTREAM CEILING THICKNESS 1993 & 1996 VAPOUR SIDE



**TABLE 1 - SITRA POWER AND WATER STATION  
DISTILLER 1A & 1B PERFORMANCE FROM 1991 - 96**

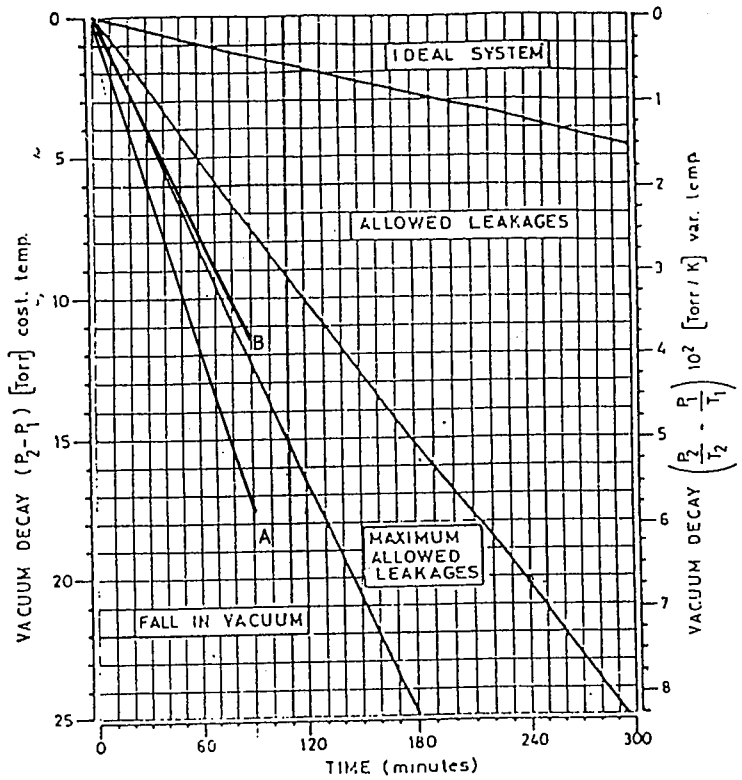
YEAR	RELIABILITY %		FORCED OUTAGE RATE %		AVAILABILITY %		PRODUCTION RATE M <sup>3</sup> /h	
	DIST. 1A	DIST. 1B	DIST. 1A	DIST. 1B	DIST. 1A	DIST. 1B	DIST. 1A	DIST. 1B
1991	89	98	13.30	2.40	70.39	78.39	408	433
1992	99	93	1.32	7.73	98.29	92.87	395	400
1993	99	98	0.94	2.82	68.43	62.91	385	395
1994	95	96	5.25	4.44	83.75	83.11	417	395
1995 *	65	76	46.76	33.63	39.59	46.38	372	392
1996	98	97	2.50	3.00	72.00	73.00	358	396

- \* 1. Reliability poor due to excessive corrosion.  
 2. Highest Forced Outage Rate was recorded during 1995.  
 3. Forced outage increased relatively because of poor vacuum conditions.



**TABLE 2 - SITRA POWER AND WATER STATION  
DISTILLATE WATER PRODUCTION STATISTICS**

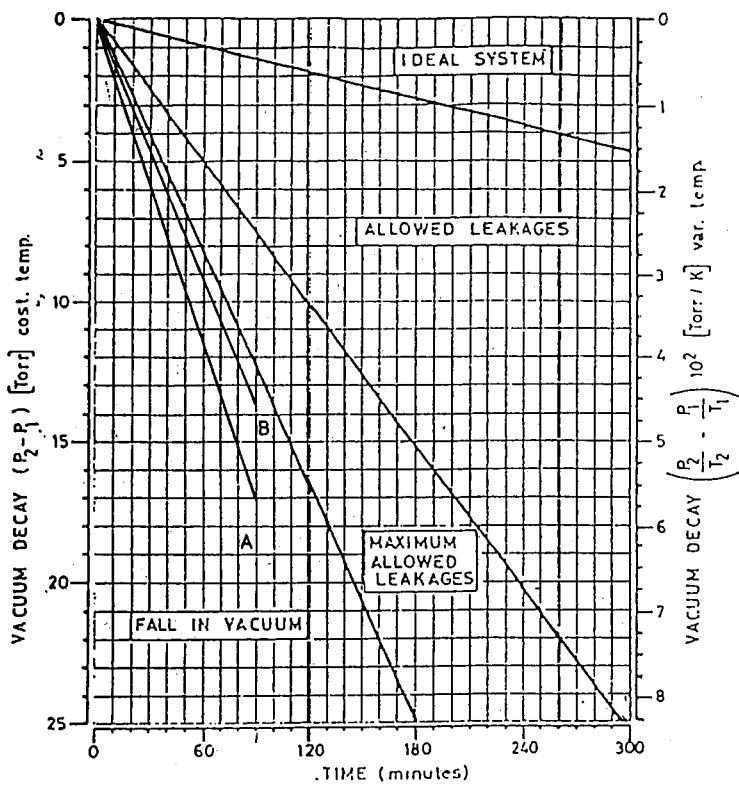
YEAR	PHASE I		PHASE II	PHASE III	TOTAL PRODUCTION MM <sup>3</sup>	REMARKS
	DIST. 1A	DIST. 1B	DIST. 5	DIST. 2, 3 & 4		
1976	0.42	1.12	--	--	1.54	Distiller 1A & 1B Commissioned.
1977	0.78	0.72	--	--	1.50	
1978	0.60	0.80	--	--	1.40	
1979	1.85	2.28	--	--	4.23	
1980	2.05	2.12	--	--	4.17	
1981	1.86	1.98	--	--	3.84	
1982	3.00	2.59	--	--	5.59	
1983	3.19	3.46	--	--	6.65	
1984	3.60	3.16	2.19	1.41	10.36	Distiller 2 & 5 Commissioned.
1985	3.15	2.73	6.51	15.95	28.34	Distiller 3 & 4 Commissioned.
1986	2.68	2.60	6.86	22.29	34.43	
1987	1.52	1.28	6.26	20.74	29.80	
1988	3.06	2.58	6.21	24.12	35.97	
1989	3.42	2.84	6.66	23.77	36.69	
1990	2.56	2.82	7.05	27.19	39.62	
1991	2.51	2.99	6.96	25.72	38.18	
1992	2.46	2.99	7.38	24.23	37.06	
1993	2.29	2.18	7.23	27.05	38.75	
1994	2.89	2.68	7.20	27.08	39.85	
1995	1.27	1.54	7.02	24.91	34.74	
1996	2.28	2.53	6.67	24.92	36.40	



**LEGEND :-**

- A - VACUUM DECAY DURING COMMISSIONING IN FEBRUARY 1994
- B - VACUUM DECAY DURING COMMISSIONING IN JULY 1995 AFTER ROOF REPAIR

**FIGURE NO. 3**  
**DISTILLER - 1 A**  
**VACUUM DECAY TEST IN STAGE 15**



**LEGEND :-**

- A - VACUUM DECAY DURING COMMISSIONING IN FEBRUARY 1994
- B - VACUUM DECAY DURING COMMISSIONING IN JULY 1995 AFTER ROOF REPAIR

**FIGURE NO. 4**  
**DISTILLER - 1 B**  
**VACUUM DECAY TEST IN STAGE 15**

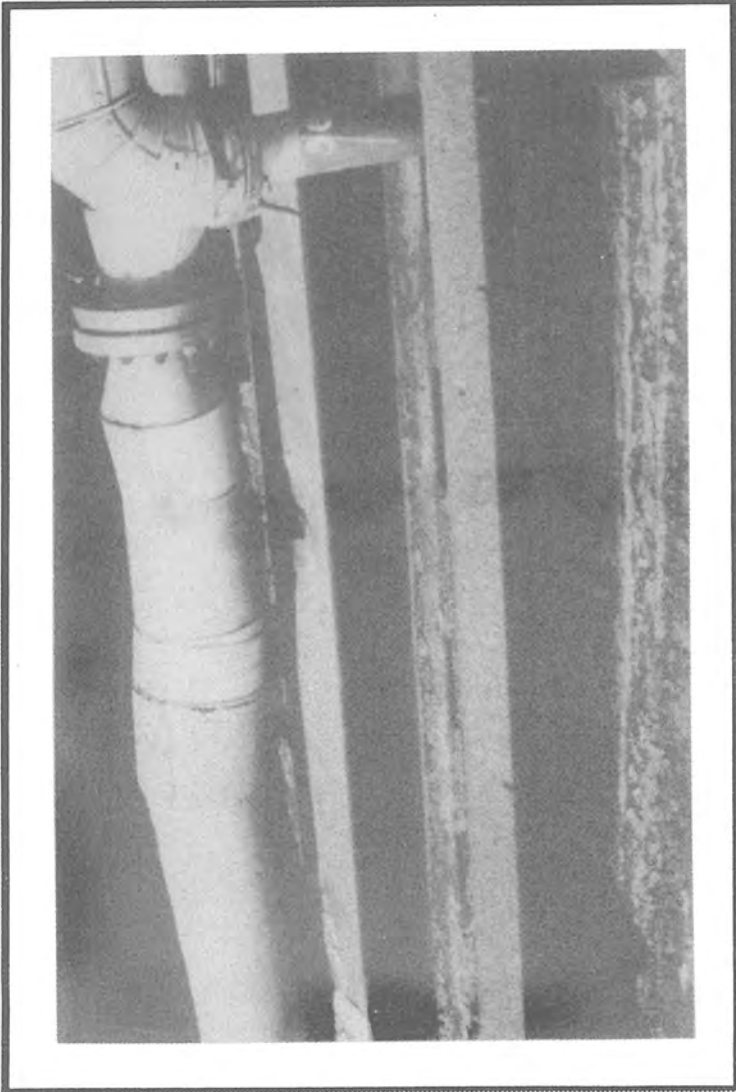


PHOTO NO. 3- DISTILLER 1A REPLACED AND CORRODED ROOF I-BEAM

# **Rehabilitation of Long Tube Parallel Flow Evaporator Al-Ghubrah Power Plant & Desalination**

*A.R. Abu Dayyeh, Ribi Hamdan, P.K. Mukerjee  
and P.A. Vijay Kumar*

# **REHABILITATION OF LONG TUBE PARALLEL FLOW EVAPORATOR AL-GHUBRAH POWER PLANT & DESALINATION STATION**

**A.R. Abu Dayyeh, Ribi Hamdan, P.K. Mukerjee & P.A. Vijay Kumar**  
SOGEX Oman Co. LLC  
Ghubrah Power & Desalination Station  
P.O. Box. 1170, Ruwi- 112 Sultanate of Oman

## **ABSTRACT**

The Desalination Plant No. 1 of Al-Ghubrah Power & Desalination Plant, Sultanate of Oman, is Multistage Flash long tube parallel flow type with 18 stages of heat recovery and 2 stages of heat reject in five vessels. The plant was commissioned in the year 1976. It had experienced severe corrosion in vapour space, more in high temperature stages. Tube support plate, inter stage walls, top roof plate were badly corroded. Tube bundles began to sag and some collapsed in vessel no. 1. Tube leak was encountered frequently. It was analysed that corrosion was due to build up of non-condensable gases in these stages. The plant venting system was designed to have series venting (cascaded) from stage No. 1 to 20. The plant was rehabilitated in the year 1990. The paper describes the study of corrosion, modifications of venting system and preventive measures being carried out to prevent the accumulation of non-condensable gases. After modification and tube bundle replacement in vessel No. 1, no significant corrosion is observed in this vessel even after five years of operation.

## INTRODUCTION

The desalination plant consists of five rectangular vessels. First vessel comprises of 6 stages, i.e. Stage No. 1 to Stage No. 6, second, third and fourth vessels have 4 stages each and fifth vessel has two stages (heat reject stages). The evaporator has separate deareator and decarbonator. The decarbonator is no longer used as the plant is running on polymer based antiscaling additive, Caustic soda is dosed in stage No. 1 distillate tray to maintain a final pH of greater than 8.5 in the distillate. The plant venting system was designed to have cascaded venting from stage No. 1 to Stage No. 20. Refer Figure No. 1. The tube bundles of recovery and reject section are divided into two, each bundle consists of 5036 tubes. There is one metallic expansion joint installed in the middle of each side between bundle tubes of each vessel 1, 2, 3 and 4.

### The material of construction of the plant were:

	<u>Material</u>	<u>Thickness</u>
Tube stages No. 1 to 18	CuNi 10 Fe	1.0 mm
stages No. 19 & 20	Titanium 0.5 mm	
Evaporator Shell	Steel St 37 - 2	
	Bottom plate (floor)	25 mm
	Top plate (roof)	20 mm
	East & West wall	
	(partition wall)	30 mm
	North & South wall	25 mm
	Distillate tray & condensing shell	15 mm

The vessels were constructed from bare carbon steel with no painting.

### DESIGN TECHNICAL DATA

Type	***	MSD long Tube
Make	***	SOGEX/DEMAG
Year of Make	***	1975 / 76
Plant Capacity	***	18200 M <sup>3</sup> /d (4 MIGPD) at TBT =90°C using low temp. chemical scale control. 27600 M <sup>3</sup> /d (6 MIGPD) at TBT = 113°C. using high temp. improved chemical scale control or acid (H <sub>2</sub> SO <sub>4</sub> )
Economy Ratio	***	6.8 <u>Kg of distillate</u> Kg of Steam
Concentration Factor		1.5
Quality of Distillate		100 ppm TDS
Seawater Temperature (Design)		35°C
Cooling water flow to heat reject		11,800 M <sup>3</sup> /hr

Brine recycle flow	10,000 M <sup>3</sup> /hr
Heat recovery section:	
No. of stages	18
No. of tubes in each stage	10072
Outside diameter of tubes	16 mm
Tube material	CuNi 10 Fe
Heat Rejection section:	
No. of stages	2
No. of tubes in each stage	10072
Outside diameter of tubes	16 mm
Tube material	Titanium

## HISTORY OF CORROSION

The plant was commissioned in 1976 and initially it was run on Polyphosphate producing design and guaranteed values of 4 MIGPD. The 24 hours performance test of desalination plant was carried out on 17th/18th March 1979, after the plant has produced water for almost three years. The contractual and actual values are tabulated in Table No. 1 - I.

The plant is also capable of producing 6 MIGPD (non-guaranteed) with acid dosing at top brine temperature of 113°C. It is well known fact that plant on acid dosing will suffer more corrosion, hence in 1979 plant was run with high temperature antiscaling additive Belgard and performance test run was carried out on 2nd March 1981, refer to performance data Table 1- II. During test run it was observed that pressure in Stage No. 1 was at 1.15 bar (Abs) and therefore first stage vent to atmosphere was opened which was emitting lot of steam, making surrounding area near stage No. 1 wet and corrosive. Afterwards plant was run around 5 MIGPD capacity. Typical values are tabulated in Table No. 1 - III.

Yearly plant is shut down for one month for annual maintenance and inspection. During annual inspection and shutdown from 08/04/83 to 05/05/83, it was found that tube support plate of stage No. 6 had severe corrosion at the bottom. As there were no manhole to go inside distillate tray, inspection was made with the help of baroscope.

First tube leak was observed on 24th October 1983. As this was the first tube leak, various tests viz: change in brine flow and pressure, change in cascade venting were carried out. Ultimately plant was shut down on 18th December 1983 to find out the tube leak, vacuum test was carried out, subsequently two tubes of stage No. 4 - 6 South were plugged.



During next annual shut down from 19/02/1984 to 24/03/1984, plant was inspected by M/s. Incon Anlagentechnik GmbH, Hamburg, Germany. [Ref 1]

It was ascertained that support plates of tubes bundles in the region of Stage No. 5 and No. 6 in vessel No. 1 were badly corroded. In the passage of non-condensable gases of stage No. 5 & 6 an approximately 1 mm thick deposit was found adhering to CuNi tubes. This material also partly covered the support plates and inner surface of distillate duct. The colour of the deposit was red and lightly adhered to the material surface. The chemical analysis undertaken in Germany showed the compositions CuO - 36.9%, Fe<sub>3</sub>O<sub>4</sub> - 61.2%.

The CuNi 10Fe tubes under the deposits showed no visible signs of corrosion while the supports, distance holding pipes and distillate duct were attacked by corrosion. Some of the supports were totally corroded upto the 1st few rows of tubes.

1983 onwards tube failure occurred frequently and in 1988 alone 644 tubes were plugged in vessel No. 1. Before rehabilitation, the following tubes were plugged.

Stages	Tubes Plugged	Total Tubes	% age
1 - 3	1135	10072	11.25
4 - 6	72	10072	—
7 - 8	2	“	—
9 - 18	0	“	—
19 - 20	13	“	—

Tube failures were confined to first vessel. Failures tended to increase in Stage No. 1 to 3 compared to No. 4 to 6. They were more frequent in lower parts of the bundle, near the non-condensable gases entrance.

Galvanic corrosion was also observed between tube and tube support plates due to displacement of insulation material between them. Consequently the hole in the tube support plate enlarged causing rattling of tubes. Tube support plates and holding pipes were badly corroded and missing in some plates causing tubes to sag. [Picture No. 1]

There was no provision to enter the distillate duct. Hence manholes were made in distillate duct of Stag No. 6 in 1986, Stage No. 1, 2, 3, 4 & 5 in 1987 and for all other stages in 1988 for close inspection of condensing chamber. Extra saddle support were also installed with Teflon sheet on top of saddles to prevent sagging in the same year of making manholes. Severe corrosion was also observed in vapour space of distillate duct. Black flakes of iron oxide

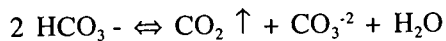
were found all over the vapour space. It was also noted that corrosion product formed on the steel broke off and on tubes. Corrosion was usually most severe in the inter stage walls.

## ANALYSIS OF CORROSION

In 1987, 25 tube samples were extracted from vessel No. 1 and delivered to Nickel Development Institute to examine them. [Ref 2]

The analysis showed that corrosion was confined to the exterior surface. The inside (brine side) surface was in good condition and covered with light scale and no evidence of serious corrosion.

Analysis of deposits on tubes showed mainly oxides of Cu/Fe. The deposit on tubes exterior was probably caused by soluble corrosion product dripping through the bundle and depositing as their oxide. The evidence, in the tube sample and distribution of failure indicated vapour side corrosion as the cause of the problem. It was clear that corrosion must be caused by non condensable gases. The main component of these gases is carbon dioxide which is evolved by thermal decomposition of bicarbonate in seawater.



The second most likely gas is oxygen. As MSF plant is operated at reduced pressure air ingress will occur, through gasket joints, level gauges, manhole cover, any leakage in the upper section of the plant is unlikely to enter the brine which is flashing. It will however, be swept into the vapour space by the flow of vapours. It is therefore evident that quite a high oxygen level could exist in the vapour space even when the oxygen level in brine recycle is at an acceptable limit of 50 ppb.

Oxygen scavengers such as hydrazine are often added to the boiler waters, These decompose to form ammonia which in the presence of oxygen, is extremely corrosive to copper base alloys. In MSF plants the steam to brine heater will contain ammonia if hydrazine is used for boiler water treatment. If brine heater is vented to stage #1 of the evaporator, then very severe vapour side corrosion can occur as oxygen is usually present.

Corrosion of copper alloy in vapour space requires the presence of both carbon dioxide and oxygen [Ref 3]. The use of carbon dioxide makes condensate acidic. The developed acidity does not cause copper alloys to corrode because these alloys are more noble than the hydrogen release reaction and in the absence

of oxygen corrosion would be negligible. [Ref 4]. The acidity however removes the protective film and in the presence of the oxygen corrosion can proceed. This corrosion normally takes place in the form of uniform thinning of tube. This is the type of corrosion observed in the samples.

## REHABILITATION

The plant was rehabilitated in the year 1990. Eddy current test and ultrasonic thickness measurement was carried out during rehabilitation in order to assess the plants life [Ref 5].

Eddy current test was carried out for the 10% of 5036 tubes in each bundle for Cu-Ni tubes of Stages No. 7 to 18 and Titanium tubes of Stage No. 19 and 20. The thickness reduction ratio in almost all the tubes tested was within the range of 20% to 30% and there was no any tube more than 30% in reduction ratio of tube thickness. On the other hand allowable thickness reduction ratio in structural strength (no requirement of corrosion allowance) is 75% in 90-10 Cu/Ni tubes and 50% in titanium tubes. Accordingly the tube life was assessed to be durable for another 10 years. During the eddy current test, conditions of tube support plate were also checked. Defect / damage on tube support plates was found in vessels No. 2 and 3.

The designated position of end plate, partition plates, side plate, top plate and condensing chamber plate were measured by ultrasonic thickness indicator. In vessel No. 1 between stage No. 2 and 3, thickness reduction ratio of partition plate (30 mm thick) was highest at 13.7% i.e. 4.1 mm of wall plate was corroded against 10 mm corrosion allowance.

Reduction ratio of top plate (20 mm thick) was highest in Stage No. 18 at 15% i.e. 3 mm of ceiling plate was corroded against 5 mm corrosion allowance.

Reduction ratio of condensing chamber plate was highest in Stage No. 12 at 16%, i.e. 1.2 mm of chamber plate was corroded against 5 mm corrosion allowance.

From the above it was concluded that body shell itself of the evaporator will be durable for another 10 years. Hence it was decided to only replace the badly corroded tubes bundles and condensing section of vessel No. 1 only.

Entire tube bundles of vessel No. 1 and condensing section was cut and dismantled. Fig. 3, 4. New tube bundle and condensing section were erected. Fabrication of condensing section, insertion/fitting of the tubes was done at the supplier's

factory.

The material of construction of new bundles were as follows:

<u>Name of part</u>	<u>Material</u>
1. Shell for condensing section	Carbon steel + SS 316L cladding
2. Tube	CuNi 10Fe1Mn (16 mm OD & 1.0 mm thick)
3. Tube Plate	CuNi10Fe1Mn
4. Tube support plate	SS 316 L
5. Partition Plate	SS 316 L
6. Distillate Tray	Carbon steel + SS 316 L cladding

Baffles were also provided in the new tube bundle to promote cross flow so that non-condensable gases are not accumulated at the bottom of the bundle. No baffles were provided in old bundle. Manholes were also provided in condensing chamber.

The plant venting system was designed to have series venting (cascaded) from stage No. 1 to Stage No. 20. The practice of cascading non-condensable gases from stage to stage with venting at just a few stages in the mid and low temperature sections of the plant means that gas concentration will increase until the vented stage is reached. For this reason the stage No. 1, 2, 3 venting was modified. Separate direct vent line to deaerator was provided to remove non-condensable gases quickly and completely from the process as possible from stages 1, 2, 3. For cascaded vent line from stage No. 4 to stage No. 5, stage No. 5 to stage No. 6, vent line angle was changed. Earlier the vent line was connected at the center of the tube bundle from side of vessel. This was done to avoid pocketing of noncondensable gases. Water hammering was observed in brine inlet line to vessel No. 1 after modification. Direct atmospheric vents with remote control valve for stages No. 1 & 2 was provided on both the bundles side to suppress the hammering/flashing in the brine outlet of brine heater/header in the case of trip of brine recycle pump at elevated temperature. Earlier brine heater vent was connected to stage # 1. In order to avoid any corrosion due to presence of Ammonia in steam supplied to brine heater, after rehabilitation, brine heater is directly vented to atmosphere. Refer fig. 2 & 5.

## **PERFORMANCE TEST PRIOR TO REHABILITATION**

Performance test at steady condition of 860 m<sup>3</sup>/hr production at TBT 99.2°C was carried out between 30th December '89 and 1st January '90. Distillate product of Vessel No. 1 was monitored by using ultrasonic meter [Ref. 6].

The result of performance test showed the product flow in close agreement with calculated production based on flash down.

The maximum output test was carried out on 2.1.1990 prior to shutdown EVAP #1 on 3.1.1990 for rehabilitation Vessel No. 1. The plant output was gradually increased to the data for maximum attainable output with the existing vacuum unit and venting all non-condensables to vacuum system (atmospheric vent not opened). The distillate conductivity shot up more than full scale (+ 1000  $\mu\text{s}/\text{cm}$ ) when distillate production reached 990 $\text{m}^3/\text{hr}$  at 104°C and dumped to waste. The analysis of the distillate samples for the stages showed pick-up of the brine from Vessel No. 1 (due to tube leak). The production was further increased upto 1120-1130 $\text{m}^3/\text{hr}$ . by increasing TBT to 106°C. Performance test results are tabulated in Table No. 2.

Based on the results of test it was recommended that the unit can be operated only at max. TBT of 104°C and recycle flow of 10,000  $\text{m}^3/\text{hr}$ . The operation of TBT in excess of 104°C could lead to corrosion of vessel No. 2 tubes and its support plate. Also venting of all the non-condensable at the vacuum unit at temperature above 104°C will cause excessive carry over and build up of salt on the nozzle periphery and diffuser which will restrict the vapour flow causing ejector to choke and secondly it will create problems of stress cracking of nozzles.

### **OPTIMISATION TEST AFTER REHABILITATION**

The test was conducted in three parts. First part on relation between TBT and brine recycle flow (BRF), second part on relation between TBT, BRF and seawater flow, third on relation and effect of venting and vent valve adjustment to temperature profile. [Ref. 7].

The maximum productions in the relation of BRF and TBT were obtained at the conditions of 113°C/9000  $\text{m}^3/\text{hr}$  and 1030  $\text{m}^3/\text{hr}$  production and 109°C/9500  $\text{m}^3/\text{hr}$  production of 1000  $\text{m}^3/\text{hr}$  using atmospheric venting pipes.

At 113°C operation requires sever control to prevent scale trouble and at 109°C operation required the atmospheric vent valves of stage No. 1 to be opened. Also operation of 107°C/9500  $\text{m}^3/\text{hr}$  required operation of two units of vacuum system. On this condition the safe operation was found at 104°C/9500  $\text{m}^3/\text{hr}$ . The limitation of brine recycle pump capacity restricted the production capacity in a certain level at high TBT. The reason was that the maximum flow rate of brine recycle pump decreases corresponding to higher TBT, where the delivery pressure had to be increased to match with increase of 1st stage pressure and pressure drop of flow line including each stage tubes.

## CONCLUSION AND RECOMMENDATION

The effect of varying sea water flow rate to the production was small. It was recommended that sea water flow rate will be within the flow range of 8500 to 9500 m<sup>3</sup>/hr. Variation of sea water temperature was observed and it is expected due to the tidal condition and to stabilise the operation variation is to control the sea water flow rate as the plant does not have tempering system.

At the end of the test operation, eight modes of vent valves were tested when the plant was operated at 104°C TBT and 9500 m<sup>3</sup>/hr BRF. It was found that the best position of vent valve is mode No. 6 as shown on attached Table No. 3 in considering the balance of venting from each stage by judging the temperature profile. Refer fig. 6.

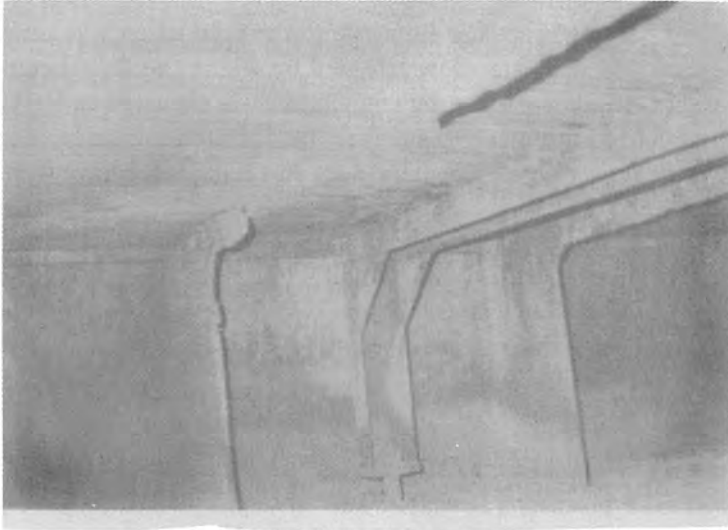
For steady operation condition, the operation conditions of 104°C TBT and 9500 M<sup>3</sup>/hr. BRF producing around 980 m<sup>3</sup>/hr. of distillate was found optimum.

A special vacuum test is being carried out at each start up to ensure all oxygen leaks are arrested.

No significant corrosion is observed in vessel No. 1 even after 5 years of operation. [Picture 2].

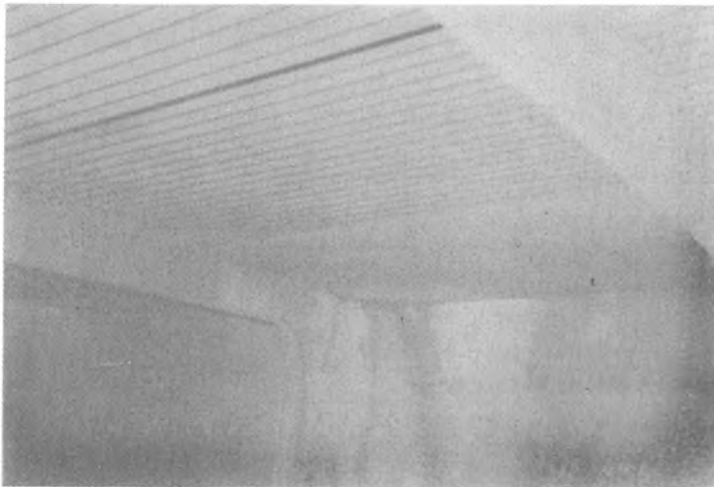
## REFERENCES

- [1] INCON ANLAGENTECKNIC GmbH, Germany. "Inspection report of Desalination Plant No. 1, Ghubrah, Oman" - 1984.
- [2] NICKEL DEVELOPMENT INSTITUTE, Birmingham, England. Report on Corroded tubing from No. 1 distiller, Ghubrah, Oman - 1987.
- [3] NICKEL DEVELOPMENT INSTITUTE (Cit) [2].
- [4] L.L SHEIR, Corrosion, Volume No. 1, Metal/Environmental reactions Newnes - Butterworth (Publishers).
- [5] HITACHI ZOSEN CORPORATION, Ghubrah Power & Desalination Plant, Plant No. 1 Replacement of Tube Bundles of Stage 1 to 6. "REPORT OF EDDY CURRENT TEST AND ULTRASONIC THICKNESS TEST HZ letter L-1711.SO/CS/280 dt. 27/06/1990.
- [6] HITACHI ZOSEN CORPORATION. Performance test prior to shut down of Desalination Plant No. 1, January 1990. HZ letter L-RT-SO/CS-028 dt. 04/01/1990.
- [7] HITACHI ZOSEN CORPORATION, Desalination Plant No. 1, Replacement of the Tube Bundles for Stage 1 to 6", Report of Optimisation Test : July 1990. HZ letter L- 1711 -SO/CS-296 dt. 16/07/1990.



PICTURE NO. 1

CORRODED TUBE SUPPORT PLATE/EXTRA SADDLE SUPPORT PROVIDED  
(BEFORE REHABILITATION)



PICTURE NO. 2

NO CORROSION OBSERVED IN NEW BUNDLE AND CONDENSING SECTION  
AFTER 5 YEARS OF OPERATION  
(AFTER REHABILITATION)

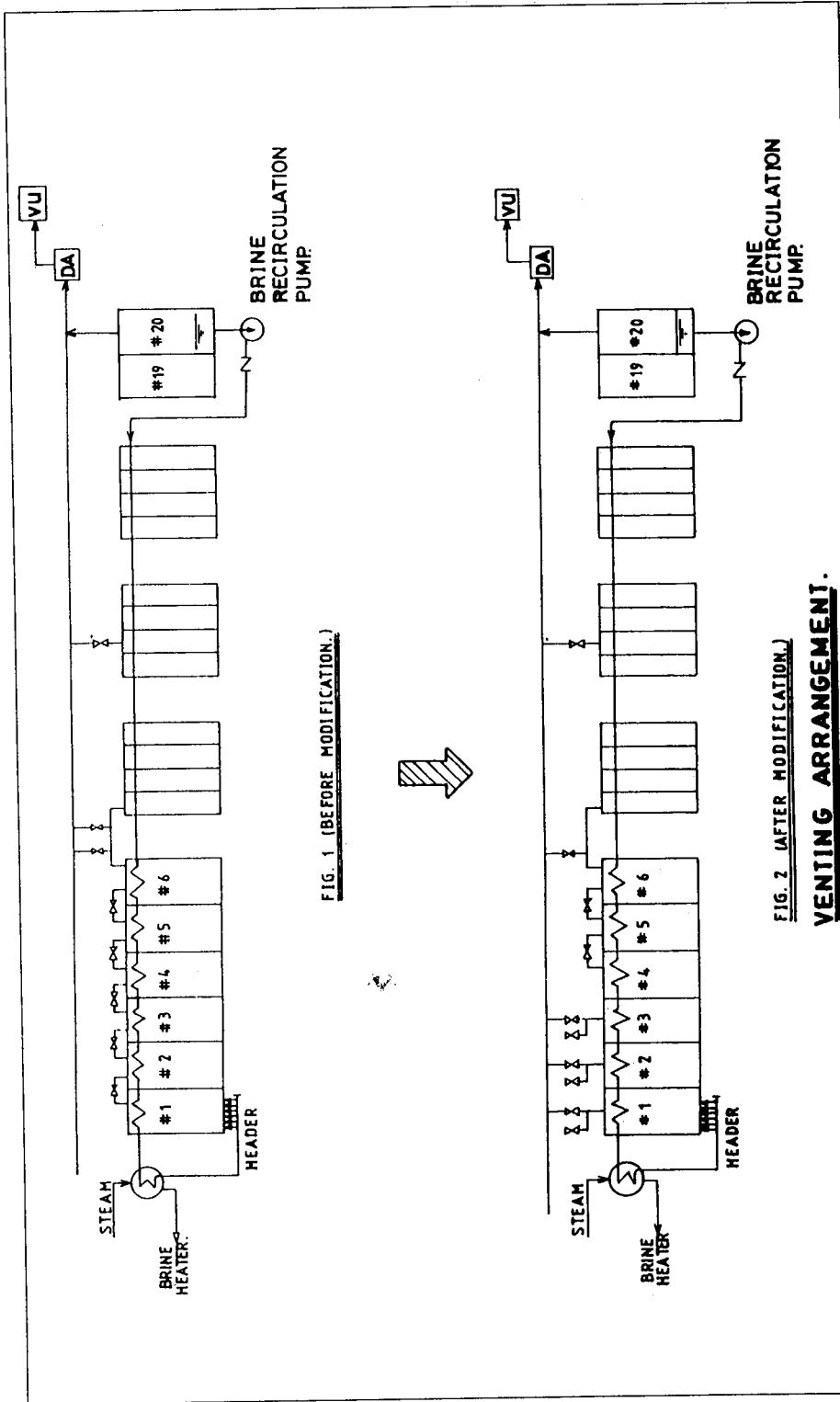
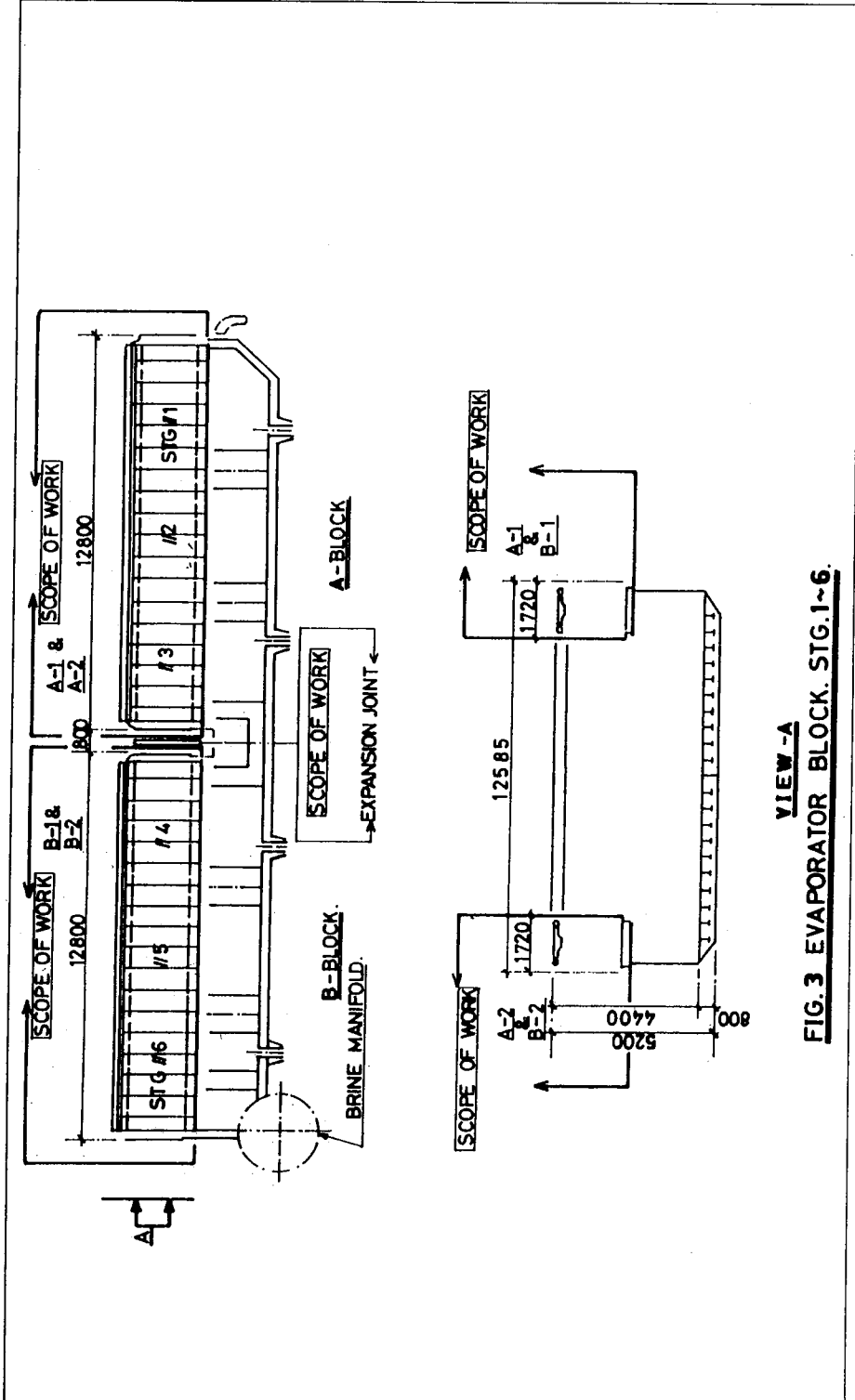


FIG. 1 (BEFORE MODIFICATION.)

FIG. 2 (AFTER MODIFICATION.)

**VENTING ARRANGEMENT.**





**VIEW -A**  
**FIG. 3 EVAPORATOR BLOCK, STG.1~6.**

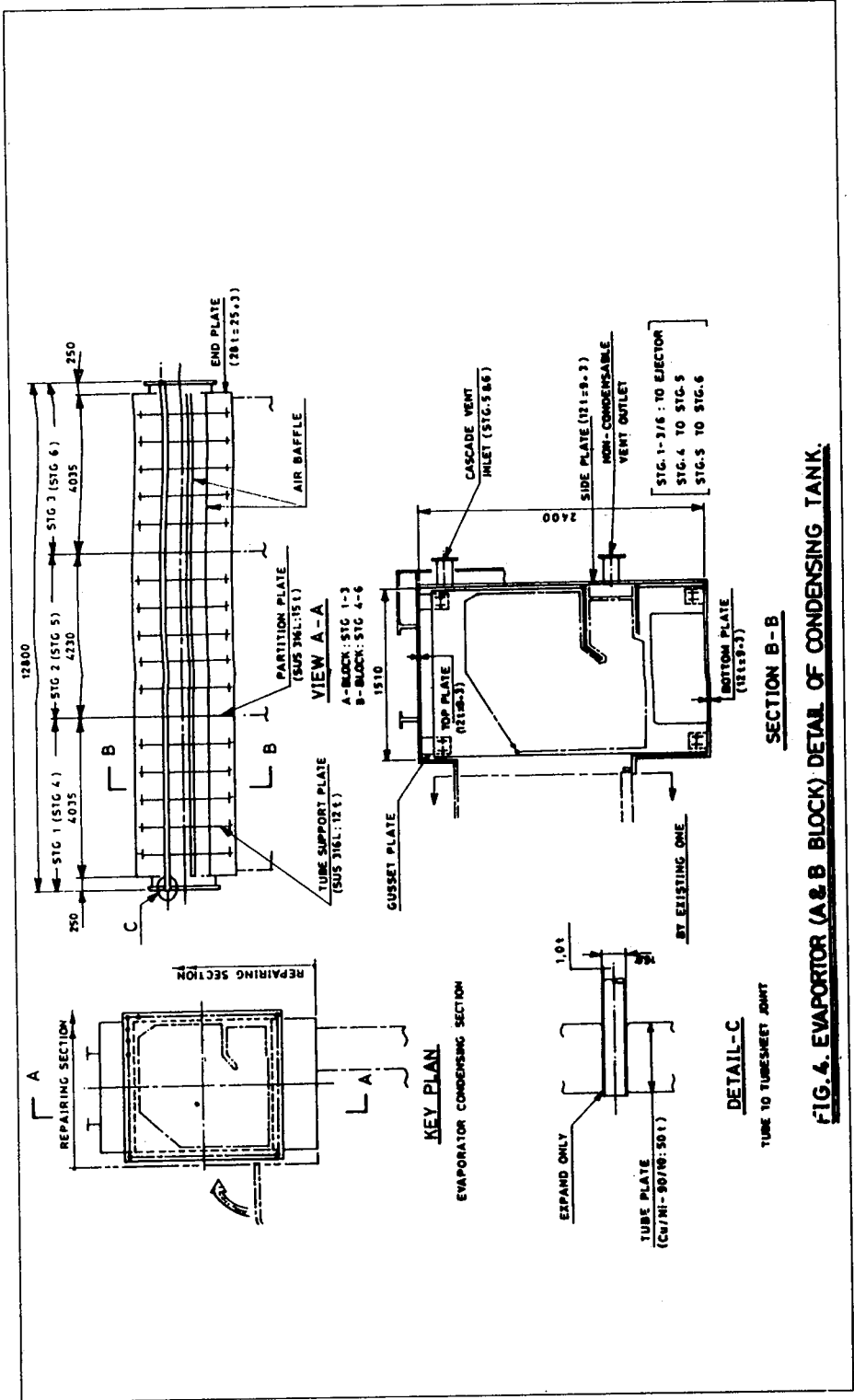


**FIG. 4. EVAPORATOR (A & B BLOCK) DETAIL OF CONDENSING TANK.**

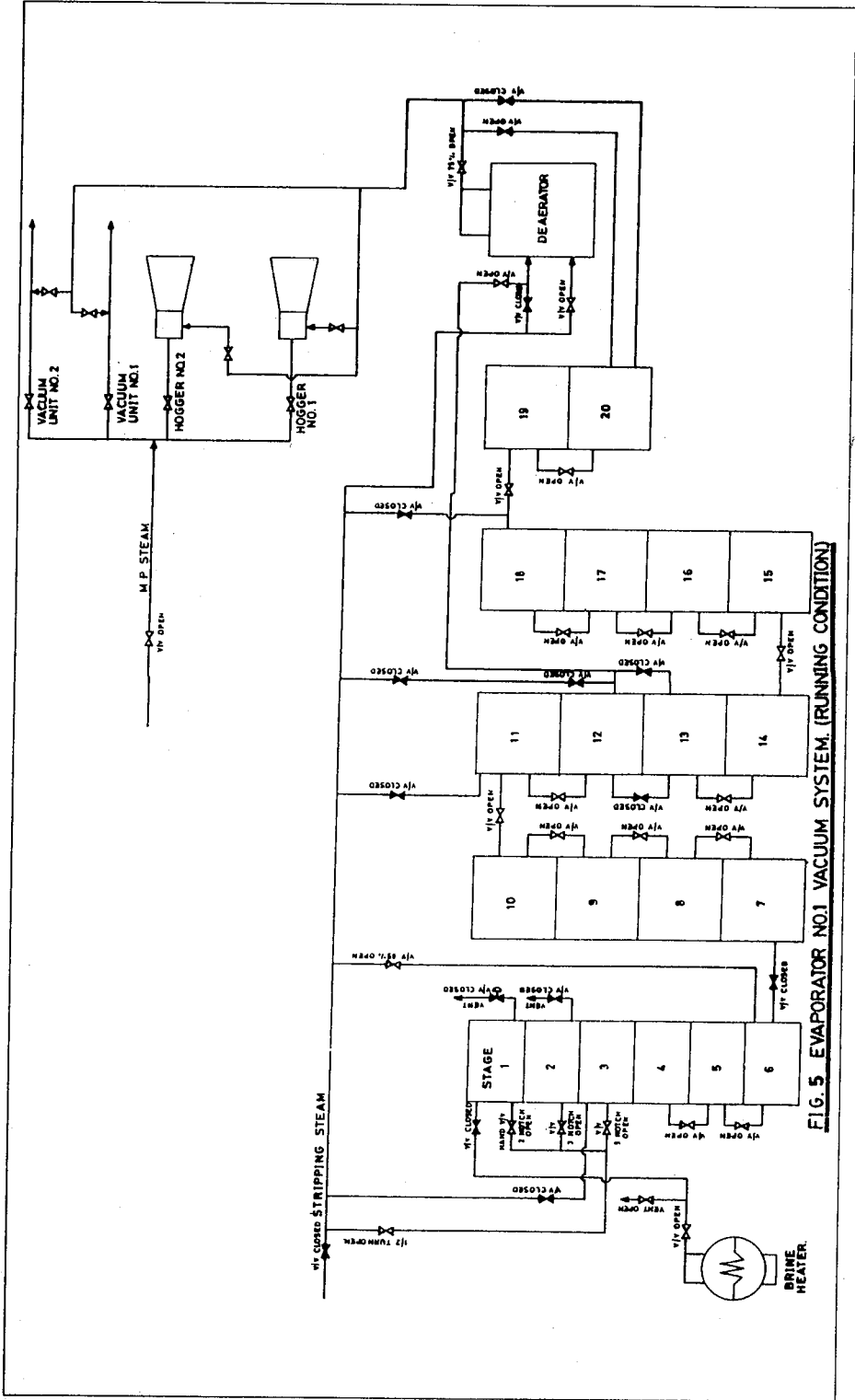
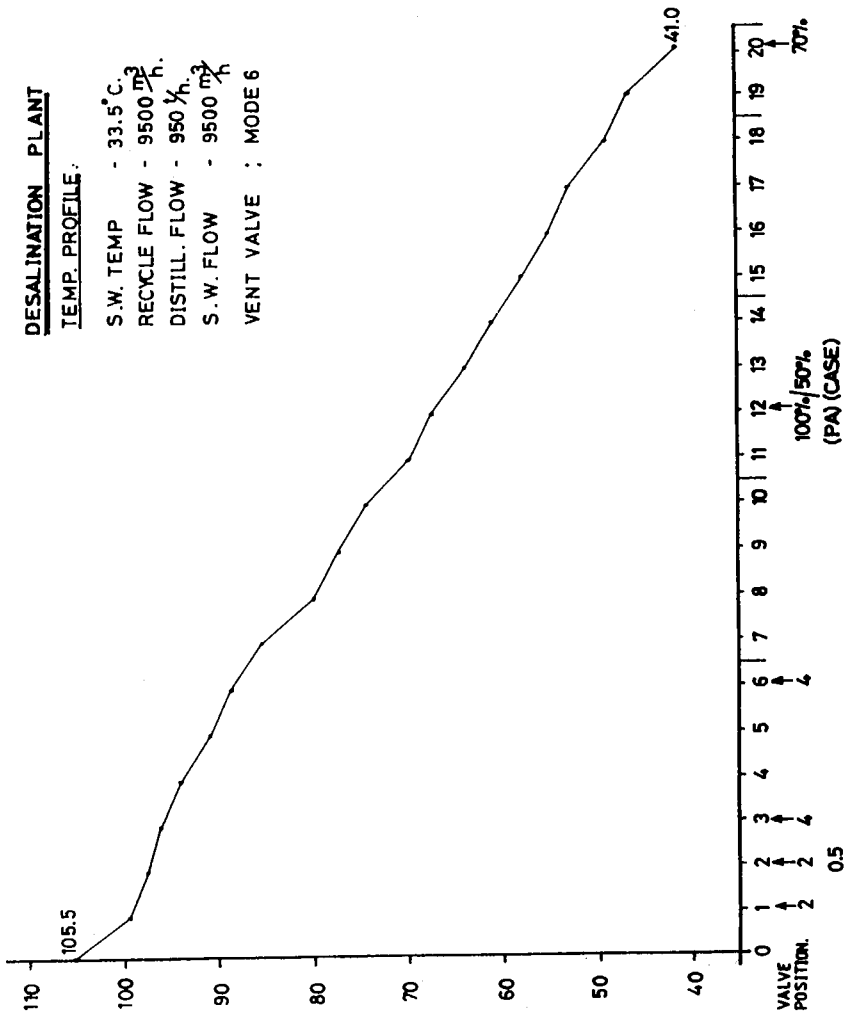


FIG. 5. EVAPORATOR NO.1 VACUUM SYSTEM. (RUNNING CONDITION)

**DESALINATION PLANT**

**TEMP. PROFILE.**

S.W. TEMP - 33.5°C.  
RECYCLE FLOW - 9500  $\frac{m^3}{h}$ .  
DISTILL. FLOW - 950  $\frac{m^3}{h}$ .  
S.W. FLOW - 9500  $\frac{m^3}{h}$ .  
VENT VALVE : MODE 6



**FIG. 6 TEMPERATURE PROFILE.**

**TABLE NO. 1**

Description	Unit	*I Contractual Value		Actual Value	**II	***III	Remarks
		757 #	797 #				
1. Distillate production.	m <sup>3</sup> /hr		797 #		1130	970	# 4.0 MIGPD, ## 4.21 MIGPD  + 194 m <sup>3</sup> /hr condensate ++ 144.4 m <sup>3</sup> /hr condensate
2. Cooling water to heat reject.	m <sup>3</sup> /hr	11800	9504		8900	11796	
3. Brine flow to Brine Heater.	m <sup>3</sup> /hr	10000	8521		9900	9300	
4. Brine Inlet Temp. to Brine Heater.	°C	85	82		97.6	96.4	
5. Brine Outlet Temp. from Brine Heater.	°C	91	90		108.3	104	
6. Steam flow to Brine Heater.	t/hr	113.3	119.3		186.5 +	139 ++	
7. Steam Pressure to Brine Heater.	Bar (Abs)	1.0	0.795		1.46	1.2	
8. Steam Temperature to Brine Heater.	°C	100	93		113	106.5	
9. Economy Ratio.	Kg distillate Kg condensate	6.8	6.7		6.05	6.98	
10. Heat Consumption.	K. Cal	79.4	82.0		—	—	
11. Purity of Distillate.	Kg distillate PPM	100	6.0		138	92.7	
12. Distillate temperature.	°C	41	33		39.1	40.8	
13. pH value of distillate after caustic dosing.	—	8 - 9	8.8		8.5	8.6	
14. pH value of Brine Recycle.	—	8.4 - 8.6	8.5		8.6	8.6	
15. Brine Recycle concentration.	PPM	—	56949		60649	59040	
16. Seawater temperature.	°C	—	23		23.9	31.1	
17. Seawater T.D.S.	PPM	—	39575		*	*	

\* Seawater T.D.S. constant between 39000 - 40000

\* I : Performance Test Data with Polyphosphate on 17/18 March, 1979.  
 \*\* II : Performance Test Data with Belgard EV on 02nd March 1981.  
 \*\*\* III : General Performance of Plant with Belgard EV, 04th June 1983 Production Approx. 5 MIGPD Non-guaranteed.



**A Kinetic Model for Scale Formation in MSF  
Desalination Plants. Effect on Antiscalants**

*A. Mubarak*

# A KINETIC MODEL FOR SCALE FORMATION IN MSF DESALINATION PLANTS. EFFECT OF ANTISCALANTS.

**A. Mubarak**

College of Technology, University of Qatar  
Doha, Qatar

## ABSTRACT

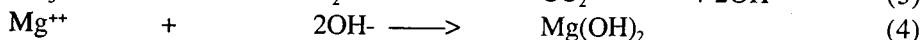
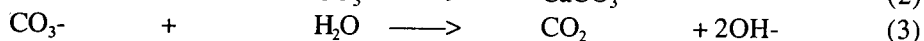
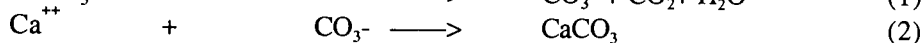
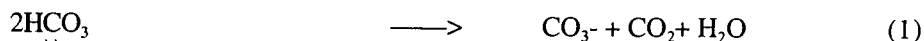
The kinetics of scale formation in MSF plants, at atop temperature of 90°C has been studied and a kinetic model for  $\text{HCO}_3^-$  decomposition /  $\text{CaCO}_3$  formation has been developed. Fitting model calculations to experimental data, obtained by refluxing seawater while either purging with nitrogen or keeping under partial vacuum, shows the bicarbonates to decompose to carbon dioxide and hydroxyl ions; the hydroxyl ions concomitantly react with the residual bicarbonate species forming carbonates which in turn react with calcium ions producing calcium carbonate. The three step mechanism follows first order kinetics with the initial decomposition step for the bicarbonates being slow. The reaction involving precipitation of calcium carbonate, while relatively faster, is also somewhat slow having a total 2nd order rate constant of  $0.01 \text{ L. Mol}^{-1} \text{ Sec}^{-1}$ . Steady state treatment of the mechanism shows the rate of scaling to depend on the concentrations of the bicarbonates, calcium ions as well as partial pressure of  $\text{CO}_2$ . Meanwhile, the presence of antiscalants was found to slow down virtually all of the three reaction rates and nearly inhibit the precipitation of calcium carbonate. Runs made with 10 ppm Belgard EV2000 produced a 2nd order rate constant, for the calcium carbonate precipitation reaction, of  $5 \times 10^{-6} \text{ mol}^{-1} \text{ Sec}^{-1}$ ; thereby making it about two thousand folds slower. Further, the equilibrium constants generated by the kinetic model approximate those calculated from thermodynamics. Magnesium hydroxide formation, on the other hand, is neither expected nor found in the precipitate accumulated at 90°C. In this paper, a) The reaction mechanism leading to  $\text{CaCO}_3$  crystallization is presented, b) The rates of the individual steps, at this operational temperature, are reported; and c) The inhibiting effects of antiscalants on all of the rates involved are quantified and discussed.

**Keywords:** Desalination. Antiscalants. Scaling. Kinetics. Seawater.  
 $\text{CaCO}_3$ .  $\text{Mg}(\text{OH})_2$

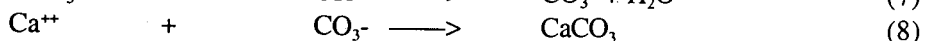
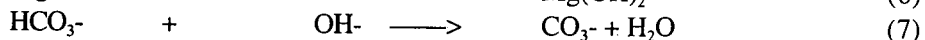
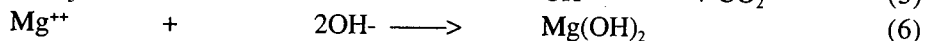
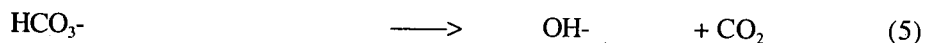


## LITERATURE REVIEW

While it is widely recognised that the breakdown of the bicarbonate species is responsible for the ultimate formation of scale in distillation plants, it is the scaling mechanism that has been a subject of a long and persisting ambiguity. Langelier [1] and more recently Shamse El Den et al [2] spoke of carbonate formation directly from bicarbonates which, in their view, will hydrolyse to produce hydroxyl groups causing the precipitation of magnesium hydroxide;



On the other hand, Dooly and Glater [3] followed by Harris and co-workers [4] contend that precipitation of magnesium hydroxide occurs simultaneously with the initial release of hydroxyl groups. Excess hydroxyl groups are then neutralised by the residual bicarbonates to form carbonates;



It is clear that the ambiguity revolves around the underlying kinetics and since the consequences to adopting either concept would, no doubt, have a great impact on the operational as well as maintenance philosophy of desalination plants, the need for a kinetic study that will hopefully contribute to the understanding of such complex system is therefore readily apparent. Likewise, since the inhibiting action of antiscalant materials (namely, Belgard of Cibe Geigy and POC of Degussa) described by vendors under the term "Threshold Effect" has never really been quantified, so to speak, a study addressing the intrinsic role of these materials in desalination processes seemed very much in order.

## EXPERIMENTAL

Sea water aliquots of four litre volume were measured in five litre flasks and refluxed at a controlled temperature of 90°C using a compenstat apparatus, of Gallenkamp, and employing an oil bath. Some runs were made while purging nitrogen through the solutions at a flow rate of 0.5 l/min. Others were refluxed under partial vacuum (ca 10 psia) generated by vacuum pumps model 123v supplied by Lacy-Hulbert of the UK. After the temperature of the solutions had reached

90°C, samples were drawn out by siphoning; they were then cooled first in an ice water bath to room temperature then analysed for  $\text{HCO}_3^-$  and  $\text{CO}_3^{2-}$  using 0.02N HCl. The Ph measurements were made using Philips Ph meter PW 9418 of Pye Unicam supplied with a combined glass electrode and a temperature compensation probe. Ph readings of 8.2 and 3.8 were used for calculating the  $\text{CO}_3^{2-}$  and  $\text{HCO}_3^-$  concentrations. Calcium as well as magnesium were also determined, before and after refluxing, using atomic absorption techniques. Cooling water was controlled at 10°C using an alcohol water mixture and a frigomix 1495 coupled to a Thermomix 1449 of B. Braun, Germany. Refluxing was carried out for 5.5 hrs. Belgard EV2000 was used in parallel runs (at 10 ppm) to study the effect of antiscalants on the rates involved.

In order to develop a feel for the underlying kinetics, several preliminary runs were first made by refluxing seawater at varying temperatures for various time intervals and analysing the solutions for bicarbonates, carbonates, Ca and Mg. The precipitates were also analysed for Ca and Mg. Initial kinetic measurements were also made on the systems  $\text{NaHCO}_3$  - NaOH and  $\text{MgCl}_2$  - NaOH for comparing the rates of formation of  $\text{Mg}(\text{OH})_2$  vs.  $\text{CO}_3^{2-}$  species.

Further, solutions of sodium carbonates were boiled for several time intervals to check the degree of  $\text{CO}_3$  hydrolysis. Several kinetic runs were then made at 90°C in the manner described earlier using either nitrogen purge or partial vacuum (aimed at removing the evolved  $\text{CO}_2$ ). The results are recorded in tables 1 and 2, respectively. Runs made without employment of either nitrogen or vacuum produced no significant change in the parameters tested.

## KINETIC MODEL

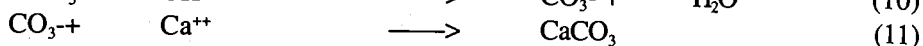
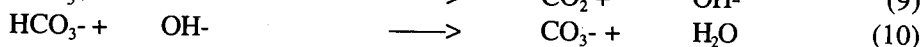
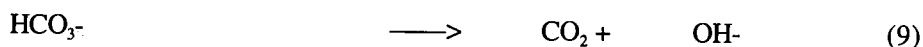
Examination of the data of tables 1 and 2 shows that the  $\text{CO}_3^{2-}$  species and simultaneously the Ph to increase with time indicating no severe consumption (through the formation of i.e.,  $\text{Mg}(\text{OH})_2$ ) of the hydroxyl ions produced. Further, analysis of the refluxed solutions as well as the precipitate indicated no appreciable change in the initial magnesium concentration in solution and only about 2 ppm was detected in the precipitate.

Although that precipitation of magnesium hydroxide (rx.4) is thermodynamically more favorable (having a Gibbs free energy change of  $-64.22 \text{ KJ.mol}^{-1}$ ) compared with rx.7 of  $-20.9 \text{ KJ.mol}^{-1}$  even at elevated conditions, initial kinetic measurements showed the later to be considerably faster. This is somewhat expected however as the later reaction (rx.7) involves a proton transfer the rate of which is imminently high. The charge density and consequently the hydration properties for Mg ions, on the other hand, may very well be the reason influencing the slow rate of

Mg(OH)<sub>2</sub> crystallization observed here.

The hydrolysis of CO<sub>3</sub><sup>-</sup> ions (rx. 3) was also experimentally checked. Measurements of Ph, CO<sub>3</sub><sup>-</sup> and HCO<sub>3</sub><sup>-</sup> (made on Na<sub>2</sub>CO<sub>3</sub> solutions refluxed for one hr at boiling temperature) showed negligible release of hydroxyl ions and/or loss of CO<sub>3</sub><sup>-</sup> species. This is very much in line with theoretical expectations however. This reaction, even at the test temperature of 90°C, has a fairly small equilibrium constant calculated to be  $1.1 \times 10^{-6}$ .

Having established the above criteria, the following mechanism was then constructed,



The days when the kineticist had to struggle with the data for obtainment of straight lines conforming to some rate order have been long gone. Today, with the powerful and fast processing capabilities of computers and PCs, analysing kinetic data (however complex the system might be) has become less formidable, less time consuming and certainly much more accurate. After devising a mechanism and setting up the corresponding kinetic equations (assuming a certain order) and writing up a program for handling of the calculations and graphics, the rest is a matter of zeroing in (by trial and error) on the right rate constants both forward and reverse. This is accomplished by fitting the calculated concentrations to those obtained from experimental measurements. This way the rate constants produced are virtually determined by the experimental data; more like the way it ought to be.

Following are the associated rate equations for this mechanism,

$$R_1 = K_f1 [\text{HCO}_3^-] - K_r1 [\text{OH}^-] [\text{PPCO}_2] \quad \text{A}$$

$$R_2 = K_f2 [\text{HCO}_3^-][\text{OH}^-] - K_r2 [\text{CO}_3^{2-}][\text{H}_2\text{O}] \quad \text{B}$$

$$R_3 = K_f3 [\text{CO}_3^{2-}][\text{Ca}^{++}] - K_r3 [\text{CaCO}_3] \quad \text{C}$$

Where R<sub>1</sub> denotes rate of reaction 1; K<sub>f1</sub> the forward rate constant for reaction 1; K<sub>r1</sub> the reverse rate constant for reaction 1, etc. From material balance considerations and the law of mass action, the reaction components (reactants and products) will increase / decrease by the following quantities after time T,

$$Q_1 = R_1 \times T \quad \text{D}$$

$$Q_2 = R_2 \times T \quad \text{E}$$

$$Q_3 = R_3 \times T \quad \text{F}$$

and the kinetic concentrations would then be,

$$\begin{array}{rclclcl}
 [\text{HCO}_3^-] & = & [\text{HCO}_3^-]_o & - & Q_1 & - & Q_2 & \text{G} \\
 [\text{PPCO}_2] & = & [\text{PPCO}_2]_o & + & Q_1 & & & \text{H} \\
 [\text{OH}^-] & = & [\text{OH}^-]_o & + & Q_1 & - & Q_2 & \text{I} \\
 [\text{CO}_3^-] & = & [\text{CO}_3^-]_o & + & Q_2 & - & Q_3 & \text{J}
 \end{array}$$

Where the symbol o denotes initial concentration. The computer then calculates and plots these concentrations for a given set of chosen rate constants both forward and reverse. The initial concentrations (based on actual measurements) used in these calculations are as follows,

$$\begin{array}{rclcl}
 [\text{HCO}_3^-] & = & 0.002643 & \text{M} & \\
 [\text{PPCO}_2] & = & 0.0006 & \text{atm} & \\
 [\text{OH}^-] & = & 0.000001585 & \text{M} & \text{calculated from Ph 8.2} \\
 [\text{CO}_3^-] & = & 0.000001 & \text{M} & \text{approximately 1ppm} \\
 [\text{Ca}^{++}] & = & 0.013 & \text{M} &
 \end{array}$$

The fits obtained for the runs with and without Belgard EV2000 using either nitrogen purge or vacuum are shown in figs 1 - 4 and the corresponding rate constants are recorded in Table 3.

### STEADY STATE TREATMENT

The differential equations describing the rate laws for the various species involved in reactions 9, 10 and 11 are as follows,

$$-d[\text{HCO}_3^-]/dt = Kf_1 [\text{HCO}_3^-] - Kr_1 [\text{PPCO}_2][\text{OH}^-] + Kf_2 [\text{HCO}_3^-][\text{OH}^-] - Kr_2 [\text{CO}_3^-][\text{H}_2\text{O}]$$

$$d[\text{OH}^-]/dt = Kf_1 [\text{HCO}_3^-] - Kr_1 [\text{PPCO}_2][\text{OH}^-]$$

$$-d[\text{CO}_3^-]/dt = Kf_3 [\text{CO}_3^-][\text{Ca}^{++}] - Kr_3 [\text{CaCO}_3] + Kr_2 [\text{CO}_3^-][\text{H}_2\text{O}] - Kf_2 [\text{HCO}_3^-][\text{OH}^-]$$

$$d[\text{CaCO}_3]/dt = Kf_3 [\text{CO}_3^-][\text{Ca}^{++}] - Kr_3 [\text{CaCO}_3]$$

Considering the species, OH<sup>-</sup> and CO<sub>3</sub><sup>-</sup> as intermediates and equating the rate of change of their concentrations to zero and assuming further the activities of both [H<sub>2</sub>O] and [CaCO<sub>3</sub>] to be unity and solving for [OH<sup>-</sup>] and [CO<sub>3</sub><sup>-</sup>] and substituting for their values in the 1st differential equation gives the rate law for decomposition

of  $\text{HCO}_3^-$  species,

$$-d[\text{HCO}_3^-]/dt = \frac{[Kf_1 * Kf_2 * Kf_3 [\text{HCO}_3^-]^2 [\text{Ca}^{++}] - Kr_1 * Kr_2 * Kr_3 [\text{PPCO}_2]]}{Kr_1 * Kf_3 [\text{PPCO}_2] [\text{Ca}^{++}] + Kr_1 * Kr_2 [\text{PPCO}_2]}$$

Similar treatment for  $\text{CaCO}_3$  formation would yield the same rate law. One needs to be careful however when applying the steady state approximation. Boudart [5] recommends its use after the relaxation time  $T_r$  defined as the time required for the species to decay to a fraction  $1/e$  of its original value. King [6] defines it as 1.4 times the half life of the species in question. The calculated results for residual  $\text{HCO}_3^-$  using the above equation match closely those obtained from the runs having no Belgard material.

## DISCUSSION

The initial reaction describing  $\text{HCO}_3^-$  decomposition (rx.9) is thermodynamically unfavorable at ambient conditions having a Gibbs free energy change of +33  $\text{KJ.mol}^{-1}$ . The kinetics is also expected to be slow due to involvement of  $\text{CO}_2$ . The reaction's fairly large positive enthalpy (+68.48  $\text{KJ.mol}^{-1}$ ) however helps it proceed at moderately elevated temperatures (ca. 65°C). The calculated equilibrium constant at the test temperature of 90°C is  $9.8 \times 10^{-5}$ ; almost two orders of magnitude higher than what it is at ambient conditions. At 25°C, for instance, the calculated equilibrium constant is  $6.9 \times 10^{-7}$ .

Reaction 10, on the other hand, while thermodynamically quite favorable (with a Gibbs free energy change of -20.9  $\text{KJ.Mol}^{-1}$ ) is, being exothermic, much less favored by heat. But since it merely involves a proton transfer, it is expected to be kinetically fast. Reaction 11, meanwhile, while thermodynamically favorable even at ambient conditions ( $K_{eq} = 2.06 \times 10^8$ ) should become more favorable yet (being endothermic with an enthalpy of +13.05  $\text{KJ.Mol}^{-1}$ ) at the test temperature ( $K_{eq} = 5.17 \times 10^8$ ). The fact that it involves a cation / anion interaction, this reaction is also expected to be relatively fast.

Fig. 1 depicts the best fit produced for the run involving nitrogen purge. Of prime importance is the close coherence (obtained by zeroing in on the right set of rate constants) between both experimental (the circled points) and calculated (the line points) bicarbonate concentrations. Equally important is that the calculated concentrations of  $\text{OH}^-$  and  $\text{CO}_3^-$  were checked and found in line with the experimental ones.

It should be noted here that for getting genuine fits, it is imperative that all parameters' concentrations (calculated and tested) need to match. In my experience,

one can accidentally (with some combination of rate constants) get fairly decent looking fits (i.e., matching of the bicarbonate concentrations in this case) while the other parameters ( $\text{CO}_3^-$  and  $\text{OH}^-$  for instance) are completely off.

The equilibrium constants produced by the kinetic model approximate those calculated (at  $90^\circ\text{C}$ ) from thermodynamics. This is recorded in Table 4. Of course the noted differences (an order of magnitude or so) are very much expected and can be compensated for, as is well known, by consideration of the associated activity coefficients.

Figs 3 and 4 show the runs employing vacuum with and without Belgard, respectively. The corresponding rate constants are recorded in Table 3. While the equilibrium constants were not altered in going from nitrogen purge to partial vacuum (Table 4) since the runs were made at the same temperature, the rates were somewhat higher for the runs with nitrogen (Table 3). This is to be expected however due to the stripping as well as stirring action of the gas. This is also in line with the data of Tables 1 and 2.

Of particular interest is the lowering effects observed for the antiscalant material on all of the rates involved particularly those of reactions 9 and 11 (Table 3). The rate constants  $Kf_1$  and  $Kf_3$  were lowered by 25% and nearly 100%, respectively. This is very much in line with the higher  $\text{HCO}_3^-$ ,  $\text{OH}^-$ ,  $\text{CO}_3^-$  and  $\text{Ca}^{++}$  concentrations found in the refluxed solutions having the Belgard material.

Of more interest is that in figs 1 and 3 (with no Belgard), the  $\text{CO}_3^-$  ions concentration increases up to the point of supersaturation (presumably that is when  $\text{CaCO}_3$  starts precipitating) and then levels off. Whereas in the case of figs 2 and 4, where Belgard was used, the  $\text{CO}_3^-$  concentration keeps rising with time presumably for as long as there is still undecomposed bicarbonate species.

A further confirmation to the retarding action of Belgard on the underlying kinetics involved lies in the fact that the tested carbonate species' concentrations are almost those theoretically expected. From reactions 9 and 10, for every two moles of bicarbonates decomposed, one mole of carbonates is produced. Performing calculations on the data of part B, Table 1, proves just that.

The decomposed bicarbonates at the end of 330 minutes comes to,

$$161.21 - 48.8 / 61 = 1.8 \text{ millimoles } \dot{\text{HCO}}_3^-$$

and the formed carbonates also at 330 minutes comes to

$54.86 / 60 = 0.9$  millimoles  $\text{CO}_3^-$

Further, the tested carbonates as well as calcium concentrations in the refluxed solutions having the Belgard material are very much in line with the inhibition action expected of antiscalant materials. Of course there will be a small amount of calcium ions lost to the antiscalant material or vice versa, due to the chelating action of Maleic acid. Formation of calcium maleate is also expected. This was substantiated by measurements of the free calcium ions, using calcium electrode, before and after addition of the antiscalant. Other metal ions, notably Fe, are presumably chelated by this material.

An important consequence to this mechanism is that as long as there are undecomposed bicarbonate species present in the recirculating brine, which I expect will always be at this operational temperature, intrinsic formation of magnesium hydroxide is not expected anywhere in the system. This is very much substantiated by the undetectable change in the Mg concentration found in the solutions before and after refluxing. Magnesium was also nearly completely absent in the precipitate. A further consequence is that the rate of scaling of the HIS units, compared with those of the downstream flashing/condensing stages, is governed by the higher partial pressure of  $\text{CO}_2$  as well as the higher temperature. A good venting system therefore can be of mixed blessing under the circumstances. On one hand, while a higher partial pressure of  $\text{CO}_2$  would, in principle, retard scaling, it would, on the other hand, promote corrosion. From experience associated with plant inspections however, the effects of operating the plants at a higher temperature (than design) seem to induce more scaling.

## REFERENCES

1. Langelier, M. A., Journal American Water Works Assoc., 28, PP 500-,1936.
2. Shams El-Din, A. M. and Mahmoud, R. A., Desalination, 71, PP 313 - 324, 1989.
3. Dooly, R., and Glater, J., Desalination, 11, PP 1-, 1972.
4. Harris, A., Finnan, M. A and Elliot, M. N., Desalination, 14, PP 325-, 1974.
5. Boudart, M., "Kinetics of Chemical Processes", Prentice Hall Inc., 1968.
6. King, E. L., "Basic Chemical Kinetics", The American Chemical Society, 1987.

Table 1. Data pertaining to the runs made at 90°C with (part A) and without Belgard (part B) using N<sub>2</sub> Purge. CO<sub>3</sub><sup>-</sup> and HCO<sub>3</sub><sup>-</sup> species concentrations are in PPM.

Time.Min	Part A			Part B		
	Ph	CO <sub>3</sub> <sup>-</sup>	HCO <sub>3</sub> <sup>-</sup>	Ph	CO <sub>3</sub> <sup>-</sup>	HCO <sub>3</sub> <sup>-</sup>
0	8.2	—	161.21	8.2	—	161.21
15	8.3	5.14	149.88	8.35	12.85	134.2
30	8.3	5.14	142.91	8.4	15.43	128.97
45	8.3	5.14	132.45	8.4	15.43	130.71
60	8.3	6.85	116.77	8.5	21.43	118.51
80	8.3	6.85	108.06	8.55	24.00	113.28
100	8.35	7.72	94.12	8.6	27.43	104.57
120	8.35	7.72	88.88	8.65	30.85	98.47
150	8.4	10.28	74.94	8.75	34.28	91.50
180	8.45	11.99	67.97	8.8	38.57	82.78
210	8.45	11.99	62.74	8.85	42.85	74.07
240	8.5	12.0	54.03	9.0	46.28	67.97
270	8.5	12.0	54.03	9.0	50.57	58.38
300	8.5	12.0	48.80	9.1	51.43	56.6 <sup>d</sup>
330	8.5	12.85	41.83	9.1	54.86	48.8

Table 2. Data pertaining to the runs made at 90°C with (part C) and without Belgard (part D) using partial vacuum (10 psia pressure). CO<sub>3</sub><sup>-</sup> and HCO<sub>3</sub><sup>-</sup> concentrations are in PPM.

Time.Min	Part C			Part D		
	Ph	CO <sub>3</sub> <sup>-</sup>	HCO <sub>3</sub> <sup>-</sup>	Ph	CO <sub>3</sub> <sup>-</sup>	HCO <sub>3</sub> <sup>-</sup>
0	8.2	—	157	8.2	—	157
15	8.3	7.5	140	8.25	3.8	151
30	8.3	8.1	135	8.3	6.4	143
45	8.35	9.4	129	8.3	7.2	140
60	8.35	9.8	124	8.3	7.6	140
80	8.35	9.6	117	8.4	12.6	131



100	8.35	7.3	113	8.4	14.6	127
120	8.35	9.1	97	8.45	19.6	117
150	8.35	9.0	91	8.45	22.4	111
180	8.4	11.7	79	8.6	30.3	93
210	8.45	12.4	70	8.7	33.4	90
240	8.5	13.8	58	8.7	37	78
270	8.5	16.1	54	8.75	36.8	73
300	8.5	15.3	52	8.8	40.4	71
330	8.55	16.2	48	8.85	43.3	67

Table 3. Corresponding rate constants for the data of Tables 1 and 2. Fits are shown in figs. 1 - 4.

Data	$K_{f_1}$	$K_{r_2}$	$K_{f_2}$	$K_{f_2}$	$K_{f_3}$	$K_{r_3}$
Table 1 Part A Fig. 1	0.00007	0.072	0.11	0.0000165	0.01	$5 \times 10^{-12}$
Table 1 Part B Fig. 2	0.000052	0.055	0.1	0.000015	0.000005	$2.5 \times 10^{-15}$
Table 2 Part C Fig. 3	0.000055	0.056	0.095	0.000014	0.0075	$3.75 \times 10^{-12}$
Table 2 Part D Fig. 4	0.000035	0.037	0.08	0.000011	$1 \times 10^{-6}$	$5 \times 10^{-16}$

Table 4. Comparison of Equilibrium constants produced by the kinetic model and the corresponding Equilibrium constants calculated from Thermodynamics at the test temp. of 90°C. The letters A - D correspond to the runs / data recorded in Tables 1 and 2.

<u>Reaction</u>	<u>Run</u>	<u>Kinetic <math>K_{eq}</math></u>	<u>Thermodynamic <math>K_{eq}</math></u>
9	A	$9.7 \times 10^{-4}$	$9.8 \times 10^{-5}$
	B	$9.4 \times 10^{-4}$	
	C	$9.8 \times 10^{-4}$	
	D	$9.4 \times 10^{-4}$	
10	A	$6.6 \times 10^3$	$2.36 \times 10^2$
	B	$6.6 \times 10^3$	
	C	$6.7 \times 10^3$	
	D	$7.2 \times 10^3$	
11	A	$2 \times 10^9$	$5.2 \times 10^8$
	B	$2 \times 10^9$	
	C	$2 \times 10^9$	
	D	$2 \times 10^9$	

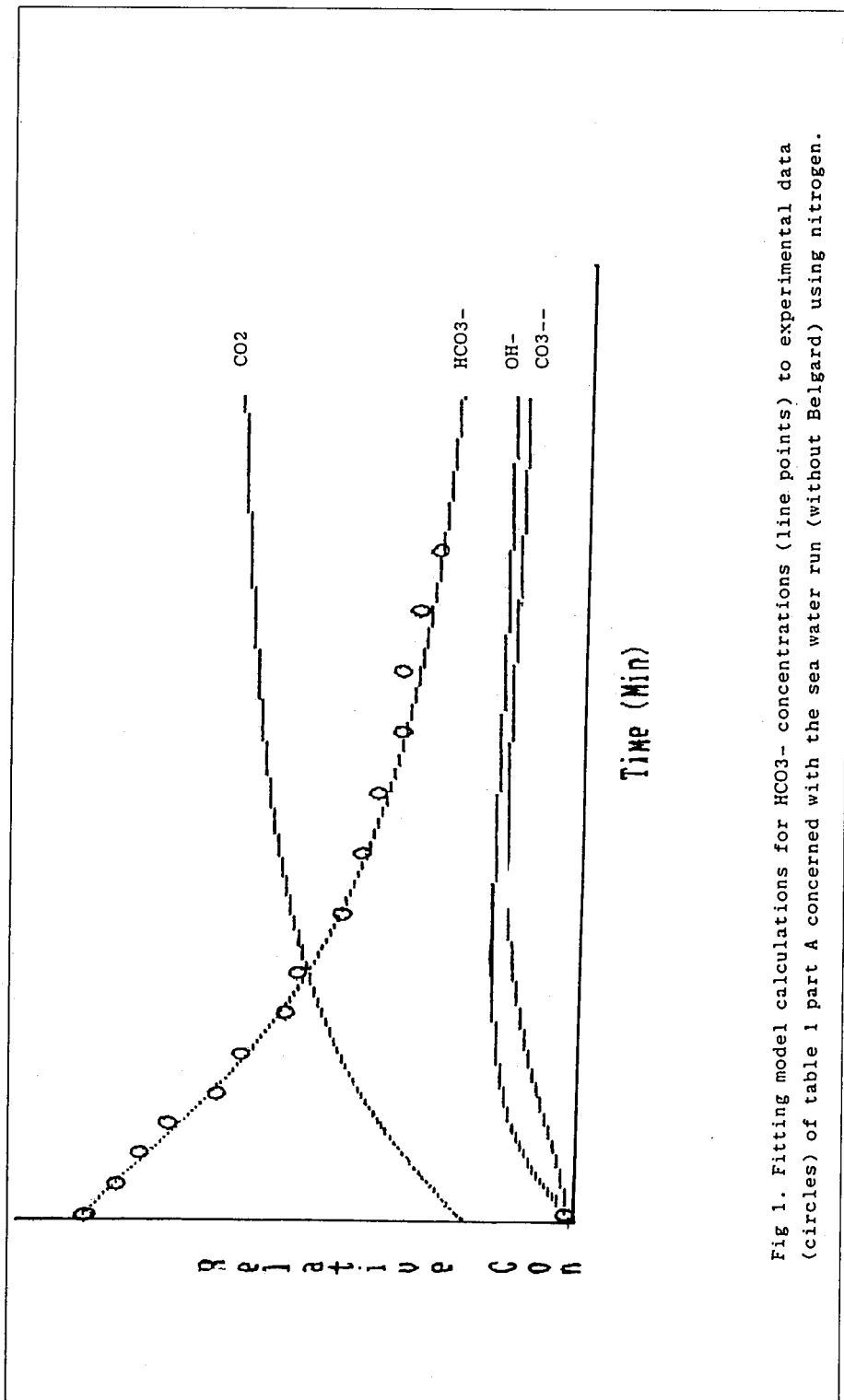


Fig 1. Fitting model calculations for  $\text{HCO}_3^-$  concentrations (line points) to experimental data (circles) of table 1 part A concerned with the sea water run (without Belgard) using nitrogen.

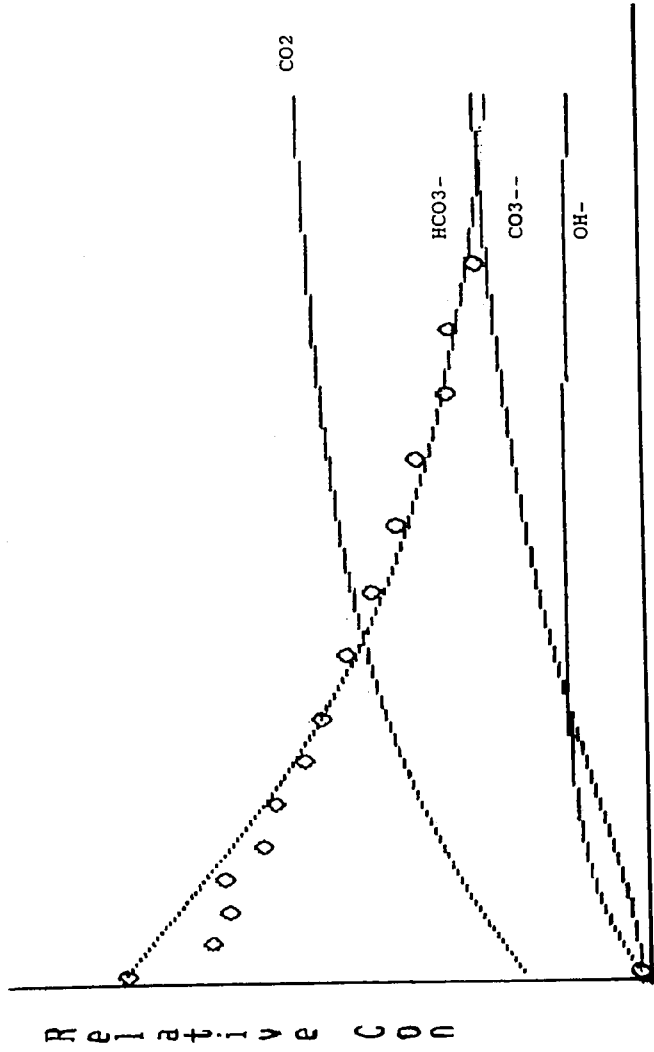


Fig 2. Fitting model calculations for HCO<sub>3</sub><sup>-</sup> concentrations (line points) to experimental data (circles) of table 1 part B concerned with the Belgard run using nitrogen purge.

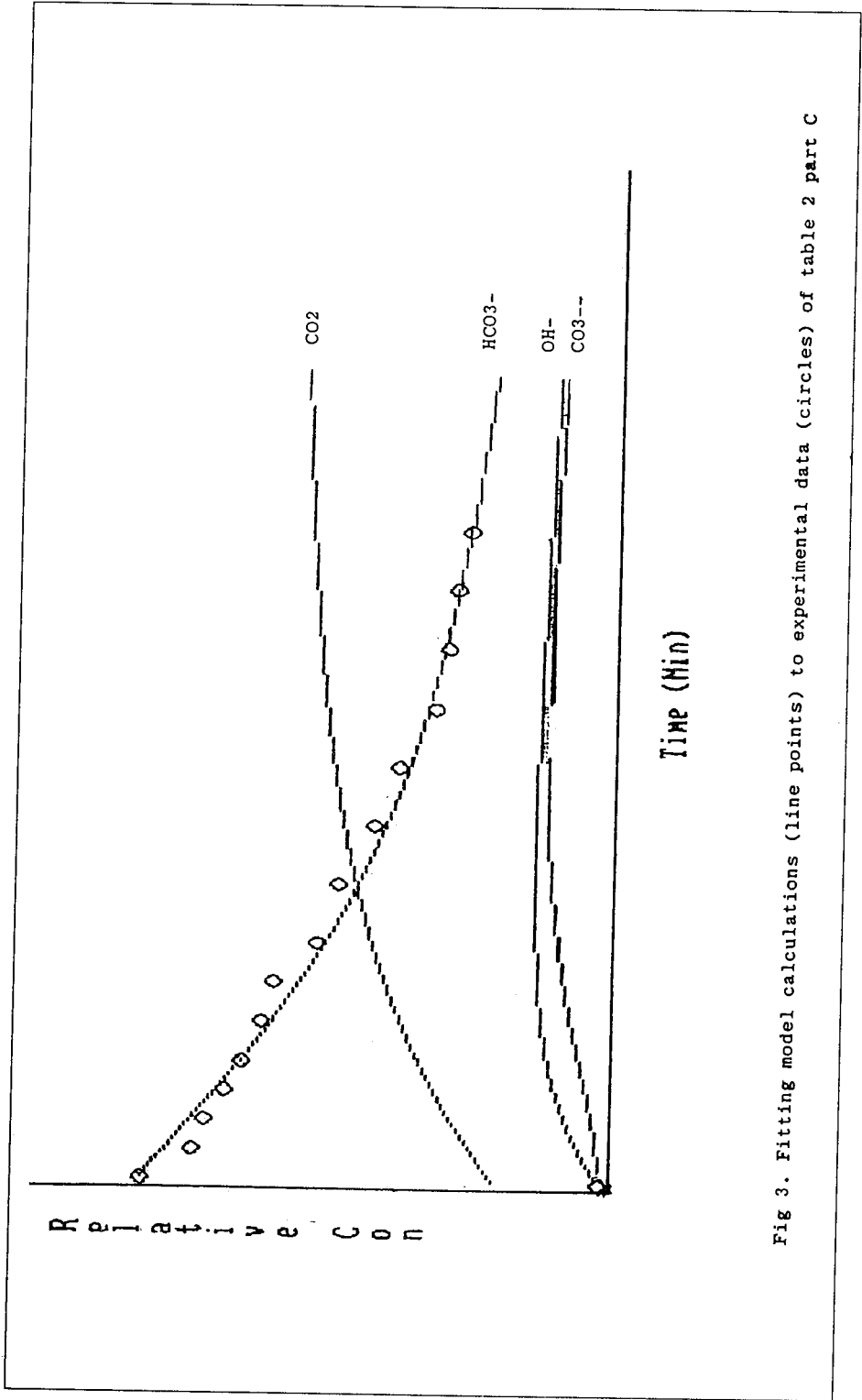


Fig 3. Fitting model calculations (line points) to experimental data (circles) of table 2 part C

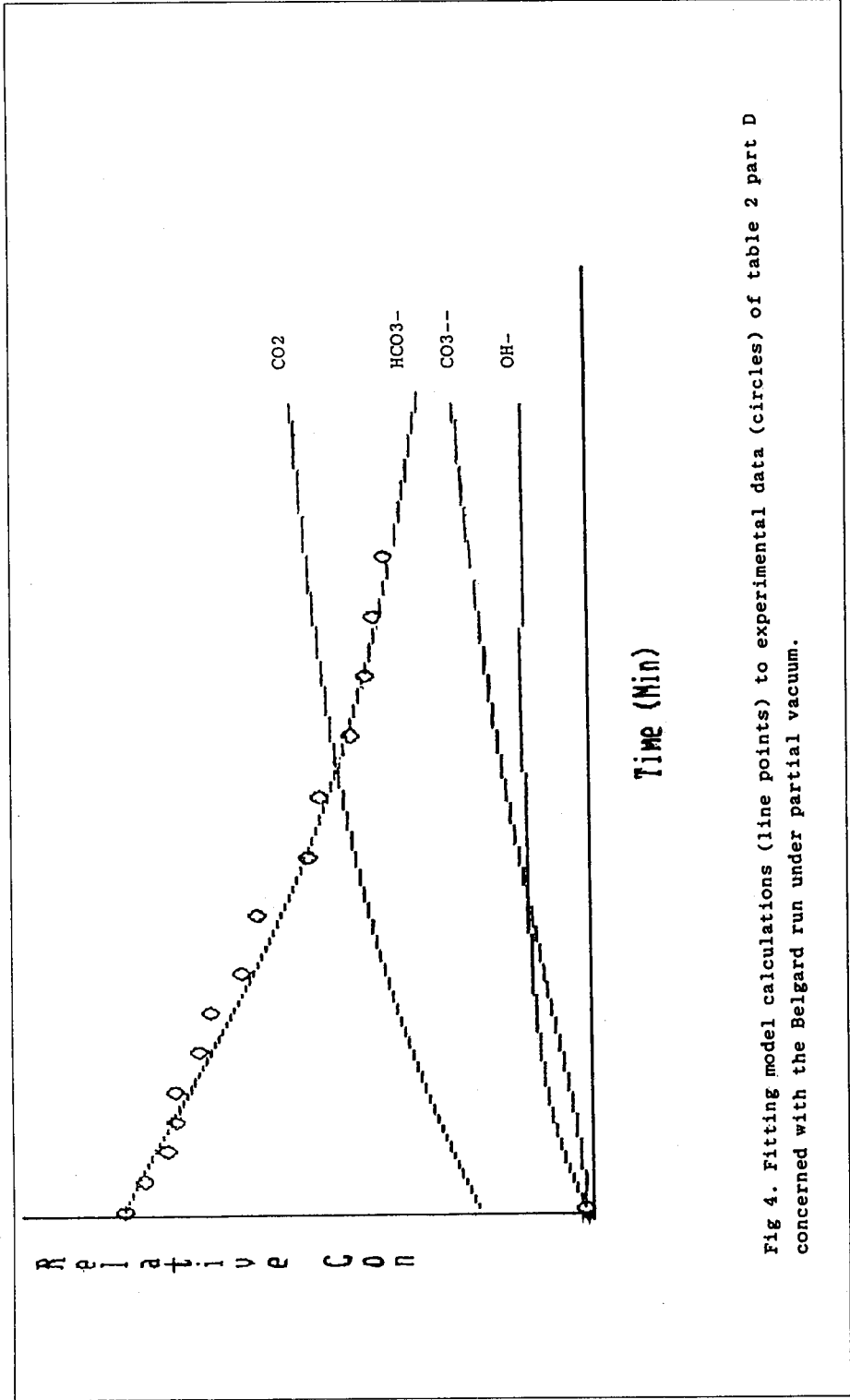


Fig 4. Fitting model calculations (line points) to experimental data (circles) of table 2 part D concerned with the Belgard run under partial vacuum.

# **Kinetics of Hydrolysis of Chloroform and Bromoform in Aqueous Solutions**

*A.M. Shams El Din and Rasheed A. Arain*

# KINETICS OF HYDROLYSIS OF CHLOROFORM AND BROMOFORM IN AQUEOUS SOLUTIONS

**A.M. Shams El Din and Rasheed A. Arain**

Material Testing Laboratory, Water & Electricity Department  
Abu Dhabi, U.A.E.

## ABSTRACT

The base-catalyzed hydrolysis of chloroform (CF) and bromoform (BF) was examined in water-methanol solutions. The progress of reaction is determined by following the decrease in  $[\text{OH}^-]$  and the increase in [halide] ions as function of time. The effects of temperature,  $\text{OH}^-$  ion concentration and the water: methanol ratio on the rates of reaction were tested in some detail.

The hydrolysis of CF was first order with respect to  $[\text{OH}^-]$  and the overall reaction followed second order kinetics. In 1: 1 water methanol solutions the reaction has an activation energy of 18.84 kcal mole<sup>-1</sup>. The rate decreases with the decrease of  $[\text{OH}^-]$  and with the increase in alcohol content of the solution.

Bromoform hydrolysed in 1:5 water: alcohol solutions according to two, second order kinetic consecutive reactions of different rates. The initial faster rate was ascribed to a free radical mechanism with an activation energy of 13.22 kcal mole<sup>-1</sup>. The second, slower reaction had an activation energy comparable to that of CF suggesting the same mechanism. Under identical condition BF hydrolysed twice as fast as CF. The feasibility of applying the knowledge gained from this study to the purification of THM-contaminated potable water is under investigation.

**Keywords:** Chloroform, bromoform, kinetics, hydrolysis, activation energy.



## INTRODUCTION

Most of the Gulf States suffer greatly from lack of natural resources of drinking water. The shortage is made for by desalinating seawater. This is achieved mainly by thermal distillation and, to a lesser extent, by reverse osmosis. Before being introduced into the distiller, seawater is subjected to chlorination to discourage marine organisms of gaining access to the distiller's inside. Chlorine reacts with bromide ion of the water and liberates elemental bromine:  $\text{Cl}_2 + 2\text{Br}^- = 2\text{Cl}^- + \text{Br}_2$ . Both chlorine and bromine react with naturally occurring and/or man-introduced organics present in seawater to produce a series of trihalomethanes (THM), of which chloroform (CF) and bromoform (BF) are the two main components [1]. Both compounds constitute over 98% of the total formed THMs. When desalination is carried out by the multi-stage flash evaporation technique (MSF), most of the formed THMs is removed with the non-condensable gases, and with the reject brine. However, a small amount condenses and collects together with the distillate. As these compounds represent health hazards, their concentration in potable water should not exceed 30  $\mu\text{g}/\text{l}$  for  $\text{CHCl}_3$  and 5  $\mu\text{g}/\text{l}$  for  $\text{CHBr}_3$ , respectively [2,3]. Removal of the THMs from waters containing higher concentrations can be affected through adsorption on activated carbon [4] or through strong aeration [5]. Theoretically the two compounds are liable to hydrolyse in water in the overall hypothetical reaction:



In neutral aqueous solutions hydrolysis does not occur to any measurable extent. The reaction is, however, base catalysed and numerous studies were devoted to the determination of the rate and the establishment of an adequate mechanism [6-11]. The results confirmed the bimolecular nature of the reaction but disagreed on the final product of the elimination reaction. This was said to be carbon monoxide and formate ions [8] or carbon monoxide [12-14] phosgene [14]. In the present paper the kinetics of base-catalyzed hydrolysis of CF and BF in aqueous methanolic solutions is examined in some detail with the aim of developing a workable procedure to control the concentration of the two agents in the distillate in case of a pollution incident [1]. The study is further extended to cover the hydrolysis of the two compounds in the brine-reject.

## EXPERIMENTAL

The kinetics of the base-catalyzed hydrolysis of CF and BF in distilled water was investigated in the temperature range 23 - 60°C. Because of the limited solubility of the two compounds, water/methanol solutions of definite volume compositions were used. All chemicals used were of Analar quality. The purity of  $\text{CHCl}_3$ ,  $\text{CHBr}_3$  and  $\text{CH}_3\text{OH}$  was confirmed by gas chromatography to a single peak. The molarities of the two halomethanes were calculated from their densities ( $d \text{CHCl}_3 = 1.4832 \text{ g/ml}$ ,  $d \text{CHBr}_3 = 2.8899 \text{ g/ml}$  [15]) and volumes (measured with calibrated micropipettes).

To carry out a kinetic experiment, eight 10 ml portions of the same  $\text{TMH}/\text{H}_2\text{O}/\text{CH}_3\text{OH}/\text{NaOH}$  composition were introduced into 30 ml capacity Pyrex glass test tubes fitted with Teflon stoppers. The tubes were provided with small magnetic stirrer and were well thermostated. The moment of addition of the halocompound to the alkaline solution was considered as the zero time of reaction. At increasing time intervals the contents of one of the tubes were quenched in distilled water, cooled to 0°C, quantitatively transferred to 100 ml volumetric flasks and the volume completed to the mark with water/alcohol mixture of the same composition of the experiment. From this stock solution, 10 ml portions were titrated against standard (0.10 or 0.05M) HCl using phenolphthalein indicator. For the estimation of halide ion concentration other 10 ml portions of the solution were acidified with  $\text{HNO}_3$  and titrated against standard (0.10 or 0.05M)  $\text{AgNO}_3$ , using a drop of 0.05 M  $\text{Na}_2\text{CrO}_4$  as indicator (Mohr's method). Titrations were repeated at least twice, and the volumes of the titer, not exceeding 0.1 ml, were averaged.

Experiments on the hydrolysis of CF and BF in seawater were similarly carried out. Due, however, to the presence of  $\text{Mg}^{2+}$  ion in seawater, the alkalinity of the solution was first adjusted after the complete precipitation and filtration of the formed  $\text{Mg}(\text{OH})_2$ .

Unless otherwise stated, experiments were carried out in  $\text{H}_2\text{O}/\text{CH}_3\text{OH}$  solutions of volume composition of 1:1 in case of CF and 1:5 in case of BF.

## RESULTS AND DISCUSSION

In agreement with previous authors [8, 10], the results of the present investigation reveal that the hydrolysis of CF and BF follows bimolecular kinetics. For the sake of clarity, each compound will be treated separately, then a comparison between the two sets of measurements, will be given.

## A - Hydrolysis of Chloroform (CF)

Chloroform was found to be stable in 1:1 H<sub>2</sub>O/CH<sub>3</sub>OH mixtures at temperatures up to 60°C; no Cl<sup>-</sup> ion was detected in solution for more than 18 hr. Hydrolysis readily occurred, however, in alkaline solutions. The various parameters affecting the reaction were examined in some detail.

The curves of Fig. (1A) represent the decrease with time of the NaOH concentration of solutions initially 0.978M, when reacted at different temperatures with 0.324M CF. The curves reveal the continuous consumption of OH<sup>-</sup> ion at rates increasing hand in hand with rise in temperature. Simultaneous with the disappearance of OH<sup>-</sup>, there occurs a corresponding build-up of the Cl<sup>-</sup> ion content of the solution, Fig. (1B). Apparently the two phenomena are related. Reference to both sets of figures reveals that the production of 1 mole Cl<sup>-</sup> is accompanied by the disappearance of 1.2 to 1.3 moles of OH<sup>-</sup>. The significance of this finding will be discussed later.

The results of the present investigation show that hydrolysis of CF follows second order kinetics. This is evidenced from the fact that plots of the quantity  $2.303 / (a - b) \log[b(a - x) / a(b - x)]$  as function of reaction time, t(min) yield straight lines [16]. The constants "a" and "b" represent, respectively, the initial concentrations of NaOH and CF, and x is the amount of either substance reacting till time t.

Since CF is the only source for Cl<sup>-</sup> ion, the value of its x was taken as [Cl<sup>-</sup>] at any time. The corresponding quantity for OH<sup>-</sup> was experimentally determined through titration. The straight lines of Fig. (2) represent the kinetic treatment of the results for solutions of initial composition: [OH<sup>-</sup>] = 0.978M, [CHCl<sub>3</sub>] = 0.324M, [OH<sup>-</sup>]/[CHCl<sub>3</sub>] = 3 in 1:1 H<sub>2</sub>O/CH<sub>3</sub>OH solutions at various temperatures. The linear plots describe the behaviour over the first 75 to 85% of the reaction. Thereafter, deviation from linearity, suggestive of reduced rates, is recorded. The lines of Fig. (2) do not pass through the point of origin.

The slopes of the linear plots of Fig. (2) are the rates of the reaction at the corresponding temperatures. The plot of the logarithm of these values as function of the reciprocal of absolute temperature, curve 1, Fig. (3), is a straight line. From the slope of this curve, the activation energy of the hydrolysis of CF under our experimental conditions, is calculated to be 18.84 kcal/mole.

A number of experimental parameters, other than temperature, were found to influence the rate of hydrolysis of CHCl<sub>3</sub>. These were examined in some detail:

The curves of Fig. (4A) are second order kinetic plots for the hydrolysis of 0.324M CF in 1:1 H<sub>2</sub>O/CH<sub>3</sub>OH solutions of varying NaOH contents at 50°C. As is clear from these curves the rate of reaction (slope of the line) increases with the increase in [OH<sup>-</sup>]. A plot of the rate constant as function of the NaOH molar concentration on a double logarithmic scale is linear with a slope of +0.82. This shows that hydrolysis of CF is first order with respect to OH<sup>-</sup>. Although not examined, a similar dependence of *k* on the molar concentration of the halo compound is expected to govern also.

The rate of hydrolysis of CF depends also on the methyl alcohol content of the solution. This was proved by running experiments on solutions of 0.324M CHCl<sub>3</sub> and 0.98M NaOH in 1:1, 1:3 and 1:5 H<sub>2</sub>O/CH<sub>3</sub>OH at 50°C. The results of this series of measurements are illustrated by the curves of Fig. (4B). These reveal that an increase in the organic solvent content of the medium reduces the rate of the hydrolytic reaction. This solvent effect is not uncommon and is attributed to solubility, solvation, dielectric constant and repulsion energy effects [17].

## B - Hydrolysis of Bromoform (BF)

Because of the limited solubility of BF in H<sub>2</sub>O and in 1:1 H<sub>2</sub>O/CH<sub>3</sub>OH solutions the study of hydrolysis of the compound was carried out in 1:5 vol/vol H<sub>2</sub>O/CH<sub>3</sub>OH solutions. By and large the general features of the reaction are similar to those reported above for the case of CF. Thus, for example, the results show that hydrolysis occurs with the simultaneous consumption of OH<sup>-</sup> and the release of Br<sup>-</sup> ions. Curves similar to those of Fig. (1) were also obtained in case of BF. One interesting feature of these curves, however, is that the molar ratio [OH<sup>-</sup>] consumed/[Br] produced changed according to a definite pattern with the progress of the reaction. During the first 20-25 min of mixing of the reagents, the ratio is very near to 1.35:1 (i.e. 4:3). At more advanced times the value drops to 1.24 to 1.26 (3.72 to 3.78:3). Although the difference is not large, yet the fact that it is consistent and temperature-independent gives confidence to its meaning. The significance of this parameter will be presented shortly when dealing with the mechanism of reaction.

Similar to the case of CF, the hydrolysis of BF follows second order kinetics. This is evidenced from the linear nature of the curves relating the function  $2.303/(a-b) \log [b(a-x)/a(b-x)]$  to the reaction time, Fig. (5). This set of curves corresponds to the conditions where the initial concentrations of NaOH and BF are 0.981 and 0.322M, respectively ([OH<sup>-</sup>]/[BF] = 3.05), at increasing temperatures.

The base-catalyzed hydrolysis of BF differs from that of CF in that the kinetic data fall nicely on two straight lines of different slopes. This suggests that hydrolysis occurs through two consecutive reactions, each following a second order

mechanism. The first reaction, with a higher rate, accounts for the hydrolysis of some 20 to 30% of the BF of the solution. Depending on temperature, this occurs during the initial 15 to 30 min of mixing the reagents. The second, slower reaction extends over longer times and corresponds to the hydrolysis of the main part of BF. The variation of the ration  $[\text{OH}^-] \text{ consume}/[\text{Br}^-] \text{ produced}$ , mentioned above, is taken to support the idea of dual hydrolysis mechanisms. Another evidence will be presently given.

The peculiar behaviour of BF, as compared to its chloro-analogue has been observed by previous authors in other solvents [10]. This was attributed to the occurrence of a parallel reaction path involving free radicals [10, 18]. Free radical formation is said to be favoured by the voluminous bromine compound and is stabilized by the high methanol content of the solution. We assume that this mechanism accounts for the initial segments of the curves of Fig. (5). On the other hand, the upper parts of the curves correspond to an  $\text{S}_\text{n}^2$  mechanism, similar to that operating in the case of CF.

The two rates of hydrolysis of BF,  $k_1$ , and  $k_2$ , were determined from the slopes of the curves of Fig. (5). These were used to construct the corresponding Arrhenius plots shown by curves (2) and (3) of Fig. (3). The initial fast reaction, attributed to free radicals, is characterized by a relatively small activation energy,  $E_1$ , of 13.22 kcal/mole, curve (2). The low value of  $E$ , complies with the faster rate of hydrolysis. On the other hand, the hydrolysis of the main part of BF has an activation energy,  $E_2$ , practically equal to that of CF, viz., 18.84 kcal/mole. On the basis of this equality, one is justified in concluding that the rate determining step in both reactions is one and the same.

Of interest is to compare the rates of hydrolysis of CF and BF. Comparison is only meaningful when all experimental parameters, known to influence the rates, the same. As is seen from the curves of Fig. (4B), the rate of hydrolysis of CF at 50°C in 1:5 water/methanol solutions amounts to  $6.0 \times 10^{-3} \text{ l-mole}^{-1}\text{-min}^{-1}$ . The corresponding value for BF under the same conditions of temperature,  $[\text{OH}^-]$  and  $[\text{OH}^-]/[\text{CHX}_{23}]$  was  $12.1 \times 10^{-3} \text{ l. mole}^{-1}\text{-min}^{-1}$ . The hydrolysis of BF occurs, therefore, at a rate twice as fast as that for CF. The facile decomposition of BF is attributed to the large size of the bromine atoms, causing greater polarization of the C-Br bonds, making easier their cleavage.

### **C - Hydrolysis of Chloroform in Seawater**

Since a good part of the formed THM remains in the brine, it was of interest to establish the effect, if any, of seawater components on the stability of the halocompounds. The study was carried out on CF as example. Hydrolysis experiments in natural seawater were performed on 0.324M CF in 112 ml of 1:1

seawater/methanol solutions at 23 and 50°C. At increasing time intervals, portions of the mixture (10 ml) were diluted 10 times with distilled water and the chloride ion contents therein determined argentometrically. For times up to 52 hours, no detectable change in the Cl<sup>-</sup> ion content of the solution was measured. This denotes the stability of CF in neutral seawater.

Addition of NaOH to seawater resulted in the precipitation of Mg(OH)<sub>2</sub>. To overcome this difficulty, enough alkali was added to remove all the Mg<sub>2+</sub> content of seawater (1762 ppm [19]). The Mg(OH)<sub>2</sub> precipitate was filtered off and the Mg<sub>2+</sub> free seawater was diluted 1:1 by methanol. The mixture was used to prepare solutions 0.324M and 0.978M with respect to CF and NaOH, respectively. The kinetics of hydrolysis of CF under these conditions were followed in the way described above, at 23° and 50°C, successively. The results obtained are shown by the curves with black circles of Fig. (2). Similar to the results in distilled water, CF breaks down following second order kinetics. It does so, however, at considerably lower rates. The rates at 23° and 50°C amount to 0.25x10<sup>-3</sup> and 5.5x10<sup>-3</sup>, mole<sup>-1</sup>-min<sup>-1</sup> compared to 0.45x10<sup>-3</sup> and 10.75x10<sup>-3</sup> mole<sup>-1</sup>-min<sup>-1</sup> 1:1 distilled water/methanol solutions. The rates of hydrolysis in distilled water are almost twice those measured in seawater at the same temperature. The retarding effect of neutral salts was noted also by previous authors [8,9] and was attributed in the case of sodium chloride to common ion effect [9].

#### D - Mechanism of Hydrolysis

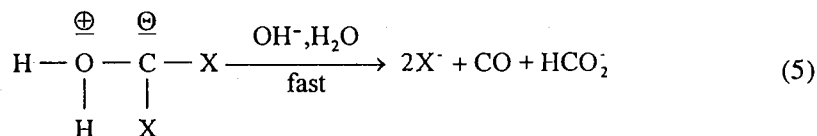
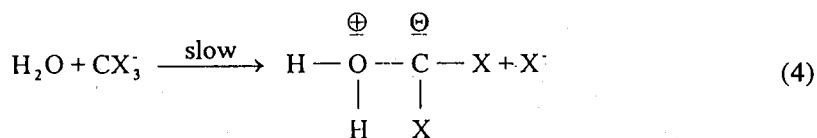
Any mechanism accounting for the hydrolysis of haloforms in aqueous solutions should be in agreement with the following experimental findings:

- a) Hydrolysis consumes OH<sup>-</sup> ions.
- b) The reaction liberates halogen ions simultaneous with the disappearance of OH<sup>-</sup> ions.
- c) The ratio [OH<sup>-</sup>] consumed/[X<sup>-</sup>] produced is always larger than 1.
- d) The reaction is first order with respect to both haloform and hydroxyl ions; the overall reaction is second order.

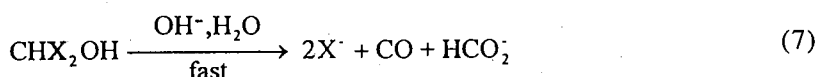
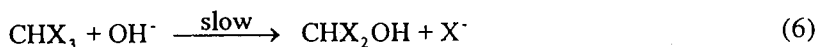
A number of mechanisms have already been suggested. These were reviewed by Hine [20].

- A) The first mechanism proposes the primary fast formation of trihalomethyl anion, followed by an SN<sup>2</sup> attack by a water molecule [20]

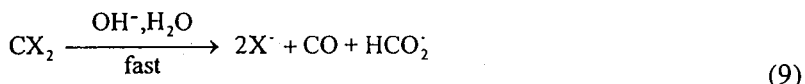
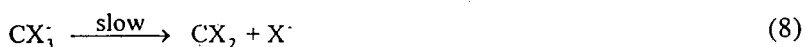




B) An alternative path presumes a primary rate-determining SN2 attack through a hydroxyl anion as



C) The nowadays more accepted mechanism, assumes, in agreement with scheme (A), the primary, reversible extraction of a proton from the haloform, with the formation of trihalomethyl anion (reaction 3). This is followed by the slow, rate-determining step involving the extraction of a halogen anion by an SN1 reaction. This produces dihalocarbene as intermediate, which reacts rapidly with solution components to yield CO and formate ion as end products [9]:



Support to this mechanism comes from the difference in effect of additions of sodium fluoride-, nitrate- and perchlorate-, on the one hand, and chloride, bromide- and iodide-, on the other, on the rate of hydrolysis of CF [9]. The last three anions decrease the rate markedly, due to recombination with dichloro carbene. According to the authors [9], "these data rule out all the other alternative mechanisms".

According to any of the above mechanisms hydrolysis of a haloform should consume as many OH- moles as it liberates of halogen ions. This condition is, however, seldom realized experimentally. Usually the amount of disappearing

OH<sup>-</sup> exceeds that of released halide ion. In view of the mono-molecular dependence of the reaction on [OH<sup>-</sup>], on the one hand, and the bimolecular kinetics of the overall reaction, on the other, one is bound to conclude that the excess of OH<sup>-</sup> ion is consumed in a fast reaction following the rate determining step. Irrespective of the reaction mechanism the end products of hydrolysis of haloforms are considered to be carbon monoxide and formic acid. It is the neutralization of the acid which accounts for the difference between [OH<sup>-</sup>] consumed and [Cl<sup>-</sup>] liberated. Accordingly, the ratio [OH<sup>-</sup>]/[X<sup>-</sup>] determines the percentage of each product. A value of 1 (i.e. 3:3) corresponds to the formation of CO alone. On the other hand, the value of 1.33 (4:3) indicates the exclusive formation of formate ion. Intermediate values of the ratio allow the determination of the percentage of each product [8].

### **E - Comparison with Available Data**

In Table (1) values of the rate constant for the hydrolysis of CF solutions determined in the present investigation are listed together with those reported by previous workers, for comparison. In Table (2) the same is given for the hydrolysis of BF. Consideration of the figures given in both Tables allows a number of interesting conclusions to be drawn. Thus:

- a) the rate of hydrolysis depends primarily on the nature of the reaction medium. In pure water the rate constants are relatively high, when one takes into consideration the very limited solubility of CF.
- b) The solubility of CF increases when a miscible organic solvent is admixed with water. The rate of hydrolysis is, however, inversely affected. The decrease in reactivity depends on the type of solvent used, as well as on its amount.
- c) The reaction rate increases hand in hand with both the CF content and the [OH<sup>-</sup>] concentration.
- d) Additions of Cl<sup>-</sup> ion to the medium reduce the rate of hydrolysis. The decrease in *k* is more the higher the concentration of the added Cl<sup>-</sup> ion.
- e) An increase in reaction temperature leads invariably to the promotion of hydrolysis and the increase of reaction rate.
- f) The hydrolysis of BF occurs at rates markedly faster than those of CF under similar conditions.
- g) Despite differences in the nature of the medium, the rate constants of CF and BF determined in the present investigation are of the same order of magnitude as those reported by other authors.



## CONCLUSIONS

The base catalysed hydrolysis of chloroform and bromoform was examined in 1:1 and 1:5 water-methanol solutions, respectively in the temperature range 23 to 60°C. The progress of hydrolysis was followed by determining the reduction in alkali concentration and the production of halide ions as function of time.

Based on the results obtained the following conclusions were drawn:

- 1) Chloroform hydrolyses in 1:1 water-methanol solutions following second order kinetics. The disappearance of the halocompound is first order with respect to OH<sup>-</sup> ion and probably so also respect to the haloform. Hydrolysis of CF is characterized by an activation energy of 18.84 kcal/mole.
- 2) The rate of hydrolysis of CF decreases with the increase in the alcohol content of the medium and also in 1:1 Gulf water-methanol solutions.
- 3) The hydrolysis of bromoform in 1:5 water-methanol solutions occurs along two consecutive second order kinetics of different rates corresponding to two different mechanisms. It is suggested that the first involves free radicals while the second proceeds via carbene formation. Two activation energies, amounting to 13.22 and 18.84 kcal/mole were computed for the two reactions, successively. Under the same conditions, BF hydrolyses twice as fast as CF.
- 4) The feasibility of gasification of distillates contaminated with traces of CF and BF, followed by their neutralization, as means of eliminating their halomethanes, is currently being investigated.

## ACKNOWLEDGMENT

The authors wish to express their thanks and appreciation to Dr. Darwish M.K. Al-Gobaisi, Director General Power and Desalination Plants for his interest in the work and continuous encouragement.

**Table (1)**  
**Rate constants for the basic hydrolysis of  $\text{CHCl}_3$**

#	Medium	$[\text{CHCl}_3]$ mole	$[\text{OH}^-]$ mole	Temp. $^\circ\text{C}$	$k \times 10^3$ $\text{l}\cdot\text{mole}^{-1}\cdot\text{min}^{-1}$	Ref.	Remarks
1	$\text{H}_2\text{O}:\text{CH}_3\text{OH}$ 1:1	0.324	0.978	23	0.45	(*)	
2	$\text{H}_2\text{O}:\text{CH}_3\text{OH}$ 1:1	0.324	0.978	30	1.5	(*)	
3	$\text{H}_2\text{O}:\text{CH}_3\text{OH}$ 1:1	0.324	0.978	35	2.5	(*)	
4	$\text{H}_2\text{O}:\text{CH}_3\text{OH}$ 1:1	0.324	0.978	40	4.5	(*)	
5	$\text{H}_2\text{O}:\text{CH}_3\text{OH}$ 1:1	0.324	0.978	45	6.25	(*)	
6	$\text{H}_2\text{O}:\text{CH}_3\text{OH}$ 1:1	0.324	0.978	50	10.75	(*)	
7	$\text{H}_2\text{O}:\text{CH}_3\text{OH}$ 1:1	0.324	0.978	60	20.05	(*)	
8	$\text{H}_2\text{O}:\text{CH}_3\text{OH}$ 1:1	0.324	0.698	50	8.0	(*)	
9	$\text{H}_2\text{O}:\text{CH}_3\text{OH}$ 1:1	0.324	0.455	50	6.1	(*)	
10	$\text{H}_2\text{O}:\text{CH}_3\text{OH}$ 1:3	0.324	0.978	50	7.25	(*)	
11	$\text{H}_2\text{O}:\text{CH}_3\text{OH}$ 1:5	0.324	0.978	50	6.0	(*)	
12	Gulf Water: $\text{CH}_3\text{OH}$ 1:1	0.324	0.978	23	0.25	(*)	
13	Gulf Water: $\text{CH}_3\text{OH}$ 1:1	0.324	0.978	50	5.5	(*)	
14	$\text{H}_2\text{O}$ (deoxygenated)	-	-	0	0.036	10	
15	$\text{H}_2\text{O}$ (deoxygenated)	-	-	20	1.38	10	
16	$\text{H}_2\text{O}$ (deoxygenated)	-	-	35	14.46	10	
17	$\text{H}_2\text{O}$ (deoxygenated)	-	-	50	112.8	10	
18	$\text{H}_2\text{O}$ (deoxygenated)	0.031	0.019	35	12.90 - 12.96	9	in presence of 0.08M NaCl
19	$\text{H}_2\text{O}$ (deoxygenated)	0.031	0.035	35	11.88 - 12.36	9	in presence of 0.16M NaCl
20	$\text{H}_2\text{O}:\text{Dioxane}$ 1:2	0.00381	0.0289	36	20.4	8	
21	$\text{H}_2\text{O}:\text{Dioxane}$ 1:2	0.3736	0.0286	36	15.2	8	
22	$\text{H}_2\text{O}:\text{Dioxane}$ 1:2	0.1280	0.0291	36	19.1	8	
23	$\text{H}_2\text{O}:\text{Dioxane}$ 1:2	0.1280	0.0075	36	19.8	8	
24	$\text{H}_2\text{O}:\text{Dioxane}$ 1:2	0.1280	0.0077	36	7.3	8	in presence of 0.286M NaCl
25	$\text{H}_2\text{O}:\text{Dioxane}$ 1:2	0.1280	0.0287	36	7.4	8	in presence of 0.286M NaCl
26	$\text{H}_2\text{O}:\text{Dioxane}$ 1:2	0.1280	0.0288	36	13.5	8	in presence of 0.095M NaCl
27	Anhydrous $\text{CH}_3\text{OH}$	-	-	50	1.83	10	

(\*) present investigation.

**Table (2)**  
**Rate constants for the basic hydrolysis of  $\text{CHBr}_3$ .**

#	Medium	$[\text{CHBr}_3]$ mole	$[\text{OH}^-]$ mole	Temp. $^{\circ}\text{C}$	$k \times 10^3$ $\text{l-mole}^{-1}\text{-min}^{-1}$	Ref.
1	$\text{H}_2\text{O}:\text{CH}_3\text{OH}$ 1:	0.322	0.981	35	2.9	(*)
2	$\text{H}_2\text{O}:\text{CH}_3\text{OH}$ 1:	0.322	0.981	40	5.0	(*)
3	$\text{H}_2\text{O}:\text{CH}_3\text{OH}$ 1:	0.322	0.981	45	8.0	(*)
4	$\text{H}_2\text{O}:\text{CH}_3\text{OH}$ 1:	0.322	0.981	50	12.13	(*)
5	$\text{H}_2\text{O}:\text{CH}_3\text{OH}$ 1:	0.322	0.755	50	8.0	(*)
6	$\text{H}_2\text{O}:\text{CH}_3\text{OH}$ 1:	0.322	0.540	50	5.75	(*)
7	Gulf Water- $\text{CH}_3\text{OH}$ 1:5	0.322	0.981	23	0.13	(*)
8	Gulf Water- $\text{CH}_3\text{OH}$ 1:5	0.322	0.981	50	6.46	(*)
9	$\text{H}_2\text{O}$ (deoxygenated)	-	-	0	0.144	10
10	$\text{H}_2\text{O}$ (deoxygenated)	-	-	25	11.94	10
11	$\text{H}_2\text{O}$ (deoxygenated)	-	-	35	57.24	10
12	$\text{H}_2\text{O}$ (deoxygenated)	-	-	50	504.0	10
13	Anhydrous $\text{CH}_3\text{OH}$	-	-	50	14.5	10

(\*) present investigation.

## REFERENCES

1. A.M. Shams El Din, R.A. Arain and A.A. Hammoud, *Desalination*, 85 (1991) 13.
2. WHO: *Guidelines for Drinking Water Quality*, vol. 1, (1984) p.63.
3. WHO: *Guidelines for Drinking Water Quality*, vol. 2, (1984) 241.
4. Degremont, *Water Treatment Handbook*, Lavoisier Pub. (Paris) (1991) 1185.
5. N.F. Gray, *Drinking Water Quality*, John Wiley (N.Y) (1994) 196.
6. A.P. Saunder, *J. Phys. Chem.*, 4(1900) 660.
7. E. Abel, *Z-Elektrochem.*, 29(1923) 391.
8. J. Hine, *J. Am. Chem. Soc.*, 72(1950) 2438.
9. J. Hine and A.M. Dowell, *J. Am. Chem. Soc.*, 76(1954) 2688.
10. J. Hine and S.T. Ehrenson, *J. Am. Chem. Soc.*, 80(1958) 824.
11. J. Hine, R. Butterworth and P.B. Langford, *J. Am. Chem. Soc.*, 80(1958) 819.
12. A. Geuther, *Ann.*, 123(1862) 121.
13. J. Thiele and F. Dent., *Ann* 302(1898) 273.
14. G. Mossler, *Montash.*, 29 (1903) 573.
15. *Handbook of Chemistry and Physics*, CRC Press Inc., Boca Raton, Florida, 66th Ed. (1985-86) p. C-350.
16. K.J. Laidler, *Chemical Kinetics*, McGraw-Hill (N.Y) (1950) p. 8.
17. Ref. 16, pp 111- 117, 123, 127 and 142.
18. C.K. Ingold, *Structure and Mechanism in Organic Chemistry*, Cornell University Press, N.Y (1953) 75 and 89.
19. A.M. Shams El Din and R.A. Mohamed, *Desalination* 99(1994) 73-111.
20. J. Hine, *Reaktivitat and Mechanismus in der organischen Chemie*, G. Thieme Verlag (Stuttgart) (1960) p. 130.

Fig. (1): Variation of [OH<sup>-</sup>] consumed (A) and [Cl<sup>-</sup>] released (B) as function of time, min., during hydrolysis of 0.324M CF and initial 0.978M NaOH at different temperatures in 1:1 distilled water: methanol solutions.

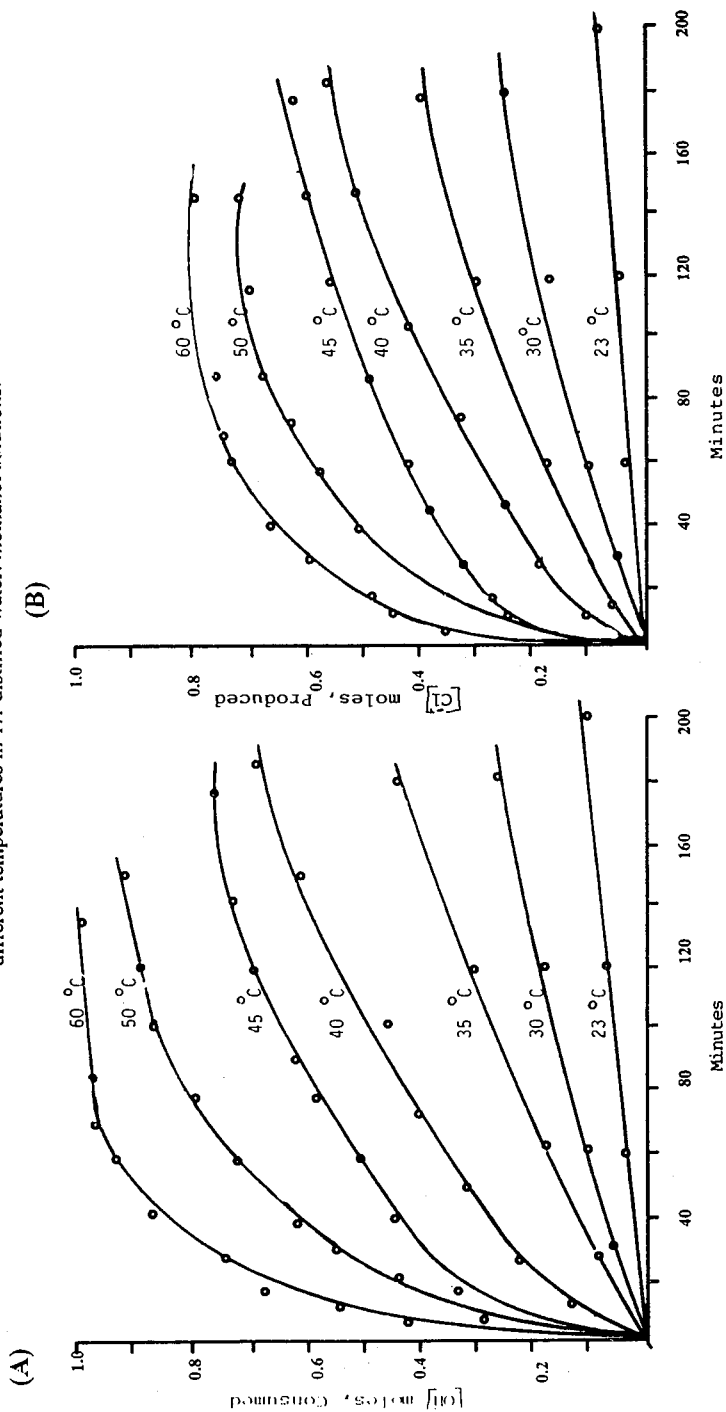


Fig. (2): Second order kinetic analysis of the results of hydrolysis of 0.324M CF + 0.978M NaOH at different temperature in 1:1 dist. water : methanol solution. Curves with black circles same as above in 1:1 Gulf water: methanol solutions.

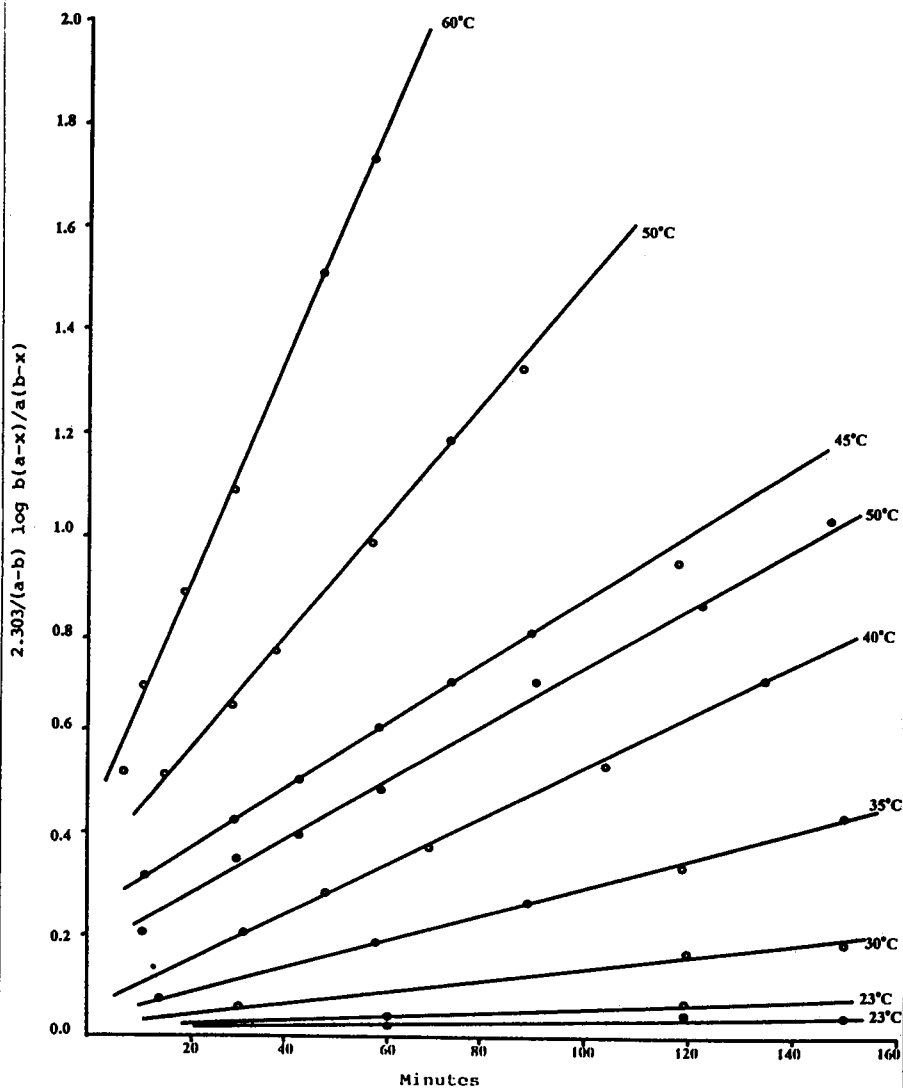
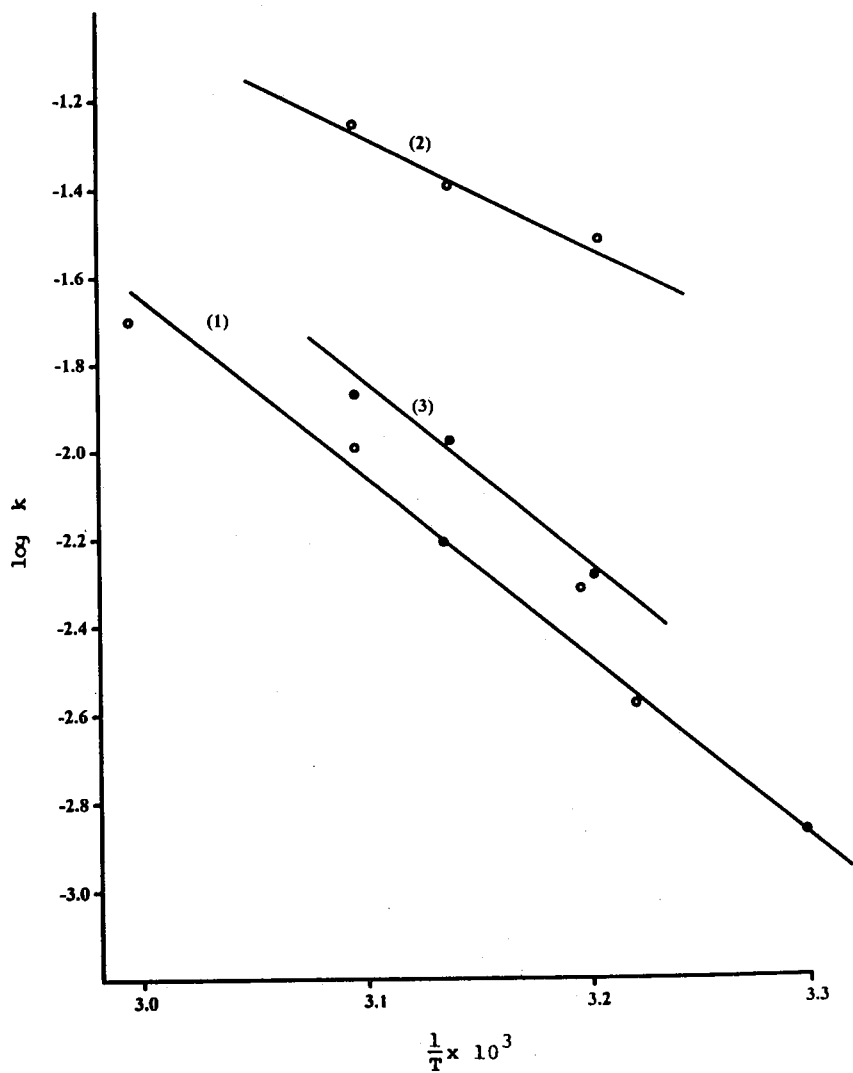


Fig. (3): Arrhenius plots for the hydrolysis of (1) chloroform (2) and (3) bromoform.



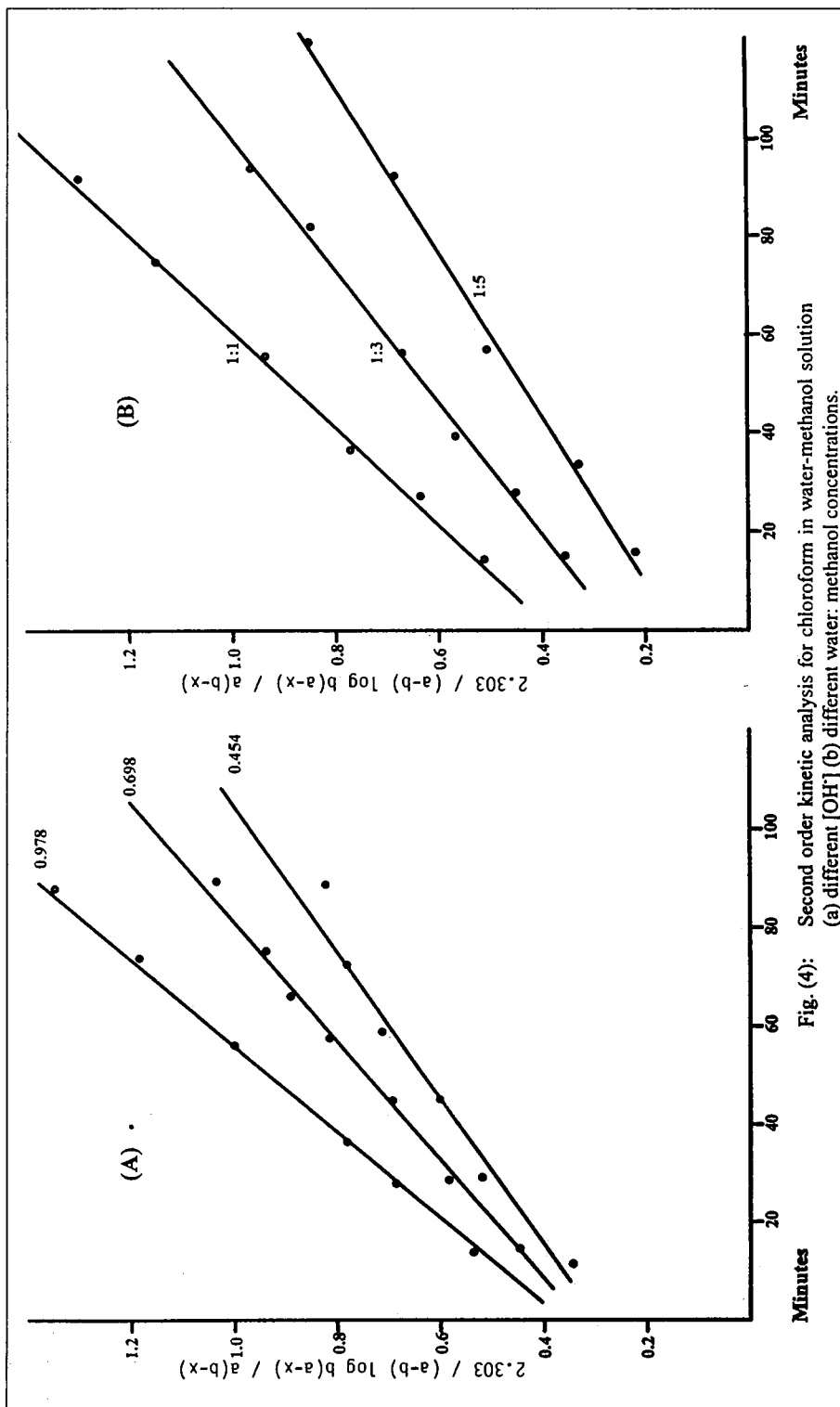
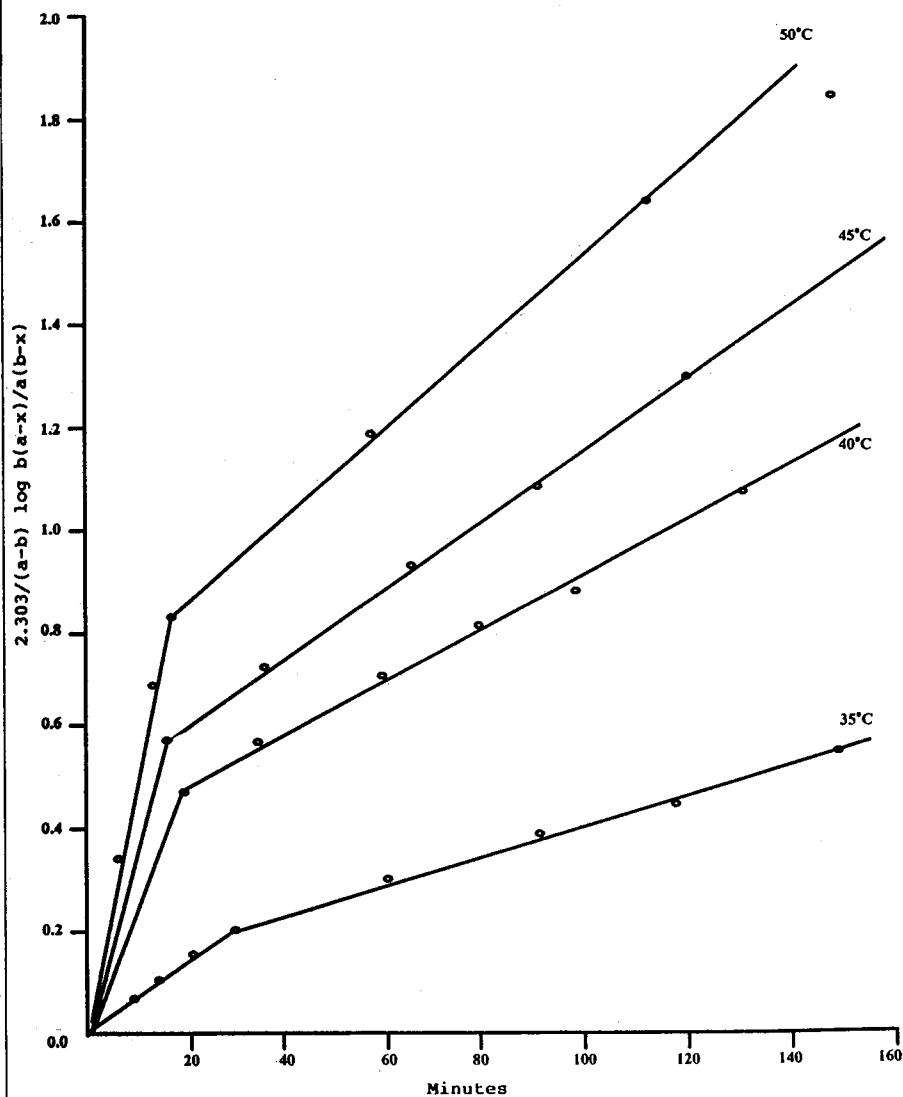


Fig. (4): Second order kinetic analysis for chloroform in water-methanol solution (a) different  $[OH^-]$  (b) different water: methanol concentrations.



Fig. (5): Second order kinetic treatment of 0.322M bromoform + 0.981M NaOH at different temperatures in 1:5 water-methanol solutions.



**The Thermovapor Compression Desalters: Energy  
and Availability analysis of Single and Multi Effect Systems**

*M.A. Darwish*

# **THE THERMOVAPOR COMPRESSION DESALTERS: ENERGY AND AVAILABILITY ANALYSIS OF SINGLE AND MULTI EFFECT SYSTEMS**

**M. A. Darwish**

College of Engineering and Petroleum  
Mechanical Engineering Dept., Kuwait University  
Kuwait

## **ABSTRACT**

Recent developments in thermal vapor compression (TVC) systems [1] and [2] by installing 4 units each having of 4 effects, 1 mgd capacity and gain ratio of 8 and another 4 units of 12 effects each, and 2 mgd capacity per unit and gain ratio close to 17 by Sidem of France, increased the interest in the system particularly for plants of low and medium capacity. This system is characterized by the following:

- (i) The compression of most of the generated vapor and its usage as a heating medium, drastically reduces the primary heat source (boiler) and heat sink (i.e. cooling water and condenser), as compared to the conventional single effect desalting system.
- (ii) Low energy consumption.
- (iii) Simple water pretreatment as compared with the reverse osmosis (RO<sub>2</sub>) system which is the main competitor of mechanical and thermal vapor compression systems in small and medium capacities.
- (iv) Low capital and operating costs.
- (v) Recently developed reliable thermo compressors.

Since very little is known about the principles and design of the system, an analysis, using the first and second laws of thermodynamics is conducted for the TVC system components, e.g. steam ejector, evaporator, condenser, as well as the system as a whole. The analysis pinpoints the deficiencies in the system and the methods of overcoming these deficiencies.

## NOMENCLATURE

$A$	=	availability rate kJ/s
$a$	=	specific availability rate A/m, kJ/kg/s
$A$	=	heat transfer area, m <sup>2</sup>
$B$	=	brine flow rate, (F-D), kg s <sup>-1</sup>
$c$	=	liquid (distillate, feed and brine) specific heat kJ kg <sup>-1</sup> K <sup>-1</sup>
$C_p$	=	Vapor specific heat at constant pressure kJ kg <sup>-1</sup> K <sup>-1</sup>
$D$	=	distillate flow rate, kg s <sup>-1</sup>
$E$	=	specific available energy consumption, kJ kg <sup>-1</sup>
$F$	=	feed flow rate, kg s <sup>-1</sup>
$L$	=	latent heat, kJ kg <sup>-1</sup>
$M$	=	mass flow rate, kg/s
mgd	=	imperial million gallon per day
$p$	=	pressure in kN
$GR$	=	gain ratio, D/S
$Q$	=	heat flow rate
$R$	=	gas constant of steam, kJ kg <sup>-1</sup> K <sup>-1</sup>
$s$	=	specific entropy kJ/kg K
$S$	=	motive steam supply flow rate, kg/s
$T$	=	temperature in Kelvin (K) or Celsius (C)
$\Delta T_s$	=	saturation temperature difference across the evaporator, C
$U$	=	overall heat transfer coefficient, kW m <sup>-2</sup> , C
$v$	=	specific volume m <sup>3</sup> kg <sup>-1</sup>
$W$	=	work done, kJ

### *Greek Symbols*

$\epsilon$	=	effectiveness or thermodynamics second law efficiency
$\eta_s$	=	isentropic efficiency

### *Subscript*

$a$	=	available heat
$b$	=	brine
$c$	=	cooling water
$c$	=	condenser
$d$	=	steam ejector discharge condition
$e$	=	evaporator
$ej$	=	ejector
$f$	=	feed
$f$	=	saturated liquid water condition
$O$	=	brine and distillate leaving the heat exchanger

s = isentropic, or steam  
t = thermal;  
v = vapor

## INTRODUCTION

A simple, and may be the first, method for desalting sea water is the single effect distillation system consisting of evaporator-condenser combination as shown in fig. 1. Steam, say, at rate  $S$  (or hot water) is supplied to the evaporator in order to heat the feed  $F$  from the feeding temperature  $T_f$  to the boiling temperature  $T_1$  and evaporate  $D$  out of it. The unevaporated, feed brine blow down  $B(=F-D)$ , leaves the evaporator at  $T_1$  and returns to the sea. The generated vapour is directed to the condenser where it loses its latent heat to a cooling seawater and thus condenses and forms the product  $D$ . The cooling seawater flow rate,  $M_c$ , enters and leaves the condenser at temperatures  $T_c$  and  $T_f$  respectively. Part of the leaving  $M_c$  forms the feed,  $F$ , to the evaporator while the balance  $(M_c-F)$  is rejected back to the sea. The gain ratio defined by product distillate per kg of heating steam  $D/S$  is usually used to rate the performance of such a system. It can be shown that if the heating steam is supplied and discharged as saturated vapor and liquid respectively the gain ratio GR is equal to:

$$GR=D/S = \frac{L_s}{(F/D)C(T_1-T_f) + L_l} \quad (1)$$

and has a value less than but close to unity, say 0.8, for normal temperature levels. The value of  $D/S$  for this system is considerably less than  $D/S$  encountered for the predominant multistage flash (MSF) or multi-effect (ME) distillation desalting systems (typical values for both MSF and ME are the range of 6-9). The main reasons for the low  $D/S$  in the single effect system are:

- (i) Most of the condensed vapor latent heat,  $L$ , is rejected to the cooling water in the condenser, except for a small fraction which is recovered by preheating the feed from  $T_c$  to  $T_f$ . Full or partial recovery of the latent heat (as in MSF or ME) would improve  $D/S$ .
- (ii) The brine and product leave the unit at relatively high temperatures  $T_1$  and  $T_{v1}$  respectively. Where  $T_{v1} = T_1 - PBE$ . Lowering their temperatures or recovery of their heat contents would also improve  $D/S$ .

One method of recovering the generated vapor latent heat is to raise the generated vapour pressure from  $P_1$  to  $P_2$  (and consequently its saturation temperature  $T_1$  to

$T_{v2}$ ) by a thermal compressor (steam ejector) and reuse it as a heating steam. This arrangement is shown in Fig. 2. The generated vapor leaving the evaporator  $D_f$  is divided to two parts. One part  $D_f$  is used to heat the feed in a condenser of  $D_f/D$  fraction capacity of that of conventional single effect conventional evaporating system. The other part  $D_r = D - D_f$  is extracted by a steam ejector where it is compressed from pressure  $P_1$  to  $P_2$  by the use of motive steam  $S$ . The mixture of compressed vapour as well as the expanding motive steam is discharged from the ejector at a higher discharge pressure  $P_d = P_2$ . It reenters the evaporator where it condenses and becomes a heating vapour.

The main advantages of the TVC system which have created more interest in the last decade are:

- (i) The reuse of the compressed vapor as heating steam drastically reduces the required steam (motive steam here), and the boiler size as well as the heat sink (i.e. cooling water and condenser).
- (ii) A low amount of energy is used to operate the system.
- (iii) Low capital and construction costs.
- (iv) Recent developments in commercially available steam ejector, thermal compressors.
- (v) The limitation of the predominant MSF system, from economical viewpoints, to large capacities.
- (vi) The simplicity of the steam ejector, with no moving part, when compared with the mechanical vapor compression system using mechanical compressor.

The amount of mechanical energy (work) added to the TVC, to run the feed, brine and distillate pumps is very low 1-2 kWh/m<sup>3</sup> distillate and usually disregarded as compared with the thermal energy supplied. The parameters affecting the performance of the TVC are studied and quantified here by presenting both energy and availability analyses in the following sections. This seems more proper since both high quality energy (i.e. work) and thermal energy are added to the TVC and because of the need to rate and compare the performance of this system with other systems consuming mainly thermal energy, such as conventional multi effect and multi stage flash systems and systems consuming mechanical energy such as reverse osmosis and mechanical vapour compression system.

## SINGLE EFFECT ENERGY AND AVAILABILITY ANALYSIS

The processes of the single effect TVC system are presented on a T-S diagram in Fig. 3. In the following analysis, some assumptions are made whenever

adequate to simplify the analysis such as:

- (i) An average specific heat  $C$  for  $C_r$ ,  $C_d$ , and  $C_b$ .
- (ii) Equal latent heats  $L_2 = L_1 = L$ .

A typical case will be discussed later and along with the analysis to give an idea about the variations of the parameters involved. For this typical case the saturation temperatures of the generated vapor and the condensing heating vapor are 60°C, and 65°C respectively; and the motive steam is saturated at 25 bar pressure.

**a) Evaporator:**

This system, usually, uses falling film horizontal tube evaporator type, see fig. 2.

In this evaporator, heating vapor (or steam) is condensing while flowing inside the tubes while the feed (seawater) is sprayed by nozzles on the outer side of the tubes. In the evaporator, heat is gained by the feed,  $F$ , to raise its temperature from  $T_f$  to  $T_1$  and to evaporate  $D$ . At the same time, heat is released by the vapour discharged from the steam ejector at condition  $d$  (due to desuperheating and condensation), So, an energy balance in the evaporator gives:

$$(S+D_r)(h_d-h_{fd}) = FC(T_1-T_f) + DL \quad (2)$$

An availability analysis, similar to an energy analysis, can be developed for the system components and the system as a whole.

In the evaporator, the availability gain by the feed due its heating from  $T_f$  to  $T_1$  and evaporation of  $D$ , can be expressed by  $A_{e,g}$

$$A_{e,l} = FC [T_1 - T_f] - T_o \ln T_1/T_f + DL (1 - o/T_{v1}) \quad (3a)$$

The availability loss by the heating vapor (discharged form the ejector, i.e.  $D_r + S$ ),  $A_{e,l}$  is

$$A_{e,l} (S + D_r) [(h_d - h_{fd}) - T_o (S_d - S_{fd})] \quad (3b)$$

So, the net availability destruction in the evaporator is

$$\Delta A_e = A_{e,l} - A_{e,g} \quad (3)$$

b) **Condenser:**

The vapor generated in the evaporator  $D$  is divided to  $D_f$  and  $D_r$ . The portion  $D_f$  is directed and condensed in the condenser in order heat the feed  $F$  from the seawater temperature  $T_c$  to the feed temperature  $T_f$ . An energy balance in the condenser gives

$$D_f L = FC(T_f - T_c) \quad (4)$$

It is noticed here that the value of the feed  $F$  is determined by the maximum allowable salt concentration in the brine leaving the evaporator. A typical figure  $F/D$  in the Gulf area is 3 for a feed concentration of 46,000 ppm, and maximum allowable concentration of 69,000 ppm. Also the amount of vapor directed to the condenser  $D_f$  is determined by the sea water temperature. In Kuwait, the seawater design temperature in summer and winter can be taken as 10°C, and 28°C respectively. So, for  $T_f = 50^\circ\text{C}$ , and  $F/D = 3$ ,  $D_f/D$  can be obtained, from  $(D_f/D)L = F/DC(T_f - T_c)$ , and it ranges from 0.1133 in summer to 0.206 in winter.

The availability gain by the feed in the condenser,  $A_{c,l}$  due its heating from  $T_c$  to  $T_f$  is

$$A_{c,g} = FC [(T_f - T_c) - T_o \ln T_f/T_c] \quad (5a)$$

and the availability loss by the heating steam  $D_f$  is

$$A_{c,l} = D_f L (1 - T_o/T_{vl}), \quad (5b)$$

and the availability destruction in the condenser is

$$\Delta A_c = A_{c,l} - A_{c,g} = D_f L (1 - T_o/T_{vl}) - [FC(T_f - T_c) - T_o \ln T_f/T_c] \quad (5)$$

(c) **Steam Ejector**

The steam ejector is the heart of the thermo vapor desalter. The motive steam (at high pressure) energizes the ejector to induce the part of the vapor generated to be compressed,  $D_r$  from its pressure from  $P$ , (evaporator pressure) at saturation temperature  $T_{vl}$  to the ejector discharge pressure  $P_d$  (equal to the evaporator heating condensing vapor side pressure). The motive steam is expanded through high pressure ratio converging-diverging nozzle to a high velocity see fig. 4. For a saturated motive steam at pressure of 25 bar (2500 kPa); and evaporator saturation temperature of 60°C ( $P_e = 19.941$  kPa), the nozzle pressure ratio is  $2500/19.94 = 125.37$ . The high velocity at the nozzle exit can be calculated, for



a nozzle efficiency of 0.9, by:

$$V_{ne} = \sqrt{2(h_s - h_{ne})} = 2\sqrt{(h_s - h_{nes})\eta_n} = \sqrt{2 \times (2803.1 - 2059.157) \times 1000 \times 0.9} = 1157.2 \text{ m/s}$$

where the enthalpies of the steam at the nozzle inlet  $h_s = 2803.1$  kJ/kg and nozzle outlet if the expansion is isentropic is  $h_{nes} = 2059.157$ , and  $h_{ne} = 2133.55$  kJ/kg is the actual enthalpy at the nozzle outlet and at wetness fraction of 20.2%. The high velocity steam issuing from the nozzle entrains the water vapor leaving evaporator and the two streams merge in a mixing section of conical shape of converges in the direction of flow. The kinetic energy of the mixture is recovered by decelerating its usually supersonic velocity to the exit velocity in constant area throat section following the Mixing section, and then in diverging diffuser.

A commonly used measure of ejector effectiveness of compression is

$$\eta_{ej,c} = \frac{(h_d - h_e)(S + D_r)}{S(h_s - h_{nes})} \quad (6)$$

where  $(S + D_r)(h_d - h_e)$  represents the actual compression energy recovered from the nozzle exit to the diffuser exit; and  $S(h_s - h_{nes})$  is theoretical energy available in the motive steam.

For the typical case conditions mentioned earlier as an example of 25 bar saturated motive steam condition, 60°C saturation temperature vapor generated, 125 nozzle expansion ratio, and 65°C saturation temperature of ejector discharge pressure,  $S/D_r = 0.25$ ,  $h_s = 2803.1$  kJ/kg,  $h_e = 2609.6$ ,  $h_d = 2648.3$ ;  $h_{sne} = 2059.1569$  kJ/kg, the ejector effectiveness for compression  $\epsilon_{ej} = 0.26$ . The low value of  $\epsilon_{e,c}$  indicates the inefficiency of the ejector in transforming available energy to compression energy.

The value of  $S/D_r$  is a function of both the motive steam expansion ratio (i.e.  $P_{steam}/P_{suction}$ ), and the compression ratio (i.e.  $P_{discharge}$  from steam ejector divided by the  $P_{suction}$ ). The relation between SID, expansion ratio, and compression ratio is given in fig. 5 taken from Power [3].

The process occurred in the steam ejector is outlined in both T-S diagram in fig.4. The energy balance for the steam ejector used to calculate  $h_d$  is given by

$$(S + D_r)h_d = Sh_s + D_e h_e$$

Although the summation of the inlet stream enthalpies is equal to the enthalpy of

the discharged stream (i.e no energy loss), it is inherently inefficient process from work or availability view point. As shown earlier, the ejector effectiveness in transferring the theoretical maximum work that can be obtained from expanding the steam in the nozzle,  $S(h_s - h_{sne})$  into the compressing work of the vapor is very low. A better evaluation of the effectiveness of the ejector can be expressed by the availability analysis/ (or, second law analysis), i.e.

$$\epsilon_{ejector,2} = \frac{\text{availability gain by the compressed vapor}}{\text{availability loss by the motive steam}}$$

An availability analysis for the steam ejector is in order now. The availability loss by the motive steam,  $A_{ej1}$ , can be expressed by

$$A_{ek,1} = S[(h_s - h_d) - T_o(S_s - S_d)] \quad (7a)$$

and the availability gain by the compressed vapor,  $A_{ek2}$  is equal to

$$A_{ej,g} = D_r [(h_d - h_e) - T_o(S_d - S_e)] \quad (7b)$$

The availability destruction by the steam ejector  $\Delta A_{ej}$  is expressed by

$$\Delta A_{ej} = A_{ej,1} - A_{e,g} \quad (7)$$

and the ejector effectiveness  $\epsilon_{ej}$

$$\epsilon_{fej} = \frac{A_{ej,2}}{A_{ej,1}} \quad (8)$$

For the typical example mentioned earlier  $\epsilon_{ej,2} = 0.27$

#### d) Overall system

The overall system energy balance can be considered as follows: The main energy consumption by the system,  $Q_{iv}$  is

$$Q_{in} = S(h_s - h_{df}) \quad (9)$$

and the specific energy consumption for a unit distillate  $q_{in}$  is  $Q_{in}/D$ ,

$$q_{in} = S(h_s - h_{df})/D = (h_s - h_{df})/GR$$

The first law energy balances for the system can be given by

$$S(h_s - h_{df}) = D_r h_{df} + D_f h_f + (F - D)h_b - F x h_c \quad (10)$$

The availability analysis gives:

The specific available energy consumed by the system is the motive  $\Delta a_s$

$$\Delta a_s = \frac{S}{D} [(h_s - h_{df}) - T_o (S_s - S_{df})] \quad (11)$$

This parameter  $\Delta a_s$  should be compared with the available energy consumption (or work consumption) of any other desalting system.

Also the motive steam availability loss

$$S [(h_s - h_{df}) - T_o (S_s - S_{df})] \quad (12)$$

is due the availability destruction in all ejector; evaporator and condenser plus the availability of the leaving streams. The availability of the leaving streams  $D_r$ ,  $D_f$  and  $B (F - D)$  can be expressed as follows; if the seawater availability is considered equal to zero, i.e.  $T_c - T_o$ ;

$$A_{Dr} = D_r [(h_{df} - h_e) - T_o C_w l_n \frac{T_{df}}{T_c}]$$

$$A_{Dr} = D_r C_w [(T_{fd} - T_c) - T_o l_n \frac{T_{fd}}{T_c}] \quad (13)$$

$$A_{Df} = D_f C_w [(T_e - T_c) - T_o l_n \frac{T_e}{T_c}] \quad (14)$$

$$A_B = (F - D) C_b [(T_e + \varepsilon - T_c) - T_o l_n \frac{T_e + \varepsilon}{T_c}] \quad (15)$$

## MULTI EFFECT-THERMO VAPOR COMPRESSION SYSTEM

In multi effect thermovapor compression system, the motive steam at medium pressure is used to compress some of the vapor generated in the last evaporator (effect at the lowest temperature) by the steam ejector in order to be used (along with the expanded motive ) as a heating source. The motive steam and compressed vapor leaving the steam ejector are condensed in the first and highest temperature effect. Part of condensate returns to the boiler and the other joins the product water. The energy consumption of TVC varies considerably with the temperature difference across the heat transfer area in the evaporator (and

consequently the pressure drop across the evaporators), temperature level in the evaporators and the state condition of the motive steam as shown in the last example. The main features of two commercially available TVC systems are given in Table 1. The TVC system can use much smaller heat transfer surface areas than both MSF and ME systems with the same gain ratio or energy consumption. The initial capital cost (for both equipment and civil work) of this thermo vapor compression system would be significantly lower than that of an MSF system.

Since the design of the multi-effect-thermo-vapor compression desalting system is not well known, Darwish et al [4], it is outlined here through an example. The system considered in the design example is similar to the four units of 1 MIGD capacity each, built by Sidem in the western remote area of Abu Dhabi in UAE [1]. Each unit has four effects and an end condenser. It is directly operated by a boiler generating saturated steam of 25 bar pressure. The flow sheet of the system is given in fig. 6. The top brine temperature,  $T_1$ , (at about 58.80°C in the first effect;  $P_1 = 0.18159$  bars), and last effect temperature  $T_4$  (at about 46.80°C;  $P_4 = 0.1$  bar) are carefully chosen to keep low compression ratio (steam ejector discharge to suction pressures). The system design can be outlined as follows:

(1) Suppose the vapor generated in the first, second and last  $i$  effects (at pressures  $P_1, P_2, P_3, \dots, P_n$ ) are  $D_1, D_2, \dots$  and  $D_n$ , respectively. The vapor generated in the first effect,  $D_1$ , (at  $P_1$ ) is directed to the second effect where it condenses. This vapor  $D_1$  acts as a heat source and heats the feed  $F_2$  to that effect from the feed temperature,  $T_f$  to its boiling temperature,  $T_2$ , and generates vapor by boiling at a rate almost equal to  $D_2$  ( $P_2$ ). Similarly, the vapor generated in an effect  $i$  (i.e.  $D_i$ ) is used as a heat source for the next effect ( $i+1$ ) and so on to the last effect. The vapor generated in the last  $n$  effect,  $D_n$ , is divided to  $D_r$  and  $D_f$ . The stream  $D_r$  is directed to the steam ejector where it is recompressed and returned to the first effect, along with the motive steam  $S$ , as a heating medium. The stream  $D_f$  is directed to an end condenser where it condenses and heats the seawater feed from seawater temperature  $T$ , to the feed temperature  $T_f$ .

(2) The rate of seawater feed to each effect, say  $F_i$  to an effect  $i$ , is determined by the seawater salt concentration in that locality  $X_f$  and the maximum allowable brine salt concentration  $X_b$ , according to  $F_i/D_i = X_b/(X_b - X_f)$ . As an example, if  $X_f = 46,000$  ppm, and  $X_b = 69,000$  ppm, then  $F_i/D_i = 3$ .

The brine leaving the first effect,  $B_1 = F_1 - D_1$ , is directed to the second effect, where its temperature is spontaneously decreased from  $T_1$  to  $T_2$  (where  $T_1 - T_2 = \Delta T$ ) by flashing part of this brine equal to  $B_1 C \Delta T / L$  into a vapor in the second effect. Similarly the brine leaving the second effect  $B_2 = (F_1 - D_1) + (F_2 - D_2)$  is directed to the third effect and so on to the last effect. The brine leaving the last

effect  $B_n$ , is the brine blow-down and is equal to

$$B_n = (F_1 - D_1) + (F_2 - D_2) + \dots + (F_n - D_n) \sum_{i=1}^n (F_i - D_i)$$

(3) Energy and Availability Analysis

Energy balances and availability loss for the steam ejector, effects and end condense are similar to that conducted for single effect case.

(i) Steam ejector

$$Sh_s + D_r h_{gn} = (S + D_r)h_d$$

$$\Delta A_{ej} = S[(h_s - h_d) - T_o(S_s - S_d)] - D_r[(h_d - h_{gn}) - (S_d - S_{gn})]$$

where  $h_s$ ,  $h_{gn}$ , and  $h_d$  are the specific enthalpies of motive steam, saturated vapor generated in the last (or  $n$ ) effect, and vapor discharged from the steam ejector respectively. The ratio of the motive steam to the recompressed vapor  $S/D_r$ , depends on the expansion ratio,  $P_s/P_n$  and compression ratio,  $P_d/P_n$ , as shown in fig. 5 [7]. Here  $P_s$ ,  $P_n$ , and  $P_d$  are the pressures of the motive steam, last effect (suction pressure), and discharge pressure.

(ii) First effect

$$(S + D_r)(h_d - h_{fd}) = F_1 C (T_1 - T_f) + D_1 L_1$$

$$\Delta A_{e1} = (S + D_r)[(h_d - h_{fd}) - T_o(S_d - S_{fd})] - FC[(T_1 - T_f) - T_o \ln T_f/T_1]$$

where  $h_d$  is the specific enthalpy of the  $(S + D_r)$  condensate leaving the first effect. Part of this condensate,  $S$ , is returned to the boiler, while the balance  $D_r$ , represents part of the distillate product.

(iii) Second effect

$$D_1 L_1 + (F_1 - D_1) C (T_1 - T_2) = F_2 C (T_2 - T_f) + D_2 L_2$$

$$\Delta A_{e2} = D_1 L_1 (1 - T_o/T_1) + (F_1 - D_1) C [(T_1 - T_2) - T_o \ln T_f/T_1]$$

$$- D_2 L_2 (1 - T_o/T_2) - F_2 C [(T_2 - T_f) - T_o \ln \frac{T_2}{T_f}]$$

where the flow rates  $D_1$  and  $(F_1 - D_1)$  are the heating vapor and brine entering the second effect from the first effect, while  $F_2$  is the feed to the second and  $D_2$  is the vapor generated in the second effect by both boiling and flashing, (i.e.  $D_2 = D_{f2} + D_{b2}$ ) where

$$D_{f1} = (F_1 - D_1)C(T_1 - T_2)/L$$

$$D_{f2} = \frac{L_2}{L_1} [D_1 L_1 - F_2 C(T_2 - T_f)]$$

(iv) An *i*-effect  $D_{i-1} L_{i-1} + [(F_1 - D_1) + (F_2 - D_2) + \dots + (F_{i-1} - D_{i-1})] C \Delta T = F_i C(T_1 - T_f) + D_i L_i$

$$\Delta A_{ei} = D_{i-1} L_{i-1} (1 - T_o/T_{i-1}) + (\sum_{n=1}^{i-1} (F_n - D_n)) C [DT - T_o L_n \frac{T_{i-1}}{T_i}] -$$

(v) End Condenser:

$$D_f L_n = M_c (T_f - T_c) C$$

$$\Delta A_c = D_f L_n (1 - \frac{T_o}{T_n}) - M_c C [(T_f - T_c) - T_o L_n (T_f/T_c)]$$

where  $D_f$  is the part of  $D_n$  directed to the end condenser, and  $M_c$  is the cooling water to the condenser. It is noticed here that in order to keep  $T_f$  constant,  $M_c$  should be varied according to the cooling seawater temperature  $T_c$ . As a typical example,  $T_c$  can vary from 16°C in winter to 32°C in summer. Part of  $M_c$  represents the feed,  $F$  to all effects,

The total product distillate output is equal to

$$D = \sum D_i = D_1 + D_2 + \dots + D_n$$

It is noticed here that part of the vapor generated in the last effect,  $D_n$  is condensed in the end condenser,  $D_f$ , and the balance  $D_r$  is extracted by the ejector i.e.  $D_n = D_r + D_f$

As a numerical example for a four-effect, thermally driven vapor compression unit of 1 MIGD (i.e. 4545 m<sup>3</sup>/d = 52.6 kg/s) distillate operating with the data given in tables 4 and 5, the vapor saturation temperature and corresponding pressures and latent heats of the steam ejector delivery and in effects are given as follows.

The motive steam is assumed to be saturated vapor at 25 bar, where  $h_g = 2802.2$  kJ/kg and  $h_f = 962.2$  kJ/kg.

The expansion ratio (25/0.1009) of 250, and compression ratio (0.21851/0.1009) of 2.165 give  $S/D_r = 0.86$  from Fig. 9.

The calculations give the following values when  $T_f$  is assumed equal to 40°C,  $h_d = 2685.1$  kJ/kg and the flow rates in kg/s are

$$D_r = 8, S = 6.88, D_1 = 14, D_2 = 13.2, D_3 = 12.86, D_4 = 12.56$$

$$F_2 = 42, F_2 = 39.6 ; F_3 = 38.58, 4 = 37.68, F = 157.86 \text{ and } D_F = 6.$$

$$D = D_1 + D_2 + D_3 + D_4 = 52.6 \text{ kg/s.}$$

The maximum temperature increase of the cooling water in the end condenser (when  $M_c = F$ ) can be calculated by

$$D_f \times L_n = F C (T_f - T_c); T_f - T_c = 21.75 \text{ C}$$

This shows that to keep fixed feed temperature  $T_f$  say 40°C, and seawater temperature 18.25°C, the seawater supply to the end condenser should be equal to the feed ( $F = 3D$ ). When the seawater temperature is increased, cooling seawater supplied to the end condenser should be increased. In this case, part of this cooling water represents the feed,  $F$ , and the other part ( $M_c - F$ ) should be rejected to the sea. As an example, if the seawater temperature is 30°C;  $M_c = D_f L_n / C(T_f - T_c) = 343.28$  kg/s. Part of  $M_c$  is  $F$  157.86 and the balance (185.42 kg/s) is rejected back to the sea.

The ratio of the distillate to the steam, that may be named Gain Ratio (GR) is 7.65. This may not simply be compared with GR of an MSF unit supplied with steam extracted at low pressure of 2 bar, say, while the steam pressure here is 25 bar. The thermal energy consumption to produce 1 kg of desalted water is  $SL/D = 332.42$  kJ/kg and the mechanical energy consumption is in the range of 5-6 kJ/kg.

## RESULTS AND DISCUSSION

It is clear that the temperature difference across the evaporator  $\Delta T_e$  is the main factor affecting the performance of the TVC system. The decrease of this temperature (saturation temperature of the recompressed heating vapor minus the boiling temperature of the evaporating feed) can be achieved by increasing the heat transfer area of the evaporator and/or increasing the heat transfer coefficient inside the evaporator.

- (1) In the case of the single effect TVC system, the decrease of  $\Delta T_e$  increases the heat consumption per unit distillate and the ratio of distillate per unit mass of the motive steam ( $D/S$ ) see fig. 7. The value of  $D/S$  is increased from 1.2 for  $\Delta T_e = 16$  K to 8 for  $\Delta T_e = 2$  K.

The later case of  $D/S = 8$ , and specific heat consumption of 315 kJ/kg distillate corresponds to the typical case of all multi stage desalting (MSF) units operating in Kuwait or a conventional multi effect (ME) desalting system of at least 10 effects. However, it is noticed here that the availability of the motive steam supplied to the TVC at 20 bar for example is higher than that required for MSF or conventional ME system of 1.25 bar for example. For saturated steam at 20 bar, and 1.2, the available energy difference when both condensed to saturated liquids are 730 kJ/kg and 479 kJ/kg. If both systems (MSF and TVC) are directly operated by a boiler, there should be no concern on the available energy consumed. However, if both systems are operated by steam extracted from cogeneration steam turbine, the loss of this steam turbine work when steam is extracted at 20 bar is much higher than that extraction at 1.25 bar.

It is noticed here also that the value  $D/S$  has no direct relation with the number of the effects as in the conventional ME system. Here for one effect,  $D/S$  of 8 can be achieved.

(2) The decrease of  $\Delta T_e$ , increases the heat transfer area of the evaporator (and that of the whole system) and consequently the unit cost. See fig. 8. The increase of the evaporating temperature from 60 to 62, for heating condensing vapor of 65°C increases the specific heat transfer area required in m<sup>2</sup> per (kg/s distillate) from 185 to 370.

(3) The main availability destruction occurs in the evaporator and the steam ejector as shown in fig. 9. So, real improvement in this system lies in better designs of steam ejectors and evaporators. For the typical case of  $T_{v1} = 60^\circ\text{C}$ , and  $T_{v2}$  of 65°C, the specific availability loss (per kg of distillate) by evaporator steam ejector, and condenser are 41.7, 96.0, and 21 respectively.

(4) The system outlined in fig. 6 can be more efficient if the heat content of the leaving brine and distillate steam are utilized in heating the feed to the system; and the feed to the first effect is regeneratively heated as outlined in fig. 10. However, the extra cost of using preheaters for the feed (usually plate type heat exchangers), and the complexity of adding regenerative heaters between the effects should be accounted against the reduction of steam cost gained by increasing the system efficiency.

(5) The temperature of the generated vapor in the 4 effects units shown in fig. 6 are 56, 54, 50, and 46°C. By assuming an average of 1°C as boiling point elevation, the real temperature difference across the heat transfer area in each effect is 3°C. If more two effects are added for the same saturation temperatures of the first and last effects, the value of  $D/S$  would stay the same while  $\Delta T_e$  will be reduced to 2°C. The new six effect units would give about 50% more distillate



for almost the same steam consumption and consequently the gain ratio  $D/S$  become little less than 150% of the original  $D/S$ . However, the disadvantage of doing that is the addition of two more effects, and each effect heat transfer area would increase more than 50% of the original area. This mean that total heat transfer evaporator would be more than doubled.

(6) The available energy consumption per unit distillate represent the theoretical maximum work that can be obtained from the motive steam if it is used to produce power by theoretically reversed heat engine. The equivalent work of this available energy can be obtained by multiplying its value by a reasonable isentropic efficiency of  $\eta_s = 0.75$ . This equivalent specific work ( $\eta$  x specific available energy) can be compared with the specific work,  $w_s$ , of other mechanically driven desalting system like reverse osmosis (typical  $w_s = 50$ ), and mechanical vapor compression system (typical  $w_s = 60$ ). The specific equivalent work of the 4 effect TVC system shown in fig. 6, is 87.5). We should mention here that the figures of  $w_s$ 's are typical figures and the real value of  $w_s$  depends on the design of each system.

## REFERENCES

1. T. Michaels, "Recent Achievement of Low Temperature Multiple Effect Desalination in Western Areas of Abu Dhabi, UAE", Desal 92 Proc. Arabian Gulf Regional Water Desalination Symposium, 15-17 Nov. Al Ain, UAE.
2. C. Temstet, G. Canton, J. Laborie, and A. Durante, "A Large lbggh-Performance MED Plant in Sicily", Desalination 105 (1996) 109-114.
3. Power, "Steam Jet Ejectors for the Process Industries", McGraw-Hill, Inc., N.Y, 1994.
4. A. Darwish and H. El-Dessouky, "The Heat Recovery Thermal Vapor Compression Desalting System: A Comparison with Other Thermal Desalination Processes", Applied Thermal Engineering, Vol. 16, No. 6, pp. 523-537, 1996

**Table 1: Features of two commercially available thermal vapour-compression (TVC) systems**

Main Data	Sidem, UAE [1]	Sidem, Sicily [2]
Capacity, tons/day (kg/s)	4500 (52.6)	9000 (104.17)
Motive steam, kg/h (kg/s)	25 (6.94)	22.5 (6.11)
Gain ratio, D/S	8	16.7
Steam supply conditions		
Pressure (bar)	25	45
Temperature (°C)	224	257
Energy consumption, kJ/kg	330	148.8
Available energy consumption, kJ/kg	116.58	58.7
Equivalent mechanical work	87.5	64.3
Specific fuel consumption, kJ/kg ( $\eta_b=0.85$ )	388	175
Number of effects	4	12
Mechanical accessory power consumption, kwhr/m <sup>3</sup>	2	1

**Table 2: 4-Effect Thermo-vapour-compression example data**

	Delivery	Effect 1	Effect 2	Effect 3	Effect 4	Total
$T$ , °C	62	58	54	50	46	
$P$ , bars	0.21851	0.18159	0.15012	0.12344	0.100938	
$L_i$ , kJ/kg	2353.7	2363.3	2372.24	2381.87	2391.5	
$D_i$ (kg/s)	$S+D_r=14.88$	14	13.2	12.86	12.56	52.6
$F_i$ (kg/s)		42	39.6	38.56	37.68	157.86
enthalpy, kJ/kg	$h_s=2802.2$	$h_d=2685.1$	$h_{d1}=259.5$		$h_{g4}=2585$	
entropy, kJ/kgK	$s_s=6.257$	$s_d=8.081$	$s_{d1}=0.8561$		$s_{g4}=8.147$	

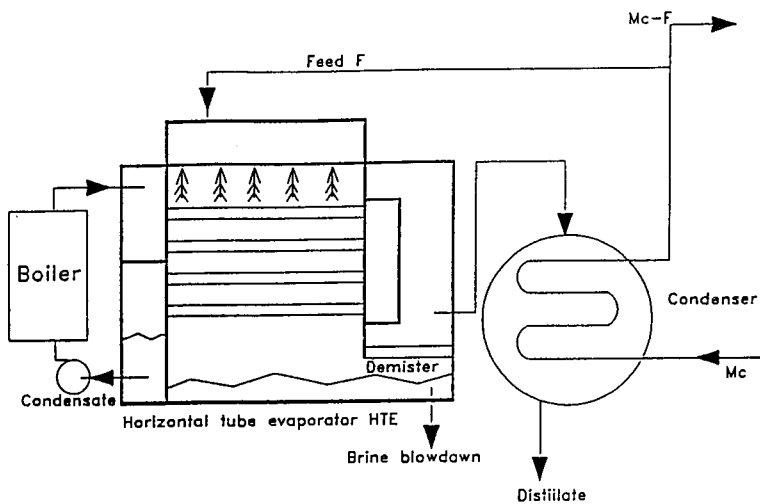


Fig. 1: Conventional single effect desalting system

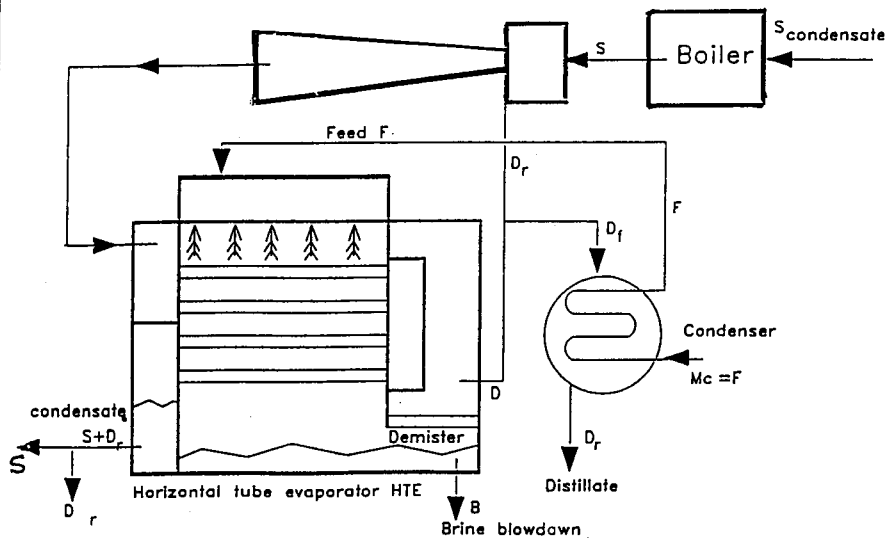


Fig. 2: Thermovapor single effect desalting system

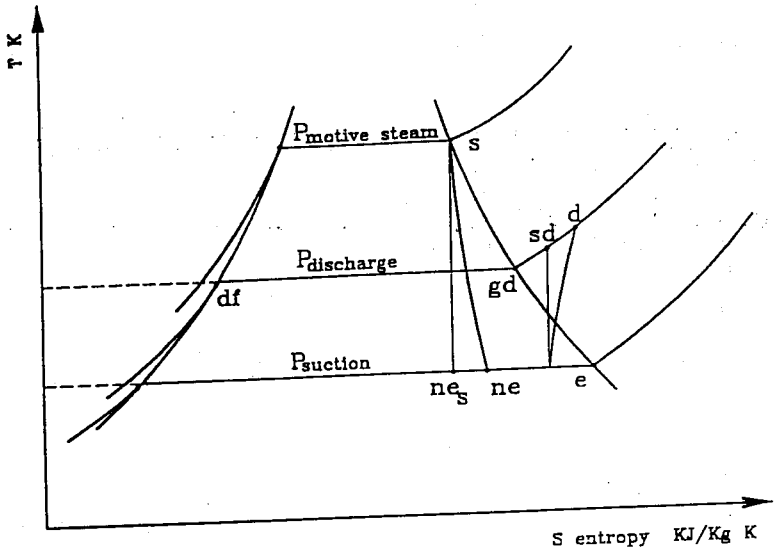


Fig. 3: Typical thermovapor compression process and steam ejector process represented on T-S diagram.

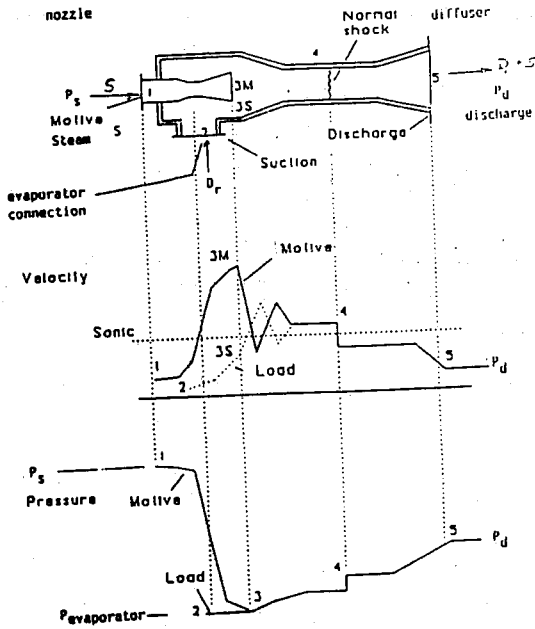


Fig. 4: Schematic diagram of a steam ejector with variation of both velocity and pressure.

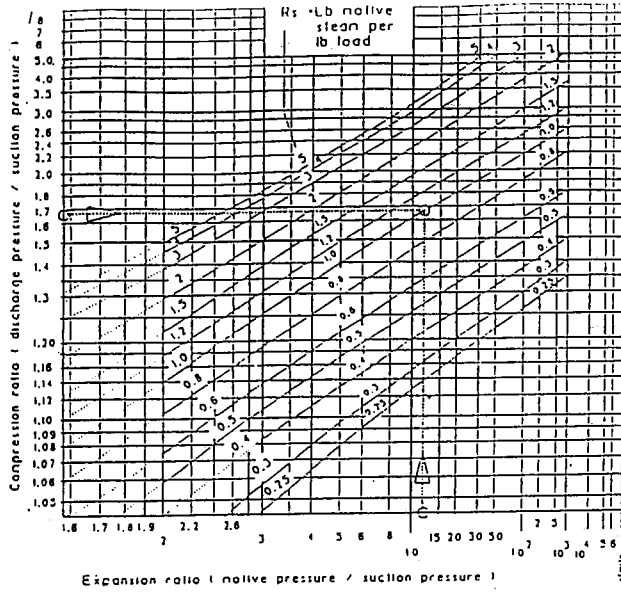


Fig. 5. Ratio of motive steam to entrained vapor as function of both expansion and compression ratio, Power [5]

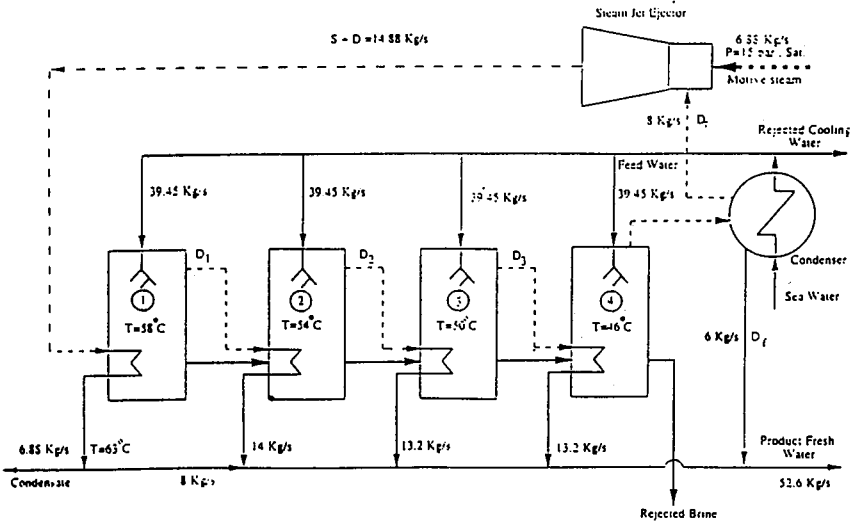


Fig. 6: Schematic diagram of 4 effect thermovapor desalting system similar to that outlined in Ref. 1.

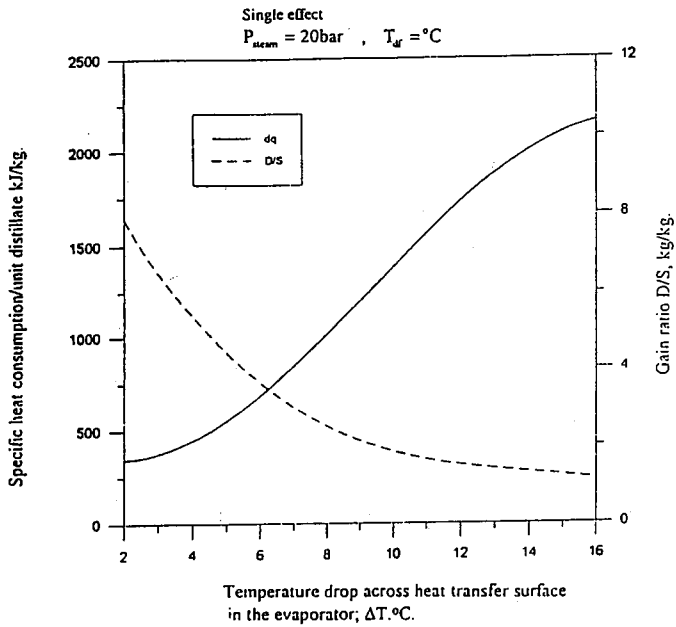


Fig. 7 Specific heat consumption per unit distillate and gain ratio  $D/S$  as function of temperature drop across the evaporator heat transfer area

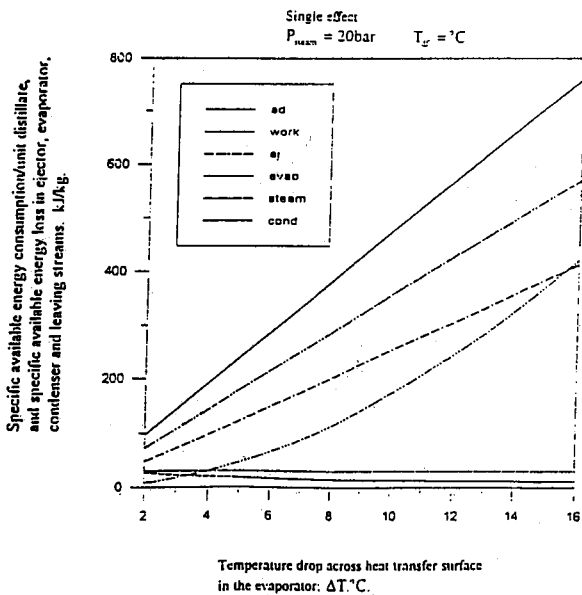


Fig. 8: Specific available energy loss in steam ejector, evaporator, condenser, and leaving streams, and available air consumption per unit distillate as function

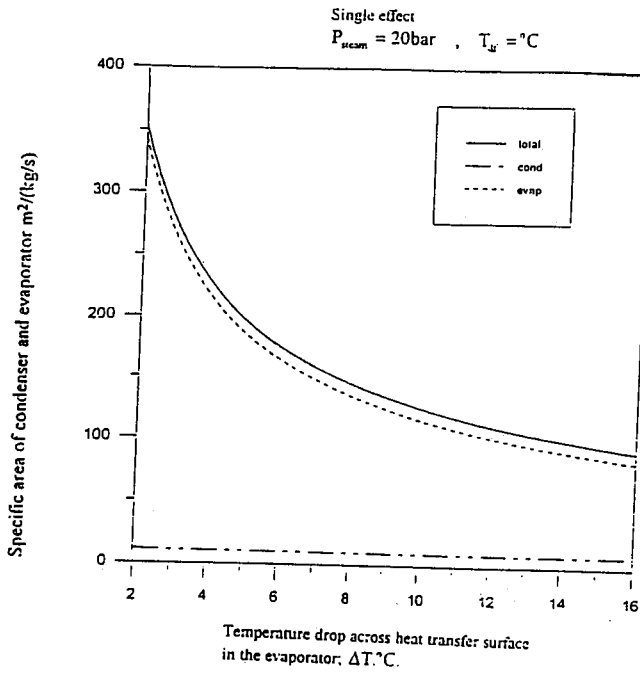


Fig. 9 : Specific heat transfer area requirement for both evaporator and condenser as a function of the temperature drop across heat transfer surfaces of the evaporator.

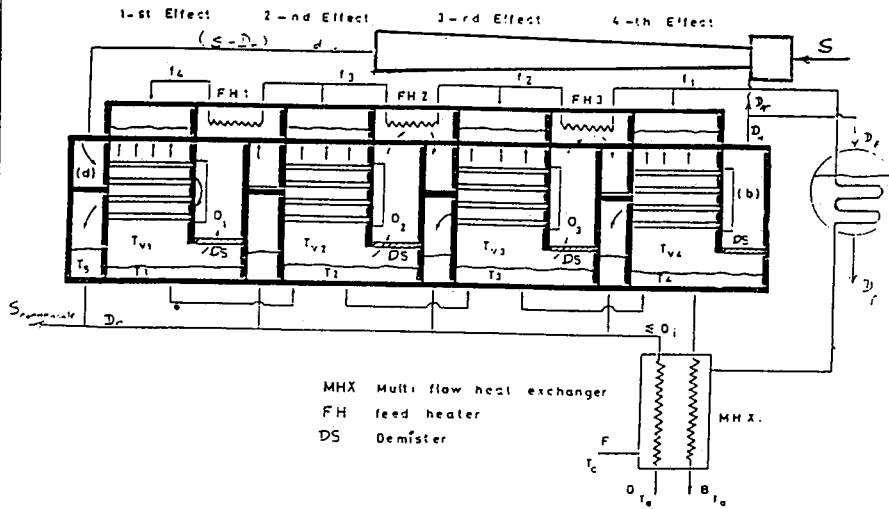


Fig. 10: Modified 4-effects TVC system with regenerative feed heaters and feed preheater by distillate and brine streams.

**Experience with the Three Different Cogeneration  
Arrangements at Al-Ghubrah Power and  
Desalination Station**

*A.R. Abu Dayyeh, Ridhi Hamdan, Wasfi F. Zaki,  
Salah Abunayib and Joshua Mathew*



# **EXPERIENCE WITH THE THREE DIFFERENT COGENERATION ARRANGEMENTS AT AL-GHUBRAH POWER & DESALINATION STATION**

**A.R. Abu Dayyeh, Ribhi Hamdan, Wasfi F. Zaki, Salah Abunayib &  
Joshua Mathew**

Sogex - Oman, Ghubrah Power & Desalination Station  
Sultanate of Oman.

## **ABSTRACT**

Ghubrah Power and Desalination Station, located 20 Km west of Muscat City, Sultanate of Oman, has undergone four construction phases since its inception in 1976. Ghubrah is still expanding as Phase V is under construction and is expected to come into commercial production by the beginning of 1997. The existing plant has an installed capacity of 509 MW Power and 29 MIGPD of Desalinated water. Around 60% of the power is generated from cogeneration while the remaining 40% power is from peaking Gas Turbine units. The cogeneration plant mainly consists of five MSF desalination units, four condensing / extracting steam turbines, one back pressure steam turbine, seven fuel fired boilers, two frame 9 gas turbines with two waste heat recovery boilers and two auxiliary boilers. The peaking gas turbines are nine frame 5 and two frame 6 units. This study discusses the method used for fuel allocation between Power and Water and the energy based efficiencies applied for the three different cogeneration configurations at Ghubrah i.e. condensing / extracting steam turbines, back pressure steam turbine and the gas turbine with waste heat recovery boilers. It also addresses the practical operational aspects of the three different cogeneration arrangements.

## INTRODUCTION

The fact that dual purpose power / water plants are of considerable cost economy compared to single purpose plants, has become one of the basics. However, the division of the total overall cost between power and water is not yet settled as there are several energy and exergy based methods. These different methods are, of course, contributing to the prime aim of arriving at some standard method. Privatisation which has already started in the field of power in Oman, may make the need for standardization more necessary.

The major portion of the total cost of power and desalinated water production is the fuel cost. In 1995, Ghubrah Power and Desalination Station fuel cost for power generation was 68.6% of the total power cost and fuel cost for water production was 42.8% of total water cost [Ref. 1]. This paper presents the methods used for fuel allocations for the three different cogeneration configurations at Ghubrah Power and Desalination Station and also discusses the practical operational aspects of these three configurations. The recent Phase-IV extension is two x 95 MW gas turbine units with two waste heat recovery boilers (WHRB) which utilize the exhaust heat of the gas turbine units to supply steam to two x 6 MIGPD existing MSF Desalination Plants (Phase-II) which were earlier getting steam from fuel fired boilers. This resulted in a considerable decrease in the amount of fuel consumed by Phase-II fired boilers during the year 1995, which brought to the surface the argument that the steam for Phase-II desalination units from the WHRBs is fuel cost free which necessitated reviewing of the fuel allocation method.

## PLANT DESCRIPTION

Ghubrah Power and Desalination Station is a cogeneration plant with installed capacity of 509 MW power and 29 MIGPD desalinated water. Ghubrah power plant along with Rusail Power Station, which is six x 83 MW Gas turbine units, meet the power demand of the Muscat region. Ghubrah desalination plant is the major drinking water source for the capital Muscat. Since its inception 1976 Ghubrah has undergone four extension phases which can be described as follows:

### Phase-I

This can be divided into two main areas. One is the peaking Gas Turbine units area which is nine x 17.5 MW and two x 27 MW simple cycle gas turbine units. The other is the cogeneration power / water plant (Fig. 1a) which consists mainly of:

- Steam Generating Plant :

These are water tube, dual fuel fired boilers. Three units are 80 t/hr. capacity each at 30 bar and 380°C and the other three units are 150 t/hr. capacity each at 50 bar and 480°C.

- Steam Turbine Alternators :

Three x 8.5 MW and one x 50 MW extracting / condensing type steam turbine units.

- Desalination Plant :

One x 5 MIGPD long tube and one x 6 MIGPD cross tube MSF desalination units. Process heat energy for desalination is mainly from steam turbine extraction. Low pressure steam reducing stations are provided as by-pass for the steam turbine extraction to ensure continuous supply of process steam for desalination in case of low load or outage of steam turbines.

### Phase II / IV

Phase-II and Phase-IV together form one cogeneration plant (Fig. 1b). Phase-II was first commissioned in 1986 as a single purpose desalination plant consisting of two x 6 MIGPD MSF desalination plants and two fuel fired medium pressure water tube boilers. Phase-IV, commissioned in the summer of 1995, consists of two x 95 MW gas turbine units and two WHRBs which utilize the exhaust heat from the gas turbines to generate medium pressure steam for Phase-II desalination plants. Phase-II fuel fired boilers are now rendered as auxiliary boilers for this cogeneration plant.

### Phase-III

Phase-III cogeneration plant (Fig. 1c) commissioned in 1993, consists of one x 30 MW Back Pressure Steam Turbine (BPT), one x 6 MIGPD MSF desalination plant and one fuel fired water tube boiler of 230 t/hr. MCR at 60 bar, 485°C. Desalination process energy is mainly from the BPT exhaust with by-pass steam pressure reducing station to ensure supply of steam to the desalination plant during low load or outage of the BPT. On the other hand, a dump condenser is provided to admit the exhaust steam during low load or outage of the desalination plant and hence the BPT can remain in operation as per the system power requirement.

In all of the five desalination plants at Ghubrah, the Brine Recirculation Pumps (BRP) are driven by back pressure steam turbines, the exhaust of which is connected to the low pressure line entering the respective Brine Heater.

## **LOAD VARIATION**

It is known that the total cost of both Power and Desalinated water decrease as the Power and Desalination plants are run at or close to their full capacities. Another cost effective factor is to maintain the maximum heat energy required for desalination, from the cogeneration cycle and not directly from fuel fired boilers.

Water demand is relatively constant and it is also buffered by a big storage system. This allows all Ghubrah desalination plants to be run continuously at their full capacity except during winter when they are released one at a time for annual maintenance.

The power demand, however, does not have this flexibility. Power demand, which is mainly air conditioning, varies drastically between summer and winter and again between day and night as shown in Fig. 2. The power system maximum and minimum demand are both critical. The maximum demand, which influences stability, can absorb all the existing installed power capacity with little or no spinning reserve. On the other hand the minimum demand, which influences efficiency, falls down to only 25% or less of the maximum. The minimum power demand adversely affects both power and water costs. During minimum demand some of the big capacity machines (Ghubrah Phase-IV and Rusail Power Station) are shutdown and some are run at low loads which results in low generation efficiency. Again, the shutdown or low load of Ghubrah Phase IV requires supplementing steam to Phase II/IV desalination plants from the auxiliary boilers which increases water cost.

As shown in Fig. 3 the minimum demand trend is not encouraging as its annual rate of increase is very minimal compared to rate of increase of the maximum demand. The annual rate of increase in the maximum demand is 8 to 10%, whereas the annual rate of increase in the minimum demand is only 3 to 5%.

## **PHILOSOPHY OF OPERATION**

The general operation philosophy is as follows :

- The desalination plants are kept continuously on full production except when shutdown for forced or planned outage.
- To stabilize the power system, a spinning reserve of 95 MW (the biggest machine capacity) is maintained as far as possible.

- To ensure higher efficiency, the power system base load machines are Ghubrah cogeneration plants (Phase-I, II/IV and III) and Rusail Power Station.
- The hourly load variation is met with by starting or stopping one or more of Ghubrah peaking gas turbines (GT/A # 1 to 11).
- The main fuel is Natural Gas and a standby fuel source is Distillate Oil.
- Annual maintenance of the main equipment is during winter.

## **OPERATIONAL ASPECTS**

### Phase I

Of the three cogeneration configurations at Ghubrah, Phase-I has the maximum flexibility due to the large number of boilers, the interconnections between the steam headers and the inherent flexibility of the extracting type steam turbines in supplying process steam for desalination at different loads. Even when any one of the boilers is shutdown both desalination units and the steam turbines can be run at their full load. Also when any of the ST/A's is out of service the desalination units can have full production by using the steam reducing stations.

The medium power capacity of this arrangement is slightly affected by the minimum system power demand as during winter, the load on ST/A #4 need to be reduced.

### Phase II/IV

This arrangement has the flexibility that the GT/A's can run at their full capacity even when desalination units are shutdown or when the WHRB's are out of service by using the flue gas by-pass stack. Also desalination units can run at their full capacity by utilising the auxiliary fuel fired boilers in the event of GT/A or WHRB is not available.

One of the limitations is that during the start-up of the WHRB the respective GT/A load should not be more than 40 MW. Another limitation is that due to its larger power capacity Phase-II/IV is the most affected by the power system minimum demand factor. During system minimum demand the GT/A's may have to run at 50% or less of their base load and thus curtailing the steam generation from the WHRBs which will be supplemented by the auxiliary boilers with additional fuel consumption.

### Phase III

In this cogeneration arrangement also there is enough flexibility as the desalination unit can run at its full capacity during low load or outage of the BPT by using the steam reducing stations. On the other hand the provision of the dump condenser makes it possible to run the BPT at any load during the outage of the desalination plant. Phase III is the least affected by the system minimum demand due to its low power capacity that can be easily absorbed by the system.

However as presently there is only one boiler, in the event of boiler outage both desalination and BPT are rendered non available. This limitation will be lessened after the completion of Ghubrah Phase V extension (one x 30 MW BPT, one x 6 MIGPD MSF desalination unit and one fuel fired water tube boiler of 230 t/ hr. MCR at 60 bar, 485°C) which is going to be inter-connected with Phase III.

### **FUEL ALLOCATION AT GHUBRAH**

The method used for fuel allocation between power and water at Ghubrah Phase I and Phase III is based on the specific fuel consumption and the performance ratio of the desalination plants. These were determined during commissioning of each plant with desalination alone in service.

The method can be described as follows:

- With desalination alone in service, let

PRs = The Performance Ratio (Distillate production per unit mass of process steam flow)

Fs = Specific fuel consumption per unit mass of distillate flow

- With desalination in cogeneration cycle, let

PRa = The actual plant Performance Ratio

Ft = Total fuel consumed by the cogeneration plant

m = Distillate mass flow rate

then

$$\text{Fuel allocated for desalination} = F_w = \frac{F_s \times PR_s \times m}{PR_a}$$

$$\text{Fuel allocated for power} = F_p = F_t - F_w$$

For the case of Phase II/IV cogeneration plant the fuel consumed by the gas turbines is assigned for power only. The fuel for desalination is only that used by the auxiliary boilers.

In all the three cases the heat input to the power cycle is the fuel allocated for power multiplied by the lower calorific value of fuel. The power cycle efficiency is the heat equivalent of the power generated divided by the heat input.

As can be seen from the method used for Phase I and Phase III, the fuel allocated for desalination depends only on the performance ratio of the desalination plant. It does not show any advantage of cogeneration on the fuel cost of water. The advantage of cogeneration appears only as higher power efficiency. Earlier, when the method was used for Phase I with the extracting type steam turbines the method was somewhat rational. As quoted by Wade and Fletcher [Ref. 2], the increased steam flow through the extracting steam turbines can be assigned directly to desalination. For Phase III with the back pressure steam turbine the method is not rational. In Phase III same like in Phase II/IV it could be argued that desalination is utilizing the free exhaust of the power cycle. However, the method used for Phase II/IV is also irrational as it results in no advantage of cogeneration in the fuel cost of power. This, while the resulting fuel cost of water is too minimal. Surprisingly, with the above methods used, the fuel cost contribution to the total cost of water (43%) and to the total cost of power (69%) as shown in fig. 4a & b, is almost same as that obtained by El-Nashar [Ref. 3] who used the exergy method for a different cogeneration plant.

## REFERENCE CYCLE METHOD

With little modification\* to suit Ghubrah cogeneration plant, the Reference Cycle method proposed by Wade and Fletcher [Ref. 2] could be used for all of the three cases. This method compares the heat consumption and the efficiencies of the cogeneration plant with the thermal efficiency of an appropriate reference cycle of the same power output. As per Wade and Fletcher the reference cycle should be a practical generating plant cycle for the type of fuel available, rather than a theoretical cycle such as the Carnot cycle.

This method can be illustrated as follows, let

- F1 = Heat supplied directly to the power cycle
- F2 = Heat to auxiliary boilers or other secondary input to the desalination plant
- $\eta_{cy}$  = The actual conversion efficiency of fuel to power in a dual purpose plant
- $\eta_{ref}$  = Efficiency of a reference cycle of a practical single purpose power plant with the same power output



$w$  = Electrical auxiliary power required by the desalination plant  
 $M$  = Water production

Then

$$\text{Energy to power } E_1 = F_1 \times \frac{\eta_{cy}}{\eta_{ref}}$$

$$\text{Energy to water } E_2 = F_1 \left( \frac{1 - \eta_{cy}}{\eta_{ref}} \right) + F_2 + \frac{w}{\eta_{ref}}$$

$$\text{Energy per unit mass of water production} = \frac{E_2}{M}$$

Still, it will be debatable what reference efficiency to take. The 36% reference cycle efficiency used by the same authors as representing the efficiency of a typical large system with single purpose power plant can be used.

Both, the presently used method and the Reference Cycle method need to be modified in order to take care of the fact that at Ghubrah the steam used for driving the Brine Recirculation Pumps (BRP) constitutes a considerable portion of the total steam required by the desalination plant. Taking this into consideration, Phase II/IV cogeneration plant is different from Phase I and III. In Phase I and Phase III the steam required for driving the BRP is by-passing the power cycle and hence having a direct share of the total fuel used by the boiler. In Phase II/IV this does not by-pass the power cycle and hence does not have its separate share of fuel. The same applies for the steam used in the vacuum system of the desalination plant. However this is smaller in quantity compared to BRP steam.

The reference cycle method can be modified as follows

$$\text{Energy to water } E_2 = F_1 \left( \frac{1 - \eta_{cy}}{\eta_{ref}} \right) + F_2 + F_3 + \frac{w}{\eta_{ref}}$$

where

- $F_2$  = Heat to auxiliary boilers ( $F_2 = 0$  for Phase I & Phase III)
- $F_3$  = Secondary heat input to desalination by-passing the power cycle ( $F_3 = 0$  for Phase II/IV)



## **CONCLUSION**

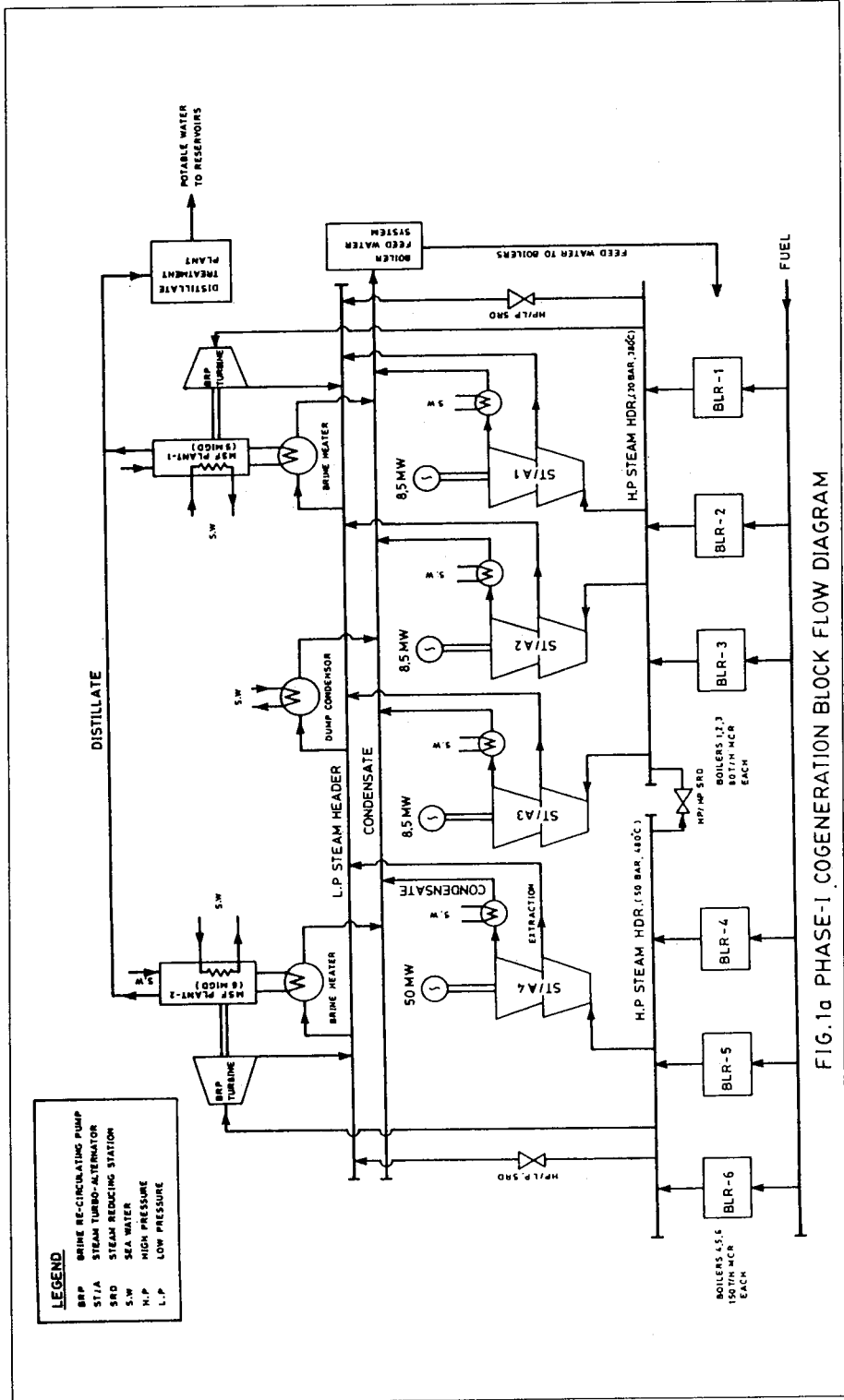
The method presently in use at Ghubrah is very simple to apply but it does not show the advantage of cogeneration as common for both power and water.

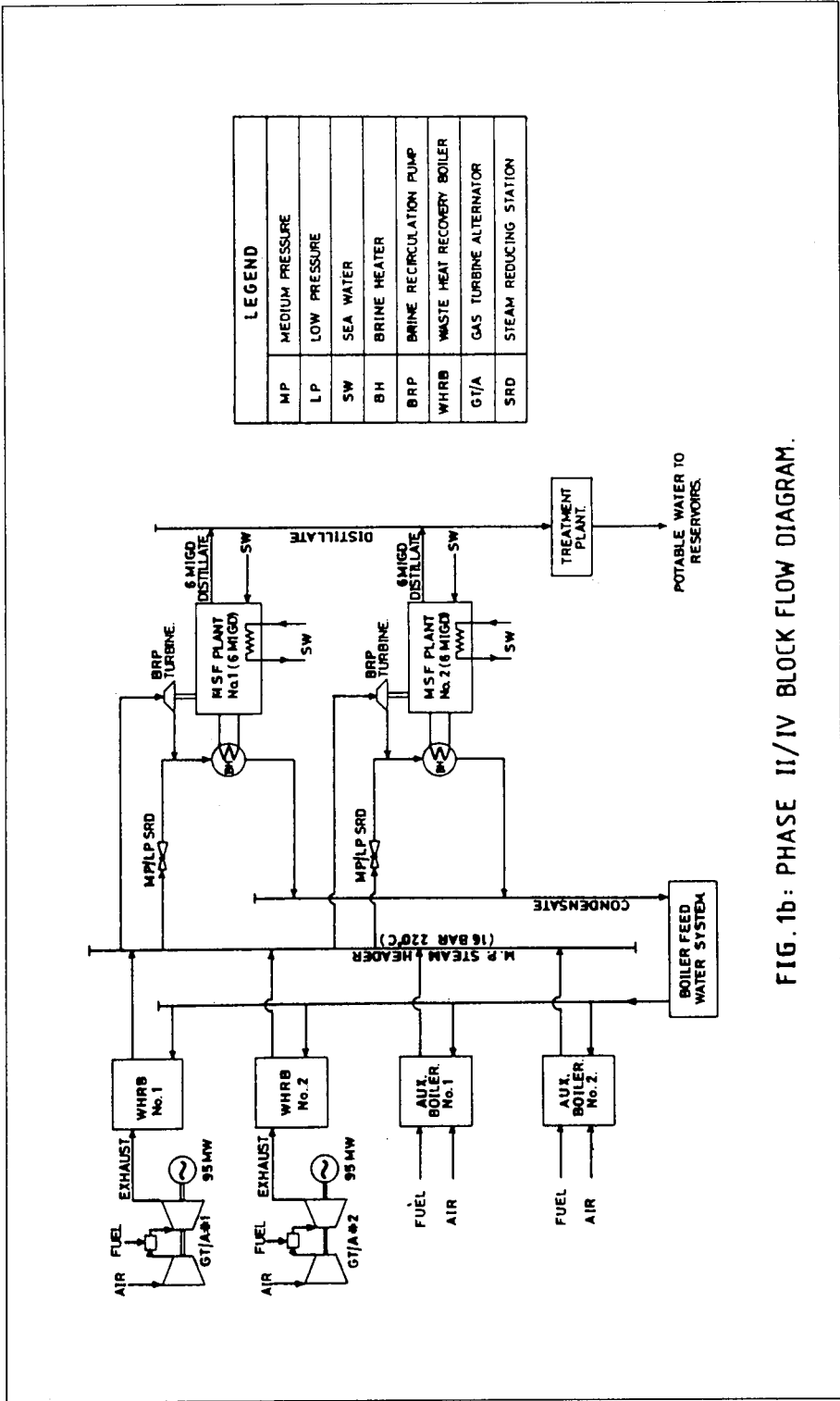
The Reference Cycle method is more rational in dividing fuel between power and water. It also takes care of the effect of power load variations on fuel allocations between power and water.

The modification introduced in this paper on the Reference Cycle method makes it more generalised in its application to the different cogeneration configurations.

## **REFERENCES**

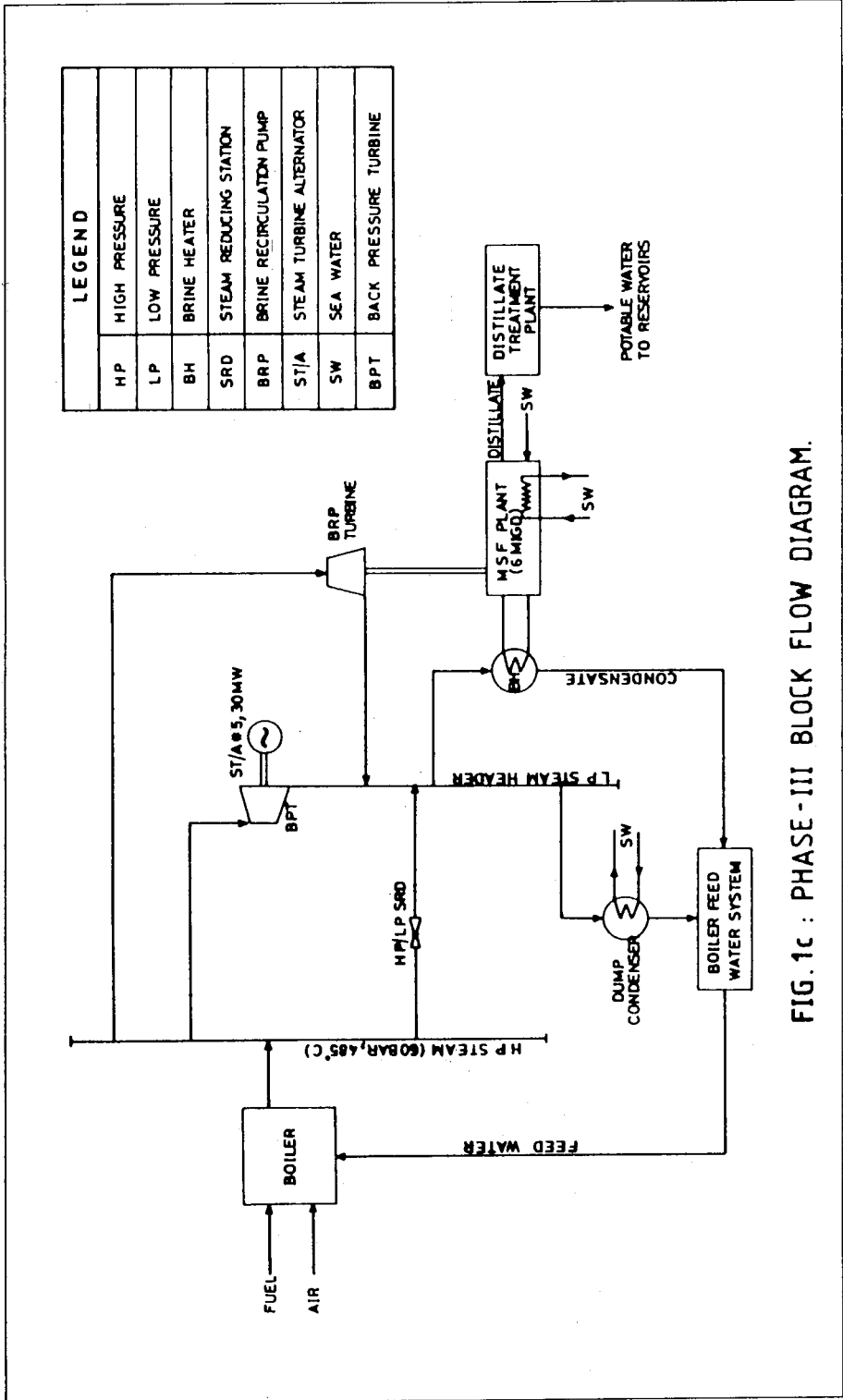
- [1] Sogex Oman Co. LLC. (O & M Contractor), Annual Report, Ghubrah Power and Desalination Station, Sultanate of Oman, 1995.
- [2] Wade N.M. and Fletcher R.S., Energy Allocation and Other Factors Influencing Water Costs in Desalination and Dual Purpose Power/Water Plants, IDA World Congress on "Desalination and Water Sciences", Volume III, Abu Dhabi, November 18-24, 1995, p363-371.
- [3] El-Nashar Ali M., The Exergetic Cost Analysis of a Cogeneration Plant for Power and Desalination : An Application to the UANE Cogeneration Plant, IDA World Congress on "Desalination and Water Sciences", Volume III, Abu Dhabi, November 18-24, 1995 p319-339.





LEGEND	
MP	MEDIUM PRESSURE
LP	LOW PRESSURE
SW	SEA WATER
BH	BRINE HEATER
BRP	BRINE RECIRCULATION PUMP
WHRB	WASTE HEAT RECOVERY BOILER
GT/A	GAS TURBINE ALTERNATOR
SRD	STEAM REDUCING STATION

FIG. 1b: PHASE II/IV BLOCK FLOW DIAGRAM.



LEGEND	
HP	HIGH PRESSURE
LP	LOW PRESSURE
BH	BRINE HEATER
SRD	STEAM REDUCING STATION
BRP	BRINE RECIRCULATION PUMP
ST/A	STEAM TURBINE ALTERNATOR
SW	SEA WATER
BPT	BACK PRESSURE TURBINE

FIG. 1c : PHASE-III BLOCK FLOW DIAGRAM.

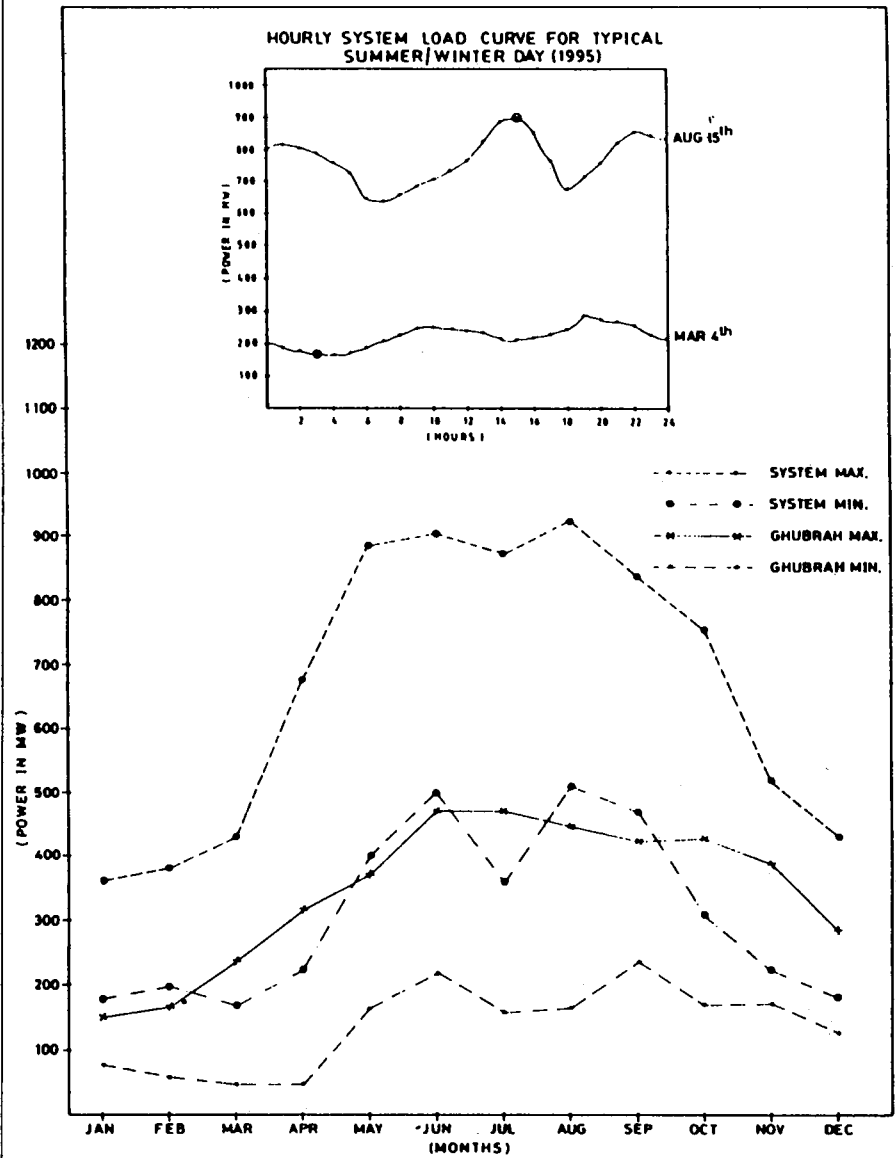


FIG.2 SYSTEM / GHUBRAH MAX/MIN LOAD (1995)

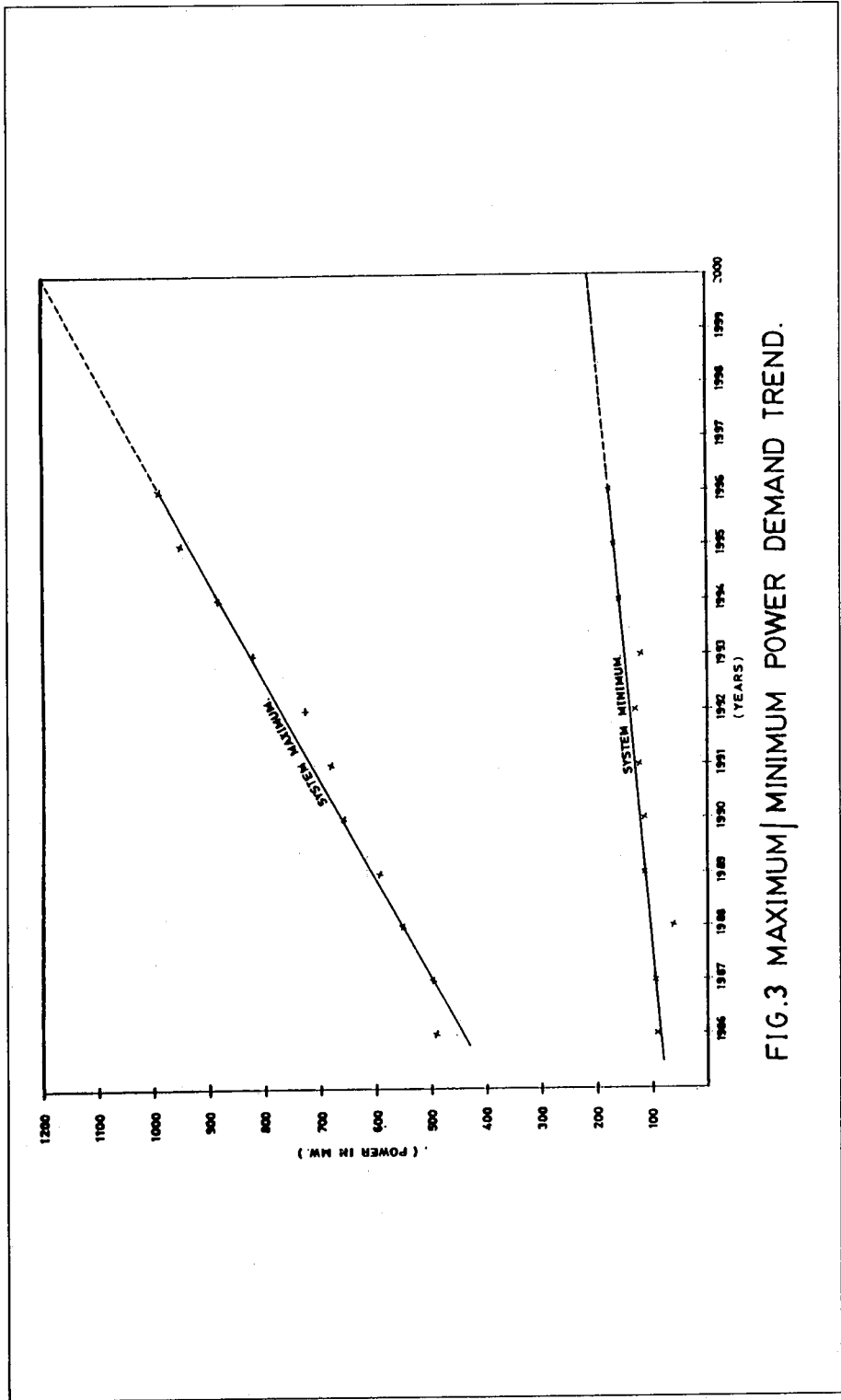


FIG.3 MAXIMUM|MINIMUM POWER DEMAND TREND.

GHUBRAH POWER & DESAL PLANT - 1995  
COST OF WATER PRODUCTION

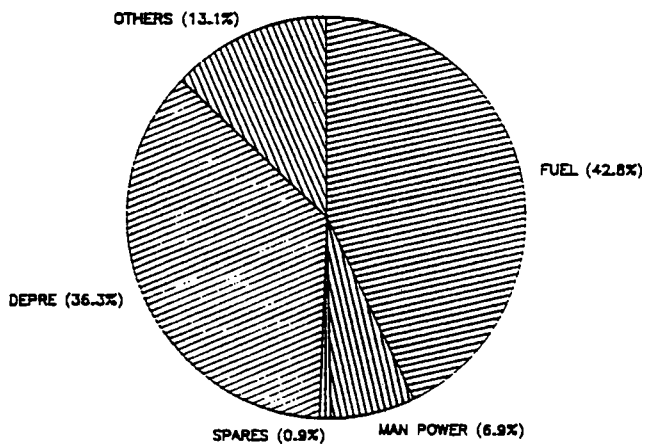


FIG. 4a

GHUBRAH POWER & DESAL PLANT - 1995  
COST OF POWER GENERATION

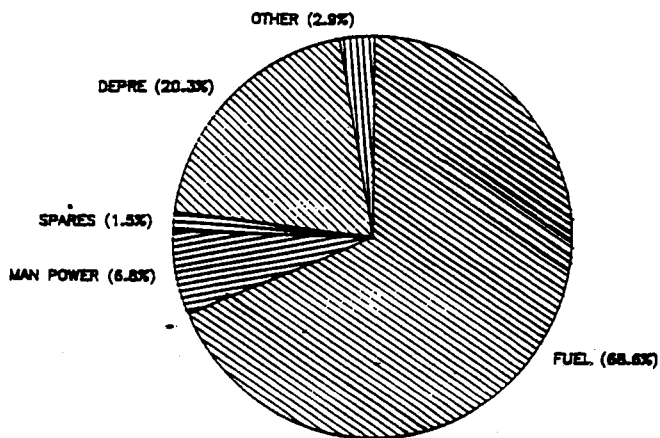


FIG. 4b

# **Performance of High Chromium Stainless Steels and Titanium Alloys in Arabian Gulf Seawater**

*Ali Al Odwani, Mohammed Al-Tabtabaei and Ahmed Abdel-Nabi*



# PERFORMANCE OF HIGH CHROMIUM STAINLESS STEELS AND TITANIUM ALLOYS IN ARABIAN GULF SEAWATER

Ali Al Odwani<sup>1</sup>, Mohammed Al-Tabtabaei<sup>1</sup> and Ahmed Abdel-Nabi<sup>2</sup>

<sup>1</sup> Water Desalination Department, Water Resources Division

<sup>2</sup> Materials Application Department, Petroleum, Petrochemicals and Materials Division

Kuwait Institute for Scientific Research

P.O. Box 24885, Safat 13109, Kuwait

## ABSTRACT

Material selection is a major design parameter for constructing new desalination plants. Over the past four decades, materials for desalination have evolved from simple, low-cost metals into special alloys that resist corrosion and erosion. Reverse osmosis (RO) is a newly emerged desalination technology. Experience with seawater RO indicates the need for materials compatible with the Gulf seawater. A study was initiated at the Desalination Research Plant (DRP), Doha in Kuwait to assess the suitability of certain alloys for seawater applications. The electrochemical impedance spectroscopy (EIS) was used to evaluate the corrosion performance of four high chromium stainless steels (316L, 317L, 317 LNMO and 254 SMO) and grade 2 titanium in natural flowing Arabian Gulf seawater. The EIS provided information concerning changes to the interfacial impedance as a function of exposure time for these alloys. The impedance spectra for all the alloys showed slight changes in the low frequency region over the exposure period. The open-circuit potentials (OCPs) of these alloys exhibited slight fluctuations around the initial exposure potential. However, the grade 2 titanium's initial potential was more active, and then gradually shifted towards the noble direction. The results of the EIS analysis and OCP indicated that grade 2 titanium performed better than the four high-chromium stainless-steel alloys. The use of 254 SMO and 317 LNMO would provide better corrosion resistance and better functional capacity than the use of 316L and 317L.

**Keywords:** Reverse Osmosis, Metallic Components, Crevice Corrosion, Electrochemical Techniques, Active, Noble, Passivation, Destruction, Cost.

## INTRODUCTION

The increasing acceptance of reverse osmosis (RO) technology in desalinating seawater and brackish water, has led many concerned specialists to further investigate factors affecting the performance of RO (NB: According to a 1993 survey, RO comprises more than 33.2% of the total world desalination capacity for all desalinating plants available [1]). The RO process is carried out at ambient temperature, easy to operate and maintain, involves no change in phase, requires less energy, and has comparatively far fewer problems than multistage flash (MSF) systems. However, a proper selection of construction material is one of the most important factors in the efficient, economical operation of an RO desalination plant [2]. It is not enough merely to provide functional capability, but one must take into account the initial cost, maintenance costs, reliability, product quality, product loss, and unscheduled shutdowns. The metallic components used in other desalination processes differ in quantity, size, application and many other aspects from those used in the RO process. However, these components are of great importance as they are included in pumps, piping systems, turbines, and many other parts of the system. The state of the art for the selection of appropriate, corrosion-resistant alloys for a specific environment is not sufficiently advanced to make choices obvious. It still remains necessary to conduct laboratory tests on candidate alloys to select those most suitable for RO of seawater.

The material on the inlet side of the RO modules is exposed to feed seawater with a total dissolved solids (TDS)  $\cong$  47,000 ppm, while those on the outlet side are exposed to a product water stream with a TDS  $\cong$  500 ppm and a reject brine stream with a TDS  $\cong$  70,000 ppm. Most systems use nonmetallic materials such as PVC, GRP, and plastic for the low-pressure piping systems [3]. On the other hand, the use of metallic components for the high-pressure piping systems, pumps and energy recovery turbines is essential [4]. The most commonly used grade of stainless steel for RO desalination plants has been type 316L [5]. At high feedwater velocities, this alloy experiences less corrosion attack than others. However, failures in the form of pitting and crevice corrosion are sometimes observed at flanges, pump seals, and at or close to weld or heat affected zones. With the advances in stainless steel, alloys of more corrosion-resistant austenitic and duplex stainless steel with better mechanical properties like 317L, 317 LNMO, 254 SMO, 904L have been introduced and are being used along with 316L. It has been found that a higher content of Cr and Mo in the composition of the alloy tends to prevent the corrosion attack, mainly pitting and crevice, in a high-chloride environment [6].

## **Experimental Setup:**

**Tested Materials:** The composition of the five commercial alloys (metals), comprising four austenitic stainless steels, and titanium that were studied in this investigation is given in Table 1. The mechanical properties of these alloys are also given in Table 2. These alloys were selected because of their reported improved crevice-corrosion resistance.

**Specifications of Test Specimens:** The test specimens were machined from plate in the as-received, mill-annealed condition. The types of specimens used were:

1. Rectangular-shaped specimens with 100 mm x 60 mm x 3 mm of exposed area and a 5 +mm diameter hole in the center. The specimens were detergent-cleaned ultrasonically, decreased and weighed. The hole in the center of each coupon was used for the attachment of the multiple crevice test assemblies. A multiple crevice assembly made of Teflon is illustrated in Fig. 1. Each washer has 12 serrations to produce a crevice-to-uncreviced ratio of 1:24 on each specimen.
2. Circular discs of 22-mm diameters were polished with 220-through 1000-grit SIC paper, detergent-cleaned ultrasonically, decreased and used for the electrochemical tests.

**Crevice-Corrosion Test Assembly:** Crevice-corrosion tests were carried out on the specimens using the multiple crevice corrosion assembly shown in Fig. 1. The multiple crevice washer was bolted to both sides of each specimen using Teflon bolts and nuts. The crevice assemblies were tightened to a torque of 8 NM. Duplicate specimens of each alloy were used, making two groups. The test specimens were exposed to the filtered seawater feed at the Desalination Research Plant (DRP) Doha, in Kuwait for 3000 h. The specimens were hung in a 100-l plastic tank at temperatures ranging between 20°C and 30°C, pH of 6.5-7, and a flow rate of 100 l/min<sup>-1</sup>. After the exposure test period, the specimens were disassembled and scrubbed with a nylon brush in deionized water. The specimens were then examined under a low-powered stereomicroscope.

**Electrochemical Test Assembly:** Electrochemical tests consisted of open-circuit potential (OCP) and electrochemical impedance spectroscopy (EIS) and were conducted in the filtered seawater feed, the chemical composition and physical properties of which are given in Table 3. The tests were carried out at ambient temperature and a pH of 6.8. The reference electrode was a saturated calomel electrode (SCE), and two graphite electrodes were used as counter electrodes. Specimens were inserted into special Teflon holders designed to prevent any leakage of solution into the existing Teflon cylinder. Daily OCP readings and interval EIS readings were performed using ACM instrument type 243.

## RESULTS AND DISCUSSION

**Crevice-Corrosion Test:** Crevice corrosion is an intense, localized form of corrosion that occurs on stainless steels in high-chloride environments. Austenitic steels owe their corrosion resistance to a passive film of  $\text{Cr}_2\text{O}_3$  that forms on the surface of the alloy [7]. In this study, all of the tested alloys were compared to one another after a thorough inspection of the severity of the attack caused by corrosion. An external view of the crevice attack of the various alloys after 3000 h of exposure in feed seawater is shown in Fig. 2. This recent study and a former study made at DRP showed that the most severe attack was observed on stainless steel 316L, followed by that on stainless steel 317L [8]. The maximum depth of crevice attack was in the range of 0.1 - 0.15 mm. Stainless steels 316L and 317L have been the most commonly used materials for the construction of brackish and seawater RO plants. They have been used in pumps, high-pressure piping systems, and in energy recovery turbines. A reasonably long-life is expected from stainless steels 316L and 317L in RO applications, provided high feedwater velocities are maintained and the design of the RO module does not encourage the formation of crevices. Even under these conditions, high-pressure piping, headers and connectors are prone to crevice-corrosion attack [3]. In such cases, the use of relatively less costlier material like 316L and 317L might not be economical in the long run.

The extent of crevice corrosion attack on the alloys, however, was found to decrease as the percentage of Mo, Cr, Ni and N increased in the alloys' compositions. Stainless steels 317 LNMO and 254 SMO with higher Mo, Cr, Ni and N contents showed little or no crevice attack. The use of these higher grade stainless steel alloys which are practically resistant to crevice corrosion and have much greater strength, is desirable.

All of the four types of austenitic stainless steel have been compared to titanium Ti(2) a metal known to have an excellent corrosion resistance in seawater up to a temperature of 100°C. The purpose was not to select titanium for RO application, but to select a stainless steel alloy with similar, excellent, passive film formation. Ti(2) showed no sign of crevice attack during the exposure period, indicating the formation of an excellent protective layer on the surface of the specimens. However, the use of titanium is not recommended over to stainless steels 254 SMO and 317 LNMO because of cost factors. Therefore, the use of stainless 317 LNMO or 254 SMO would be appropriate, since they, along with Ti(2), were immune to crevice corrosion.

**Electrochemical Test:** The findings of the OCP and EIS as a function of time were studied. Fig. 3 shows the OCP results and Figs. 4-8 show the EIS results for the alloys in flowing seawater. The potentials of stainless steel 316L fluctuated

very slightly around -220 mV for 240 h had shifted in the noble direction, reaching a maximum value of -110 mV. After 480 h of exposure, the potential of the alloy gradually shifted towards -200 mV. This type of stainless steel usually has a protective passive film, but in a chloride-containing environment, it is susceptible to pitting and crevice corrosion. The surface impedance increased with time due to the formation of a surface layer. However, the fluctuation in the potential is an indication of continuous disruption of the passive film on the surface of the steel, which is mainly due to pitting and crevice corrosion.

Fig. 3 also shows the OCP of stainless steel 317L, which started at -120 mV and then shifted in the noble direction for up to 40 h. The potential then shifted sharply in the active direction and reached a negative potential of -260 mV which was maintained for 120 h after which it shifted back in the noble direction. Beyond 240 h, the potential of stainless steel 317L fluctuated between more negative and less negative values for the duration of the experiment. This behaviour may be due to the destruction and passivation of the passive layer, and the competition between the anodic and cathodic areas on the surface of the specimen. The impedance spectra of stainless steel 317L indicates the decrease of the interfacial impedance as a function of time. The decrease in the impedance values indicate the onset of the localized corrosion on the surface of the alloy. A shift towards resisted behavior was also observed in the phase angle data.

The resistance to pitting and crevice corrosion can be improved by the addition of Mo to the stainless steel. Since Mo is a ferrite former, it is necessary to increase the Ni content to maintain the austenitic structure. The presence of N, a strong austenitic former, also remarkably improves the pitting- and crevice-corrosion resistance and increases the proof stress of stainless steels [3, 9-12]. Stainless steel 317 LNMO of higher contents of Mo, and N showed better corrosion resistance than 316L and 317L. The OCP behaviour of this alloy indicates that the passive film on the surface of this alloy was stable and resistant to chloride attack to a certain extent. The interfacial impedance also remained unchanged during the exposure time indicating good protective properties of the passive layer on this alloy.

Stainless steel 254 SMO, which contains 20.0 Cr, 6.06 Mo and 17.9 Ni, showed steadier behaviour than stainless steels 316L and 317L LNMO. The almost steady potential in the noble direction in the OCP behaviour indicates that 254 SMO passivated easily, and an oxide film developed on the surface of the specimen upon exposure to the seawater environment. There was slight change in the impedance spectra at low and intermediate frequencies as a function of time. A very slight shift in the phase angle was also observed indicating the good protective properties of the passive layer on the surface of the alloy. Titanium showed almost similar behaviour in the OCP and EIS tests during the exposure period.

There was slight change in both the impedance and the phase angle behaviour for titanium grade 2 in flowing seawater. The overall impedance values slightly fluctuated indicating minimal disturbance has occurred on the surface of titanium during the exposure period.

## **CONCLUSION**

From this study, the following conclusions can be drawn:

1. Metallic components used in the construction of an RO plant can greatly affect the plant's performance if not properly selected.
2. Increased Cr, Mo and N contents in stainless steel were significantly beneficial to the resistance of localized corrosion in seawater at ambient temperatures. Stainless steel 316L and 317L performed relatively poor under the prevalent conditions of Kuwait's seawater, compared to 317 LMNO and 250 SMO.
3. Titanium grade 2 showed superior and no signs of corrosion attack was observed.
4. The use of stainless steel 317 LMNO and 254 SMO over 316L in an RO plant would vary the price ratio in the order of 2.2 : 2.7 : 1 respectively.

## **ACKNOWLEDGMENT**

The authors wish to thank the Kuwait Foundation for the Advancement of Science and the Management of the Kuwait Institute for Scientific Research (KISR) for funding the project (Research and Development on Desalination by Reverse Osmosis) and for the provision of facilities. Gratitude is also expressed to Dr. J. Carew and Dr. Abdelhameed Hashem for their assistance in this project.

## REFERENCES

- [1] Wangnick Consulting, 1993 IDA Worldwide Desalting Plants Inventory, International Desalination Association, June 1994, p25.
- [2] Hassan, A.M., & Malik, A.V, Desalination, 74, 1989, p 157.
- [3] Olsson, J., & Wallen, J.B., Experience with a High Molybdenum Stainless Steel in Saline Environments, 1983, p241.
- [4] Oldfield, J.W, & Todd, B., Desalination, 55, 1985, p26 1.
- [5] Nordin, S, Ericson, B., & Wallen, B., Desalination, 55 (1985) p247.
- [6] Morro, H., ed., Advanced Stainless Steel for Seawater Application: Climax Molybdenum. Greenwich, Connecticut, 1980, p 12.
- [7] Herbsleb, G., Werkstoffe und Korrosion, 33, 1982, p334.
- [8] Carew, J., Abdel-Jawad., M., & Al-Wazzan, Y, Desalination, 1995 p53.
- [9] Alfonsson, E., & Quvarfort, R., Materials Science Forum, Vol. 111- 112, 1992 p483.
- [10] Reed, R.D., Journal of Metals, 36, 1984, p 16.
- [11] Bond, A.P., & Dundas, H.J., Corrosion, 26, 1984.
- [12] Larson, J.A., "New developments in high alloy cost steels, Proceedings of the 39th SFSA Technical and Operating Conference, Steel Founders of America, 1984 p229.

Table 1. Chemical Composition of the Studied Alloys.

ALLOY	UNS	C	Cr	Cu	Mn	Mo	Ni	P	Ti	OTHER
316L	S31603	0.019	16.31	0.240	1.710	2.100	10.140	0.028		CO-0.12; N-0.038
317L	S31703	0.019	18.19	0.420	1.780	3.110	13.230	0.031		CO-0.15; N-0.047
317LNMO	S31726	0.021	18.30	0.240	1.550	4.220	13.200	0.022		N-0.14
254SMO	S31254	0.011	20.00	0.700	0.580	6.060	17.900	0.021		N-0.217
Ti2	R50400	0.100							BAL	O-0.12; N-0.009

Table 2. Physical Properties of the Studied Alloys.

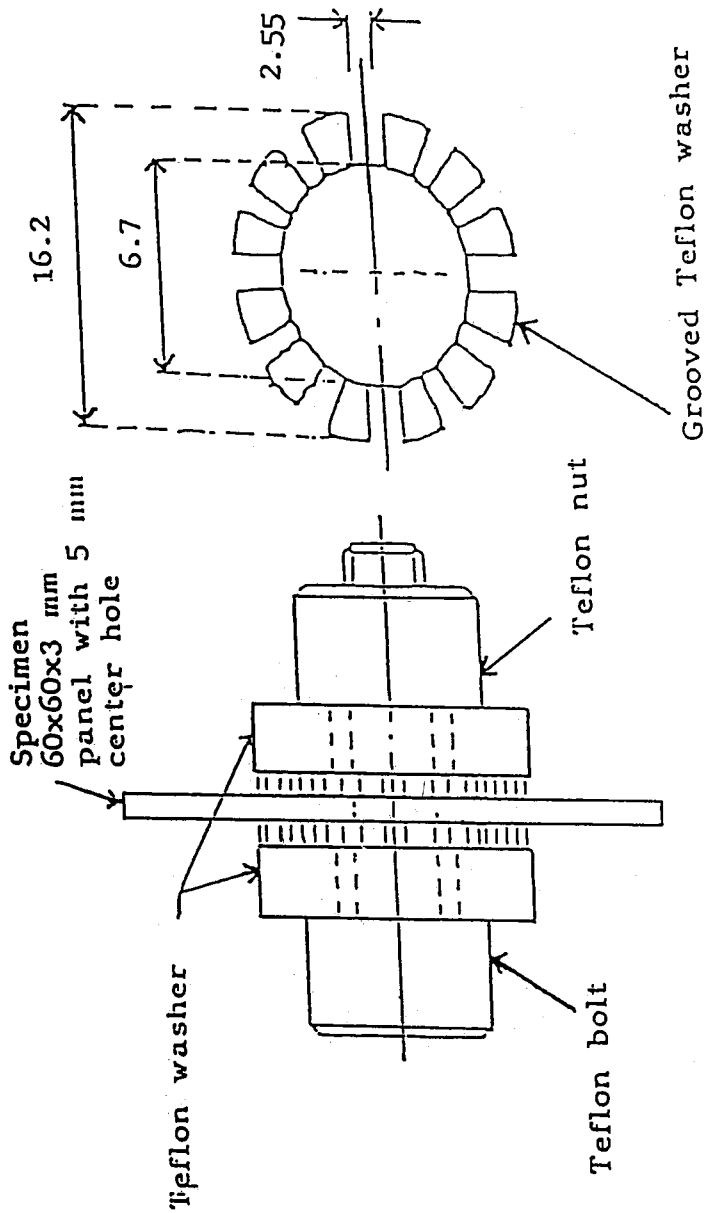
Alloy	UNS	Yield (KSI)	Elongation (%)	Tensile (KSI)	Hardness	Condition
316L	S31603	43.20		84.10	RB 80	ANLD
317L	S31703	45.00	44 (2")	87.00	RB 83	ANLD
317LNMO	S31726	50.00	50.00	93.00		ANLD
254SMO	S31254	58.00	53.00	109.00	HB 183	ANLD
Ti2	R50400	40/65	20.00	50.00		ANLD



**Table 3. Average Seawater Quality at Doha**

Parameter	Concentration* (mg/l ± SD)	
<b>TDS at 180°C</b>	<b>47000</b>	<b>± 2000</b>
<b>Total alkalinity (as CaCO<sub>3</sub>)</b>	<b>175</b>	<b>± 15</b>
<b>Carbonate</b>	<b>14</b>	<b>± 8</b>
<b>Bicarbonate</b>	<b>185</b>	<b>± 18</b>
<b>Carbon Dioxide</b>	<b>14</b>	<b>± 4</b>
<b>Sulphate</b>	<b>3400</b>	<b>± 300</b>
<b>Chloride</b>	<b>24000</b>	<b>± 700</b>
<b>Calcium</b>	<b>570</b>	<b>± 45</b>
<b>Magnesium</b>	<b>1700</b>	<b>± 150</b>
<b>Sodium</b>	<b>12300</b>	<b>± 20</b>
<b>Potassium</b>	<b>470</b>	<b>± 20</b>
<b>Total iron</b>	<b>0.08</b>	<b>± 0.08</b>
<b>pH</b>	<b>8.2</b>	<b>± 0.1</b>

\* Average concentrations of 12 samples collected monthly. SD (i.e., standard deviations) indicate variations in water quality rather than experimental errors. TDS = total dissolved solids.

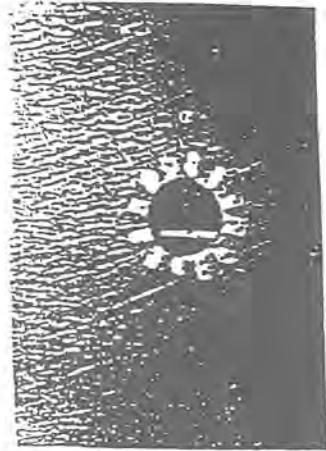


Dimensions are in mm

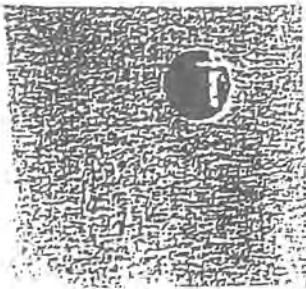
Fig. 1. Multiple crevice washer assembly.



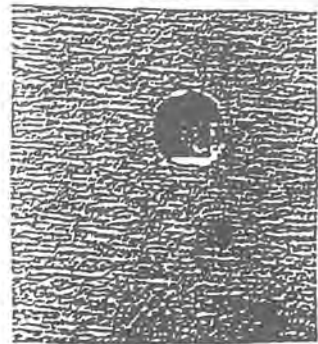
316L



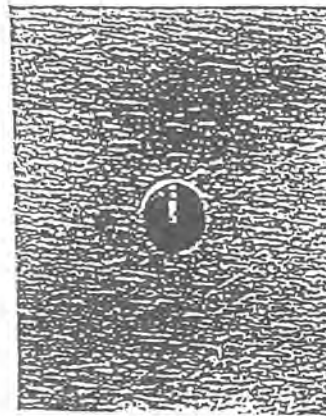
317L



317LNMO



254SMO



Ti(2)

Fig. 2. The external view of the creviced specimens after 3000 h exposure in feed seawater.

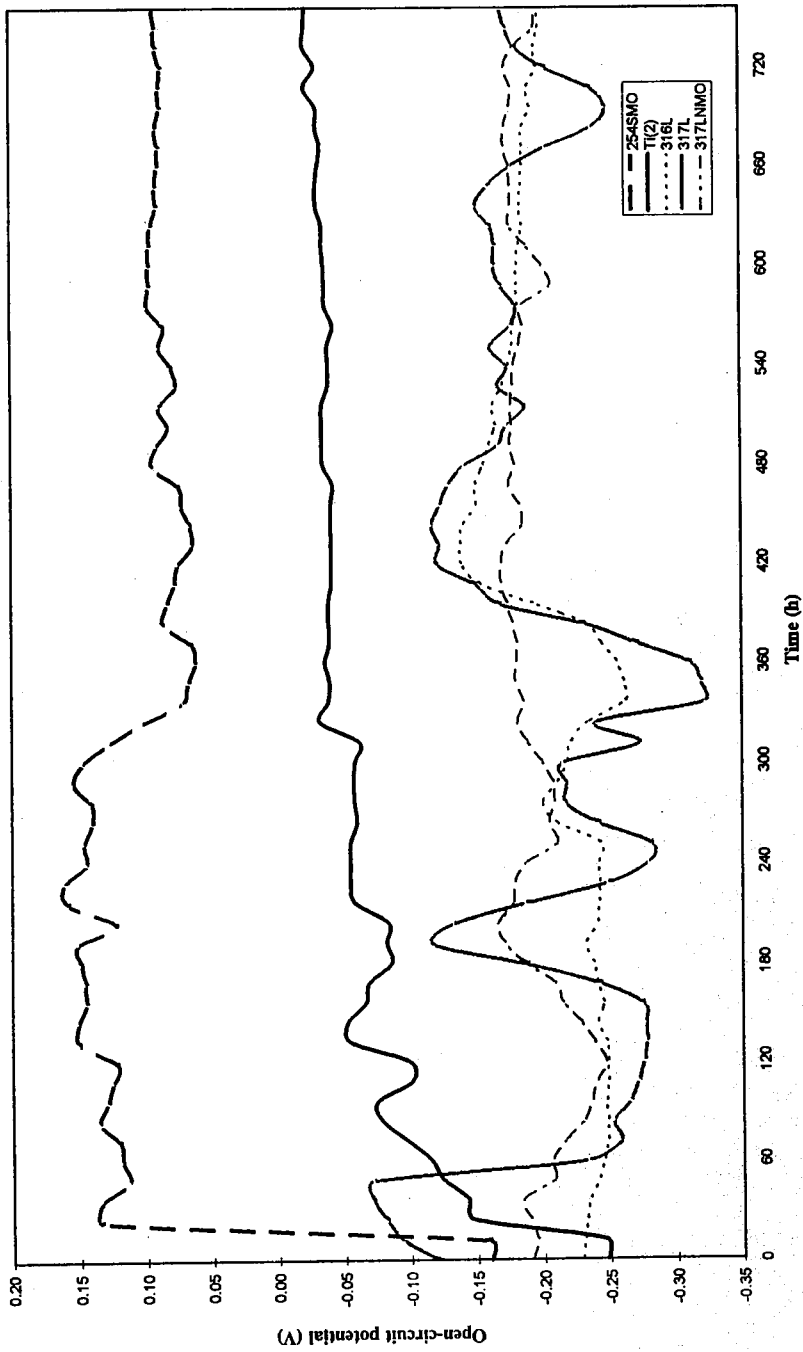
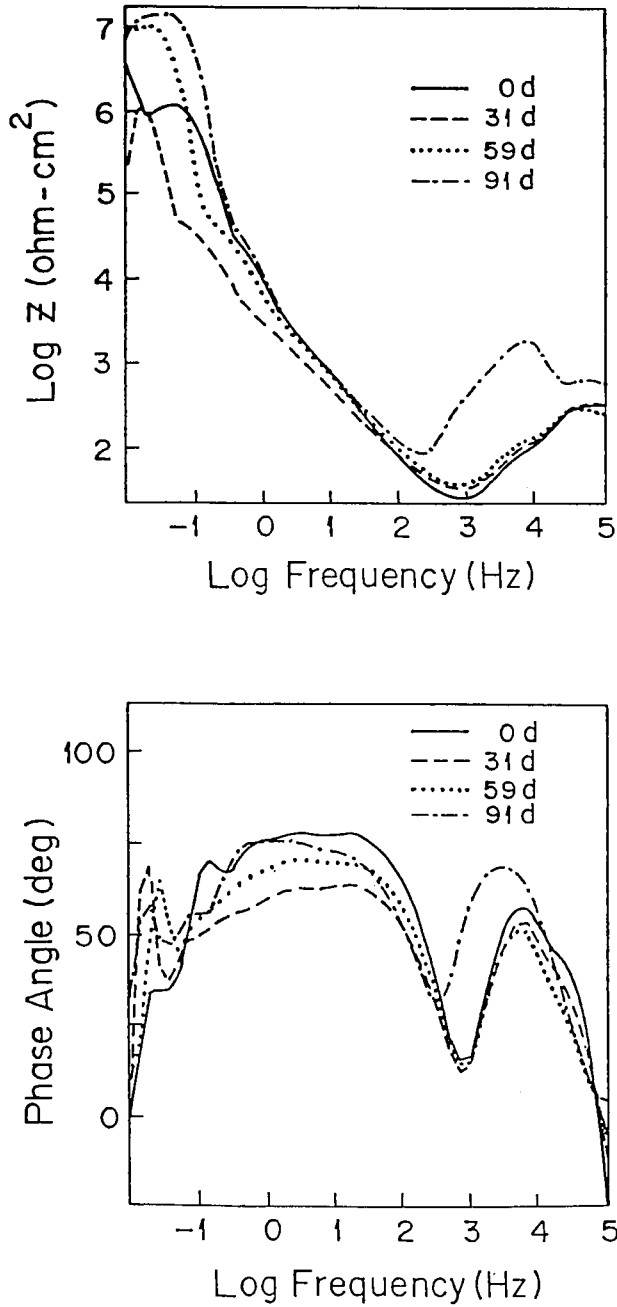


Figure 3. The open-circuit potential of the studied alloys versus time in flowing seawater.



**Figure 4.** The impedance spectra for alloy 316L in flowing seawater at ambient conditions.

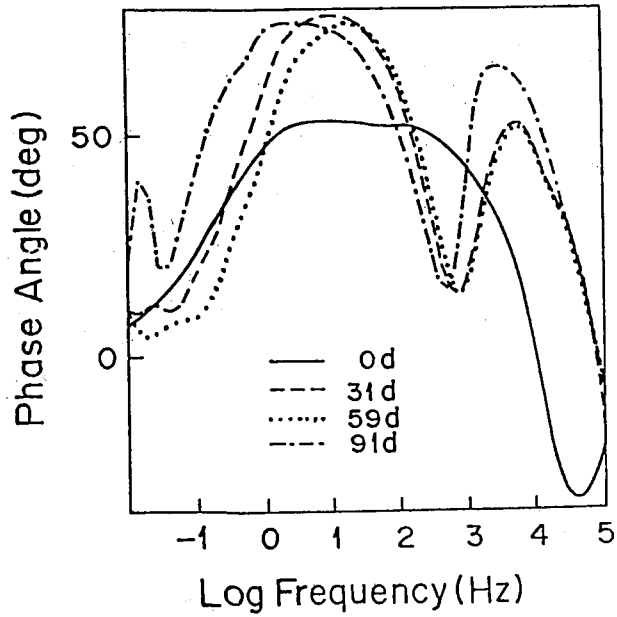
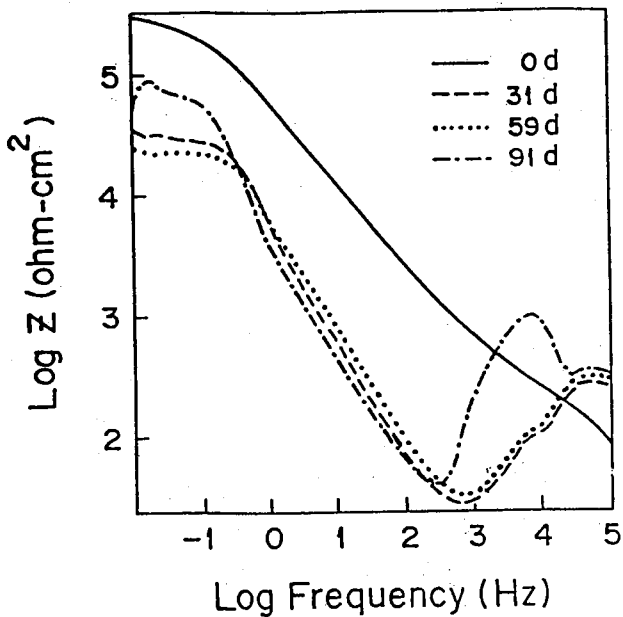


Figure 5. The impedance spectra for alloy 317L in flowing seawater at ambient conditions.

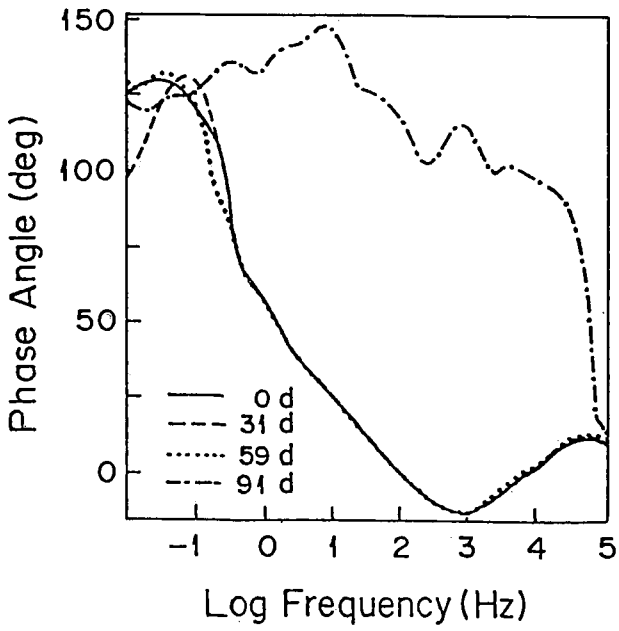
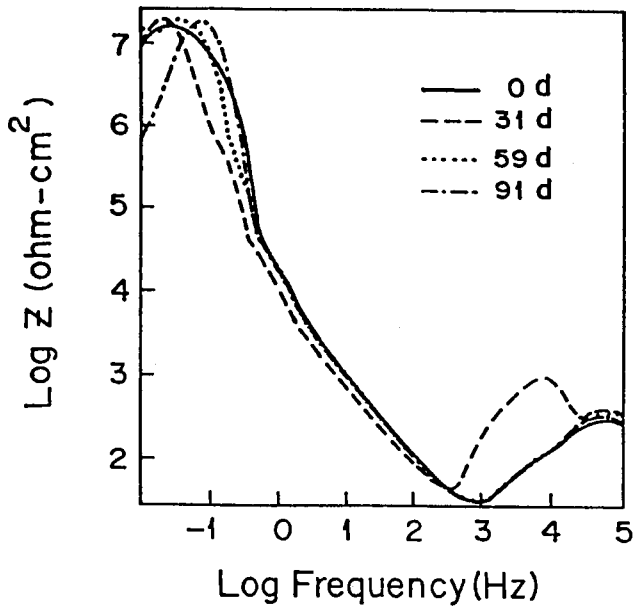
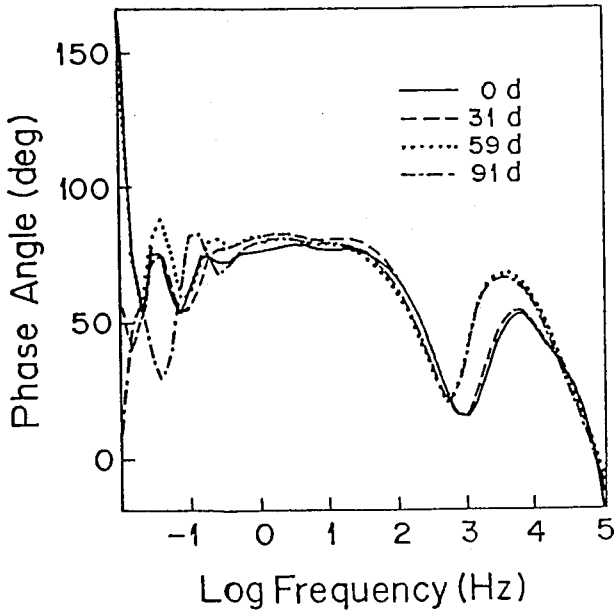
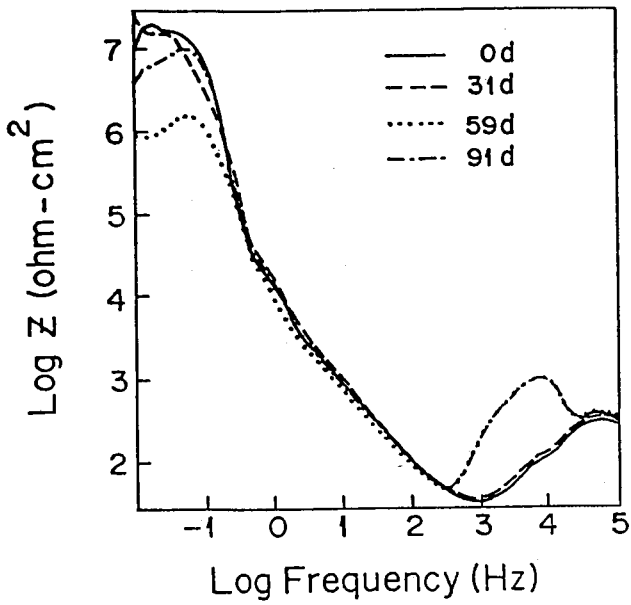


Figure 6. The impedance spectra for alloy 317 LNMO in flowing seawater at ambient conditions.



**Figure 7.** The impedance spectra for alloy 254 SMO in flowing seawater at ambient conditions



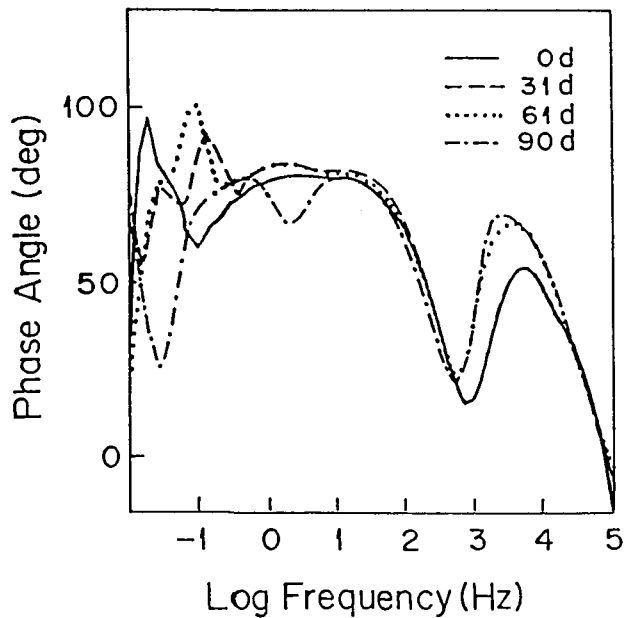
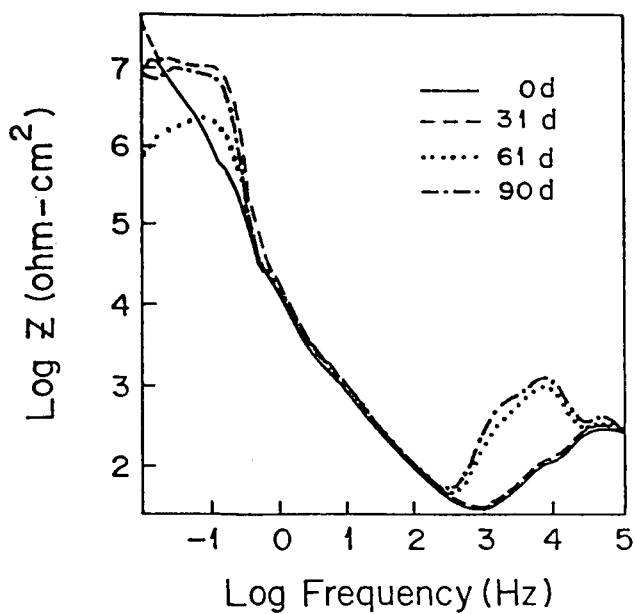


Figure 8. The impedance spectra for Titanium Grade 2 in flowing seawater at ambient conditions.

# **Use of GRP Material in Power and Desalination Plants**

*N.J. Paul, Hasan Ibrahim Al Hasani and Adel El Masri*

# **USE OF GRP MATERIAL IN POWER AND DESALINATION PLANTS**

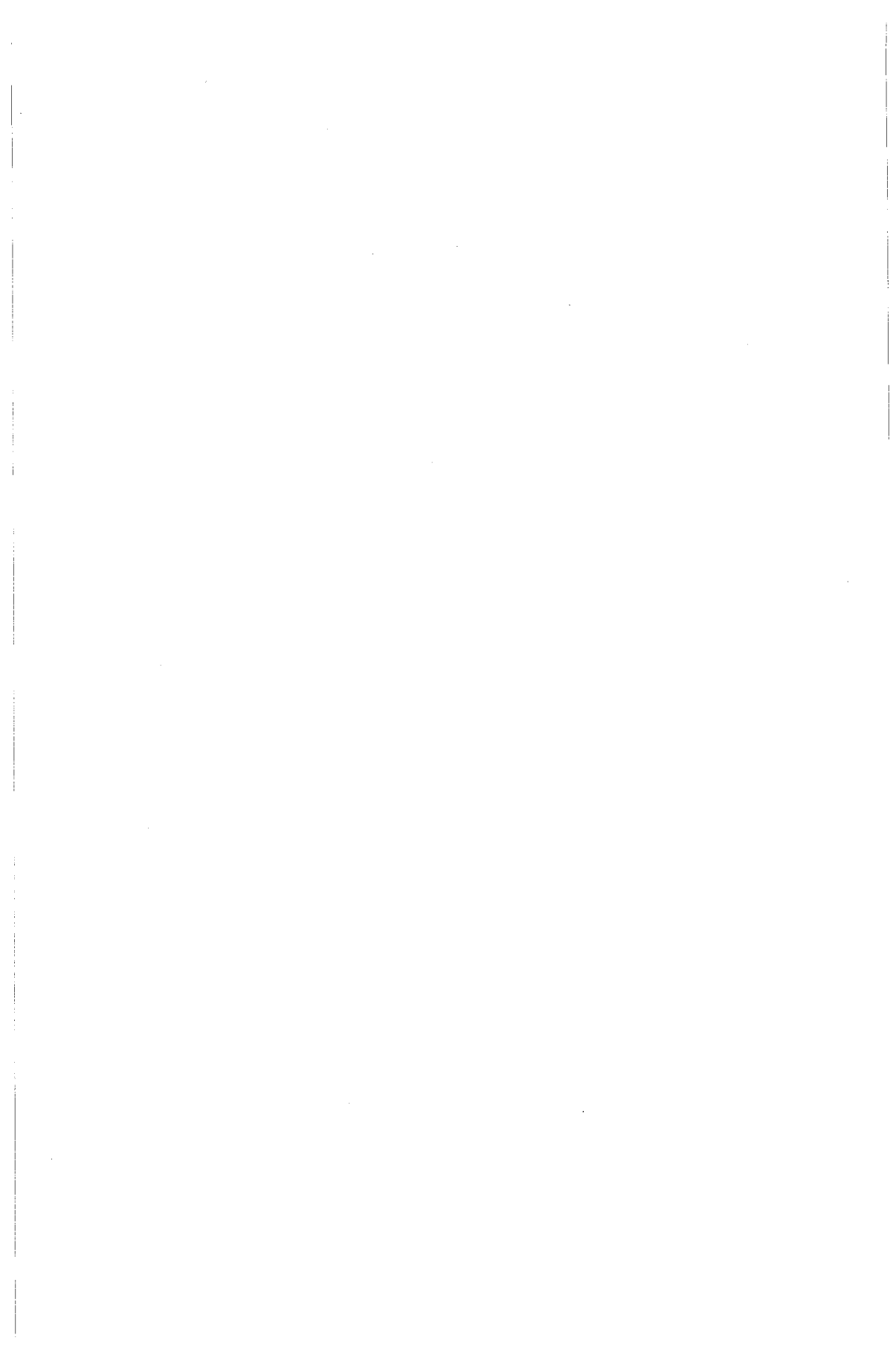
**N.J. Paul, Hasan Ibrahim Al Hosani, and Adel El Masri**

Water and Electricity Department, Abu Dhabi, U.A.E.

## **ABSTRACT**

Glass fiber and Powder Reinforced piping and vessels are used for storing and transport of various corrosive chemicals in power and desalination plants. Mostly these materials are used in conjunction with hydrochloric acid units and hypochlorination (chlorination) dosing systems. Over the years there have not been many problems; however in case of failures, repair and maintenance have caused much difficulty. Total rehabilitation/ replacement are warranted at great cost in some cases. What is the cost effectiveness of such rehabilitation measures and are there any alternative materials available in the market?

**Keywords:** Composite material, GRP, FRP, Creep, Vapor Transfer Resistance



The following are the important chemical handling systems which use these composite materials and have frequent failures.

Seawater for desalination:	Chlorine gas, hypochlorite, hydrochloric acid, alkali (soda) for neutralising in case of the chlorine gas leak
Boiler water treatment	Hydrazine, acid and alkali units
Town Water treatment	Calcium chloride, chlorine, calcium bicarbonate etc.

For the sea water treatment at the intake in one of the older plants, the gaseous chlorine is directly injected and therefore the piping system have been made of rubber lined carbon steel. However when failure occurred the extent of damage was devastating because even small leakages have caused damage to the paint and the piping material and also led to the deterioration of the concrete in the trenches. The acid for the distillers of these plants were also stored in rubber lined carbon steel tanks and several leaks occurred (Fig. 1) in the long piping because of the high pressure head that was needed. As a result the units were discarded and as an alternative the composite materials were brought in.

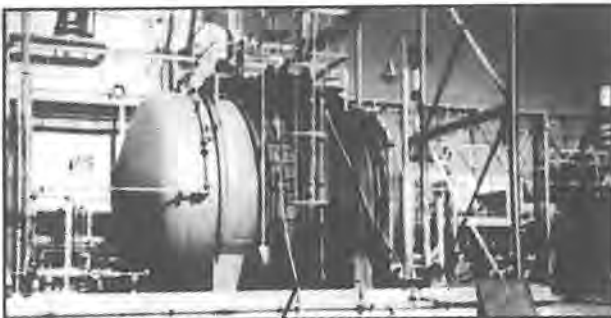
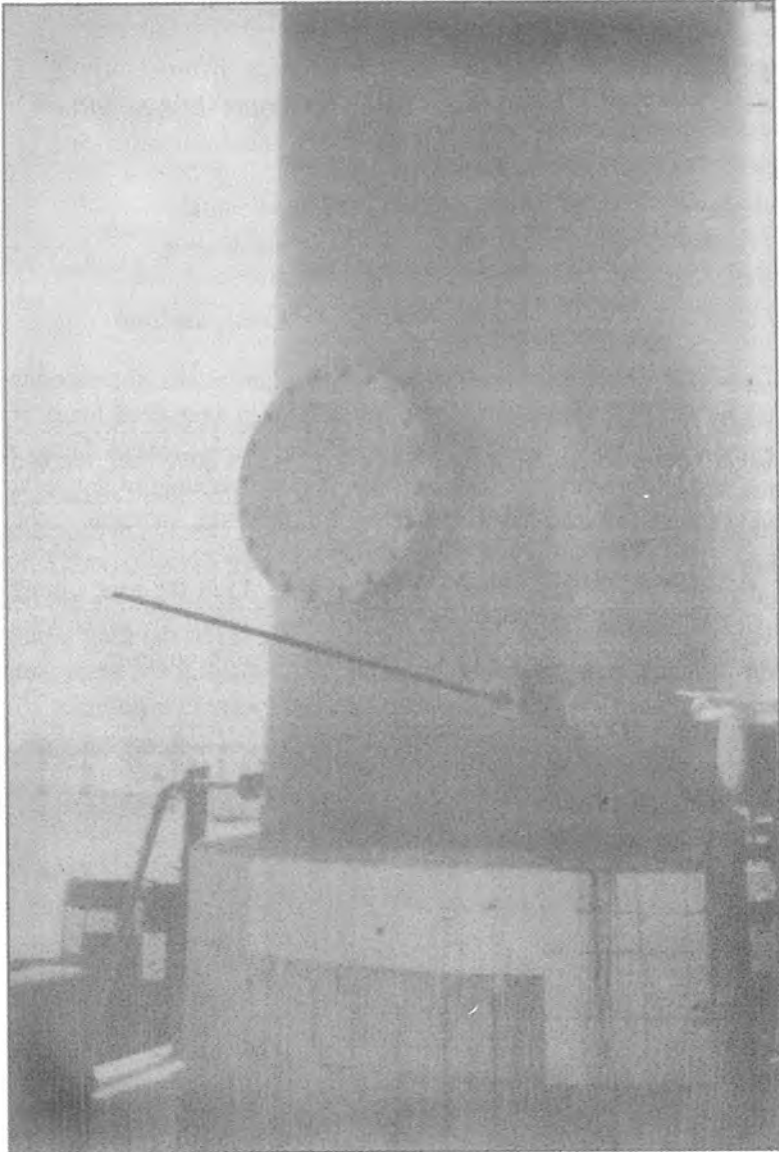


Fig. 1. Acid storage tank leaks and with spillage all over

So in the newer plants, acid is stored in fiber glass reinforced tanks. In many of the new GRP tanks there was not much of a problem for a period of 10 to 14 years but in one of the GRP acid tanks, problems began to repeat over and again. (Fig.2) A decision had to be made whether to switch over to the old rubber lined steel piping and storage tanks or to go in for a newer generation of composite material. Again the question raised was how far dependable these new materials would be? In the case of rubber lined steel, rehabilitation is easier and well known but in the case of GRP or FRP it is not clear how effective could the repairs be.



**Fig.2.** GRP acid tank with leaks and repairs near a flange.

In another GRP tank, storing hypochlorite and standing next to the above acid storage tank, severe leakage developed close to the manhole (Fig.3.). This is a very tall unit about eight meters high and four meters in diameter and mounted vertically on steel support. The accessibility for repair is difficult without scaffolding and the entry to the inside of the tank is difficult even with the help of a rope ladder.



**Fig. 3.** Hypochlorite tank with leak near manhole.

The reason for the failure to occur close to the man hole over and again (and no where else) suggested that it need not be a material failure problem (degradation due to chemical reaction) but something else. This had to be identified so that a proper preventive measure in addition to a good repair procedure had to be worked out to avoid future failures.

In the case of a couple of FRP and GRP neutralisation tanks used for storing soda as well as sodium bicarbonate, the failure has occurred at the bottom (Fig.4.) This is the location where the shell plate meets the annular plate. The bottom plate in one such case is made of thick PVC sheet and the shell is made of FRP. PVC welding has been used for bonding the bottom plate and the annular plate. The leakage has occurred at that joint. If it were a rubber lined steel the repair procedures are easy and direct and the results are guaranteed. But in the case of composite materials many uncertainties arise regarding the suitability of the repair material and the procedure for repair as the success of the procedure depends on the skill of the personnel employed for that purpose. These factors deserve serious

consideration before making decision on spending money on rehabilitation or replacement.



**Fig. 4.** Alkali storage tank leaking at the bottom.

The following questions must be answered:

1. Is this a material failure or a design cum fabrication failure?
2. Why is the failure happening after so many years and what is the cause for such failure?
3. Is the location of the failure identifiable and is the repair material compatible with the existing material?

In the case of non ferrous and ferrous metals and alloys, the cause of failure can be easily determined from the pattern of corrosion (pitting, cracking, delamination etc.) or by a suitable failure analysis. In the case of FRP or GRP, we don't expect a chemical reaction between the material and the chemical stored. So how does one account for such a sudden failure? If this is a mechanically induced problem why and how is it caused? How do failures happen in composite materials? In some cases it has happened in the joint which could be attributed to fabrication problems, but in others failures are close to the man hole. So we have to account for



1. A mechanism of failure in odd locations
2. A method by which we can repair
3. A suitable material for repair in case the original composition is unknown.

The last condition is very important because in one of the power plants a very large diameter water piping was made of glass mat and fiber reinforcement internally at the factory and at the site where pipe lengths were joined some cutting and jointing took place. At the cut joints a patch had to be done and in this case a different resin was used. As a result the joint looked fine mechanically, but chemical bonding had not taken place. Hence upon commissioning, water seeped at the joint between the parent metal and the lining and peeled off everything and finally choked the pumping system. During such failures one of the quickest and easiest things for the duty staff is to find a leak stopping material such as a putty and dab it at the leakage point. In some cases it seemed to work but soon failure repeated in the same place. No cold repair could offer a permanent answer. ***There is no simple solution such as a patch repair for GRP or FRP as in the case of metals.*** As long as the cause of the problem is not eliminated, and a right repair procedure is not adopted, the problem will recur. The difficulties arise if technical drawings or material specifications or the design details regarding the operational limitations have not been provided by the supplier of such units.

Secondly, in a composite material, it is difficult to clean and remove all trace of the chemical from the leak. In the case of a metal a simple washing could rid of the trace chemical and a mechanical grinding could bring up a polished metal surfaces ready for welding or repair. In the case of GRP and FRP and the like, the material leaked is not only locked up in the crack but also could have permeated around and unless these are removed out any bonding is ineffective. This is because in most of these cases the cracks or microcracks would have followed a staggered path so that access to total cleaning is not possible. So after emptying the tank it should be filled with dilute acid until all the alkali is neutralized and the wash water shows a pH of 7. Even then it may be difficult to remove any trace of salt that comes by neutralisation. In the case of a major leakage at the bottom, repair could be effectively achieved only by lifting the shell using cutting tools which involves safety measures for glass particle splattering while grinding off the old joint. All these have site limitations of access for crane and lifting devices. However it must be remembered that the same limitation applies to new fabricated unit to be installed (if decided ) in the place of the old one.

Thirdly we must find out what causes the cracks to develop. In the acid storage tank mentioned above, the manhole was steel lined with the GRP. The failure has occurred because of high stresses due to mechanical tightening of the bolts.

The differences in the hardness of material is less understood by the handling staff. The use of an O ring or gasket could have saved the problem rather than to use force and pressure on the GRP/Plastic faces.

It is difficult to assess the comparative efficiency of the above repair procedures. Therefore a study has to be done of all the old and new systems before any repair/ replacement procedure could be launched. Also the cost Vs lifetime of service has to be evaluated in all new decisions.

The failure of these three large sized tanks and the difficulty in making repairs of lasting nature have caused considerable rethinking. Twenty years ago, there were a limited number of coating products available for chemical plant application. They were chiefly *epoxy or ester based*. The filler material was either glass flake or powder or mat or shreadings depending on the type of equipment and the facility the applicator had. All of them were cold processes. And all of them *claimed* immunity to alkali and acid (equally good) and excellent for water storage, and transportation. Thus the client was confident about the performance capabilities of these units until problems started. A study of product data sheets of various materials available in the market these days gives us some helpful notes on do's and don'ts. Recently two excellent articles have appeared which describe the mechanism of failure of GRP and other allied products.

### **Causes of failure:**

a) **Creep:** Very few engineers know that GRP is not elastic and therefore *does not have an elasticity to an yield point like steel or metals. Like plastic, GRP therefore has visco-elasticity and creep properties under load.* This creep rate depends on not only the load but also the temperature to which the structure is exposed. Also the total creep accumulated depends on the total history of the tank with its load and temperature variations. For example in the Middle East the temperature during summer could vary between 25°C in the nights to 50°C in the day and the sway could take place within a time span of 6 hours from dawn to noon. The stretching and shrinking of GRP under these thermal shocks could lead to thinning of sections and cracking which eventually leads to seepage and failure. Thus GRP tanks operating at about 50°C is not expected to last beyond 5 years according to Hawkins. This is further explained by the fact that the coefficient of expansion for most resins are about 36 to 72x 10<sup>-6</sup> mm/mm./C which when applied to rigid steel with a coeff. of 11x 10<sup>-6</sup> mm/mm/C could cause enough strain when temperature changes are high. This is termed as cold wall effect. Water or any liquid inside the tank tries to lower the temperature of the organic coating while the steel surface gets hotter by the sun rays and ambient air.

b) **Chemical Resistance** : The other reason observed for the failure of the tanks was the lack or inadequacy to chemical resistance. Although the original claims were for a wide range and concentration of chemicals, experience has proved the contrary. Isophthalic polyesters are said to have poorer resistance to chemicals than vinyl esters and polyester based materials. Chlorinated polyesters are not suitable for strong alkaline environment like Bisphenol A Fumarate resins Vinyl ester resins are recommended for strong acid containment while chloro polyesters are suited for oxidising acids. Table 1 lists some of the resin types and their chemical handling capabilities. As mentioned above, twenty years ago neither the supplier would have mentioned these facts to the client nor would the customer understood the implications thereof.

Table 1. List of some resins and filler material.

RESIN	FILLER	LIMITATION	APPLICATION
1) Bisphenol acrylic plastic copolymer	Flake glass (F.G.)	100C max. wet	metal filler for pump impeller etc. (sea water)
2) VE/acrylic copolymer	F.G	110C	aggressive chemicals
3) isophthalin/acrylic copolymer	F.G	60C	sea water & marines
4) PE or VE /acrylic copolymer	F.G		primer & top coat
5) Brominated VE	F.G	80C	alkali potable water
7) P.E acrylic copolymer	F.G	High Temp.	not for alkali aques
8) Acrylic ester chemicals	Flake Graphite	110C	aggressive
9) Epoxy cured	100% solids (unspecified)		abrasive resistance

V.E. Vinyl Ester P.E. Phenolic Ester

c) **Vapor Transfer resistance:** As with all plastic films, water or vapor transfer resistance decides the efficiency of any coating system. In contrast to the chemical resistance which is dependant on the type of resin used, the VTE depends on the type and structure of the filler material. Although spherical or microfiner particles as glass powder fillers are easy to handle as thin uniform spreading, the flake type particles are best suited to and effective in low permeability and show the orientation pattern of such particles which claim as low 0.005 perms for a layer of 150 flakes.

Thus we find that there is more than one reasons for an old fiber glass system to fail. Some would have actually executed the guaranteed service life time but for mishandling, while others would have short lived because of wrong material for a particular storage. It is thus difficult to evaluate any particular system in the absence of sufficient documentation. In the case of acid storage it is possible to evaluate the cost of rubber lined steel tanks and the cost of refurbishment is known. In the case of alkali tanks alternative material such as stainless steel have also failed and there is rethinking why carbon steel could not be used without coating. Since this is only for neutralising leaking chlorine gas and does not flow into any processing operational path, the impurity does not count. However some authors still contend that the cost of carbon steel could be comparable to GRP. More details on such cost comparison are not available yet.

## CONCLUSION

1. History sheets for failures throw more light and evidence on the cause of failure of GRP.
2. Unlike metals there is no set pattern of failure and therefore it is difficult to pinpoint the cause of failure. Even repair procedures are not direct but could be cumbersome.
3. One of the problems in undertaking a repair is the non availability of information about the system.
4. The acid and particularly the alkali that has seeped into the gap needs to be neutralised thoroughly without which any adhesion of the patching material cannot be assured.
5. The crack pattern is not certain and the various other creep and thinning locations cannot be located. Therefore there could be other locations where failure may recur.

6. A total replacement of the unit is also not easy since the demolition and removal of the old plant and site clearing are additional costs. In the worst case the steel has its scrap value while a very old GRP/FRP item is of no value whatsoever. As per new structures costings, steel with coating is comparable to GRP.
7. The fact that GPP has creep, it is good for erection only in shaded area/ enclosure away from heat dissipating units like air-conditioners or transformers, ovens etc.

The claims made by new generation of products is yet to be seen.

## **REFERENCES**

1. Peter Goodwin - The sectional Glass coated tank - Desalination and Water Reuse - Sept. 1996 p38
2. Adrian Hawkins - The durability of GRP storage tanks in hot climates ibid p39.
3. Ko Keijman - The novel Siloxane Hybrid Polymers in Protective coatings Protective coatings Europe, July 1996 p 26
4. William R Slama - Polyester and Vinyl ester Coatings, J Protective coatings and linings, May 96 p 88.
5. Paul N.J. - WED Internal Report on GRP and FRP tank failures June 96.

# **Feed Salinity and Cost-Effectiveness of Energy Recovery in Reverse Osmosis Desalination**

*M.A. Mandil, H.A. Faroq, M.M. Naim and M.K. Attia*

# FEED SALINITY AND COST-EFFECTIVENESS OF ENERGY RECOVERY IN REVERSE OSMOSIS DESALINATION

M.A. Mandil, H.A. Farag, M.M. Naim and M.K. Attia

Alexandria University

Alexandria, Egypt

## ABSTRACT

For salinities covering the range from brackish water to highly saline sea water (50 fold range of salinities), effect of energy recovery (E.R.) on unit cost of desalination by reverse osmosis (RO) is sought. Since recovery is a primary factor in this respect, variables affecting recovery are considered in such a way that ensures trouble-free operation of RO units. Limiting conditions such as maximum and minimum allowable brine flow rates, maximum product flow, limiting brine osmotic pressure are introduced as limiting factors in design calculations for one MGD (3785 m<sup>3</sup>/d) single stage plant. Results presented graphically show possible working ranges for different feed salinities. Maximum technically feasible recovery ( $Y_{TF}$ ) is defined. ( $Y_{TF}$ ) for each salinity is determined and chosen for calculating cost-reduction expected from ER. A sensitivity analysis is also conducted to determine the effect of electrical energy unit cost. Results show that ER is expected to render cost reduction that warrants its use for sea water desalination at all normal levels of salinity. However, energy unit cost higher than 6 cents/KWh may be needed for noticeable cost reductions with brackish waters.

**Keywords :** Reverse osmosis / Feed salinity / Energy recovery / Cost-reduction.

## INTRODUCTION

Reverse osmosis has always been noted for its low energy consumption. This is not only due to its low process energy requirement but also as a consequence of the energy recoverable from brine before its disposal. Energy recovery from the brine depends on the amount of brine and on its pressure which in turn depends primarily on the salinity of the feed. Higher brine pressure and higher flow rate means more recoverable energy. That is perhaps why energy recovery has been often referred to as being more adaptable to SW rather than brackish water desalination.

The main aim of this work is to determine at what salinities, energy recovery starts to lose its cost effectiveness. For this purpose a 50 fold range of salinities have been studied including 6 brackish waters, 5 different sea water compositions in addition to 3 simulated SW compositions to fill in the gaps. Ionic compositions, reported in the literature for these waters were used for the calculation of their osmotic pressures ( $\Pi$ ) as suggested in Permasep manuals [1] using the following equation :

$$(\Pi) = 1.205 \Phi(T + 273.15) \Sigma \bar{m}_i \quad (1)$$

$\Phi$  being a function of ionic molalities ( $\bar{m}_i$ ) and ionic strength.

### R.O. system selected

DuPont permeators were chosen simply for the availability of data and parameters needed for design. For salinities above 10,000 mg/l 8" B-10 model 6840T permeators were used and 8" B-9 model 0840 for lower salinities. A single pass arrangement was used in all cases as a convenient basis for comparison.

Number of permeators ( $N_p$ ) required for the production of 1 MGD ( $Q_p$ ) of desalinated water

$$N_p = (Q_p / Q_{pe}) \quad (2)$$

$Q_{pe}$  permeator productivity at the end of 5 yrs of operation was calculated using

$$Q_{pe} = (PCF) (TCF) (MFRC) Q_i \quad (3)$$

Where  $Q_i$  is the initial permeator productivity at standard test conditions, and PCF, TCF, MTRC being pressure correction factor, temperature correction factor and membrane flux retention coefficient. Values suggested by manufacturers for these coefficients at selected conditions were used [1].



## Recovery to be used for design purposes

For all salinities, effect of changing recovery on permeator productivity was determined at selected combinations of temperatures and pressures.

For sea water (25°C/1100 psi), (25°C/1000 psi), (35°C/900 psi),  
(35°C/800 psi)

For brackish water (25°C / 400 psi), (30°C / 300 psi), (35°C / 200 psi)

However attractive it may be, to work at high recoveries from the economic point of view, there are several considerations which impose technical limitations on the level of recovery one can apply for water of a certain salinity. Increasing recovery increases brine salinity and decreases its amount. The higher the concentration of the brine, the higher its osmotic pressure ( $\Pi_b$ ), and hence the value of the driving force ( $P - \Pi_b$ ), may drop to limits that causes water permeation across the membrane to be too small or even to stop. Hence a higher limit for  $\Pi_b$  relative to  $P_b$  must be set in order to guard against such a situation. For the purpose of the present study, a ratio of  $\Pi_b/P_b$  was arbitrarily set at 0.9.

With regard to brine flow, maximum and minimum brine flow rates are to be kept at limits suggested by manufacturers [1].

Variation of permeator productivity as a function of recovery at different salinities along with superimposition of brine flow and  $(\Pi/P)_b$  limitations lead to the development of diagrams as that shown in figure 1. These diagrams show working areas that identify both productivities ( $Q_{pe}$ ) and recoveries ( $Y$ ) which are technically feasible without violating above conditions. The maximum value of  $Y$  within these areas were taken as maximum technically feasible recovery  $Y_{TF}$ . Hence  $Y_{TF}$  as defined here is the highest recovery attainable from a certain properly treated feed having a given TDS and known ionic composition, in a single stage system, operated at chosen temperature and pressure, without violating maximum and minimum brine flow rate limitations and keeping  $(\Pi/P)_b$  at a prescribed limit of  $\leq 0.9$ . In addition, presence of specific elements in brine (and/or) product water, should be within limits to avoid scaling and keep product quality as desired.

Values of  $Y_{TF}$  obtained from a series of diagrams such as that shown in figure 1 were previously reported by the authors [2].  $Y_{TF}$  as a function of salinity at selected temperatures and pressures are given in figures 2 and 3.

Rather than determining effect of energy recovery on product water cost at a fixed value of recovery for all salinities,  $Y_{TF}$  corresponding to each salinity was used instead.

## Energy calculations

Pumping energy requirements (ERQU) was calculated using the following equation [3]:

$$\text{ERQU} = \frac{6.9 P_f}{Y (3600) \text{ Epm}} \text{ Kwh/m}^3 \quad (4)$$

where  $P_f$  feed pressure in psi

$Y$  recovery

$\text{Epm}$  combined pump & motor efficiency taken here as 0.75.

Energy consumption for pre-and post-treatment was taken as suggested by Van Dijk [3] to be  $(0.5/Y)$  KWh/m<sup>3</sup>.

Hydraulic turbines were chosen for energy recovery from which recoverable energy (ERCO) was calculated using [3]:

$$\text{ERCO} = \frac{6.9 (P_f - \Delta P) F_R}{Y 3600} (1 - Y) \text{ KWh/m}^3 \quad [5]$$

where  $\Delta P$  pressure drop through permeator and piping

$E_R$  turbine efficiency, taken here as 0.8

## Capital cost

Required capital (RC) was estimated with proper cost adjustment following procedure suggested by Wade [4], including as main items cost of intake, pretreatment, membranes, pumps, energy recovery turbines, with additional allowance for civil, electrical and miscellaneous items.

## Product cost

For the calculation of water cost the following conditions were adopted

- \* Plant life 20yrs
- \* Annual amortization rate 0.1175
- \* Membrane replacement rate 20% per annum (5 yr life)
- \* Energy cost evaluated at 3 electrical energy rates 3,6 & 9 cents/KWh

- \* Cost of pre-treatment, operation, maintenance and other cost items was taken as 10% of subtotal of all other cost items.
- \* Average annual load factor 0.8

Product water cost was calculated at different feeds of sea water and brackish water, at corresponding values of  $Y_{TF}$ , for two alternatives with and without the use of energy recovery turbines. The cost saving in each case was calculated. Selected results are shown in figures [4-6].

## CONCLUSIONS

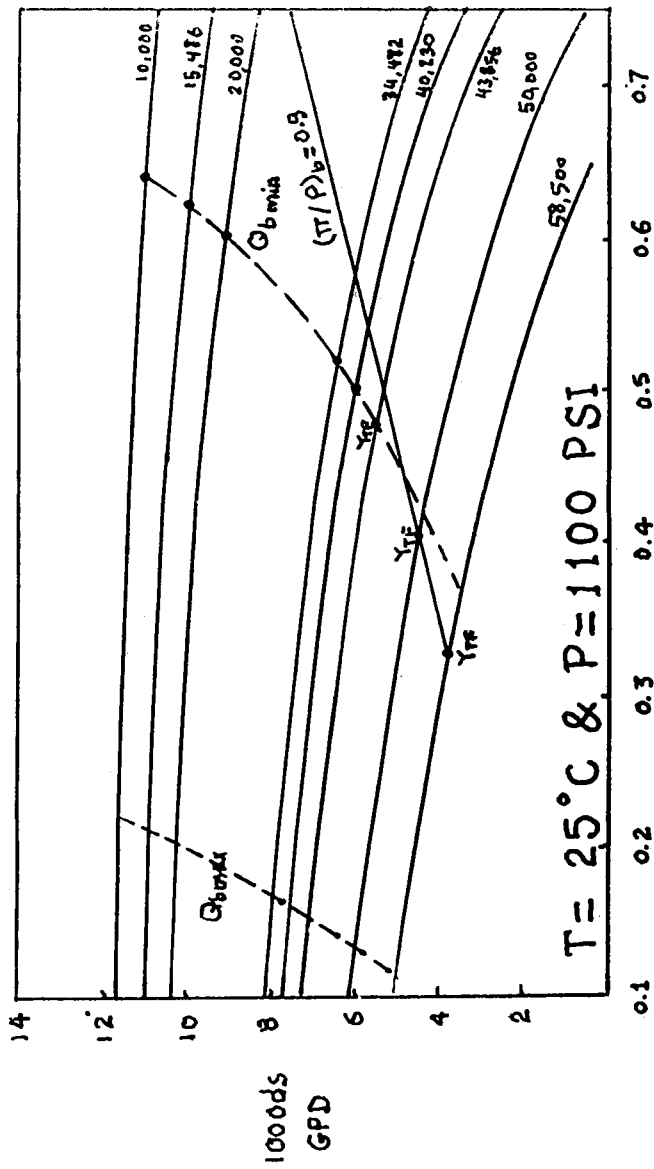
1. Cost reduction due to E.R. decreases with increase in recovery as an obvious result of reduction in brine flow rates.
2. General trend for SW is that increasing feed salinity leads to the increase in cost saving. For brackish water this trend is noticed only at relatively high salinities.
3. Increase in electrical energy unit cost leads to progressively high cost reduction for both sea water and brackish water feed.
4. Energy recovery is expected to render cost reductions that warrant their use for sea water at all normal levels of salinity (>35000ppm).
5. Energy unit cost higher than 6 cents/KWh may be needed for SW of lower salinities (< 35000ppm).
6. With brackish water, energy recovery starts to give percentage cost reductions in the order of 5% or higher at energy unit cost higher than 6 cents/KWh.
7. In general, cost reduction is found to be particularly dependent on recovery (Y), decreasing sharply at low values of Y (below 50%) then decreases slowly from there on.

## **ACKNOWLEDGMENT**

1. This work is based on M.Sc. Thesis prepared by M.K. Attia at the Chem. Eng. Dept. Alexandria Univ. Alexandria, Egypt.
2. Authors express their deep appreciation to Dr. A.H. Tewfick for availing his computer programming abilities during the progress of this work.

## **REFERENCES**

1. Permasep Engineering Manual (PEM), Bulletins 2020 & 3020, DuPont Company, Wilmington DE, (1992).
2. Mandil NU et. al., "Maximum technically feasible recoveries in SWRO," Symposium on desalination operations in Kingdom of Saudi Arabia Organized by King Saud University & SWCC, Riyadh, S. A., June 4-6 (1994).
3. Van Dijk JC et al, "Optimizing Design and Cost of SWRO systems", Desalination 52 (1984) 57-73.
4. Wade RO, "R.O. Design Optimization", Desalination 64 (1987) 3-16.



FIGURE(1) EFFECT OF SW FEED SALINITY ON PERMEATOR (B10) PRODUCTIVITY (Y<sub>TF</sub> DETERMINATION)

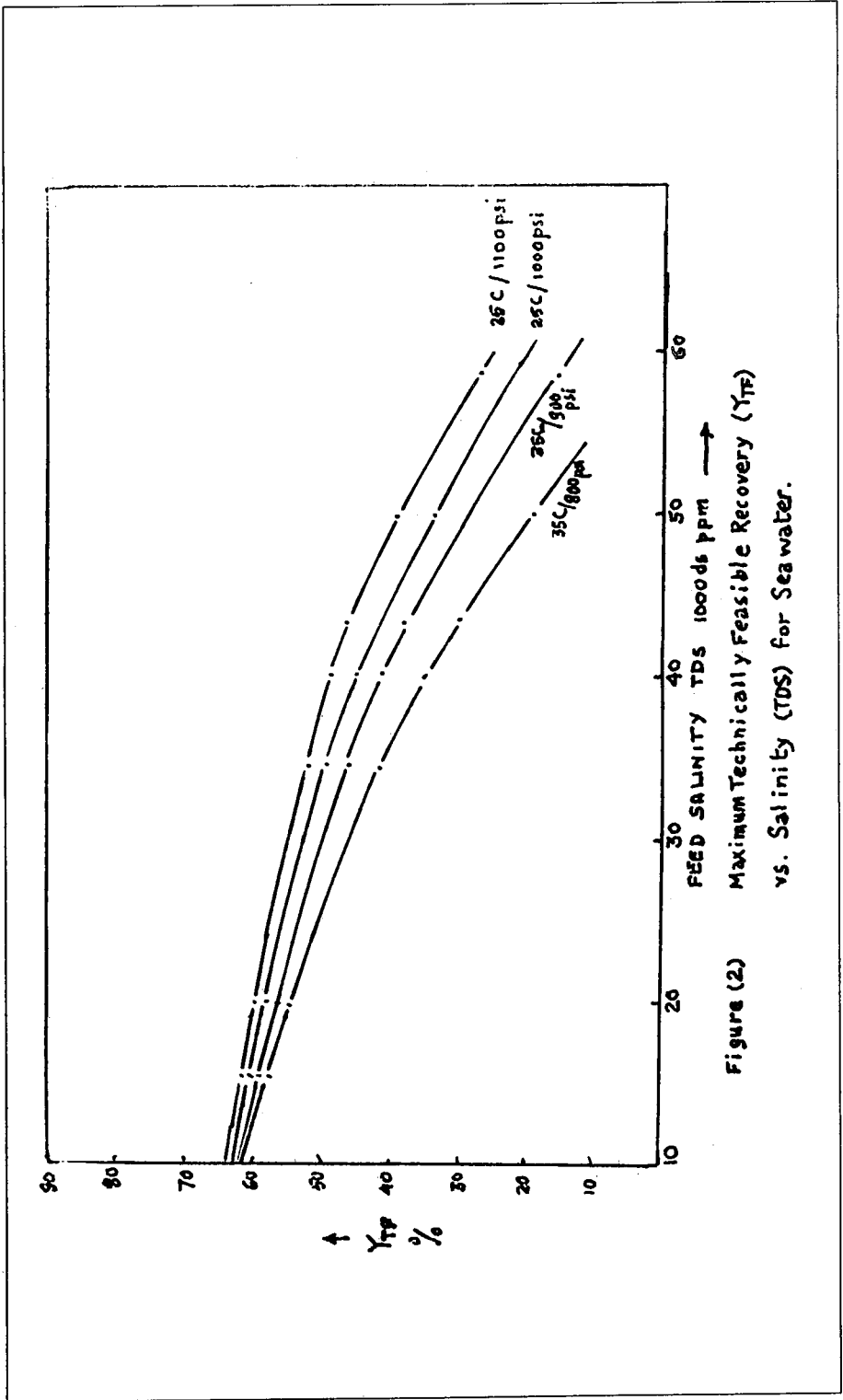


Figure (2) Maximum Technically Feasible Recovery ( $Y_{TF}$ ) vs. Salinity (TDS) for Seawater.

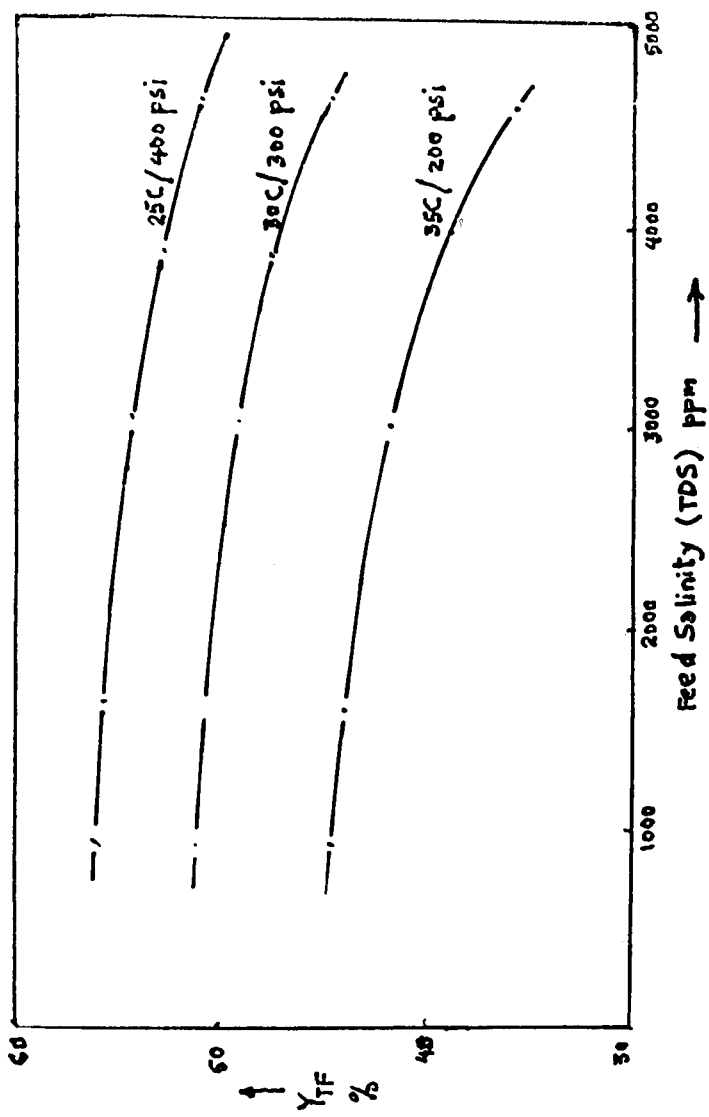


Figure (3) Maximum Technically Feasible Recovery (YTF) vs. Salinity (TDS) for Brackish Water.

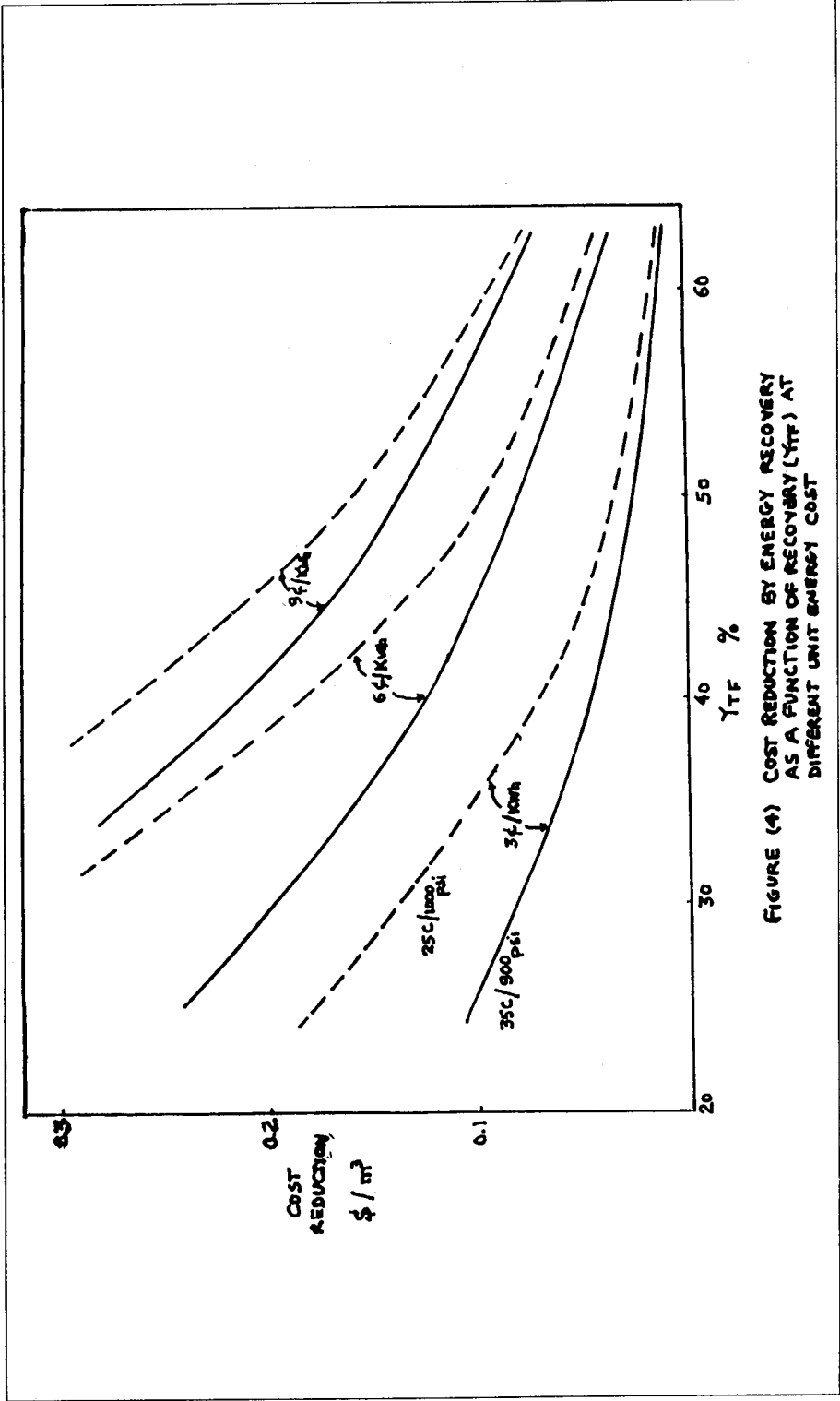
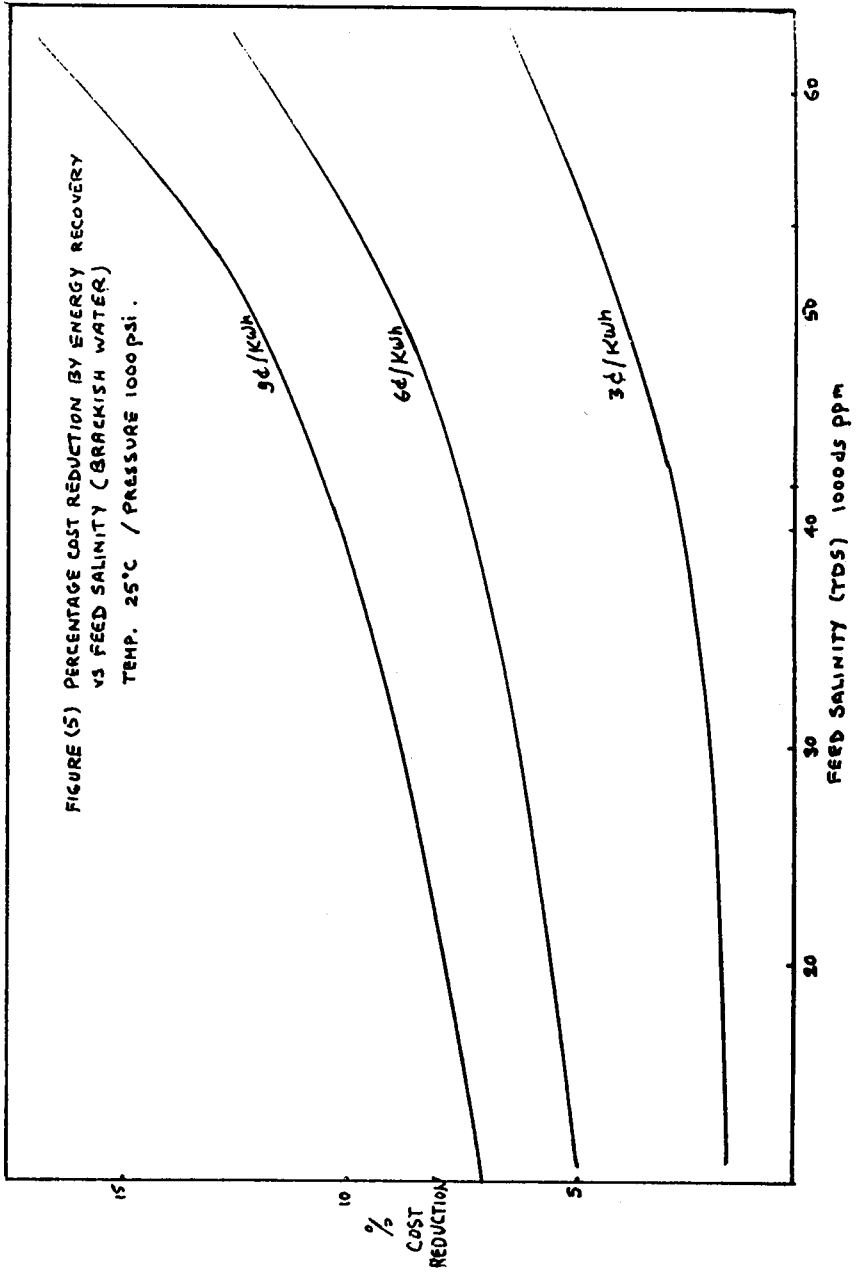


FIGURE (4) COST REDUCTION BY ENERGY RECOVERY AS A FUNCTION OF RECOVERY (YTF) AT DIFFERENT UNIT ENERGY COST



FIGURE (5) PERCENTAGE COST REDUCTION BY ENERGY RECOVERY  
VS FEED SALINITY (BRACKISH WATER)  
TEMP. 25°C / PRESSURE 1000 PSI.



**Comparative Performance Analysis of Two Seawater  
Reverse Osmosis Plants: Twin Hollow Fine Fiber  
and Spiral Wound Membranes**

*Sameer Bou-Hamad, Mahmoud Abdel-Jawad,  
Mohammed Al-Tabtabaei and Saud Al-Shammari*

# COMPARATIVE PERFORMANCE ANALYSIS OF TWO SEAWATER REVERSE OSMOSIS PLANTS: TWIN HOLLOW FINE FIBER AND SPIRAL WOUND MEMBRANES

**Sameer Bou-Hamad, Mahmoud Abdel-Jawad, Mohammad Al-Tabtabaei and Saud Al-Shammari**

Water Desalination Department, Water Resources Division

Kuwait Institute for Scientific Research

Kuwait

## ABSTRACT

In spite of the great advances in increasing the reliability, and technical and economic viability of seawater desalination by reverse osmosis (RO) made over the past decade, its commercial application is still increasing. Unit design is highly dependent on the quality of the feedwater and pretreatment method used to safeguard membrane performance. Work is in progress at Doha Research Plant (DRP), in Kuwait, to determine the performance of two seawater RO units under the prevalent seawater conditions. The RO units have a total capacity of 2x300 m<sup>3</sup>/d and are fed with beachwell seawater with a silt density index (SDI) of around 2, without any further pretreatment. The two RO plants are identical in all operational aspects, but differ in membrane configuration, i.e., twin hollow fine fiber and spiral wound. This paper discusses the analytical performance of the two types of membranes using a single-stage system. The paper covers one year of performance data and discusses the technical parameters of water productivity and permeate quality. It also covers the evaluation of membrane performance, system availability and operational problems encountered.

**Keywords:** Availability, salt rejection, productivity, permeate quality, operational problems.

## INTRODUCTION

When reverse osmosis (RO) was first commercialized in the early 60's it was considered suitable for desalting only brackish water, which is much less saline than seawater but is still too saline for human consumption and is of limited value for agriculture on a large commercial scale.

The state of the art of RO is such that the site-specific design specifications of a new plant are still far from routine. This is particularly true in the case of seawater RO (SWRO). Some of the parameters such as quality of the feedwater, recovery of fresh water and problems associated with membrane sensitivity to scaling and fouling, are highly site-dependent. However, great advances have been made in RO technology during the last decade which have resulted in a rapid increase in the use of SWRO, and consequently, its emergency as an economically viable alternative to multistage flash (MSF) for seawater desalination (Wagnick Consulting, 1994). The acceptance of this technology will increase further with improvements in feed pretreatment, plant performance, membrane performance and energy consumption. RO has already become the major competition to MSF. The abundance of electricity in the Middle East combined with increasing demands for water and restrains on capitals spending points to SWRO as a technology whose time has come. During the last 10 years, hundreds of SWRO plants have been built worldwide. With each year, the number of plant sites and their cost-effectiveness have increased.

Most of the world's desalination capacity is located in the Arabian Gulf region. In spite of the recent advances in RO, its application to seawater desalination, is still being optimized. A single-stage RO module for highly saline seawater feed is already on the market and requires operating references. Devices to reduce the energy consumption of this process are actively under development in several places worldwide. Feedwater pretreatment systems are also under development. Beachwell seawater intake has proved to be very promising wherever installation has been possible (Abdel-Jawad, et al. 1994).

This paper discusses the performance of two types of single-stage membranes (i.e., twin hollow fine fiber and spiral wound). The objective of this work is to establish membrane characteristics and identify factors that can influence membrane performance and service life. For the purpose of data evaluation, a special software package was developed to effectively evaluate system performance under standard conditions.

## PROCESS DESCRIPTION

Two seawater RO plants capable of desalting Gulf seawater through single stage were designed and installed at DRP. Each line is designed to operate independently to produce 300 m<sup>3</sup>/d using raw seawater from a common beachwell system. One plant utilizes twin hollow fiber membrane, whereas the other plant utilizes spiral-wound, thin film membrane.

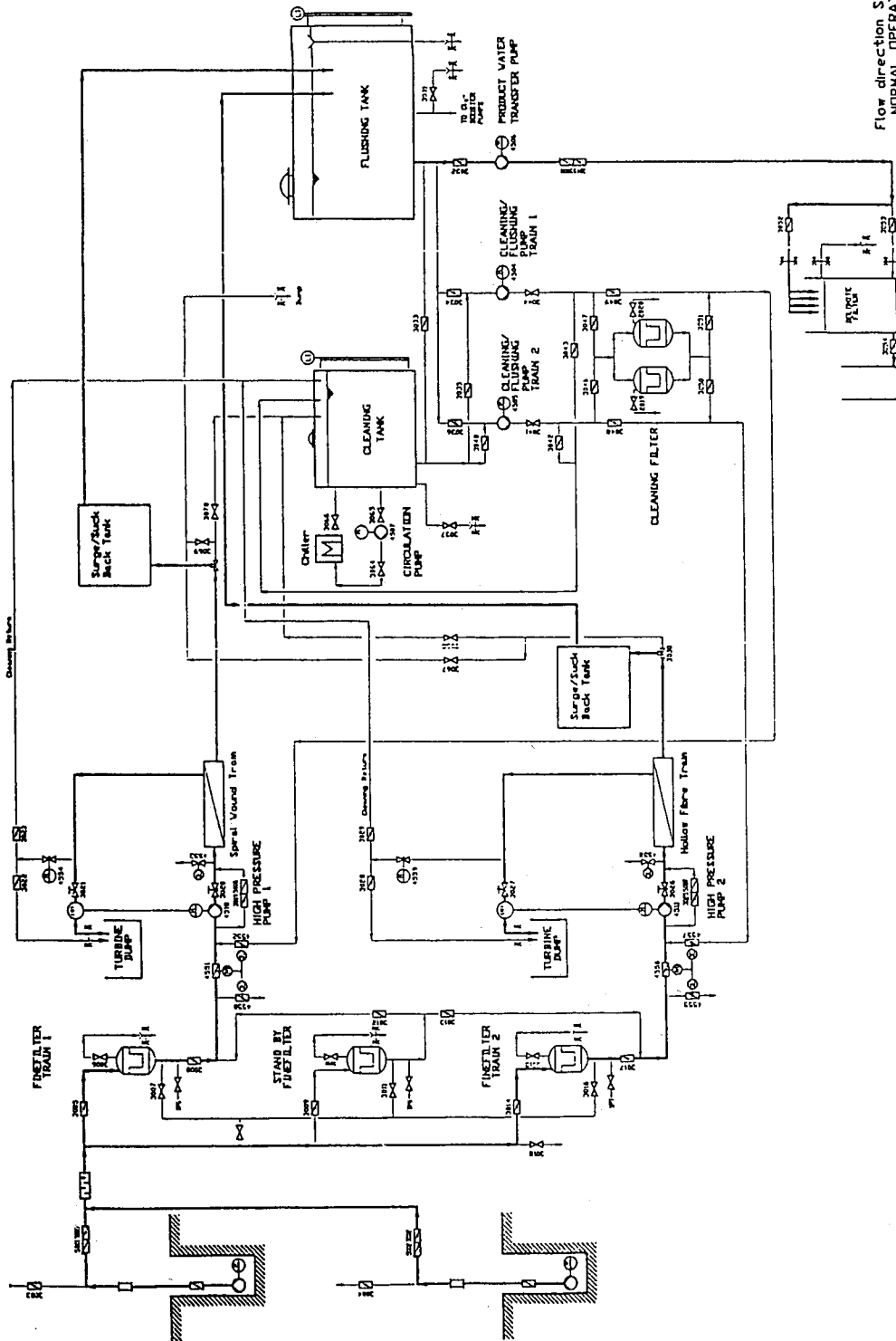
Fig. 1 shows a schematic diagram of the SWRO system installed at DRP. The seawater feed is withdrawn from two beachwells drilled at a 30-m depth near the beach at Doha. It consists of two well pumps, a complete dosing system, two independent RO trains and a complete post-treatment system. The total capacity of the plant is 2 x 300 m<sup>3</sup>/d.

The desalination plant is fed by one of two submersed pumps with a flow of 75 m<sup>3</sup>/d. The seawater feed can be chlorinated by dosing Cl<sub>2</sub> gas. If chlorination of the feed is practised, dechlorination of the seawater upstream of the membranes should be ensured. An acid dosing system was also installed to adjust the pH value to 7.1 to ensure a negative Stiff & Davis Index value. Furthermore, an antiscalant is dosed to inhibit carbonate and non-carbonate scaling on the membrane. The pretreated water then passes a fine filter system consisting of three-bag fine filters (one fine filter per train and, one filter standby) with a mesh size of 5 µm. A multistage, centrifugal, horizontal, high-pressure pump pressurizes the pretreated seawater to the required operation pressure.

The pressurized water is guided to the membrane stacks, which are equipped with suitable membranes to separate the salt in the brine stream from the fresh water permeate in one stage. The number of membranes are selected to enable the rated output of 300 m<sup>3</sup>/day per train (spiral wound train consists of five pressure vessels each housing six elements, and hollow fibre train consists of eight pressure vessels each housing a twin membrane element).

The permeate of each train flows to the holding surge/suck back tank located above the module racks and from there by gravity to the flushing tank. Each train is equipped with a Pelton wheel turbine to recover energy from the reject brine which is discharged from the RO membranes. The turbine is coupled with the motor shaft of the high pressure pump so that the recovered energy reduces the power required for running the motor of the pumps.

Automatic flushing of the modules, high pressure pump and pipe work with permeate is performed at every plant stop by means of the cleaning/flushing pump. By flushing the brine solution inside the modules and the seawater in the high pressure pump and replacing it with low salinity water, scaling and corrosion



Flow direction Scheme  
NORMAL OPERATION

due to stagnation are minimized.

In case of plugging of the membranes as indicated by increase in differential pressure across the membrane bundle, an increase in permeate salinity and a decrease in productivity, cleaning with suitable chemical solutions has to be performed. A common chemical cleaning facility comprising a mixing tank, cleaning pumps, fine filter system, water chiller and interconnecting pipe work and valves is available.

The permeate is transferred by means of the product water transfer pump to the dolomite filter. Upstream of the dolomite filter, the permeate is sterilized by injection of gaseous chlorine. The pH of the product water, which is usually lower than that of the feed, is adjusted inside the dolomite filter which is equipped with supporting gravel and dolomite material .

Finally, the product water flows by gravity from the dolomite filter to the product storage tank.

## **RESULTS AND DISCUSSIONS**

Table 1, shows typical average service parameter values of the beachwell seawater intake at Doha. Figs, 2, 3 and 4 show the feed conductivity, temperature and silt density index (SDI), respectively. In Fig 2, it can be seen that the conductivity of the feed had increased from about 49,500  $\mu\text{S}/\text{cm}$  to about 55,000  $\mu\text{S}/\text{cm}$  during the first four months of operating and remained almost steady thereafter. The low salinity of the feed can be attributed to the availability of subsurface water in the vicinity of the wells during the development of these wells. A slight drop in salinity towards the end of the operation period can be attributed to accumulation of rain water in the subsurface zone. The rain for that year was above average in Kuwait.

**Table 1. Typical Average Service Parameters of the Beachwell Seawater Intake System at Doha.**

Parameter	Value
Pressure (bar)	4.9
Temperature (°C)	24.8
Conductivity (mS/cm)	54.0
SDI (%)	1.4
pH	7.8
pH, after acid dosing	7.05
Feed to RO <sub>1</sub> (m <sup>3</sup> /h)	35.0
Feed to RO <sub>2</sub> (m <sup>3</sup> /h)	35.0
Running hours	6900
Energy Consumption (KWh/m <sup>3</sup> )	0.225

With regard to temperature, it can be seen from Fig. 3, that it varied between 23.5°C and 26°C for winter and summer, respectively. The SDI value of the feedwater was always below 3% with average value of 1.4% as can be seen in Fig 4.

The two RO lines are operated over 6000h in June 1996. RO line No. 1 (RO<sub>1</sub>) is using spiral wound membrane (Fluid system-2822 SS), where as RO line No. 2 (RO<sub>2</sub>) is using hollow fiber-twin membrane (Dupont- 688OT-B-10).

During the one year operation, RO<sub>1</sub> was chemically cleaned only one time compared to four clearings for RO<sub>2</sub>. Table 2 shows the shutdown time, the reason for shutdown and the availability of the RO<sub>1</sub> and RO<sub>2</sub> plants. It can be seen that 99.6% and 93.2% are the availabilities of RO<sub>1</sub> and RO<sub>2</sub>, respectively. The lower availability of RO<sub>2</sub> is due to increase in the salinity of the permeate which required several chemical cleanings and treatments of the modules.

Typical flow diagram for RO<sub>1</sub> and RO<sub>2</sub> are shown in Figs. 5 and 6, respectively. It can be seen that the permeate recovery of RO<sub>1</sub> and RO<sub>2</sub> after one year of operation, was 35.5%, giving the recovery design value of 35% both lines.

Operational parameters, product flow rate and salt rejection versus time for RO<sub>1</sub> (i.e., spiral wound membranes) are shown in Figs. 7, 8 and 9 respectively, whereas the corresponding data for RO<sub>2</sub> ( i.e., hollow fiber-twin ) are shown in Figs. 10, 11 and 12. After one year of operating, RO<sub>1</sub> and RO<sub>2</sub>, had productivities that were still near the design values. With regard to the salt rejection, RO<sub>1</sub> is still operating according to the design value ( i.e., 99.4 normalized value versus 99.8 design value ). As for RO<sub>2</sub>, salt rejection suffered drop from 99.8% to 96.4% during the one year of operation (i.e., loss of 3.4% in salt rejection for RO<sub>2</sub> compared with 0.4% for RO<sub>1</sub>).



Inspection of the fine filters revealed the formation of slime matter inside the 5  $\mu\text{m}$  bags. The process of elimination excluded the beachwells as the source of the slime. The exclusion of suspected sources limited the possible reasons for the formation of the slime added chemicals, i.e. antiscalant, acid and bisulphite. Work is in progress to identify the specific reason for the formation of the slime which affected the performance of the twin hollow finer fiber modules, but did not affect the spiral wound modules (figs. 9 and 12). Work will continue on operating these two lines under comparable conditions to evaluate their long-term performance.

## **CONCLUSION**

Arabian Gulf seawater is one of the most saline seawater in the world. Present RO technology has proved to be suitable for desalting this highly saline water through a single-stage configuration. Excellent availability, salt rejection and permeate productivity were demonstrated for more than 6000 h of operation under comparable conditions of two RO plants.

Spiral-wound RO modules proved to be superior to twin hollow fine fiber RO modules in resisting slime that accumulated downstream of the chemical dosing points. During the one year of operation, the spiral wound modules was cleaned one time, whereas the twin hollow fine fiber was cleaned four times. Investigating the source of slime indicated that the added chemicals (i.e., antiscalant, sulfuric acid and sodium hydrogen sulfite) could be the reason for slime formation. Work to determine its exact cause will continue. Work to evaluate the performance of the RO modules will also continue for another year.

## **ACKNOWLEDGMENT**

The authors wish to thank the Ministry of Electricity and Water (MEW) in Kuwait, for the partial financial support of this project.

## REFERENCES

- [1] Abdel-Jawad, M., & Ebrahim, S., Beachwell Seawater Intake as Feed for an RO Desalting System. *Desalination*, 99 (1994) 57-71.
- [2] Wangnick Consulting, 1994, IDA Worldwide Desalting Plants Inventory. The International Desalination Association.

**Table 2 . Shut-down Time, Reasons and Availability of RO<sub>1</sub> and RO<sub>2</sub> Plants.**

**RO<sub>1</sub> (300 m<sup>3</sup>/ day) Spiral Wound**

Shut-down Period		Reason for Shut-down	Total Hrs of Shut-down
From	To		
19/08/95 08:00	19/08/95 10:00	Maintenance of Pressure Gauge	2
24/08/95 12:00	24/08/95 14:00	Maintenance of Pressure Gauge	2
26/08/95 16:00	26/08/95 18:00	Maintenance of Feed Line	2
02/11/95 09:00	02/11/95 13:00	Adjustment of Pump Discharge Valve	4
18/05/96 08:00	18/05/96 20:00	Chemical Cleaning with (Citric acid and Ammonia)	12
03/04/96 08:00	03/04/69 12:00	Pressure Gauge Maintenance	4

*Total Running Hours*                      6674.32 hr

*Total Shut-down*                            26 hr

*Availability*                                    99.61%

**RO<sub>2</sub> (300 m<sup>3</sup>/ day) Hollow Fine Fibre-Twin**

Shut-down Period		Reason for Shut-down	Total Hrs of Shut-down
From	To		
28/09/95 12:00	09/10/95 08:00	To investigate high Conductivity of permeate	260
17/02/96 20:00	18/02/96 10:00	Chemical Cleaning (Citric acid +Ammonia +PTB)	10
15/03/96 12:00	19/08/96 08:00	Chemical Cleaning (Citric acid +Ammonia +PTB)	92
13/04/96 12:00	14/04/96 08:00	Chemical Cleaning (Citric acid +Ammonia +PTB)	20
04/05/96 08:00	07/05/96 08:00	Chemical Cleaning(Citric acid +Ammonia +PTB+EDTA+ Caustic Acid)	72

*Total Running Hours*                      6691.24 hr

*Total Shut-down*                            454 hr

*Availability*                                    93.21%

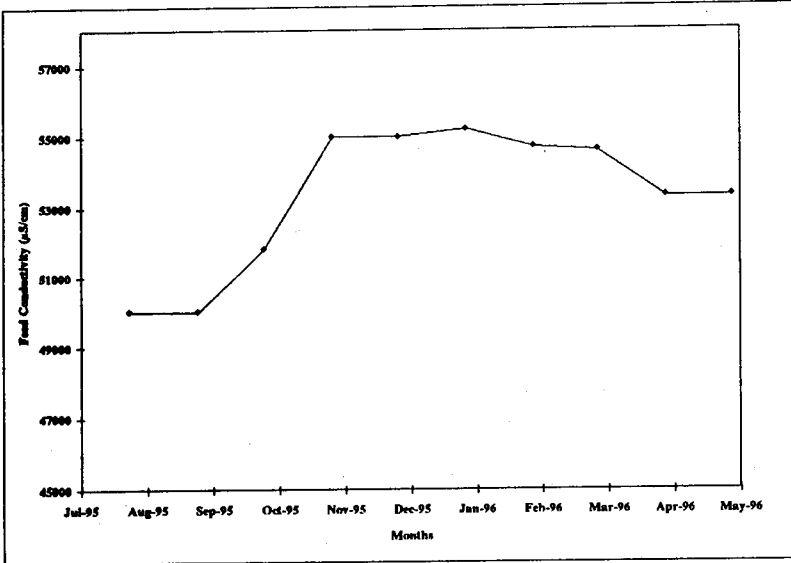


**Fig. 2. Average monthly Conductivity of the beachwell water versus time.**

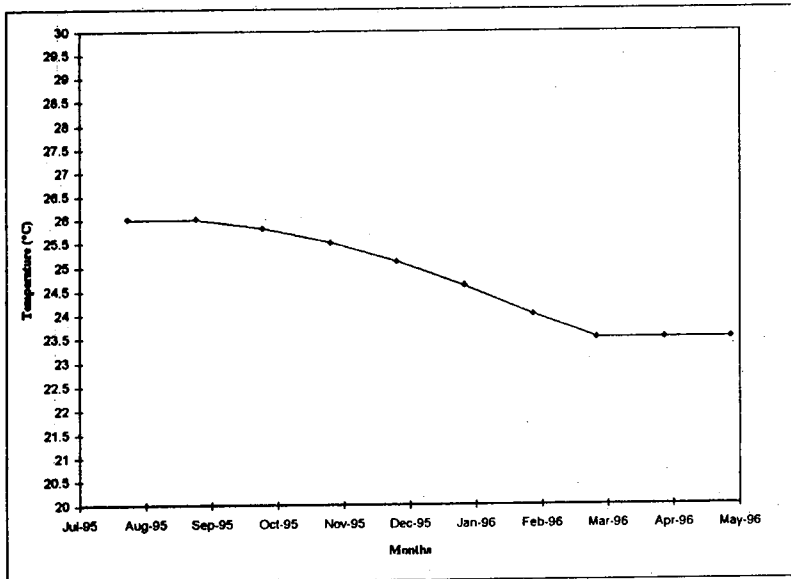


**Fig. 3. Average monthly temperature of the beachwell water versus time.**

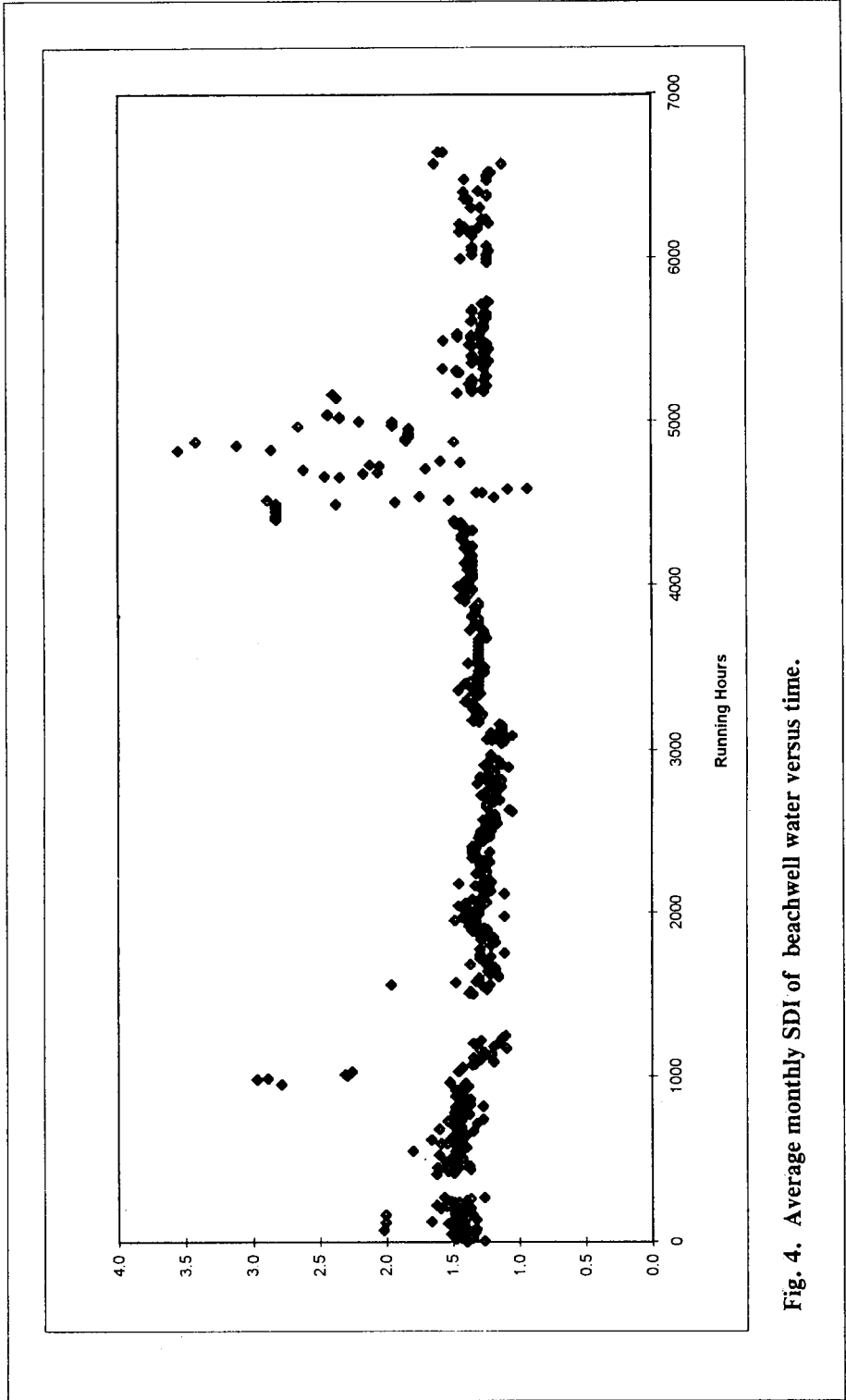


Fig. 4. Average monthly SDI of beachwell water versus time.

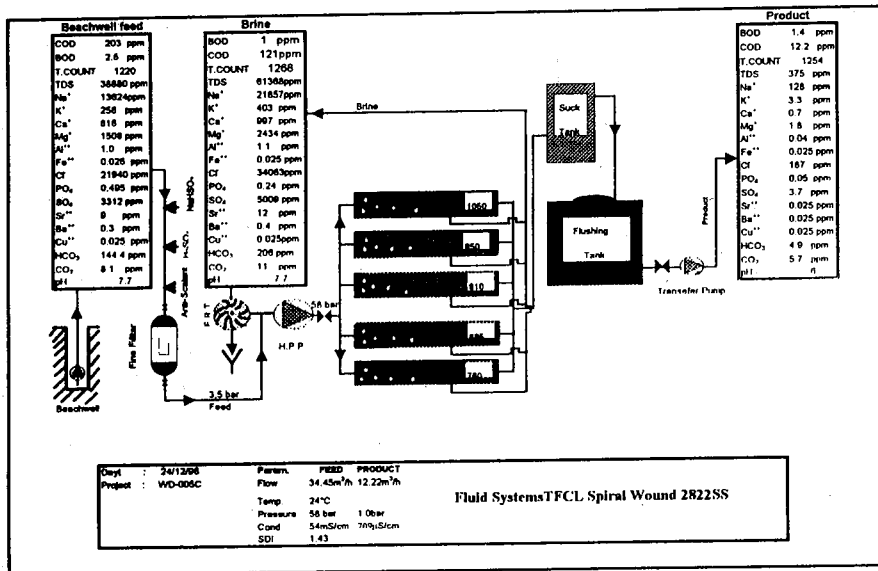


Fig. 5. Typical flow diagram of the spiral wound RO, plant.

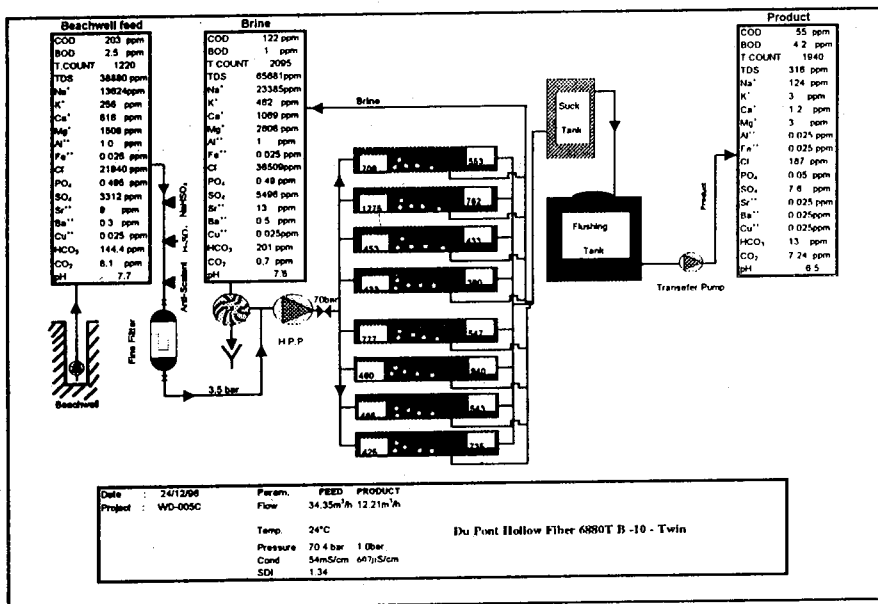


Fig. 6. Typical flow diagram of the hollow fiber RO, plant.

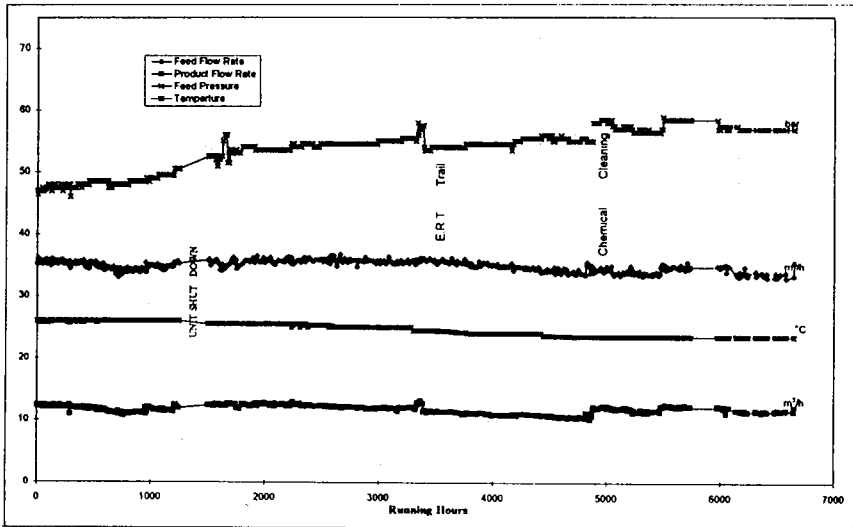


Fig. 7. Operational Parameters of RO<sub>1</sub> (i.e. spiral wound) versus time.

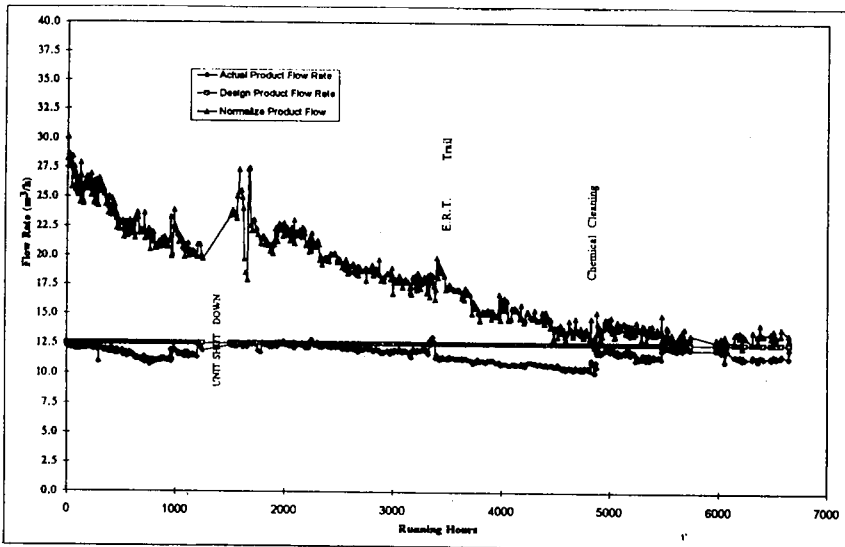


Fig. 8. Designed, actual and standardized product flow rates of RO<sub>1</sub> (i.e. spiral wound) versus time.

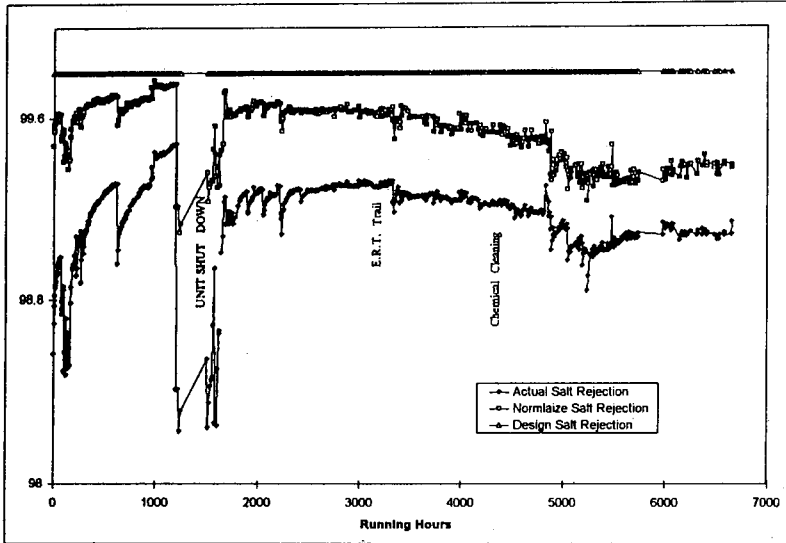


Fig. 9. Designed, actual and normalized salt rejection  $RO_1$  (i.e spiral wound) versus time.

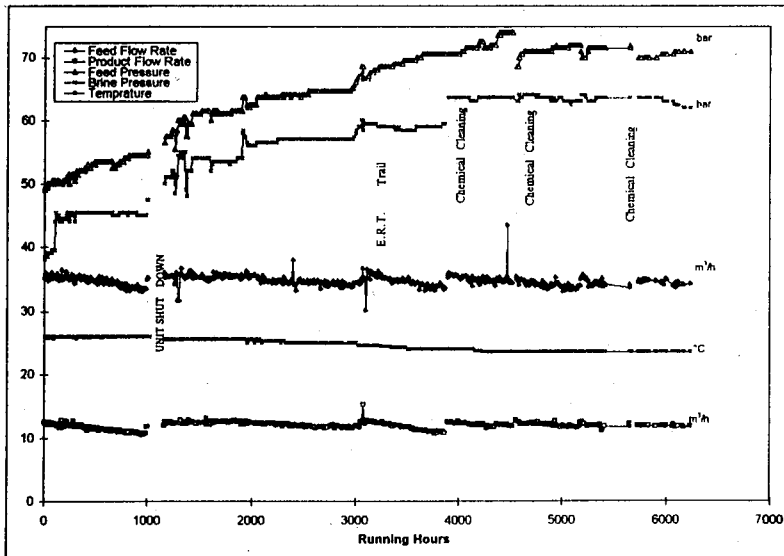


Fig.10. Operational Parameter of  $RO_2$  (Hollow Fine Fiber-twin) versus time.



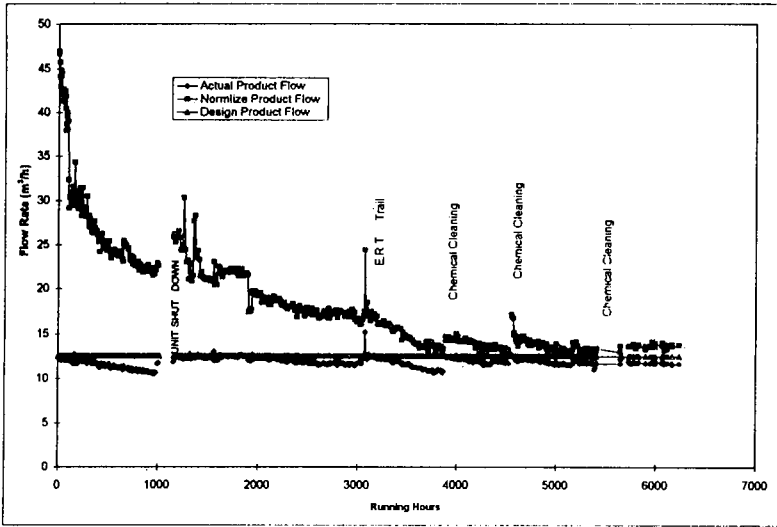


Fig. 11. Designed, actual and standardized product flow rates of RO<sub>2</sub> (i.e. Hollow Fine Fiber) versus time.

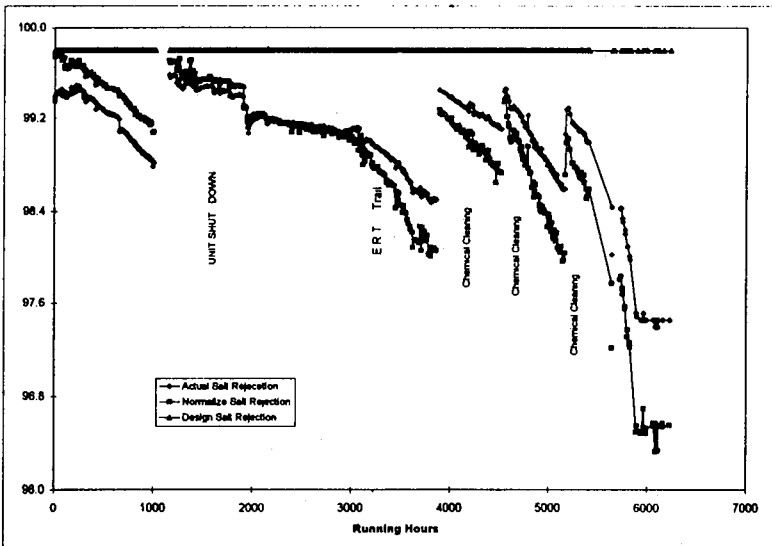


Fig. 12. Designed, actual and standardized salt rejection of RO<sub>2</sub> (i.e. Hollow Fine Fiber) versus time.

# **A Case Study of RO Plant Failure Due to Membrane Fouling, Analysis and Diagnosis**

*M. Gamal Khedr*

# **A CASE STUDY OF RO PLANT FAILURE DUE TO MEMBRANE FOULING, ANALYSIS AND DIAGNOSIS**

**M. Gamal Khedr**

Saudi Industries for Desalination Membranes & Systems Ltd. (SIDMAS)  
Riyadh, Saudi Arabia

## **ABSTRACT**

Progressive decline in performance of an RO plant, after a period of smooth operation, is described. Research for the reasons and remedy included: 1. Correlation of the recorded decline in performance to- problems in feed pretreatment. 2. Selection of elements for individual testing. 3. Elements performance together with their outer features suggested the conduction of element autopsy. 4. Chemical analysis of the fouling film, Cell Test of the sheet membrane, as well as surface analysis by SEM and X-ray.

Results revealed that the membranes suffered from accumulation of an iron-based fouling film. Scale deposition took place due to exceeding the system design parameters together with defective pretreatment. Instead of cleaning, the system was forced by increase of pressure so as to maintain the original product rate. This led to element telescoping and localized damage of the thin film surface.

Brief discussion of the adequacy of the techniques used is given in view of the characteristics of membrane fouling films.

## INTRODUCTION

System design of a reverse osmosis plant is the basis which determines the operating conditions e.g., feed temperature, feed pressure, pH and, percent recovery which are required for a specific feed water analysis and membrane performance, i.e. product rate and quality. The main design equations are those which control the precipitation of sparingly soluble salts and oxides, the equations which refer to the membrane performance as the flux of salt through the membrane and the hydraulic permeability and finally, the equations of the hydrodynamic balance of flow of the different streams included in an RO element.

It is evident that for correct operation of an RO plant, the operation conditions specified by the RO system design projection should be precisely respected and in preference, a wide safety margin should be kept. Deviation from these conditions usually lead to operation problems of scaling and fouling which cause decline of performance to yield lower product quantity and/or quality, to an increase in operation and maintenance costs, and could shorten the membrane life time.

The present work describes a case where the failure of pretreatment to meet the feed water quality, and exceeding the operation conditions, specified by the system design led to the failure of the plant and the damage of the membrane elements.

Inspection of the failure and systematic testing included (1) Evaluation of efficiency of feed pretreatment (2) Test of performance of RO elements removed from the different plant stages (3) Test of element tightness and dye absorption by the membrane (4) Autopsy of elements and Cell Test of samples of sheet membrane (5) Chemical analysis and surface analysis of the fouling film by SEM and X-ray.

## PLANT DESIGN

Skid Array	:	8:4:2
Number of Element Pressure Vessels	:	6
Total Number of Elements	:	84
Membrane Type	:	Thin Film Composite
Element Configuration	:	Spiral Wound
RO Feed TDS	:	1578
RO Feed pH	:	6.3
Plant Percent Recovery	:	85%
Total Product Flow	:	890 l/min
Reject Flow	:	155 l/min

Product TDS	:	35.5 ppm
Feed Temperature	:	34.0°C
Feed Pressure	:	220 psi

## CHARACTERIZATION OF THE FAILURE

After a period of eight months of steady performance where the product rate and the salt rejection were in conformity with the design projection, a gradual increase in salt transmission was observed accompanied by the decline in product rate.

The weight of the RO elements, in the 3rd stage is higher than the standard value. Increase in weight is higher in case of the last elements in one and the same pressure vessel to the range of 20 to 30%. Some elements of the second stage showed the same phenomenon but to a lesser extent.

The elements exhibited telescoping which would indicate the increase of the element resistance to the feed flow and / or the exposure to feed pressures quite higher than its normal operating pressures.

A brownish deposit is detected on the front of the element.

Rapid rise of  $\Delta P$  which imposed the shut down of operation to clean the membrane at a too high frequency (two times in one month) with only limited improvement.

Measurements of the product water TDS at the beginning and the end of the pressure vessels gave the following results.

numerous to count". No solid scales were detected.

The rise of  $\Delta P$  observed with the first stage is, therefore, due to biofouling. A fraction of the bacteria cells brought by the contaminated feed stream, adhered to the membrane surface. Upon growth and multiplication, enhanced by the convenient temperature and the availability of nutritive organic substances, the slimy life product covered the membrane surface and caused rise in  $\Delta P$  and consequently decline of the product rate.

Several membrane leaves from third stage elements were found to carry thick scales both on the membrane surface and in the feed spacer in these areas. Analysis of a deposit sample, Table 1 showed that it is mostly composed of calcium in carbonate form, silica and iron. Similar indication is given by X-ray analysis, Fig (1).

**Table 1.** Analysis of the scale deposit on membrane surface (3rd stage)

Element	% in the deposit
SiO <sub>2</sub>	51.5
CaCO <sub>3</sub>	24.8
Fe	16.8

Dye absorption is found to be concentrated around these scaled areas which suggests that the damage of the thin film is related to the scale deposition rather than to surface oxidation. The latter would have caused homogenous dye absorption on the membrane surface.

Fig (2) clearly shows the "channeling" phenomenon, where the active membrane surface area is terribly reduced due to scale deposition. The feed flow is limited to only narrow channels.

Near the thick scales, the membrane surface is rough and abrasive. In fact, fine deposit crystals, SEM, Fig (3), are tightly bind to the surface or embedded into the thin film, which would explain, in part, its damage. Together with the scale aggregates, the micrographs show strong bacterial growth and black spots.

The scaled areas are not only non-performing, but they hinder the normal feed flow and stop the turbulent agitation of the feed stream due to blocking of the feed spacer network.

Scale growth also leads to increase of element resistance to feed flow which is observed as rise of both  $\Delta P$  (feed-brine) and  $\Delta P$  (feed-product). Instead of shut down for cleaning of the membranes, verification of the feed analysis, and

rectifying the source of the chemical imbalance, the operation responsible increased the applied pressure to overcome this resistance and maintain the product rate. The membranes slid on each other and caused telescoping of the RO element. The friction of the membrane surface in presence of scales resulted in the damage of the thin film. This explains the dye absorption, and the observed decline of salt rejection.

Inspection of the plant operation data showed that the actual percent recovery prior to the decline of performance was, in fact, 90%, exceeding the design value of 85%. This is a scaling factor. It impairs the system chemical balance through creating (a) a higher brine concentration of the scale forming compounds and (b) a lower flow rate of the brine stream than the values of the RO system design, therefore, it leads to severe concentration polarization (4). Furthermore, the analysis of the feed water confirmed the presence of an iron concentration of 0.088 ppm which explains the iron content of the fouling deposit. The black spots in this deposit when collected and analysed were found to be rich in iron.

The SEM of Fig. (3), made for a membrane sample from the element of the third stage shows an example of the complex case of the membrane fouling which includes both scaling and biofouling [2]. The slime gel matrix of the biofouling film favours entrapping of the organic molecules, colloidal particles and suspended particles and microorganisms which increases the thickness and the complexity of the composition of the fouling film. This explains the higher  $\Delta P$ , the higher decline of performance and membrane damage suffered by the third stage.

This is further confirmed by the results of localized test of performance on membrane samples taken from autopsied elements (Table II) shows highly heterogeneous membrane damage. The decline in salt rejection and the parallel increase in permeation are particularly important in sample (2) covered with thick scales.

**Table II.** Results of local cell testing of sheet membrane from autopsied elements

Sample No.	Product Rate GPD	% Salt Rejection
1	10,805	90.72
2	12,508	75.48
3	10,296	92.27
4	11,286	86.24

## CONCLUSIONS AND RECOMMENDATIONS

1. The scale deposition observed in the present case is due to either or both of.
  - (a) Failure of pretreatment to meet the design required feed characteristics, mainly the contents of iron, calcium and silica.
  - b) Failure of operation to maintain the system design limits e.g., operation at higher feed pressure to raise the declined product rate and operation at higher percent recovery than the design values.
2. Scale deposition on and into RO membranes, impaired the hydrodynamic conditions of the feed flow. Since the above fouling conditions were not controlled, scaling turned out to be a self sustaining phenomenon which under conditions of severe concentration polarization led to channeling, failure of RO performance and damage of membrane surface.
3. The situation is further worsened by the combination of scale deposition and biofouling. The interference between the resulting surface deposits leads to a complex fouling film causing higher and faster rise of differential pressure, imbalance of hydrodynamic conditions, consequently failure of RO performance and also failure of cleaning and sanitization processes.
4. The procedure adopted for the study of fouling of the RO elements which combines:-
  - (a) the nondestructive testing of the RO performance, then
  - (b) autopsy of the element after Dye test
  - (c) adequate chemical analysis of the fouling deposit and
  - (d) membrane surface examination by SEM,

is shown to enable comprehensive diagnosis of the fouling case and consequently to elucidate the precautions which should be taken in order to avoid such fouling situation.

### 5. Selection of Techniques for Study of Fouling Films on RO Membranes

The membrane fouling has practically been the most important problem in RO application, upto now there is no standard method to study fouled membranes that can give results of absolute significance for the diagnosis without need of special experience for interpretation.

The main difficulty encountered in such study e.g., the case considered in the



present work, is the high heterogeneity of composition of the fouling film. Different areas of membrane surface carry different mixtures of components like mineral scale aggregates, organic material, micro-organisms and their life products. On the other hand, it is not only the relative concentration of each of these components which would influence the RO performance, but also the way they are physically arranged. Blocking of the feed spacer impairs the hydrodynamic conditions of feed flow and would lead to severe concentration polarization.

Therefore, the commonly used methods of chemical analysis give only an average composition of the complex and heterogeneous film. Same is also obtained by energy dispersive x-ray and Fourier Transform Infra Red Spectroscopy.

Even the recently introduced, highly sophisticated techniques which are claimed to offer high precision in analysis of the fouling films and diagnosis of the fouling causes such as Laser Ionization Mass Analysis, [31] include, in fact, a wide margin of approximation when they generalize results which depend on the arbitrary selection of the point of testing.

As for testing performance of a fouled RO membrane, it gives also average performance which can differ greatly from one portion of the membrane surface to another as per our results of Cell Test of the fouled membrane surface.

In the present work, and the previous related one [2], in order to deal with the above mentioned heterogeneity, the approach based upon the interpretation of the results of performance decline on basis of destructive elements autopsy, and correlation between the chemical analysis of the fouling deposit and its physical aspects observed by SEM examination of the surface were adopted. Classical chemical analysis is supported by energy dispersive x-ray and Fourier Transform Infra Red Spectroscopy. The interpretation of these results could explain all the observed aspects of the fouling case and elucidate the contributions of the factors as defective pretreatment and erroneous operation.

## REFERENCES

1. Gamal Khedr, Badran, M. and Shoukry A., *Ultrapure Water*, 9 (2), 33 (1992)
2. M. Gamal Khedr, IDA World Congress on "Desalination and Water Sciences", Volume IV, 19 (1995)
3. P. John, et al, IDA World Congress on "Desalination and Water Sciences" Volume II, 119 (1995)
4. Gamal Khedr and Varoqui, R., *Ber Bunsenges. Phys. Chem.*, 85, 116 (1981).

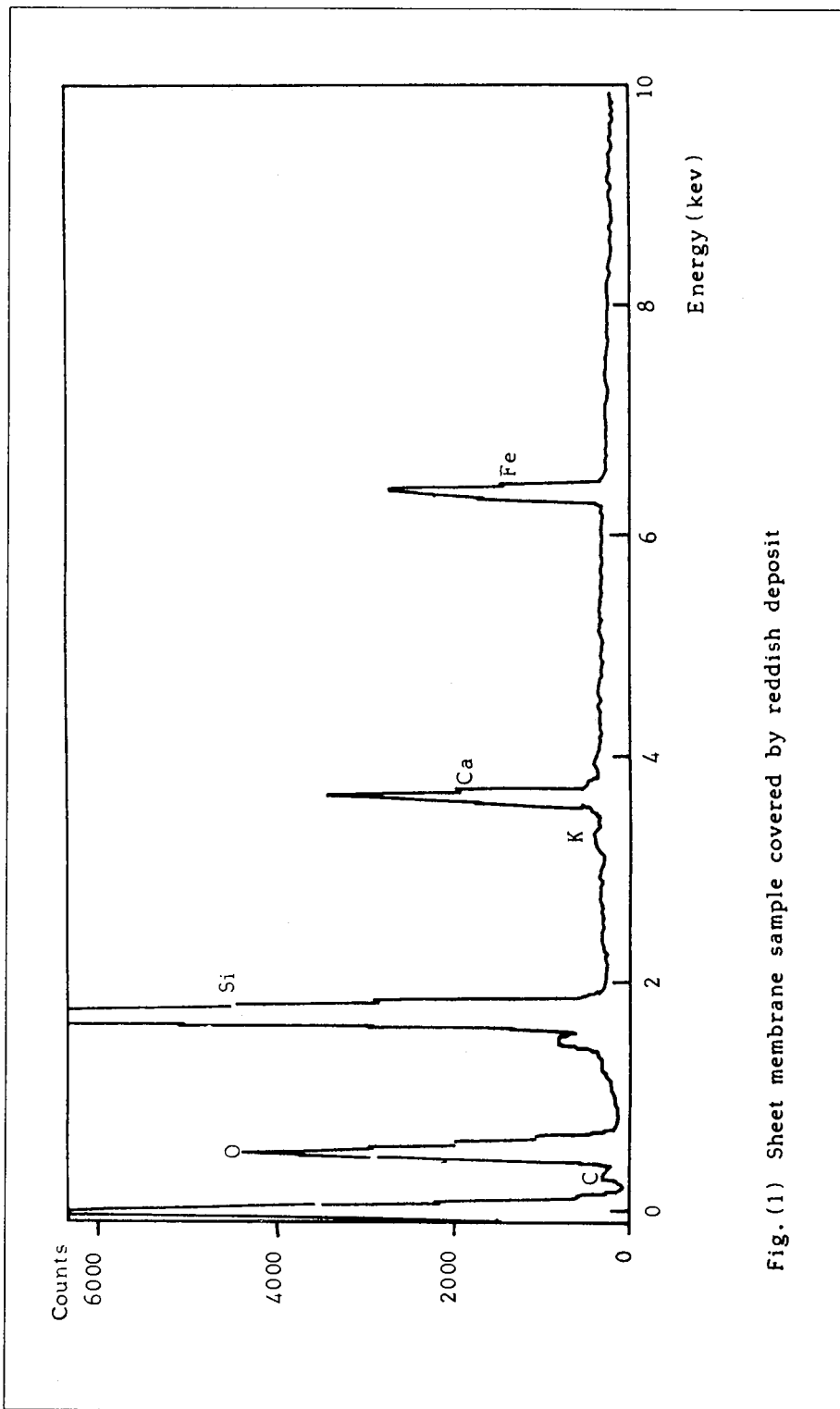


Fig. (1) Sheet membrane sample covered by reddish deposit

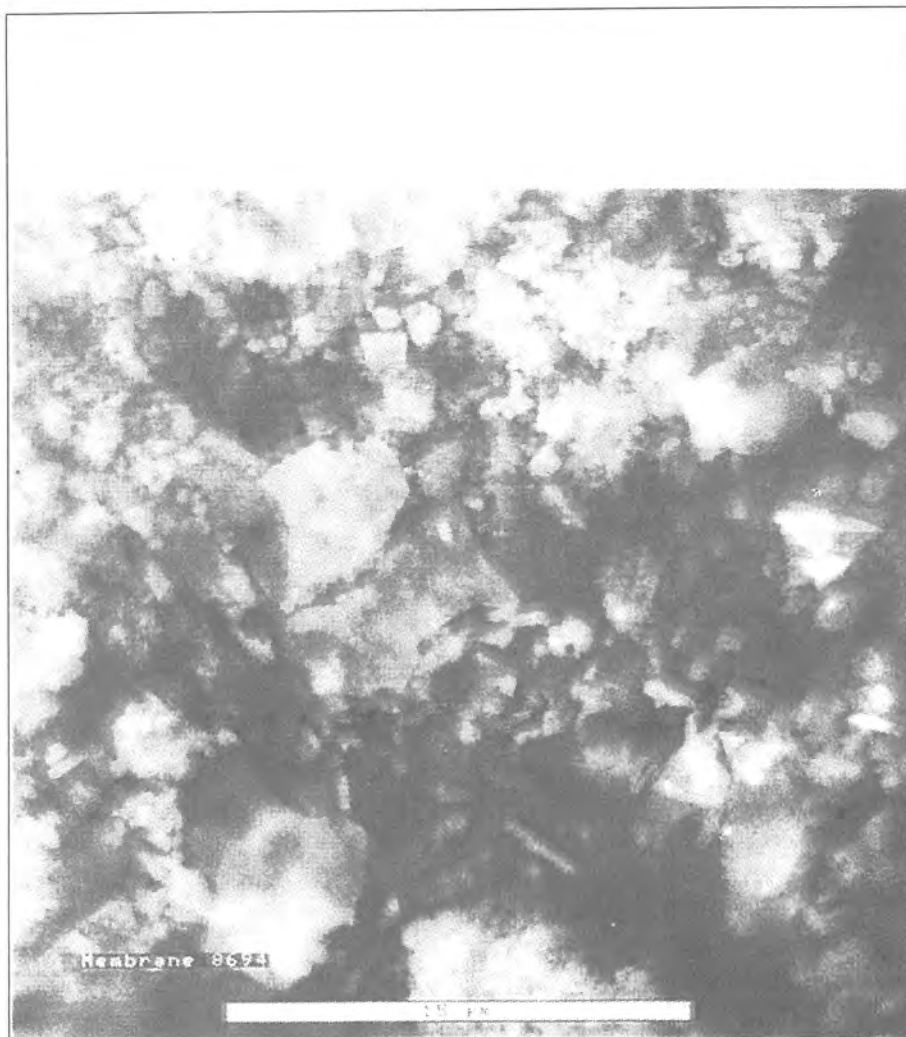


Fig.(3) Scanning Electron Micrograph showing scale aggregates and bacterial growth.

Stage	Vessel Number	Feed Side ppm	Reject Side ppm
1	1	10	11
	2	10	12
	3	14	14
	4	10	13
	5	11	12
	6	10	11
	7	11	17
	8	11	14
2	1	52	54
	2	44	55
	3	46	51
	4	40	48
3	1	197	436
	2	200	510

This shows that the decline in salt rejection is higher in the third stage than in the second one. In both cases it is concentrated in the elements towards the end of the pressure vessels. The first stage did not show any decline in salt rejection.

## EXPERIMENTAL

### Test of Element Performance

The test is conducted in a pilot plant with one-element pressure vessel under the following standard conditions.

Feed pressure	:	225 psi
Feed TDS	:	2000 ppm NaCl
Feed pH	:	6.5
% recovery	:	15

### Test of Mechanical Leak

If the performance testing shows lower salt rejection than the standard value of the element model, the Bubble Test is performed. Compressed air is applied to the element central tube where any leak will be revealed by air bubbles coming out which will enable to identify the nature of the leak.

### Dye Test

It consists simply of testing the element performance in presence of an organic

dye. The dye absorption by the thin film surface suggests that the decline of salt rejection is related to damage of the active membrane surface.

### Cell Test

It aims to determine the RO performance (% salt rejection and product rate) of sheet membrane samples having an active surface area of 80 cm<sup>2</sup> for each one of four cells. The system was described in detail elsewhere [1]. Results of salt rejection and product rate are normalized to express the performance of an RO element produced out of this sheet membrane.

### Autopsy

Membrane autopsy was carried out on elements of first and third stages.

## RESULTS AND DISCUSSION

The measured RO performance of the fouled elements is given, herewith, in comparison with the original values upon start of operation:

Element Position in Plant Design	% Salt Rejection		Product Rate GPD	
	Original	Present	Original	Present
First Stage	98.8	99.2	9020.0	6186
Third Stage	99.0	82.5	8926.0	10025

The elements removed from the first stage showed remarkable decline in product rate while the salt rejection remained unchanged. In fact, cleaning by the usual alkaline mixture could restore the original performance which confirms that the thin film was intact but covered by a fouling film of organic nature.

On the other hand, the fouled elements removed from the third stage showed increase of both salt passage and product rate. In this case the alkaline cleaning gave an only limited improvement while the acid clean further worsened the salt rejection. These results, together with the increased weight of the element, suggest that the nature of fouling in the last stage is mainly deposition of thick mineral scales, which would have damaged in part the thin film surface.

The tightness test of the elements confirmed the absence of mechanical leaks. Non cleaned elements, were selected for autopsy after being dye tested.

Autopsy showed that all the membrane leaves from first stage elements were covered by a thick slimy fouling deposit. The bacterial count result was "too

**Performance Evaluation of Ten Years Operation  
Experience of Brackish Water RO Desalination  
in Manfouha Plants, Riyadh**

*Raed I.S. Al Mudaiheem, Sami O.A. Al Yousef,  
A.K.M. Amirul Islam and Tamer Sharif*

# **PERFORMANCE EVALUATION OF TEN YEARS OPERATION EXPERIENCE OF BRACKISH WATER R.O. DESALINATION IN MANFOUHA PLANTS, RIYADH**

**Raed I.S. Al Mudaiheem, Sami O.A. Al Yousef,  
A.K.M. Amirul Islam**  
Riyadh Water & Sewage Authority  
Riyadh, K.S.A.

**Tamer Sharif**  
Permasep\* Products, DuPont Company  
Jeddah, K.S.A.

## **ABSTRACT**

There are two sources that provide Riyadh city with potable water:

1. Desalinated sea water from Al Jubail plants pumped from Saudi Arabia's east coast. (represents about 60%).
2. Brackish water from deep and shallow wells which are primarily treated by eight plants of which six are followed by reverse osmosis desalination plants. (represents about 40%).

Among the six R.O. plants supplying Riyadh are Manfouha plants (1 & 2). While receiving raw water from deep wells, the two plants are designed to produce about 84,000 m<sup>3</sup>/day.

The Manfouha R.O. plants were commissioned starting in 1984 and are still operating at close to design capacity. The two plants are presently operated and maintained by Riyadh Water and Sewage Authority.

This paper covers plant design parameters of Manfouha plants, while highlighting membranes performance after more than ten years of operation.



## **INTRODUCTION**

In view of the phenomenal economic growth in all sectors experienced in Saudi Arabia which was associated with an equally phenomenal growth in water demand, the Government of Saudi Arabia was eager to find ways to meet growing demand for potable water in one of the world's fastest growing capitals - Riyadh. Desalination of brackish waters in the Riyadh area by the Reverse osmosis process was looked upon as one of the favored techniques.

Located in one of Riyadh's oldest neighborhoods, Manfouha plants were among five plants purchased by the Ministry of Agriculture and Water to supply city of Riyadh with 205,000 m<sup>3</sup>/day of potable water. All five plants (Manfouha 1 & 2, Salboukh, Shumaisy, & Malaz) were built by Degremont, France and use reverse osmosis technology with B-9 (0840) permeators manufactured by DuPont, Permasep\* Products. The Manfouha plants with a design capacity of 84,000 m<sup>3</sup>/day (22.2 million GPD) of blended product water was commissioned starting in 1984. The R.O. portion designed to produce 63,840 m<sup>3</sup>/day which is blended with 20,160 m<sup>3</sup>/day with pre treated raw water.

The Riyadh Water and Sewage Authority has been operating and maintaining the plant for the last ten years. The plant was designed to produce potable water with TDS less than 500 mg/l from deep wells where their water wells salinity range between 1,300 to 1,700 mg/l.

It is extraordinary to note that after more than ten years, the plants are still producing at > 93% of R.O. design capacity (when all trains are operated simultaneously). Permeator replacement rate has been around 2% per annum.

## **PLANT & PROCESS DESCRIPTION**

The brackish water R.O. desalination facility was commissioned in 1984. Its design product capacity was 27,360 m<sup>3</sup>/day for Manfouha 1 and 36,480 m<sup>3</sup>/day for Manfouha 2 (see Fig. 1 for a plant overview).

### **Water Wells & Water Quality**

A total of 24 deep feed wells supply brackish water (18 in service and others standby). Depth of each well is about 1,200 meters with a capacity around (150 - 200) m<sup>3</sup>/h and a temperature of 60-70 deg. C. Well water TDS quality varies between 1,300 to 1,700 mg/l (max.). The average feed water TDS to Manfouha plants is about 1,400 mg/l (see Table 1 for water analysis):

Table 1: Water analysis at Manfouha plants.

ITEM	RAW WATER (COOLED)	RO FEED	RO PROD.	NET	S.A.S.O.
Temp. Deg. C	33	max. 35	-	32	-
pH as CaCO <sub>3</sub>	8	6	5.8	7.5	6.5-8.5
Total H. ppm as CaCO <sub>3</sub>	670	360	42	180	500
Ca. H. ppm as CaCO <sub>3</sub>	470	170	22	100	200
Mg. H. ppm as CaCO <sub>3</sub>	200	190	20	80	150
Total alk. ppm as CaCO <sub>3</sub>	160	10	12	55	-
Cond. as uS/cm.	2000	2010	350	770	160-1600
TDS mg/l.as ion	1350	1350	200	490	100-1000
Ammonia mg/l.as ion	<0.24	-	0	0	-
Nitdte mg/l.as ion	<0.016	-	0	0	-
Nitrate mg/l.as ion	10	17	9	8.5	-
Chlodde mg/l.as ion	265	310	60	100	250
Sulfate mg/l.as ion	500	420	60	170	400
Iron mg/l.as ion	0.4	0.015	0.004	0.06	0.3
Alu. mg/l.as ion	0	0.01	0	0.009	0.2
Chlodne mg/l.as ion	0	0	0	0.36	-
Silica mg/l.as ion	<26	1.5	4	-	-

Note: (H.) Hardness.

S.A.S.O: Saudi Arabian Standards Organization.

### Cooling Towers

Raw water is pumped to 28 cooling towers each designed for 150 m<sup>3</sup>/hr. The cooling towers reduce the raw water temperature to 29-35 deg C. While some iron oxidation and silica coruscation occurs. The cooled water proceeds to the distribution chamber.

### Chemical Conditioning / Turbocirculators

From the distribution chambers, the water is admitted into eight rapid contact clarifiers (capacity of each is 600 to 700 m<sup>3</sup>/hr) where per design dosing of the following chemicals is done: 340 mg/l sodium carbonate, 140 mg/l calcium hydroxide (hydrated lime), 45 mg/l sodium aluminate and 0.2 mg/l coagulation aid (A 100). Considerable reduction in dosing was achieved which in turn resulted in considerable cost savings. The current dosing is limited for lime around 110 ppm, sodium carbonate around 240 ppm, sodium aluminate around 12 ppm and coagulation aid around 0.02 ppm.

Softened water is taken to an intermediate tank prior to which primary sulfuric acid dosage @ 30 mg/l is done. The feed water pH is reduced to (6.5. - 7).

### Media Filters

Acidified, softened water is diverted to 12 coarse and fine media gravity two stage open sand filters (see Tables 2 & 3). Filtration is done in two stages with the water traveling upward through coarse sand media in the first stage and downwards through fine sand media in the second. Support media is gravel for both filter tanks.

**Table 2:** Loading media for 3.5 X 10 meter filter concrete tank (first stage, course)

Depth	Dimension	Weight
10 cm.	10 - 18 mm (gravel)	3 Tons
240 cm	3- 5 mm (course sand)	87 Tons

**Table 3:** Loading media for 4.66 X 10 meter filter concrete tank (second stage, fine)

Depth	Dimensions	Weight
10 cm.	10 - 18 mm (gravel)	6 Tons
15 cm.	3 - 5 mm (course sand)	12 Tons
90 cm.	0. 8 - 1.2 mm (fine sand)	61 Tons

Filtered water is then stored in R.O. feed storage tanks. SDI value of <1.5 is achieved at this point. In order to minimize water waste, filter effluent (upon back washing and rinsing) is circulated back to clarifiers inlet for repeated chemical conditioning.

Nine low pressure feed pumps (500 m<sup>3</sup>/hr, 95 kW motor) pump R.O. feed water to single stage centrifugal (SS 316) high pressure pumps. Preceding the H.P. pumps a second dosage of sulfuric acid @ 25 mg/l which reduces feed pH to 5.5 (presently and due to process optimization pH is allowed up to 6.4). Sodium hexametaphosphate is also dosed @ 4 mg/l. Also, 18 AMF Cuno (SS 316) micro filters with 5 micron cartridges are installed for micro filtration of R.O. feed water.

### High Pressure Pumps

High pressure R.O. feed (up to 27.6 Bar) is generated while using total of nine

high pressure pumps (Manfouha 1 & 2). Each pump is single stage centrifugal type and is driven by motor with a rated power of 600 kW. The amount of feed water delivered per pump is about 450 m<sup>3</sup>/hr. at 27.6 Bar. Pumps are connected in parallel and each pump is designed to support two full trains in operation. All high pressure piping is made of SS 316.

### **Desalination Membranes**

Pressurized R.O. feed water is admitted to brackish water reverse osmosis unit with a 4:2:1 brine staged configuration (total of 14 trains). Each train has about (100-113) permeators. The maximum number of permeators which can be installed per train is 140. Brine control is maintained by calibrated control valves. The feed, brine and product manifolds are vertically installed with float type flow indications.

R.O. product is post treated with sodium carbonate and transferred to a mixing chamber where it is blended with undesalinated but treated (and cooled only raw water). Post chlorination is carried out in the mixing chamber prior to distribution.

At every shut-down of each R.O. train, flushing is manual with R. O. feed water to protect the system against scaling and corrosion by the stagnant water.

### **Auxiliaries**

Four ready connected in-place cleaning systems supplied complete with a separate 4 m<sup>3</sup> cleaning tank, a cartridge filter, heat exchanger, and four cleaning pumps are used to achieve various cleaning flows and velocities in order to ensure effective cleaning.

### **PLANT PERFORMANCE OVER A TEN YEAR PERIOD**

Over more than a ten year period in which membrane addition was around 13% of the original membranes installed. Replacement started after five years of operation. During this period, the plant was cleaned only once. See Tables 4 & 5 in which performance of the plant is summarized.

Bearing in mind that each train was designed to produce 190 m<sup>3</sup>/hr, and upon studying the performance of (train 1) in Manfouha I and (train 8) in Manfouha 2 as a representative sample, train 1 is presently producing 184m<sup>3</sup>/hr, and train 8 producing 186m<sup>3</sup>/hr representing 96-97% of design requirement (see also Fig. 2).

**Table 4:** Performance of Manfouha Trains Summary:

PARAMETER	CURRENT PERFORMANCE		DESIGN
	M1(TRAIN.1)	M2(TRAIN.8)	
Total O.H. hr	28000	32000	
Product flow m <sup>3</sup> /hr	184	186	190
Reject flow m <sup>3</sup> /hr	35	32	
Feed temp. c	34	35	
Feed press. bar	25.7	26	max. 27.6
Total product. TDS ppm	195	210	

**Table 5:** Performance of Manfouha trains (per stage summary):

PARAMETER	M1 (TRAIN 1)			M2 (MIN 8)			DESIGN
	st.1	st.2	st.3	st1	st.2	st.3	
Product flow m <sup>3</sup> /hr	120	44	20	119	47	20	
Product Cond. us/cm	380	350	630	230	660	780	
Number of perm.	68	29	16	64	32	16	
Number of perm. SP<10%	48	20	13	43	23	12	<10%
Number of perm. 25>SP%>10	17	7	2	16	8	3	<10%
Number of perm. SP>25%	3	2	1	5	1	1	<10%
Diff. press. per.perm. bar	0.6	0.5	0.6	0.75	0.65	0.8	maxl.7Bar
Diff. press. per stage bar	1.5	2.2	2.4	2	1	1.5	

The quality of product is also close to design requirements, the present overall product TDS is 210 mg/l for train 8 and 195 mg/l for train 1 (see Fig. 3).

## WATER COST

See Table 6 below where water cost at Manfouha plants (operation & maintenance only) is shown as monthly average for 1416H.

**Table 6:** Total cost for O & M (per month).

Description	Total cost (SR)	Total cost (USD)
Power (consump. 1. 712 kWNm <sup>3</sup> ), power cost = 0.2 SR / kWh	358460	95589.3
Salaries & wages	186883.2	49835.5
Spare parts	7000	1866.7
7		
Chemicals	466110	124296
Fuel, oil & lubricants	798	212.8
Total cost of O & M	1019251.2	271800.3
Cost of cubic meter	0.98	0.261

**Note: Average total water production from Manfouha plants is 1048587.4 m<sup>3</sup>/month**

## **CONCLUSION**

Excellent performance of Manfouha plants could be attributed to the following:

1. Good operation and close monitoring by properly trained operators under qualified supervision were the key to successful operation. Close follow-up and technical support by the membrane manufacturer complemented the above.
2. Appropriate plant design and workmanship on the part of the Designer.
3. Extensive investment in the pre-treatment process was worthwhile. In spite of the high cost of pre-treatment chemicals, considerable savings were achieved through process optimization and operation at high recovery > 85%, minimal downtime for membrane cleaning, and membrane life was positively influenced.
4. Monitoring and follow-up of data, and immediate trouble shooting of various machinery (including membranes) were carried out without delay.
5. The source of feed water from wells also contributed to providing clean feed, i.e. low Silt Density Index (SDI) and with steady physical properties.

## **ACKNOWLEDGMENT**

The authors gratefully acknowledge. The Riyadh Water & Sewage Authority, Riyadh, Saudi Arabia for supporting this work and providing the data for this study.

## **REFERENCES**

1. Annual reports of Riyadh Water & Sewage Authority for the year (1405 ) to present.
2. Manfouha plants O & M. catalogues & manuals.

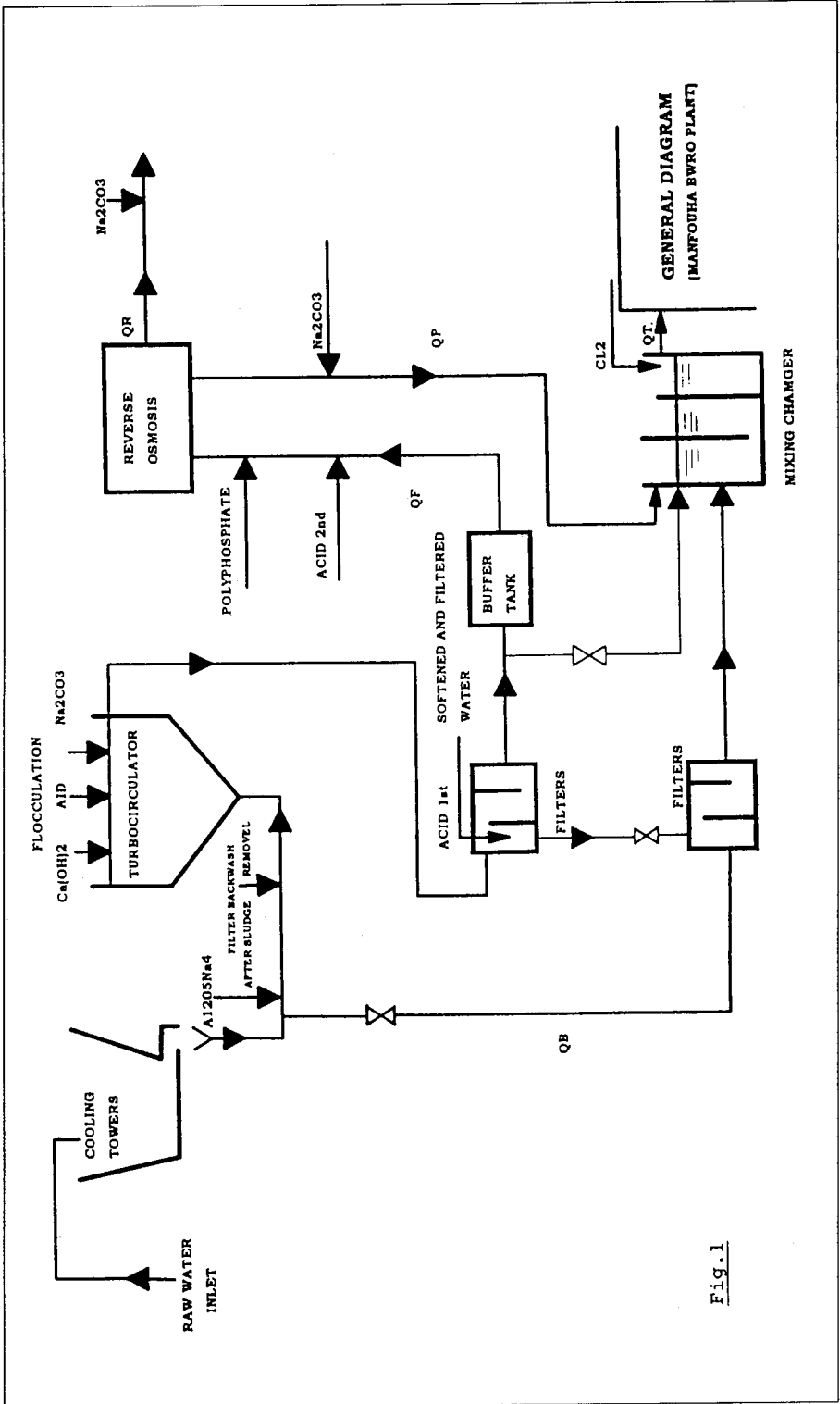


Fig.1

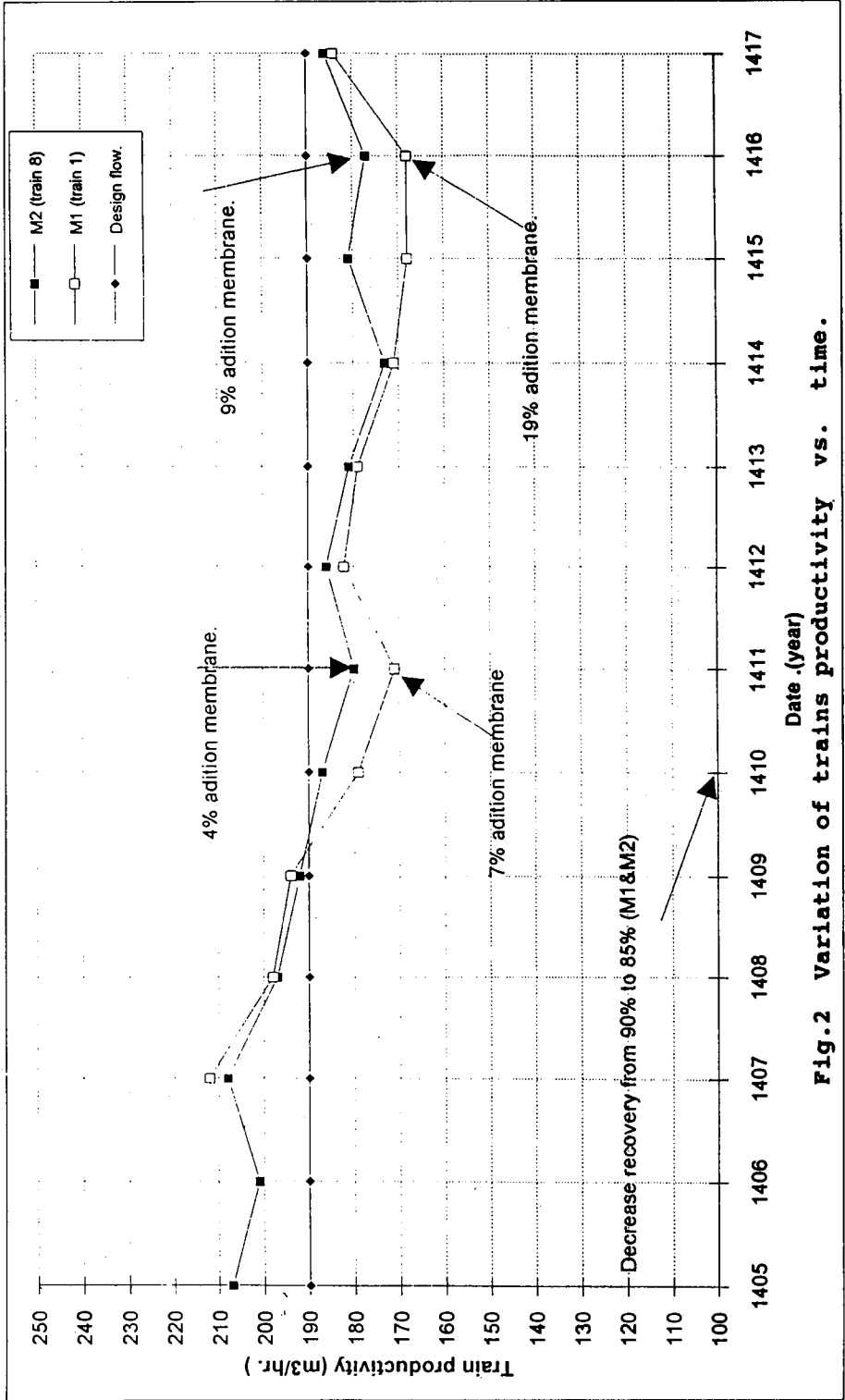


Fig.2 Variation of trains productivity vs. time.



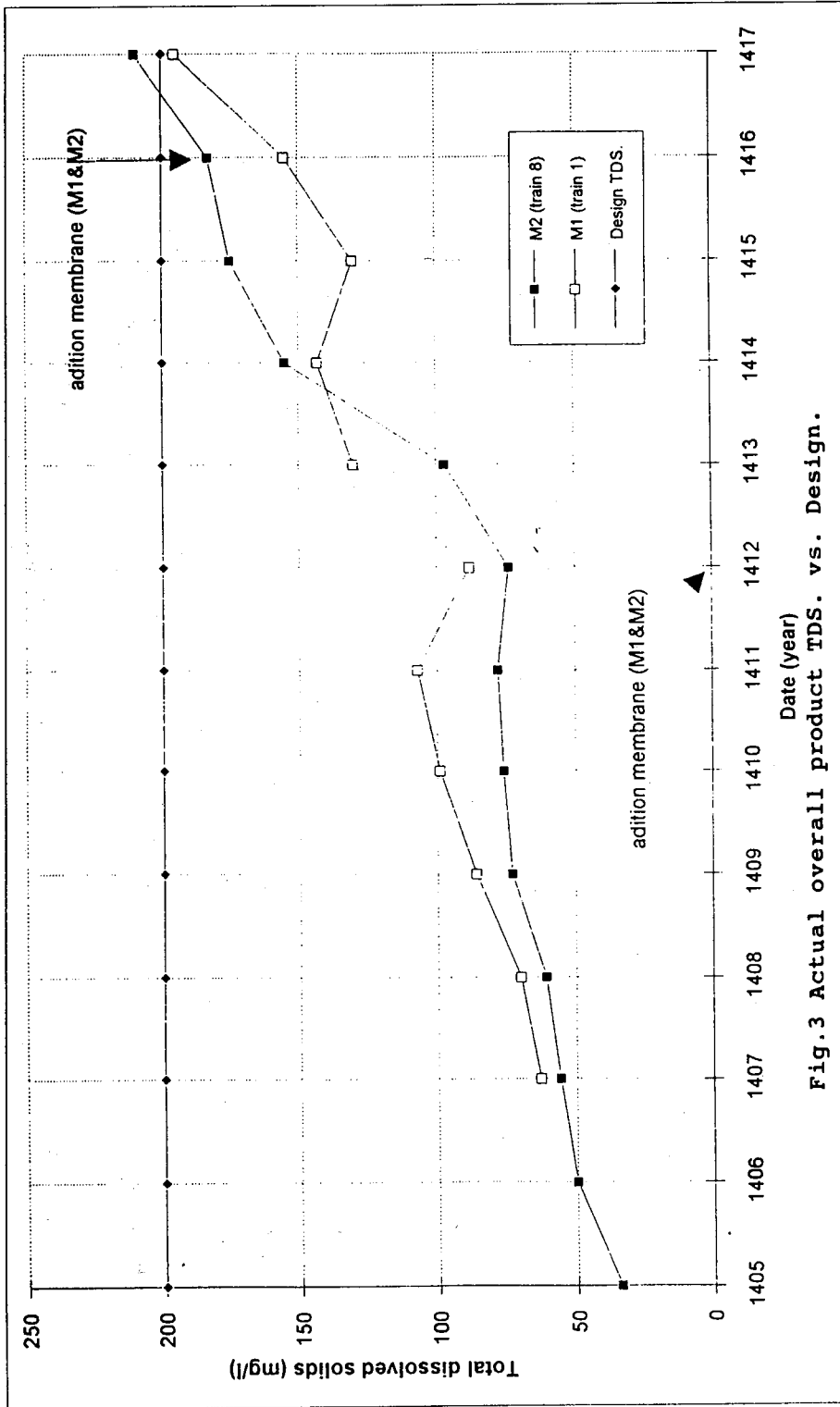


Fig.3 Actual overall product TDS. vs. Design.

# **Pilot Study of MSF-RO Hybrid Systems**

*Essam El-Sayed, Sadeq Ebrahim, Ahmad Al-Saffar  
and Mahmoud Abdel-Jawad*

# PILOT STUDY OF MSF/RO HYBRID SYSTEMS

**Essam El-Sayed, Sadeq Ebrahim, Ahmad Al-Saffar and  
Mahmoud Abdel-Jawad**

Water Desalination Department, Water Resources Division  
Kuwait Institute for Scientific Research  
P.O. Box 24885, Safat 13109, Kuwait

## ABSTRACT

Evaluation of the reverse osmosis (RO) process performance in an multi-stage/ reverse osmosis (MSF/RO) hybrid system is of particular interest due to the obvious advantages of hybrid desalination plants over isolated ones. Meaningful evaluation of the RO process performance in a hybrid model requires continuous monitoring of an RO test unit for an appreciable period of time during the winter season when the ambient seawater temperature is low. The primary objective of this study was to systematically confirm possible gains in the RO product water flow rate and to examine the overall performance of an RO plant operating in a hybrid environment. Experiments were carried out at the Doha Desalination Research Plant (DRP) using a carefully designed and equipped 20 m<sup>3</sup>/d RO test unit linked with the nearby MSF unit A-1 of the Doha East Distillation Plant. Actual hybrid testing of the RO unit started during the cold season and continued for about 1,800 h. The temperature of the RO seawater feed withdrawn from the MSF reject stream ranged from 24 to 31°C. Operating data collected from the RO test unit included temperature, pressure, flow rate, concentration, silt density index (SDI), and pH according to the function of each stream. A description of the experimental model, including the MSF/RO arrangement, performance data, and a discussion of the results obtained are included in the course of this paper. It was shown that an increase of up to 49% in the RO product water recovery was realized when data from before and after hybridization were compared. Also, a 42-48% gain in RO product water recovery was estimated for a seawater feed temperature of 33°C as compared to an isolated RO plant using surface seawater at a temperature of 15°C and at a reference feed pressure of 55 bar. Higher SDI values, increased frequency of backwash and chemical dosing, and loss of the membrane's salt rejection were also encountered during the hybrid testing.

**Keywords:** Reverse Osmosis, Multistage Flash, Hybrid, Integrated, Systems, Plants, Seawater, Desalination, Desalting.

## INTRODUCTION

Kuwait has been, for over thirty years, very much dependent on seawater distillation, exclusively by the multistage flash (MSF) process, as its primary source of freshwater. Kuwait has adopted MSF distillation as part of dual-purpose plants for the cogeneration of electricity and water. Five power/water complexes located along Arabian Gulf coast house a total of forty operating MSF units with nominal capacities ranging for each from 22,700 to 27,300 m<sup>3</sup>/d [1]. The total installed capacity of all operating MSF plants in Kuwait currently exceeds one million cubic meters per day. Naturally, under such circumstances and with the existence of such heavy investments, one should think of desalination by reverse osmosis (RO), even with its obvious advantages, as a process that can coexist with MSF rather than a process that should replace it. In fact, due to its nature, the RO process seems to be the most suitable desalination process for side-by-side coexistence with the MSF. Moreover, it has been reported that integration between MSF and RO systems can be significantly beneficial [2-7]. Some of the benefits that may be cited are the greater flexibility in dual-purpose power/water production plants which helps overcome the operational difficulties caused by the seasonal variations in electricity and water demands, higher RO product water recovery and less power consumption by RO due to preheated feed from the MSF system, possible use of RO membranes with maximum permeability, common seawater intake with lesser capacity, lower chemical consumption and membrane replacement rates, and probably, prolonged membrane life.

Several conceptual studies have been made on MSF/RO hybrid systems, in which different integration schemes and design configurations have been proposed and discussed [3-8]. One of the simplest integration schemes is one in which the reject stream leaving the heat rejection section of a recirculation-type MSF plant is fed to the RO plant. Also, in this scheme, the distillate from the MSF plant is blended with the permeate from the RO plant to achieve the required product water quality, thus eliminating the need for blending the distillate with local groundwater [3]. The use of such a scheme is suitable for situations where an MSF plant already exists, and alterations to or interruptions in its operation cannot be permitted. This scheme helps keep the RO feed water temperature range narrow, i.e., 28 to 35°C, relative to the conditions in Arabian Gulf coast of Kuwait where the seawater temperature varies between 13 and 35°C. The resulting higher average temperature of the RO feed water is estimated to increase the RO membrane flux, for certain membranes at certain temperature by about 2.5 to 3% per degree Celsius.

The RO plant can be a single-stage configuration with high product water recovery as the main objective, while high salt rejection is of much less importance. Complete elimination of the RO's second-stage not only reduces capital cost, it should also reduce membrane replacement and energy costs. Based on operating experience gained at the Doha Desalination Research Plant (DRP), about 22% of the total RO energy consumption is estimated to be utilized in the second stage [9].

An MSF/RO hybrid model based on the selected integration scheme was established at the DRP as part of the research and development program on desalination by RO. The primary objective was to systematically confirm the possible gains in the RO product water flow rate and to examine the overall performance of an RO plant operating in the selected hybrid environment.

## **EXPERIMENTAL TESTING OF RO IN THE HYBRID SYSTEM**

Meaningful measurement of the RO process operational parameters in the hybrid model required that the RO test unit, including its pretreatment system, should be carefully designed and equipped, and linked with one of the existing MSF plants. Excessive volume of feed water, transfer lines, tanks, and filters was avoided and thermal insulation for these vessels was considered in order to minimize heat dissipation from the hot feed water to the surroundings. The instruments and data acquisition system facilitated continuous monitoring of the operation, and recording of the measured and/or the computed parameters. The RO test unit was operated for an appreciable period of time during the winter season when the ambient temperature was low. Fig. 1 shows a simplified schematic diagram of the experimental model including the MSF/RO arrangement, and the connecting pipeline which transports a small portion of the seawater reject from MSF unit A-1 of the Doha East Distillation Plant to the DRP.

The RO test unit was constructed to yield a nominal capacity of 20 m<sup>3</sup>/d using four modules, each of which contained one RO membrane element of the hollow fiber configuration. Instruments for measuring temperature and turbidity were installed upstream of a 5 $\mu$  cartridge filter system, while those for measuring electrical conductivity and pH were installed downstream of the cartridge filter on the feed water line and downstream of the RO modules on the product water line. Two flowmeters were installed, one on the product water line and another on the reject brine line. Four pressure measurements were available, two of these were across the cartridge filter while the other two were across the membrane modules, i.e., feed water and reject brine headers. An automatic SDI measuring system was installed on the filtrate line

feeding the RO unit; SDI measurements were checked manually on daily basis. Prior to entering the RO unit, the feed water was filtered through a simple pretreatment unit which consisted of four multimedia filters, and chemical dosing of acid, coagulant, and flocculant. The pretreatment unit was optimized for filtrate with acceptable SDI values as specified by the membrane manufacturer. However, maintaining acceptable SDI values was not easy during the hybrid testing. Using seawater feed from the MSF plant caused the SDI values to exceed the upper limits much more often than using surface seawater feed before hybrid testing began. The frequency of filter backwash and the rates of chemical dosing were also higher during the hybrid testing than before.

The actual hybrid testing of the RO unit was started during the cold season and continued for about 1,800 h. During this period, the RO seawater feed temperature fluctuated between 24 and 30°C. These lower than-expected temperatures were dictated by the operational constraints in the MSF plant, from which the RO seawater feed was taken.

## RESULTS AND DISCUSSION

Fig. 2 shows the variations in seawater feed temperature and pressure, and the measured product flow rate and concentration versus the accumulated operating hours of the test unit since its start-up. Experimental data for the operation period of 500 h prior to the commencement of the hybrid testing are included in Fig. 2 for a comparison of the data from before and after hybridization. An average difference in the seawater feed temperature of about 6°C was realized as the hybrid tests began at about the 4550-h operating time mark. This difference was effectively increased to about 10°C due to the fact that the average ambient temperature started to drop rapidly during the hybrid tests, as indicated by the recorded temperatures of the cold seawater feed to other test units which showed values of 15°C and below. The RO seawater feed pressure, which averaged about 60 bar before hybridization, was reduced to an average of about 56 bar during the hybrid testing. Such a reduction in the feed pressure was necessary to keep the product flow rate at the same level as that before hybrid testing began; yet a moderate increase in the measured product flow rate was noticed. For proper comparisons, the effect of variations in the feed pressure on the product water flow rate data should be eliminated. For this purpose, a correction factor based on the ASTM standardization procedure [10] was applied using a value of 55 bar as a reference feed pressure. Also, similar procedures were applied to the data on the product water concentration, as total dissolved solids (TDS), which exhibited a gradual increase during the hybrid tests.

Fig. 3 shows the actual and corrected values of the product water flow rate and concentration plotted versus the operating time before and after hybridization. Differences between the actual and corrected values for product water flow rate appear quite significant, while in the case of the product water concentration, the differences are not as large. The corrected values show that the product water flow rate was at an average of about 410 l/h before the hybrid testing began, and increased to an average of about 520 l/h over the first 500 h of hybrid testing, during which the average temperature was at the 25°C level. With the exception of some wide fluctuations during the following 800 h of testing, a product water flow rate average of 540 l/h corresponded to an average feed water temperature of 27°C. As the feed water temperature continued to increase, i.e., from 28 to 31°C over the final 500 h of testing, the product water flow rate values climbed significantly from 560 l/h to an average of 660 l/h. In other words, average increases in product water flow rate of about 27%, 32%, and 48% were observed for average temperature rises of 7°C, 9°C, and 12°C.

It is also shown in Fig. 3 that the gradual increase in the corrected product water concentration, i.e., TDS in the product water, followed a pattern that was almost similar to that of the feed water temperature. This does not suggest that higher operating temperatures negatively influence a membrane's capability for salt rejection. In fact, based on basic membrane transport equations [11], it seems logical to assume that an increase in the operating temperature would cause the membrane's pure water permeability to increase more than the ion's diffusivity through the membrane phase. Since other contributory factors, such as concentrated membrane boundary phase, membrane thickness, membrane fouling, are not known at the moment, and are not within the scope of this paper, no attempt was made to draw any conclusion with regard to salt rejection.

Product water flow rates were calculated at two temperatures, 15 and 33°C using a temperature correction factor based on the ASTM standardization procedure [10]. With 15°C being the average seawater temperature in the Arabian Gulf during the winter season, it represents the seawater feed temperature to an isolated RO plant, while 33°C represents the possible seawater feed temperature to the RO in the hybrid system. Fig. 4 shows the RO product water flow rates at the reference feed pressure of 55 bar for three feed temperatures: 15°C, 33°C and the actual temperature during hybrid testing. The range of the product water flow rate data before hybridization, for the same reference pressure of 55 bar, is represented by the shaded area in Fig. 4. Most of the predicted data for the product water flow rate at 15°C fall within this range with the exception of the data for the last 300 h of hybrid testing, when the predicted data appeared to be above that range. Based on

the average predicted values at 15°C and 33°C, and the given range of the actual data, it can be shown that a gain of about 42-48% in RO product water flow rate can be achieved through hybridization. Fig. 5 is also presented to emphasize the effects of feed temperatures on the product water flow rates during the hybrid testing. From an energy consumption perspective, an isolated, two-stage RO plant without an energy recovery consumes 9.5 kWh/m<sup>3</sup> [9], while a single-stage RO plant in an MSF/RO hybrid system is estimated to consume only 5.2 kWh/m<sup>3</sup>. That is a 45% saving in energy consumption alone.

## CONCLUSIONS

Experimental testing of RO performance in an MSF/RO hybrid model was performed for about 1800 h with an RO feed water temperature ranging from 24 to 31°C. Significant increases in the RO product water flow rate were observed when the data from before and after hybridization were compared. It was demonstrated, on the basis of the experimental data, that a 42-48% gain in the product water flow rate could be achieved for a temperature of 33°C, over that of an isolated RO plant operating at 15°C during the winter season. The results imply that the energy consumption of RO can be reduced, without involving any form of energy recovery, to the level of 5.2 kWh/m<sup>3</sup> using a simple MSFRO hybrid arrangement in which the RO plant is fed the preheated seawater rejected from the MSF heat rejection section.

The results obtained in this study are encouraging; however, they should be viewed as a qualitative background only, and are less than adequate for the drawing of concrete conclusions. Further studies are needed in which the performance of different types of RO membranes in an MSF/RO hybrid environment can be substantially examined for such qualities as salt rejection, quality of preheated seawater and the effectiveness of its pretreatment.



## ACKNOWLEDGMENT

The work presented in this paper is part of the R&D project WD-002 sponsored by the Kuwait Foundation for the Advancement of Sciences (KFAS), State of Kuwait. The authors wish to express their sincere thanks to KFAS for its financial support of this project.

## REFERENCES

- [1] Statistical Year Book, Water edition 20-B, Ministry of Electricity and Water, State of Kuwait, 1995.
- [2] Hassan, A.M.; Abanmy, A.; Jamaluddin, A.T.; Iwahori, H.; Kitigawa, M.; Hirai, Y; Taniguchi, Y; Haseba, S. & Goto, T., "Membrane Evaluation for Hybrid System." IDA World Congress on Desalination and Water Sciences, Abu Dhabi, November, 1995, 5, p79-95.
- [3] Al-Sofi, M.A.; Hassan, A.M. & El-Sayed, E.E., "Integrated and Non-Integrated Power/MSF/SWRO Plants." The International Desalination and Water Reuse Quarterly, 2/3, 1992, p 10- 16 & 2/4, 1992, p42-46.
- [4] Al-Sofi, M.A., "Integrated Production of Power and Water." Desalination, 76, 1989, p89-105.
- [5] Kamal, I.; Schnieder, W. & Tusel, G.F., "Process Arrangement for Hybrid Seawater Desalination Plants." Desalination, 76, 1989, p323-335.
- [6] Awerbuch, L.; May, S.; Soo-Hoo, R. & Van Der Mast, V, "Hybrid Desalting Systems." Desalination, 76, 1989, p189-197.
- [7] Al-Mutaz, J.S.; Soliman, M.A. & Dagtham, A.M., "Optimum Design for a Hybrid Desalting Plant." Desalination, 76, 1989, p 177-189.
- [8] El-Sayed, E.; Abdel-Jawad, M.; Ebrahim, S.; Al-Nuwaibit, G. & Al-Saffar, A., "Research and Development on Desalination by Reverse Osmosis." Final Report WD-002, Kuwait Institute for Scientific Research, 4, 1996.
- [9] Abdel-Jawad, M. & Franke, W. "Doha Reverse Osmosis Plant, A Joint Program Between Kuwait and the Federal Republic of Germany on Water Desalination by Reverse Osmosis." Final Report MS-17, Kuwait Institute for Scientific Research, 3 (Operation Results), 1988.
- [10] ASTM Designation: D4516-85 (Reapproved 1989).
- [11] Sourirajan, S., "Reverse Osmosis." Logos Press Ltd., London, 1970.

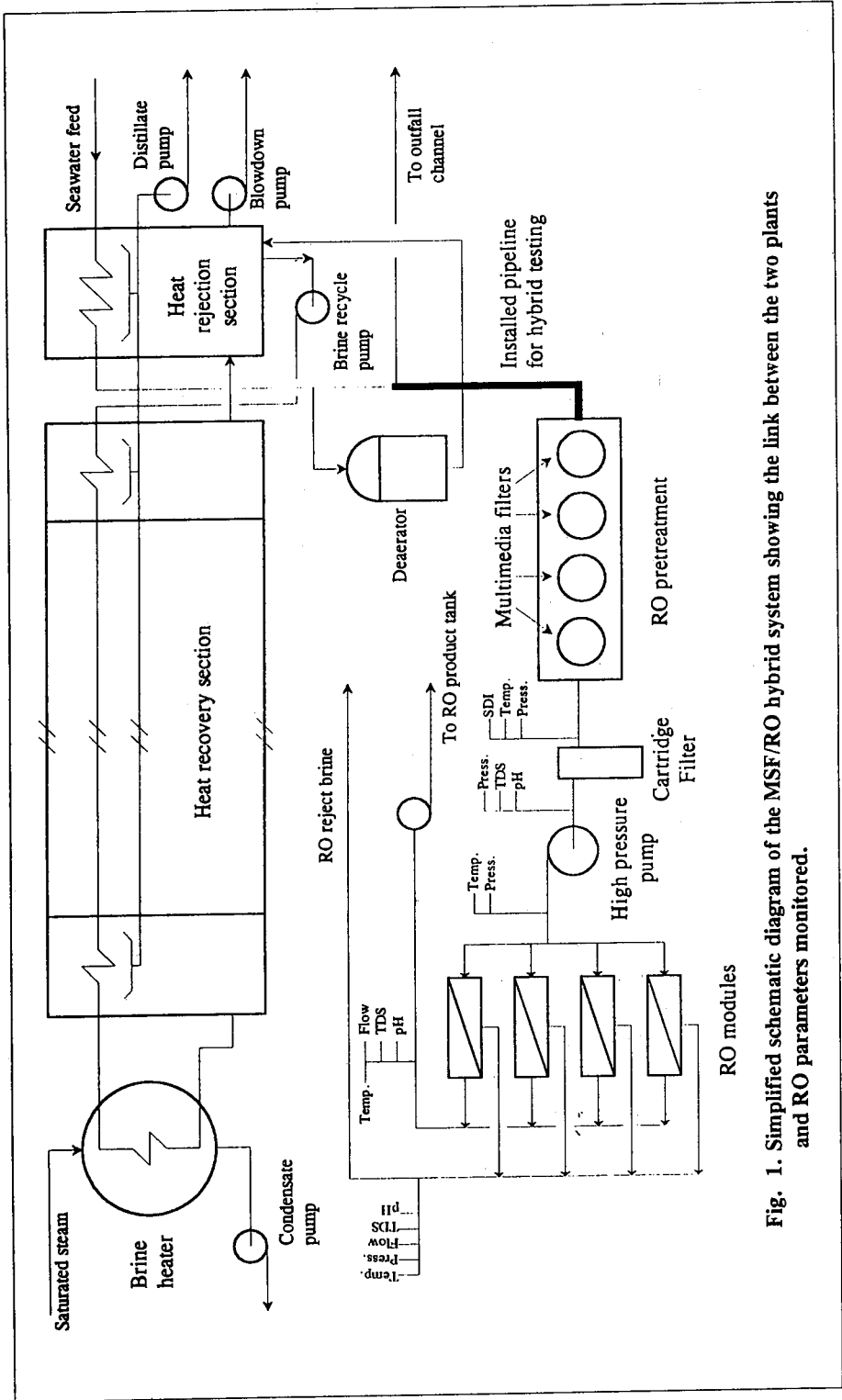


Fig. 1. Simplified schematic diagram of the MSF/RO hybrid system showing the link between the two plants and RO parameters monitored.

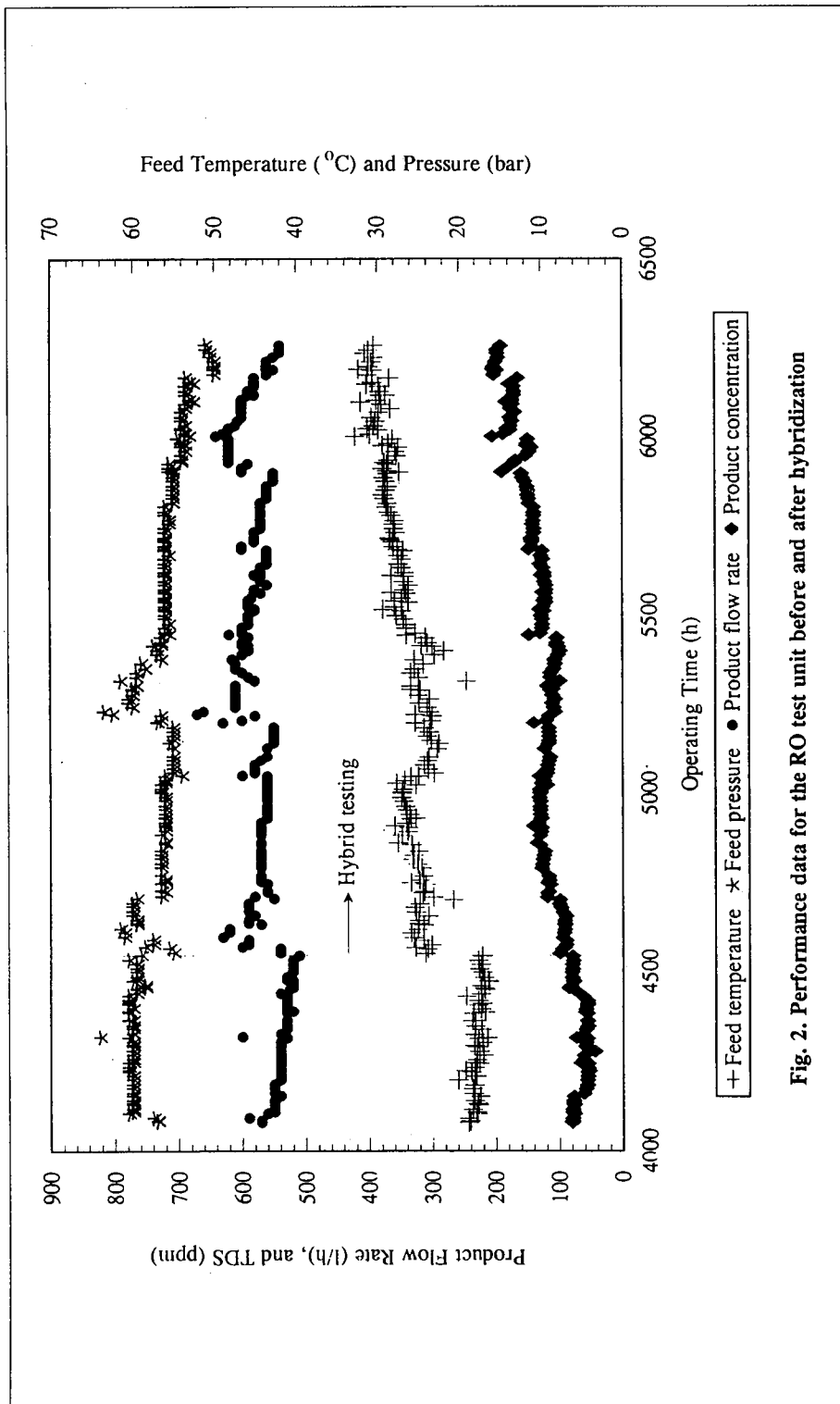


Fig. 2. Performance data for the RO test unit before and after hybridization

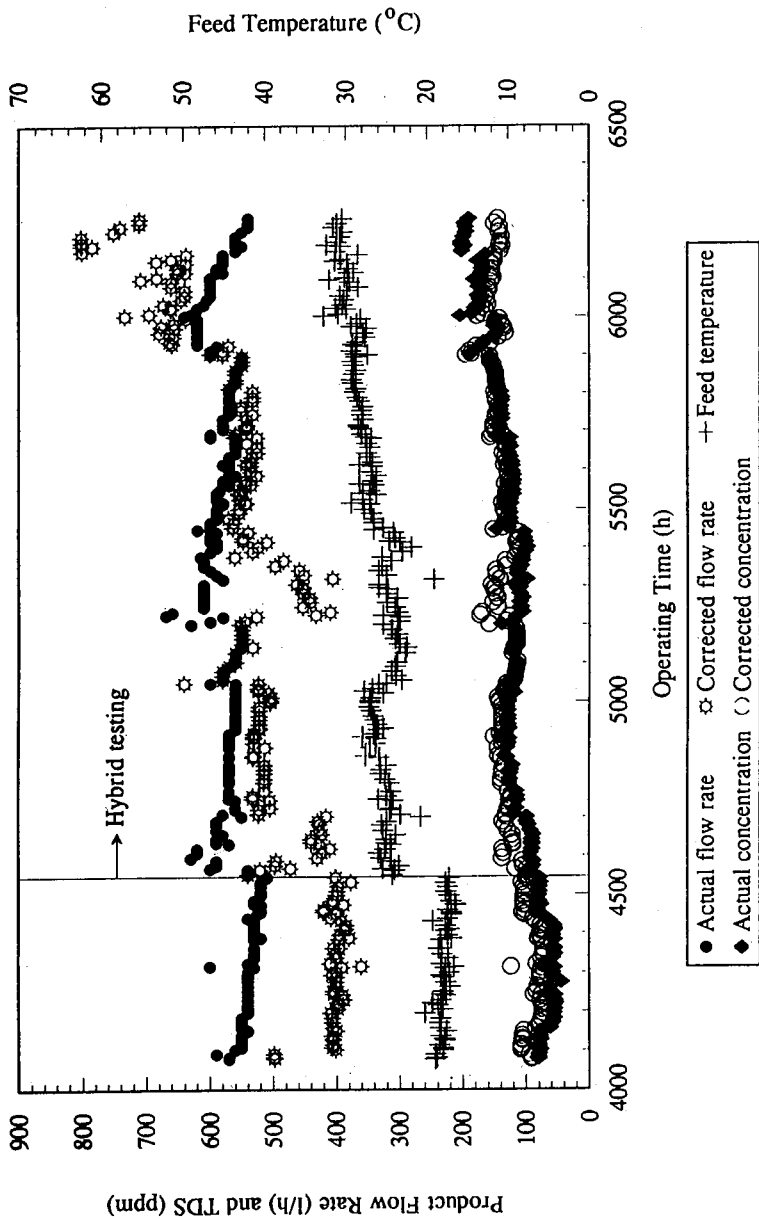


Fig. 3. Actual and corrected values for RO product water flow rates and concentration at 55 bar feed pressure before and after hybridization.

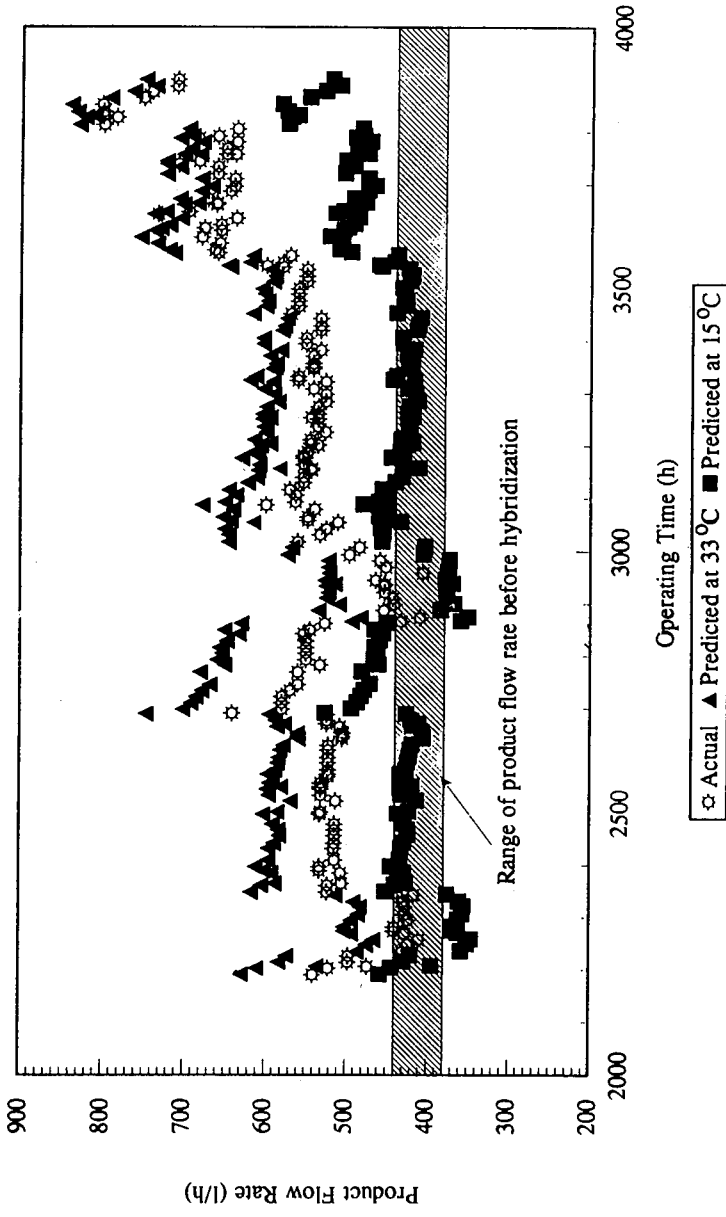


Fig. 4. Comparison of RO product flow rate, actual and predicted values, at 33°C during hybrid testing along with the predicted values at 15°C of an isolated RO system. (All values are given at a reference feed pressure of 55 bar.)

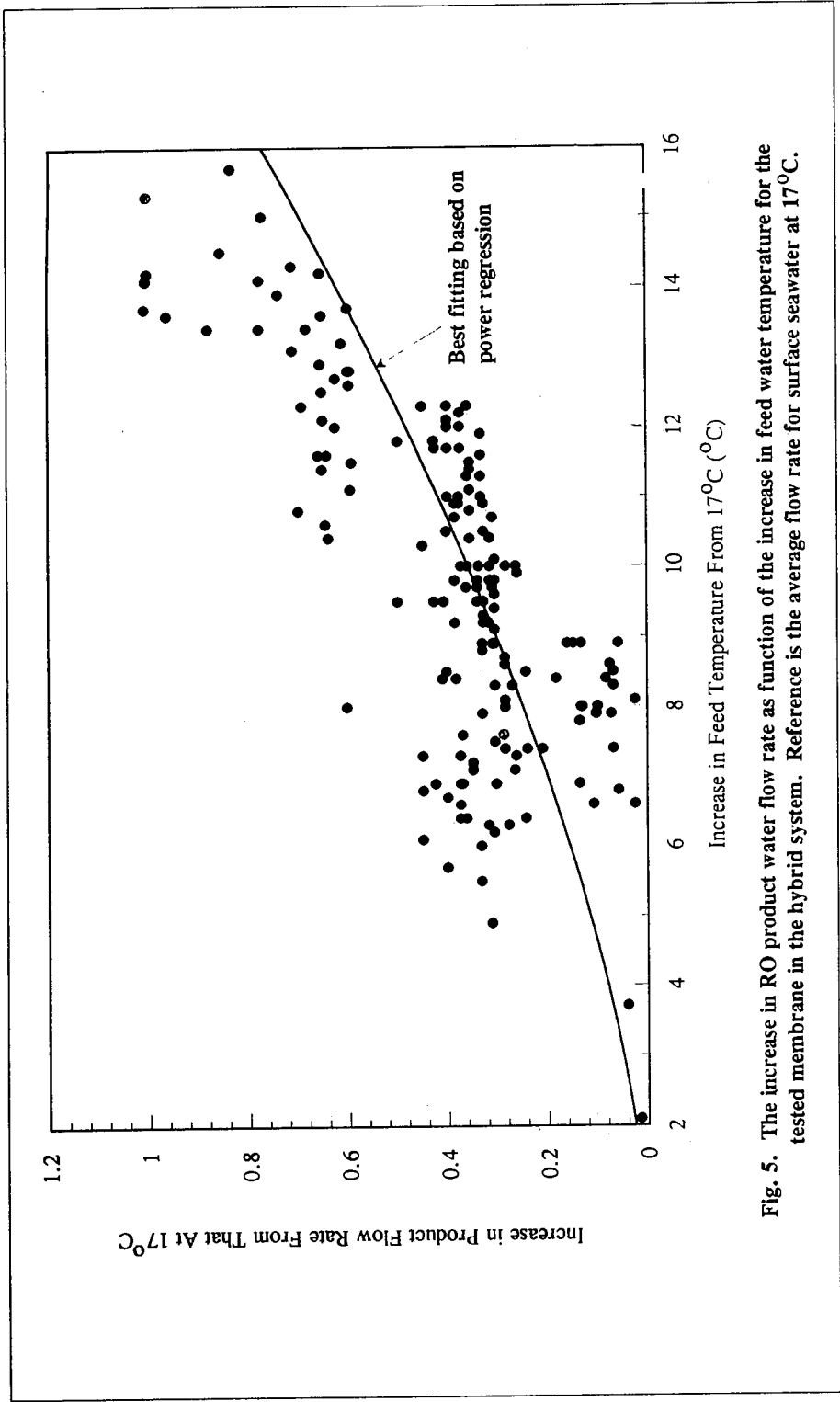


Fig. 5. The increase in RO product water flow rate as function of the increase in feed water temperature for the tested membrane in the hybrid system. Reference is the average flow rate for surface seawater at 17°C.

# **PRACTICAL SOLUTIONS TO PROBLEMS EXPERIENCED IN OPEN SEAWATER RO PLANTS OPERATING ON THE ARABIAN GULF**

**Mohammed Obaid**

Water and Electricity Department - Abu Dhabi, UAE

**Ali Ben Hamida**

DuPont Permasep Products - Manama, Bahrain

## **ABSTRACT**

In 1991, the Water and Electricity Department of Abu Dhabi (WED) commissioned a two million imperial gallons per day (9000 M<sup>3</sup>/D) seawater reverse osmosis plant in Jabel Dhana, United Arab Emirates. Initially, the high salinity, hot Gulf seawater RO plant being operated on open sea intake has suffered from biological fouling, low plant availability and high total water cost. Today the plant is operating with a new simplified process, the availability has reached 98% and the running cost has substantially been reduced. The plant represents an outstanding example of the application of several biofouling control technologies recently developed for RO seawater desalination plants. This paper presents in detail the various actions taken at Jabel Dhana to control biological fouling, increase the plant availability to 98% and reduce the plant running cost.

**Keywords:** reverse osmosis, biological fouling control, plant availability, running cost.

## **INTRODUCTION**

Significant pretreatment improvements have been made at Jabel Dhana open sea intake plant which has led to an availability of 98%. Jabel Dhana is about 250 kms. south west of Abu Dhabi. The plant running with an open sea intake on the Arabian Gulf is operated and maintained by the Water and Electricity Department of Abu Dhabi (WED). The plant was built by Aqua Engineering using DuPont B-10 membranes and commissioned in 1991.

During the first three months of start up, the plant was running smoothly then later a rapid increase in bundle pressure drop was observed. Conventional membrane chemical cleaning which involved sodium bisulfite (SBS) and detergent, were used to clean the membranes. The cleaning procedure was elective but lengthy since it required up to 5 days of continuous chemical cleaning in order to restore the bundle pressure drop.

During the chemical cleaning, the portion of piping after dechlorination was not cleaned since it was bypassed. Therefore following the membrane chemical cleaning, the biofilm accumulated in the piping sloughed off and carried to the RO membranes, rapidly fouled the permeators. Thus the bundle pressure drop increased and the membranes required again chemical cleaning. This has affected the plant availability which was in the vicinity of 75%.

In 1992, DuPont introduced a short chemical cleaning for removing biomass from RO membranes. The new developed cleaning procedure has been more effective, shorter and less expensive than the conventional method. In August 1995, a simplified pretreatment process was implemented. Since then, chemical cleaning has substantially been reduced, the plant availability increased and the total water cost reduced.

## **PLANT DESCRIPTION**

The plant consists of an open sea intake with a raw water silt density index (SDI) of 18, test for 5 minutes. A simplified schematic process flow is shown on Figure 1 and a general view of the plant on Figure 2.

About 1260 M<sup>3</sup>/H raw seawater from a depth of about 5 meters is sucked through an intake screen. Band screens with compressed air cleaning facility are installed preceding the seawater intake pumps. Continuous chlorine used to be injected at the intake chamber. The pretreatment consists of horizontal type dual media filters (aquafilt + fine sand), Figure 3. Ferric chloride (FeCl<sub>3</sub>) is added along with sulfuric acid (H<sub>2</sub>SO<sub>4</sub>) prior to media filters. Facility for



polyelectrolyte is provided but not in use. Dechlorination using SBS is done after the five micron cartridge filters.

The RO single pass system consists of 4 trains, each equipped with 134 B-10 permeators Model 6845T, Figure 4. Operating conditions are 1200 psig and 30% recovery.

Permeate from the RO trains flows to horizontal suckback tanks kept on the floor from where it is diverted to flushing and permeate tank. Permeate pumps forward water to final product storage tanks. Lime and chlorine are added for RO product water posttreatment.

## **COMMISSIONING AND PERFORMANCE TEST**

The open sea intake plant at Jabel Dhana was commissioned in 1991. The raw seawater characteristics are given below:

Raw Seawater TDS = 47,000 - 50,000 ppm

Raw Seawater Temperature = 18 - 39°C

However, the design feed water TDS was 48,000 ppm and maximum feed water temperature of 33°C. After system stabilization, the reliability period/performance test commenced, the plant met the required design product flow (9000 M<sup>3</sup>/d) and product salinity (less or equal to 500 ppm).

Three months later, a rapid increase in bundle pressure drop was observed. Frequent chemical clearings using the conventional method, SBS followed by detergent, were conducted to lower the bundle pressure drop. In addition to the conventional cleaning, SBS flushing was used every 3 to 5 days to control the rapid increase in pressure drop across the bundle.

Several sections of piping have been physically inspected. Section where chlorine is present, before SBS addition, was free from biomass. Piping section after dechlorination was full of slimes. It was then concluded that aftergrowth occurred after introducing SBS into the system.

When membrane chemical cleaning is carried out, the portion of piping after dechlorination is not cleaned since it is bypassed. Following the cleaning, the slime accumulated in this portion of piping sloughed off and carried out to the RO membranes, rapidly increased the bundle pressure drop. Thus, the RO membranes were again required for cleaning. Mechanical cleaning of contaminated piping was used to clean accumulated slime.

## **PROCESS IMPROVEMENT**

It was found that the growth of micro-organisms occurred in the piping section after dechlorination using SBS. The number of bacteria in several samples taken after SBS addition showed higher number than the raw seawater samples. This phenomenon has been experienced in all surface reverse osmosis plants running on the Arabian Gulf where the SBS injection point is not at the suction of the high pressure pump.

An intensive research program was conducted by the membrane manufacturer. This led to the development of a biofouling package that was used successfully by other Gulf plants. This package consists of:

1. Intermittent chlorination,
2. A faster and more effective new membrane cleaning method.
3. Improved B-10T membrane with a stronger substrate to withstand high pressure drop.

After consultation with the membrane manufacturer, WED has decided to implement this package at Jabel Dhana. In August 1995, the chlorine dosing pump was turned off and close monitoring of the system was done to see the effect of the intermittent chlorination process. To avoid clogging of the intake screen, intermittent chlorination is implemented once every 7 to 10 days for 4 hours.

After several months of operation without continuous chlorination, the slime which used to be present in the low pressure piping after SBS addition has not been observed. Since the use of intermittent chlorination, the rate of permeator pressure drop buildup has been substantially decreased. The frequency of chemical cleaning is every 5 to 6 months, no SBS flushing is needed.

Frequency of cartridge filters replacement has increased due to exhausted media filter which has been in operation for more than five years. Consequently organic fouling is passing through the media and fouling the cartridge filters, No slime has been detected neither on the cartridge filter elements nor on the housing, indicating the elimination of biological fouling.

The plant performance has been outstanding without continuous chlorination/dechlorination. Early January 1996, WED has implemented the same pretreatment process in other open sea intake plants running on the Arabian Gulf (Mirfa, Sila, Sir Baniyas, Dalma, Rafeek, Abu Kashisha).

## **CLEANING IMPROVEMENT**

The conventional chemical cleaning consisting of SBS and detergent was lengthy and costly. The train used to go for up to 5 days of continuous chemical cleaning in order to restore the bundle pressure drop. The biomass deposited in the membranes was never fully eliminated.

In 1992, DuPont introduced a new chemical cleaning for biofouling. The new technique involves cleaning of the RO B-10 polyamide hollow fine fiber membranes with sodium hypochlorite at high pH (11.8 - 12.0). This new method was applied few times at Jabel Dhana and the results obtained were excellent. In addition to the excellent cleaning results, the hypochlorite cleaning is short since it requires only 6 to 8 hours while the conventional cleaning used to require up to 5 days of continuous cleaning. This cleaning technique is cheap, short and effective in restoring the bundle pressure drop.

Since the implementation of new technology, the chemical cleaning frequency is every 5 to 6 months.

## **PLANT PERFORMANCE**

Due to the biological fouling experienced in the plant with the original pretreatment, the plant total production decreased after about 4500 operating hours. Figure 5 shows the product flow before the implementation of the new developed biofouling package.

In August 1994, new membranes were installed on train 1 & 2. Those new membranes were with a stronger substrate made of nylon which can tolerate higher bundle pressure drop than the previous polyester material.

As shown on Figure 6, the product flow was above the design for the first 12 months with the continuous chlorination. The following months with intermittent chlorination process, the product flow has been steady, higher than the design flow by about 25%.

The product water TDS over 14,000 hrs. averaged 350 ppm from a single pass seawater RO system running on Arabian Gulf from a very high feed salinity of 47,000 to 50,000 ppm. Figure 7 shows individual points.

From the above mentioned treatment and process modifications, we have achieved outstanding results which were not expected by many experts. The obtained results are summarized in Table A:

## CONCLUSIONS

Implementations of the new simplified process has substantially improved the performance of the open sea intake plant at Jabel Dhana.

Today, with intermittent chlorination, the plant availability is 98% and is producing a potable water at low water cost as compared to plant availability of about 75% when continuous chlorination/dechlorination of feedwater was applied. Moreover, water cost came down as a result of lower chemical cost and higher availability.

The outstanding performance of Jabel Dhana has regained WED's confidence in the RO technology as an efficient and reliable process for seawater desalination. This simplified process has been implemented in all WED open sea intake reverse osmosis plants running on the Arabian Gulf.

## ACKNOWLEDGMENTS

The authors gratefully acknowledge the advice and co-operation of His Excellency the Undersecretary of Water and Electricity Department of Abu Dhabi, Engineers at Jabel Dhana and other RO WED staff for their assistance and help.

Chemicals	Avg. Consumption, kg/month		Reduction in Chemicals, %	Use
	Before 8/95 Chlorination /Dechlorination	After 8/95 Intermittent Chlorination		
Chlorine Gas	2150	25	99	Disinfection
Sodium Bisulfite	7000	3000	57	Remove Chlorine
Citric Acid	1100	57.5	95	Remove Iron
DMCA-14	700	Zero	100	Remove Deposits
Tannic Acid	12.5	0.9	93	Improve Rejection
Lutanol M40	5	1	80	Improve Rejection
Ammonium Hydroxide	550	30	95	pH Adjustment
Caustic Soda	22.5	3	87	pH Adjustment

**Table A: CHEMICAL COMPARISON**

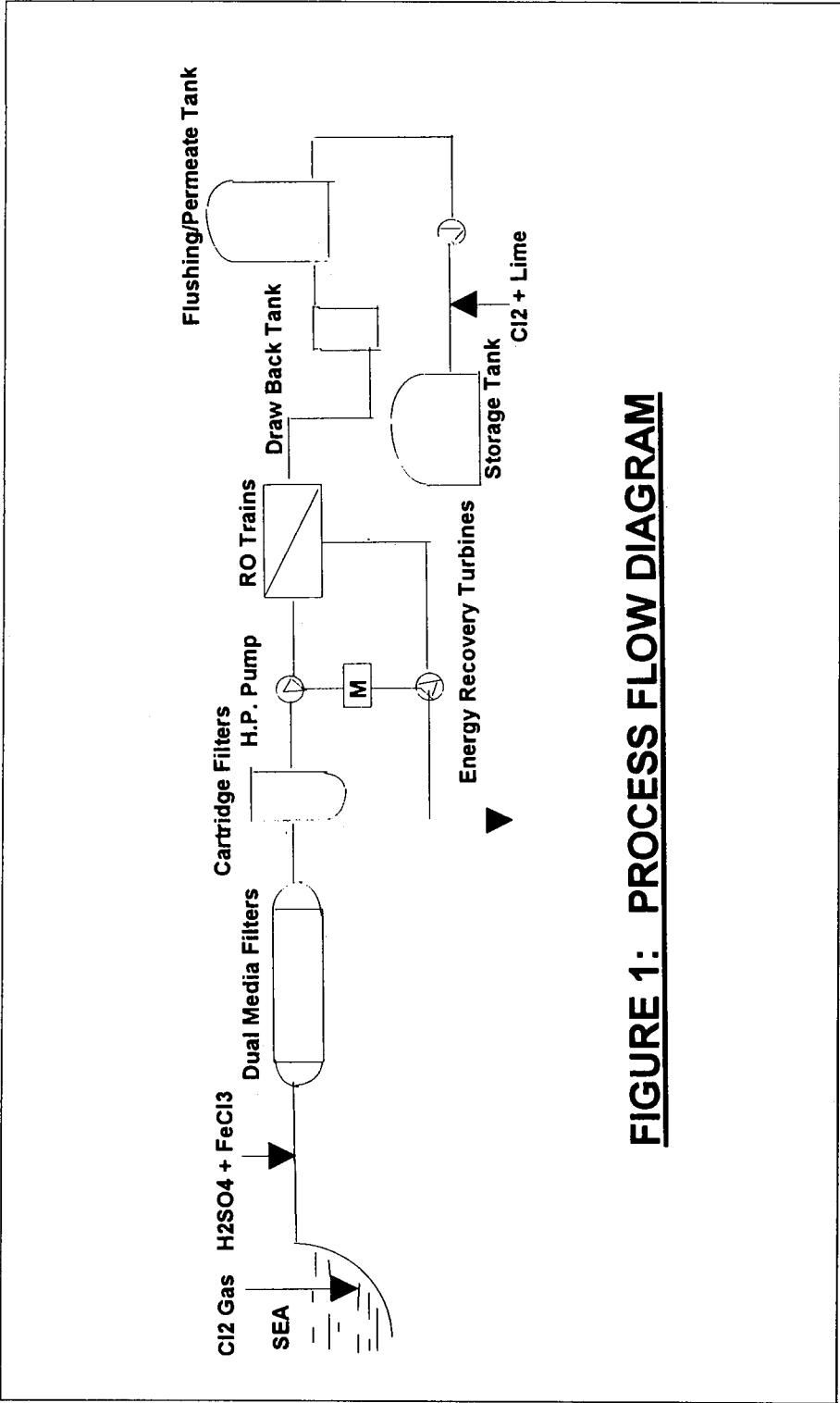


**FIGURE 1: PROCESS FLOW DIAGRAM**

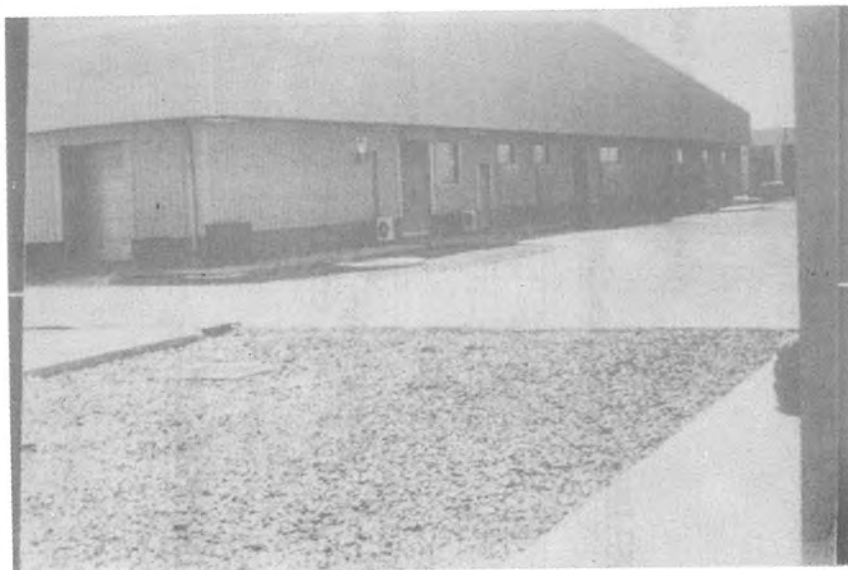


**FIGURE 2: GENERAL VIEW**

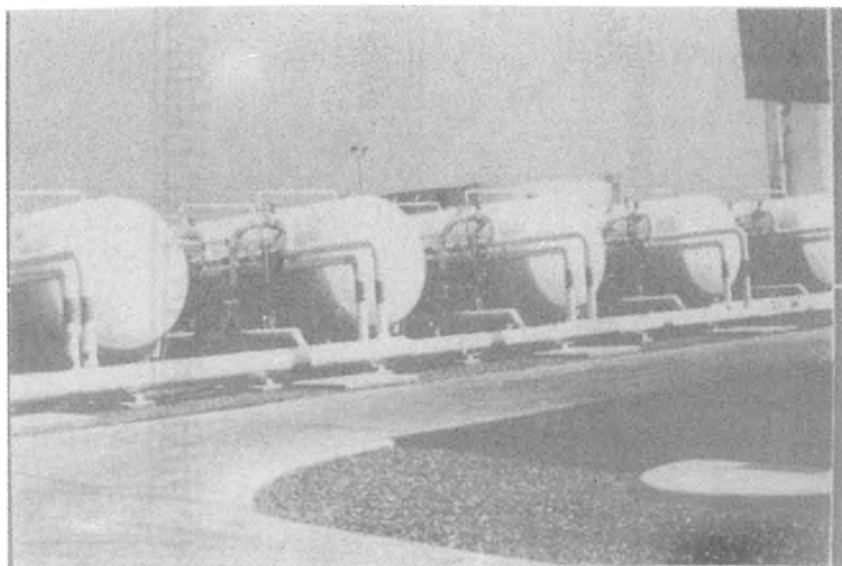


**FIGURE 3: DUAL MEDIA FILTERS**

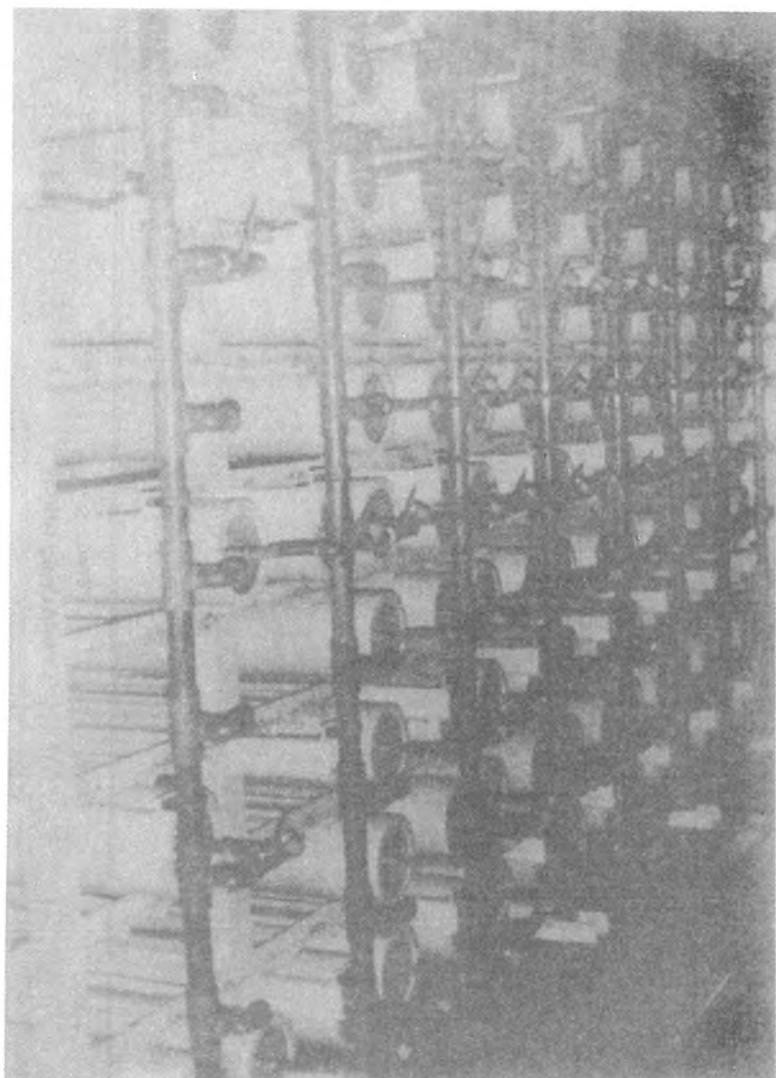


**FIGURE 4: B-10 PERMEATORS**

**NORMALIZED PRODUCT FLOW WITH ORIGINAL PRETREATMENT - TRAIN 1**  
**JABEL DHANA SWRO PLANT**

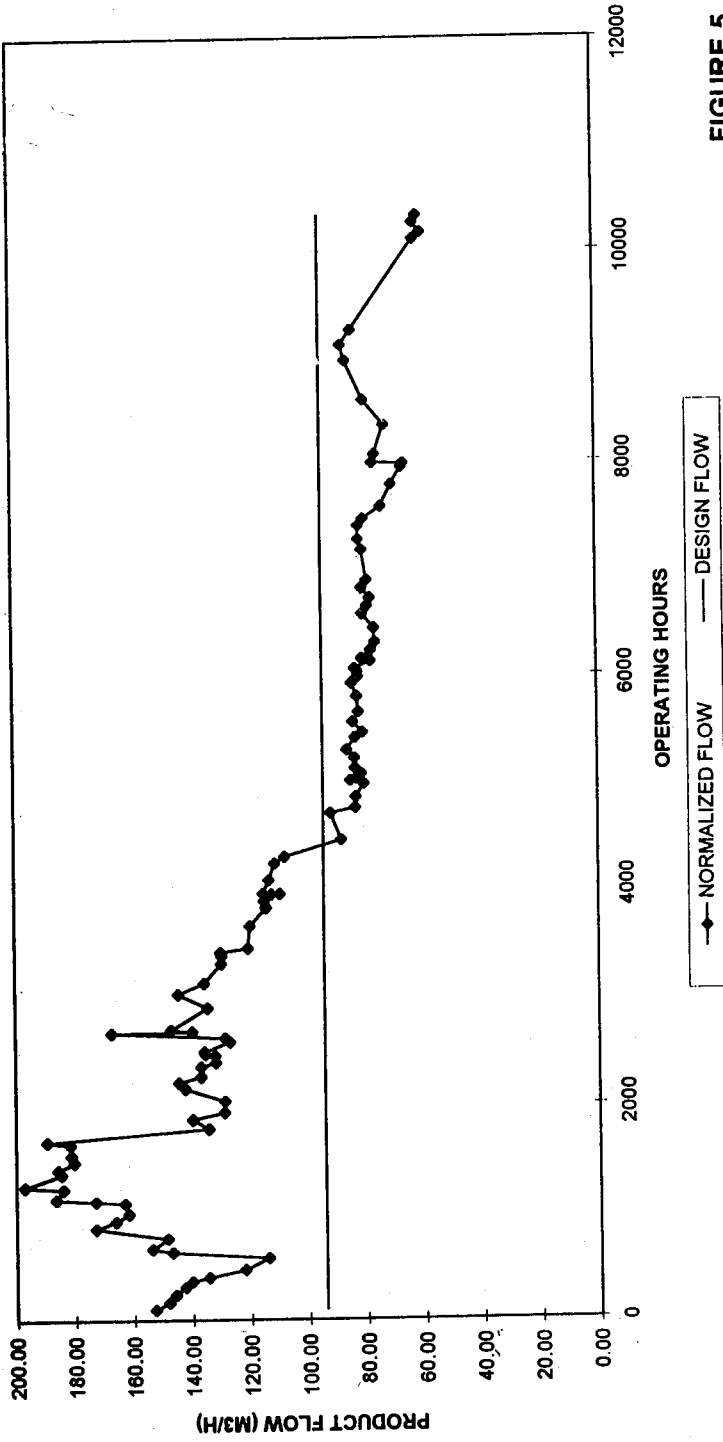


**FIGURE 5**



**NORMALIZED PRODUCT FLOW - TRAIN 1**  
**- JABEL DHANA SWRO PLANT**

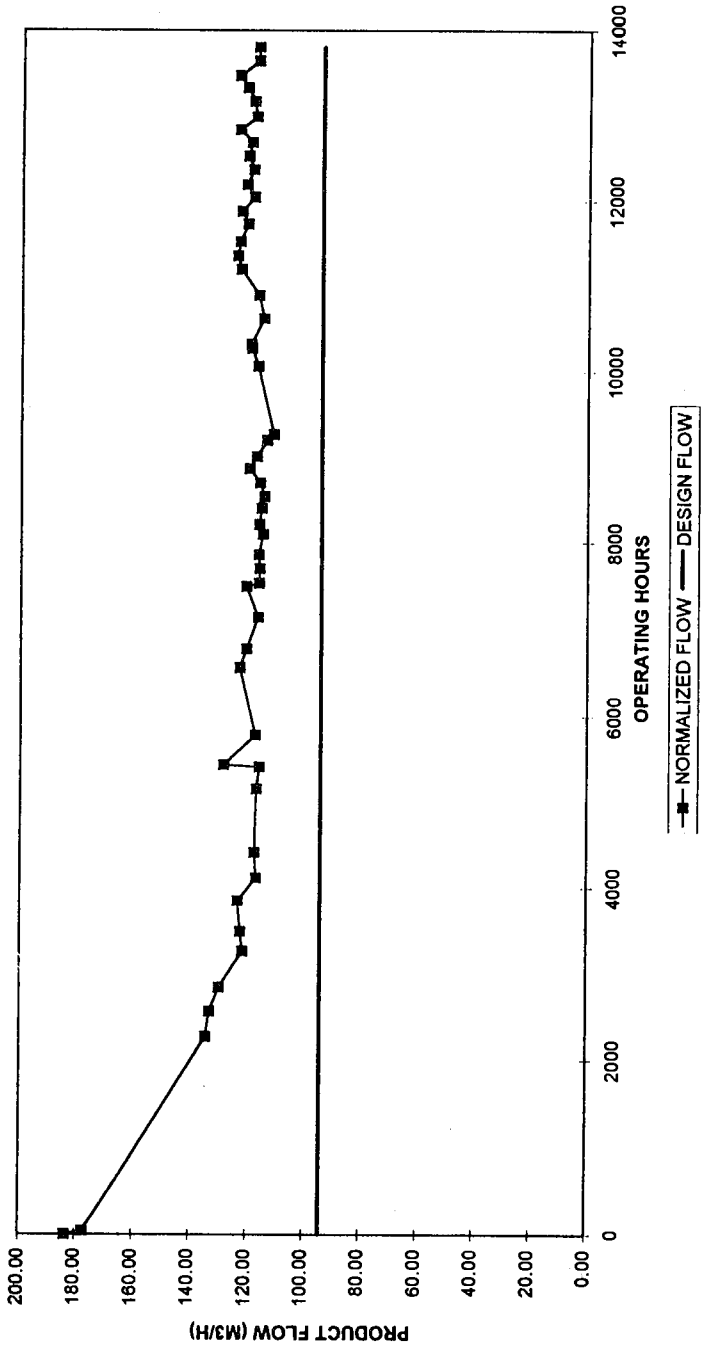


**FIGURE 6**

**NORMALIZED PRODUCT TDS - TRAIN 1**  
**JABEL DHANA SWRO PLANT**

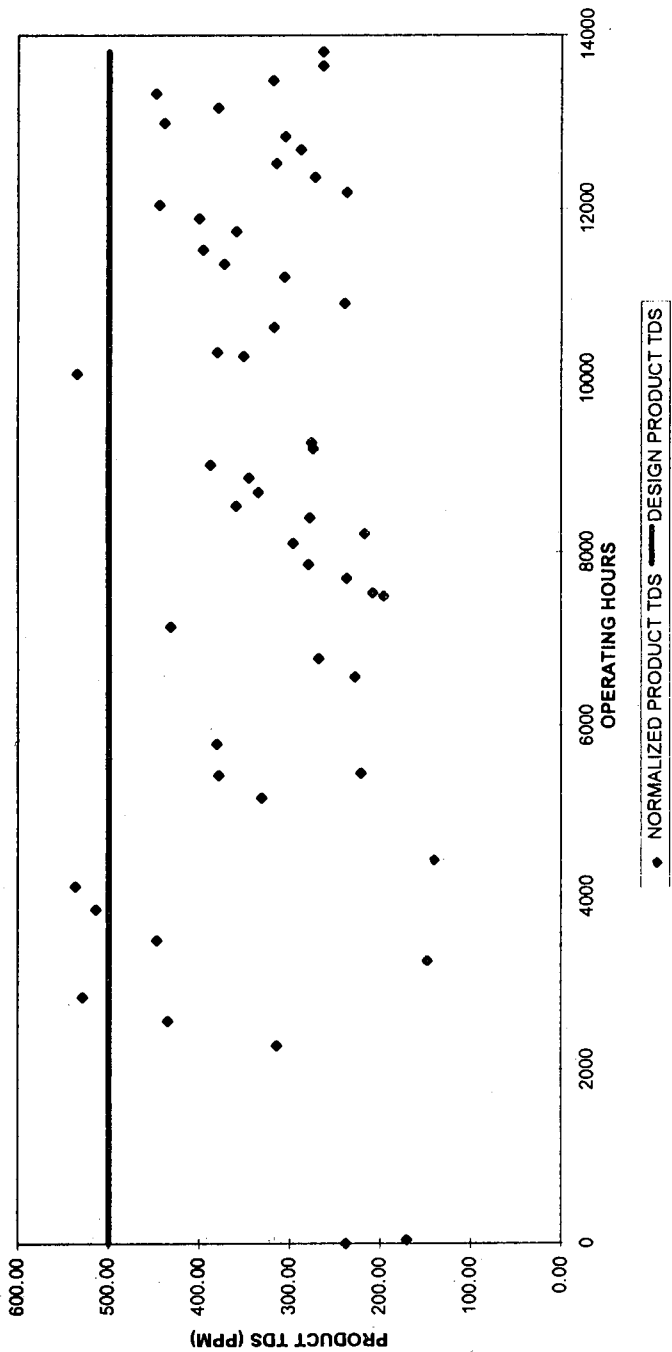


**FIGURE 7**

TABLE NO. 3

Report of Optimization Test (vent valve adjustment)  
After Rehabilitation

(Vent Valves Position)	(Vent Adjust Mode No.)	M-1	M-2	M-3A	M-3B	M-4A	M-4B	M-5	M-6
Valve from stage 1	notches	2	2	2	2	2	2	2	2
Atmospheric valves	notches	0	0	0	0	0	0	0	0
Valve from stage 2	notches	3	2	2	2	2	2	2	2
Atmospheric valves	notches	0	0	0	0	0	0	0	0
Valve from stage 3	notches	3	4	4	4	4	4	4	4
Valve from stage 1,2,3	turns	1/2	1/2	1/2	3/4	1/2	1/4	1/4	1/2
Valve from stage 6	notches	4	4	4	4	4	4	4	4
Valve from stage 12	%	0	50	100	100	100	100	100	100
cascade 12 to 13	%	100	0	0	0	20	20	40	50
Valve from stage 20	%	70	70	70	70	70	70	70	70
Stripping Steam Flow to DA	m <sup>3</sup> /hr.	6.6	6.8	7.0	6.9	6.8	6.7	6.8	6.6
Heat Performance(Distill/Condensate)	kg/kg	7.22	7.35	7.61	7.35	7.57	7.45	7.38	7.23
(Ratio of HP to Final Position)	%	99.9	101.7	105.3	101.7	104.7	103.1	102.1	100.0
Temp. of Stages									
Stage 1	deg.C	99.0	99.0	99.5	99.2	98.5	98.2	99.2	99.3
Stage 2	deg.C	96.8	97.0	97.5	97.0	96.5	96.2	97.0	97.3
Stage 3	deg.C	96.0	96.0	96.2	95.0	95.2	95.7	96.2	96.0
Stage 6	deg.C	88.7	88.2	88.7	87.2	87.2	88.0	89.0	88.5
Stage 7	deg.C	85.0	85.0	85.8	84.2	84.2	84.2	85.8	85.3
Stage 11	deg.C	68.1	68.2	69.0	68.5	68.4	68.7	69.2	69.2
Stage 12	deg.C	65.5	66.8	67.3	66.8	66.8	66.7	67.2	67.0
Stage 20	deg.C	40.0	38.2	39.0	40.0	40.0	40.0	40.3	41.0
Flash range of									
Stage 1	deg.C	5.5	6.3	6.0	5.8	6.3	6.0	5.8	6.2
Stage 2	deg.C	2.2	2.0	2.0	2.2	2.0	2.0	2.2	2.0
Stage 3	deg.C	0.8	1.0	1.3	2.0	1.3	0.5	0.8	1.3
Flash range between									
Stage 1-6	deg.C	15.8	17.1	16.8	17.8	17.6	16.2	16.0	17.0
Flash range of									
Stage 12	deg.C	2.6	1.4	1.7	1.5	1.6	2.0	2.1	2.2
Flash range between									
Stage 7-12	deg.C	23.2	21.4	21.4	20.2	20.4	21.3	21.8	21.5
Flash range between									
Stage 13-20	deg.C	25.5	28.6	28.3	27.0	26.8	26.7	26.9	26.0
Flash range between									
Stage 1-20	deg.C	64.5	67.1	66.5	65.0	64.8	64.2	64.7	64.5

**The Addur SWRO Desalination Plan,  
Towards A Full Plant Production**

*Ali Hussain and Ahmed H. Ahmed*

# THE ADDUR SWRO DESALINATION PLANT TOWARDS A FULL PLANT PRODUCTION

**Ali R. Hussain and Ahmed H. Ahmed**

The Addur SWRO Desalination Plant, Water Production Directorate,  
Ministry of Electricity and Water  
State Of Bahrain

## ABSTRACT

Since the early days of commissioning in 1990, the Addur SWRO Desalination Plant has been going through a series of predicaments. The most crucial was the inability of the RO System to attain the plant's design production of *10 MIGPD*. This is perceived as a direct reflection of the abnormal feed water condition. Mainly due to seasonal changes and high feed water SDI exiting the Pre-treatment System. In November 1995, the Addur plant went through a new phase change when the opportunity had risen for three RO Trains to be replaced with new membranes, while pre-treatment problems remain unresolved. In its entirety, this was viewed as a rewarding experience in the sense that it provided a new keystone to examine the pre-treatment system performance and its impact over the production of new membranes, which is the essence of this paper. In addition to the *one-year* operating performance assessment of the new membranes, the paper will also discuss the production prediction of these membranes under the prevailing pre-treatment conditions. The recent modifications which inspired the major step change of installing new membranes will be discussed. In addition, and more importantly, it is to provide clear illustration of the upcoming plant rehabilitation which is to move forward *the Addur SWRO Desalination Plant towards a full plant production*.

**Keywords:** Pre-treatment and RO state-of-operation; feed water SDI; performance of new membranes; plant modifications; membrane production prediction; rehabilitation.

## A CLASSICAL OVERVIEW OF THE HISTORICAL CIRCUMSTANCES AT ADDUR

The Addur Plant was designed to produce 10 MIGPD of drinking water, with a maximum TDS of 500 mg/l, at a sea water feed temperature and TDS design conditions of 29°C and 45,000 mg/l, respectively. The Plant was commissioned in 1990, whilst proved incapable of delivering neither the design production rate nor the anticipated product water quality as the result of multiple reasons. These were principally due to the fact that the RO productivity was greatly affected by the seasonal changes of the sea water (temperatures reaching as low as 15°C during winter), and higher salinity approaching 68000 PPM at times. (Figure 1 illustrates a Schematic Process Diagram of the Addur SWRO Desalination Plant).

By mid 1993, the Addur total plant production was barely averaging 50% of the design, with a product TDS about 1,300 mg/l (Figures II & III illustrate Train E Product flow and salinity, 1993). The persisting problems were recognized fundamentally as a shortfall in the Pre-treatment System, wherein the Dual Media Filters were unable to produce their design filtered water SDI of  $\leq 2.7$ . This has caused a continual rise in the differential pressures ( $\Delta P$ ) across the membrane bundles, deteriorating RO Trains productivity and the ever-rising product salinity.

Despite the serious endeavors to recover the deteriorated membrane conditions, it was evident that most of the 3,696 membranes at Addur were fouled. Since that moment in time, the symptoms of the ailing membrane condition was detected and various remedies were investigated, while the condition was ceaselessly becoming worse.

The severity of this membrane fouling problem was long suspected but the evidence was incidentally come across when a sticky foreign matter was discovered at the feed header of one of the Trains. Subsequently, a thorough examination of this feed header was performed which led to the discovery of a diversified type of fouling in the form of a thick brownish frothy sludge attaching on to the inner walls of the header. This finding indicated the probable fouling of all pipes and headers within the RO system, which reflected the magnitude of the conceivable membrane fouling severity being encountered.

Fourteen Membranes with high product conductivity yield [ $>> 8,000 \mu\text{S}/\text{cm}$ ] were examined followed by a careful internal inspection to verify the suspected membrane fouling adversity. All the 14 Membranes were found to have sustained the same obscure fouling. The foulants were in the form of a dark-brown elusive and ill-smelling substance covering a large percentage of fibers and reemay within the fiber bundles, which authenticated the absolute certainty of the extent of fouling of the membranes at Addur. Further, about six out of the 14 fiber bundles

were found suffering from a torn reemay circumstance, in addition to the endless number of broken hollow fibers.

The next area of investigation was the internal inspection of piping within the Pre-treatment System; one convenient location was the Cartridge Filters outlet header. Upon inspection, foulants of a type and texture similar to that found inside the Trains' feed headers were discovered clinging to the internal header-walls with their density growing traveling towards the High Pressure Pumps, which indicated that this fouling was originating at this exact point, perhaps just after dechlorination. Primary analysis of a retrieved specimen indicated, fundamentally, the existence of both biological and iron (and possibly scaling) as the principal foulants, with a ratio identified as, roughly, 70% biological to 30% iron.

As the foulants were identified, the endeavor was then for them to be removed from the system, while revised and newly formulated chemical cleaning methods were exploited. Conventional sterilization using formaldehyde was employed to inhibit the biological growth within the RO system, followed by citric acid (pH 4.0) and detergent cleaning to reduce bundle  $\Delta P$ , and PT-B post-treatment to improve permeate quality. A different type of membrane cleaning was also envisaged and employed, the "Enhanced sodium hypochlorite high-pH cleaning", which was a new procedure developed with the assistance of DuPont and engineered for the type of fouling adversity encountered at Addur; however, there was no consequential improvement in RO performance following the Enhanced cleaning. This episode did not only acknowledge, again, the membrane fouling severity, but also indicated that it could not be eliminated. The fouling layers within the pipes and headers was removed using a blend of hydrogen peroxide and sodium hydroxide.

Moreover, there were two remedial methods performed to attain a brief recovery in bundle  $\Delta P$ , permeate flushing and chemical cleaning. Both involved taking the Train out-of-service for a period of time to be applied, and both were (and are still) being employed with the latter offering a higher drop in bundle  $\Delta P$ ; however, having 33 Banks in the RO system makes the task extremely difficult and time consuming. Further, the frequent stopping and starting of the High Pressure Pumps could lead to serious ravage of the motors and may result in harmful consequences to the hydrodynamics of the membrane bundles.

It was very obvious at that time that recovery of plant productivity was an impossible task, though many trials were inaugurated just to maintain the 50% plant production. The ventures were targeted towards the improvement of the Pre-treatment System in order to resolve certain doubts concerning the high SDI being obtained and, most importantly, to prevent future reoccurrence of the same

fouling circumstance. The trials performed involved the regulation of pH across the Dual Media Filters, the varying of chlorine concentration across the pre-treatment, establish new guidelines for Coagulant and Coagulant Aid dosing rates, a revamp of the Dual Media Filters back-wash sequence, investigate the efficacy of the Dual Media Filters and the Cartridge Filters performance, and others.

Nevertheless, the prevailing understanding remained apparent, the RO membranes at Addur had long been exhausted, and all would require to be replaced if 10 MGD production was contemplated.

In October/November 1995, though pre-treatment problems remained unresolved, the demand for drinking water necessitated the replacement of old membranes from three RO Trains with new membrane-bundles, which was essential to increase plant production by approximately 20%. By the end of September 1996, the old membranes of the remaining five RO Trains were taken out-of-commission and considered retired; in doing so, an important Chapter in the history of the Addur SWRO Desalination Plant was wrapped-up and concluded.

## **SYSTEM MODIFICATIONS**

There were three major system modifications performed during the past one year (1995/96) which inspired the major step change of installing new membranes at Addur, a stride foreseen essential prior to reclaiming the plant to its maximum possible output.

During the final quarter of 1995, the sodium bi-sulphite dosing point was relocated from the Cartridge Filters outlet header to the immediate suction points of the individual High Pressure Pumps. The relocation of the point of dechlorination was fundamental to provide an extended chlorine exposure (i.e. sterilization) of the piping upstream the RO Trains and to delay the biological re-growth, which normally succeeds dechlorination, till after the water had exited the membranes. This modification was constituted to overcome the membrane biological fouling being experienced and to impede its reoccurrence when new membranes were placed on stream. The prevalent bio-count test results demonstrate, to an extent, the fruition of this modification step.

During the same period of time, the Coagulant (Ferric Chloride) and Coagulant Aid (Polyelectrolyte) dosing points were brought slightly upstream the Contact Tank. Essentially to provide more residence time for coagulation and flocculation to take effect.



In April 1996, as the requirement for feed water was ascertained to be more than the available quantity, thus, it was essential to remove the baffles from the In-Line Mixer upstream the Contact Tank. This is to provide lower hindrance to sea water supply to the Dual Media Filters and providing sufficient feed water for both RO and Dual Media Filters back-wash operations.

## **THE DUAL MEDIA FILTERS TRIALS**

During 1996, various challenging attempts were launched to reinvigorate the Dual Media Filters performance in order to reduce the consistently high-SDI across the pre-treatment, which was directly reflecting on the RO Trains production. Many of the trials concentrated on the operation and back-wash of the Dual Media Filters, hitherto, no significant reduction in SDI was visible. The main observations and conclusions on the trials yet performed on the Dual Media Filters follow.

The Ferric Chloride and Polyelectrolyte dosing rates were varied within a range of 2.5 - 4.5 PPM and 0.25 - 0.5 PPM, respectively. No significant drop in SDI was recognized, possibly because the SDI of the feed water exiting the Dual Media Filters is already too high to echo any noticeable change, (which remained > 3.5).

In July 1996, all Dual Media Filters underwent an extensive back-wash operation, involving a timed-sequence of water back-washing, air-scouring and sedimentation, repeated 10-times over for each filter. This was intended to extract as much as possible the embedded floc-matter from within the innermost depths of the beds. Observations demonstrated very encouraging results, though not reflected on the SDI being obtained.

Air-scouring and water back-washing duration and flow rates were varied throughout numerous experimentation, with the major objectives of removing as much floc-matter as possible from the beds. It was pertinently determined that the following sequence was offering best back-wash results:

3-minute fast drain-down; 5-minute air-scour; 3-minute sedimentation; 8-minute water back-wash; 3-minute sedimentation; and 30-minute filter stand-by (as a minimum). Twice this sequence appeared more effective in floc-matter removal, as viewed throughout the many trials performed.

Filter running time (i.e. filtration duration) was varied over a reasonable period of time, and was concluded that 17 hours was adequate.

## ONE-YEAR RO PERFORMANCE ASSESSMENT

During October/November 1995, and as the demand for drinking water had raised some concern, a sanction was granted for the replacement of old membranes from three RO Trains with new membrane-bundles, which was a very crucial step to increase plant production even though problems at the pre-treatment were not resolved. The discussion which follows is to bring to light the operating conditions and future prospects at Addur, with an explicit focus on the perceivable performance of the Pre-treatment and RO Systems.

The performance of any RO system, as it is always the case, is ordained by the performance of the pre-treatment system. Thus, under the current prevailing condition of the pre-treatment at Addur, primarily in terms of the high feed water SDI, naturally, the consequence would be a continuing decline in the overall RO performance, as characterized by low productivity, high permeate salinity and high average  $\Delta P$ .

It would be conveniently practical to review a one-year performance of one of the new Trains (RO Train "A"), which was commissioned with new B- 10 bundles (6835TR type, that are tolerant to a higher bundle  $\Delta P$ , hence offering more flexibility in RO system operation). The illustrative figures arranged at the back of this paper are to provide a clear visual understanding of the pre-treatment and RO Train "A" state-of-operation at Addur during the past one-year. Figure IV illustrates the Sea Water and Pre-treated Water SDI. Figures V, VI, and VII are trend graphs of RO Train "A" Normalized Flow, Product Conductivity, and Average  $\Delta P$  respectively.

Since commissioning in November 1995, RO Train "A" continued to remain in a very stable state-of-operation for several months, in terms of availability, productivity and operability. It remained producing the anticipated design product flow of 245 m<sup>3</sup>/h, with a good permeate quality and an acceptable rise in bundle  $\Delta P$ .

The Train maintained this operating condition for a reasonable period of time (well over 6 months), even under the unstable nature of pre-treatment conditions. However, it was not until August 1996 when it's performance began to deteriorate by taking a rough turn towards a lower productivity and an increasing trend in bundle  $\Delta P$  (though managed to retain permeate quality).

This had occurred as a result of an aggressive seasonal change which took place during that period where the sea water condition became very harsh and unpredictable, as reflected by the abnormally high SDI of the filtered water exiting the Dual Media Filters (which was exceeding 4.5).

The one-year operating data evidently show that RO Train "A" had in fact exhibited low productivity and an increase in average-bundle  $\Delta P$ . Although productivity and average-bundle  $\Delta P$  were slightly reclaimed by permeate flushing and reasonably recuperated by chemical cleaning, however, as attributed to the complex nature of the feed water exiting the pre-treatment, performance regress begins soon after restarting.

Soon and within a 4-week operating period the average-bundle  $\Delta P$  were reaching the maximum allowable limit while product flow could never be restored back to its initial rate. This can only be ascribed to the persisting iron-oxide and/or colloidal-iron deposition within the fiber bundles, including, perhaps, some organic fouling. With regard to product quality, on the other hand, it was holding within an average of 500 PPM.

### COST ESTIMATES

Assessing plant performance in terms of the overall operating cost for the years 1993, 1994 and 1995 (Table 1), it is apparent that as the condition of the old membranes was worsening, the unit operating cost was drastically climbing. However, for the first 6 months when new membranes were placed in-operation, i.e. from November 1995 till April 1996, plant productivity very sharply improved as the unit operating cost dropped to an amazing figure of 0.269 BD/M<sup>3</sup> [0.70 \$/m<sup>3</sup>].

Furthermore, as the performance of the new membranes was getting gradually affected during July and August 1996, the unit operating cost adopted again an increasing trend. Table 1 illustrates the typical production unit cost throughout the period 1993 to 1996. This clearly signifies the revenue gained when new membranes are in-operation, which can only be maintained all year round if pretreatment deficiencies are resolved.

**Table 1 WATER PRODUCTION COST 1993-1996**

ITEM	YEAR			
	1993	1994	1995	1996
Total Expenditure (BDx 10 <sup>6</sup> )	3.47	3.4	3.0	3.55
Net Production (m <sup>3</sup> x 10 <sup>6</sup> )	4.65	3.70	1.5	7.1
Unit Cost BD/m <sup>3</sup> (US\$/m <sup>3</sup> )	0.75 (2.0)	0.9 (2.4)	2.0 (5.3)	0.5 (1.3)

## **ADDUR REHABILITATION**

Furtherance to the trials at the Dual Media Filters may again lead to obtaining similar indeterminate results, thereupon, making it only logical for Addur to move forward towards the next phase of improvement, plant rehabilitation; a phase which should not only focus on process deficiencies alone but to go beyond to cover the overall adversities of the plant.

When it comes to the success of the Addur rehabilitation scheme, there is, in fact, a large scope-of-work which needs to be professionally examined and ventured. An explicit emphasis on the extent of work which needs to be construed are explained in the following systematic approach:

1. Perhaps the matter which concerns the possibility for having insufficient sea water supply to achieve the desired plant production can be over come by replacing the existing Sea Water Supply Pumps with larger-capacity pumps. Such investment would be justified in the light of the rapidly deteriorating pump material.
2. Based on the present experience, the existing Electro-Chlorinator Unit (the Annular-Tubes Cell Module type), is becoming very expensive to maintain in terms of repair difficulties and the high cost of spares. It is recommended to replace this unit with another having a different configuration (e.g. the Vertical Dipolar Plates type) and a larger output capacity, altogether.
3. Since the SDI of the filtered water exiting the Dual Media Filters never achieved the design value of (2.7) the below recommendations are concerned with the improvement of the Dual Media Filters to attain a better performance:
  - Introduce rapid-mixing for an effective coagulation/flocculation process.
  - Expanding the coagulation/flocculation chamber (Contact Tank) volume, with the addition of agitating equipment, to achieve the required residence time.
  - As anthracite is being depleted from the Dual Media Filters beds in large quantities during backwashing, it is suggested to raise the height of the back-wash water outlet weir and to cater for the expansion of the filter beds in the event that the air-scour and water back-wash flow rates are increased.
  - Since the SDI across the pre-treatment is showing an abnormal increase in trend, which may, amongst other things, characterize the saturation of

the Dual Media Filters beds-media (i.e. anthracite and sand) with coagulated floc-matter and debris, it is conceivable that it is about time that the beds-media be replaced, the cost of which is currently under study.

- As the Dual Media Filters design at Addur lacks the facility for a filter-rinse mode, an essential step which normally succeeds the back-wash sequence for reconditioning the bed to improve the SDI before the filter is placed to filtrate mode, modification will be required to introduce a permanent pipe-work system.
  - An assessment and civil-work repair of all damaged expansion-joints and wall-structure at the Dual Media Filters and Clearwell, is to be considered very important in the rehabilitation of the pre-treatment system, including the replacement of valves and piping
4. With respect to the specifics of the Dual Media Filters rehabilitation, it is suggested to accomplish only the most essential modifications and civil-work repair at the Dual Media Filters combined with instituting a second filtration system for treating the feed water at the Clearwell (assuming a maximum SDI of 5.0). This concept will not only be the most sensible solution to obtain a lower feed water SDI but will be very cost elective compared to other available alternatives.
  5. As the existing GRP Cartridge Filters vessels are experiencing severe structural damage, it is recommended that all vessels be replaced with stainless steel housings, robust internal metallic parts, valves and instruments in order to, essentially, avoid present structural damage problems and eliminate the carrying-over of corrosion products from the corroded Cartridge Filters internal parts into the membrane bundles.
  6. Equally important would be the replacement of the pipe-risers of the Cartridge Filters Feed Pumps, which are severely corroded beyond any expectation.
  7. The replacement of the entire Chemical Dosing Systems (i.e. the Coagulant, Coagulant Aid and Acid) is inevitable, as the existing dosing systems are not only unreliable and unsafe to operate, but also their efficiency is constantly deteriorating.
  8. With regard to the replacement of the old membranes on the remaining RO Trains, it is best that bundle-replacement be performed, following the rehabilitation phase. It is, however, absolutely inexpedient to commission any new membranes while the existing pre-treatment problems remain unresolved.

9. Matters pertaining to the issue of fire protection and safety of personnel and equipment that await plant rehabilitation, are to be dealt with as priority one.

In connection with the Addur rehabilitation, it is worth mentioning that a consultant has been assigned to study the overall condition of the plant and a report has been generated incorporating a rehabilitation action strategy to make the plant productive, reliable and, above all, safe. The outcome of this study has revealed that the consultant's views coincided with the major issues presented above.

## CONCLUSIONS

In its entirety, as the situation come into view out from the present pre-treatment condition, it would be obvious to conclude that no matter what alterations are made through either the chemical dosing rates, or filter mode change, the attained reduction in SDI across the Dual Media Filters is almost always trivial and relatively insignificant. This will always result in an adverse consequences on the overall performance of the RO Trains.

In view of the obscure condition of the pre-treatment, the new membranes were nevertheless commissioned with a clear optimism that it would be a rewarding experience in scrutinizing the pre-treatment and its impact over the performance of new membranes.

The experience was indeed very useful, though it was evident that at the end of their first-year operation the new membranes have lost some of their prolific characteristics as they fail to restore their initial production. This was attributed mainly to the seasonal changes in sea water state as well as the shortcoming of the Pre-treatment System. However, the performance of these can be considered, under the prevailing conditions, acceptable.

As a result of the deteriorated condition of the old RO Trains, as mentioned earlier, the membranes from three Trains were replaced in October/November 1995. The remaining five Trains were taken out-of-service and considered retired by the end of September 1996; hence, a Chapter in the history of the Addur era was concluded.

**Figure 1**  
**Addur SWRO Desalination Plant - Bahrain**  
**PROCESS DIAGRAM**

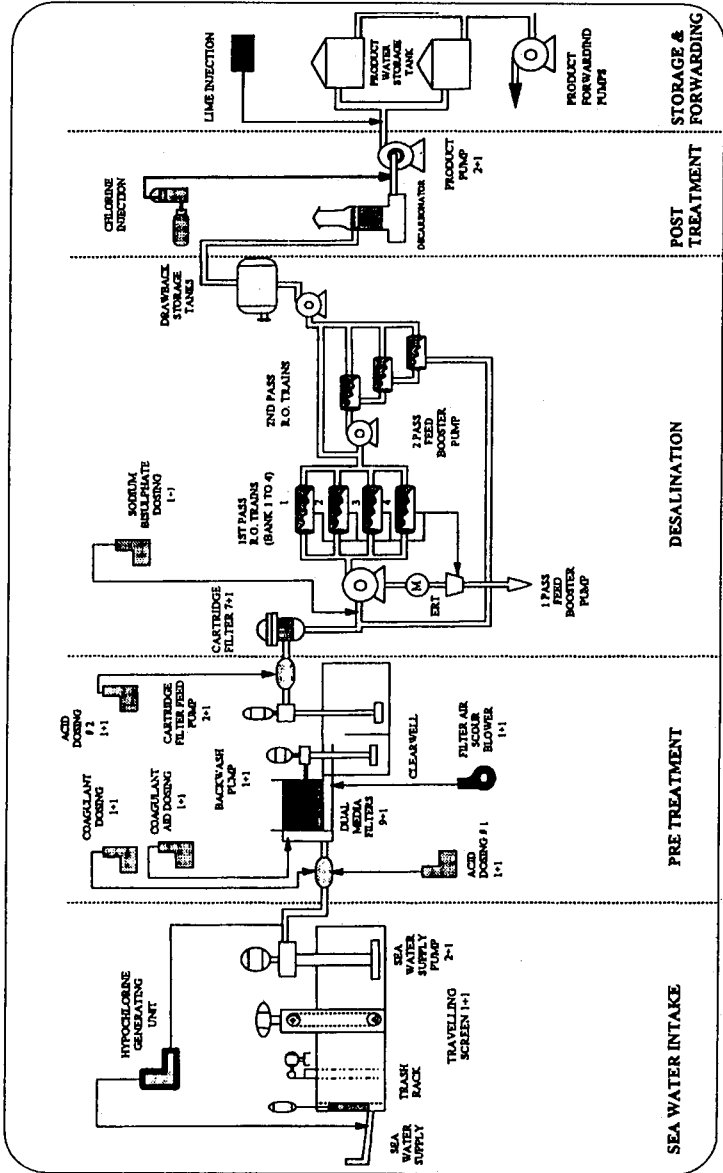


**Figure II**  
**Addur SWRO Desalination Plant - Bahrain**  
**NORMALIZED PRODUCT FLOW - OLD TRAIN E**

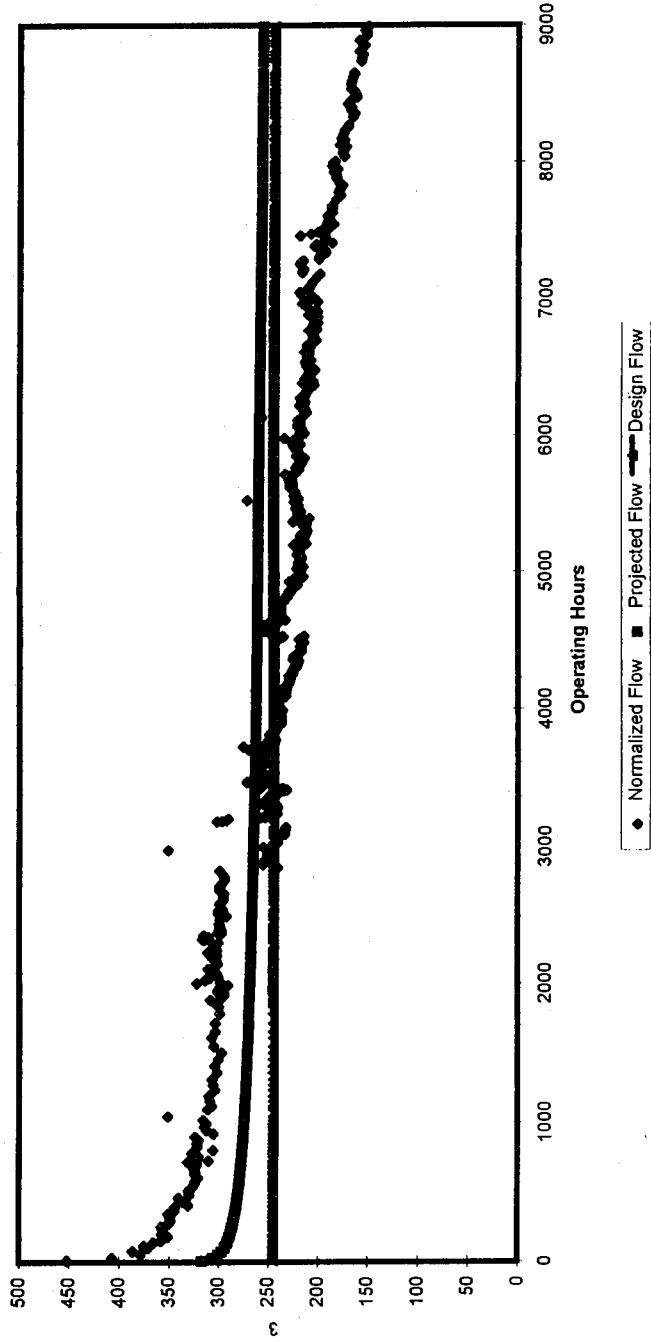




*Figure III*  
**Addur SWRO Desalination Plant - Bahrain**  
**NORMALIZED PRODUCT TDS - OLD TRAIN E**

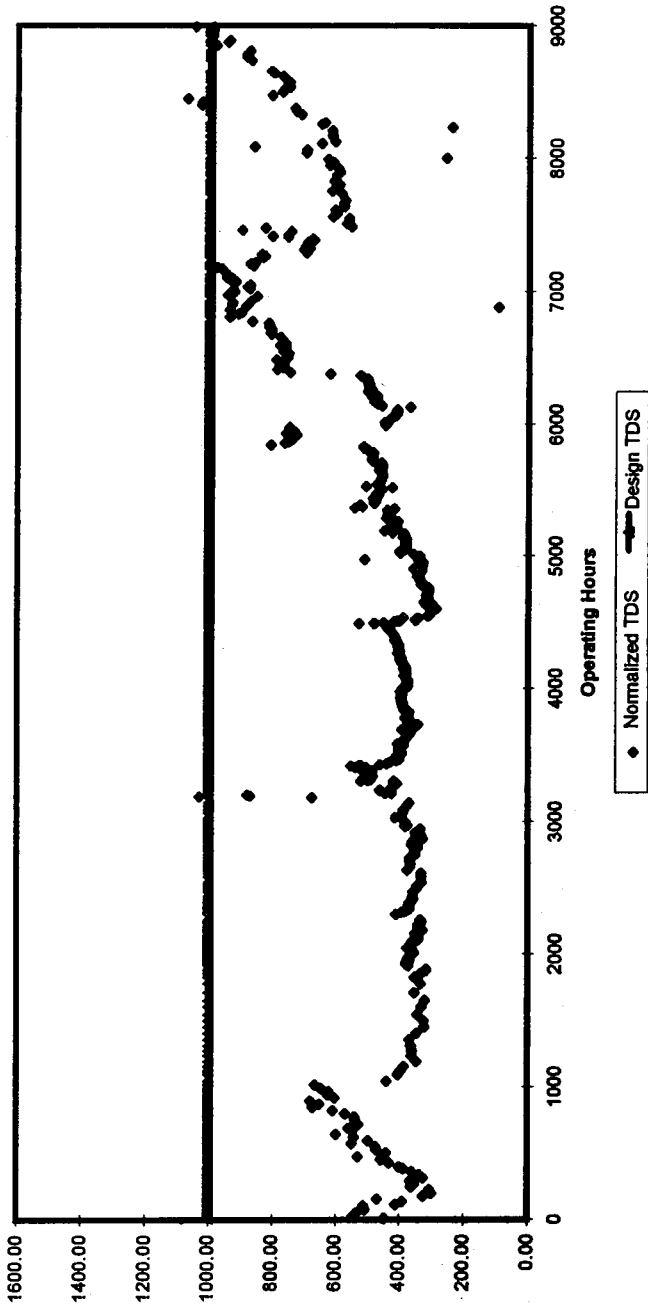
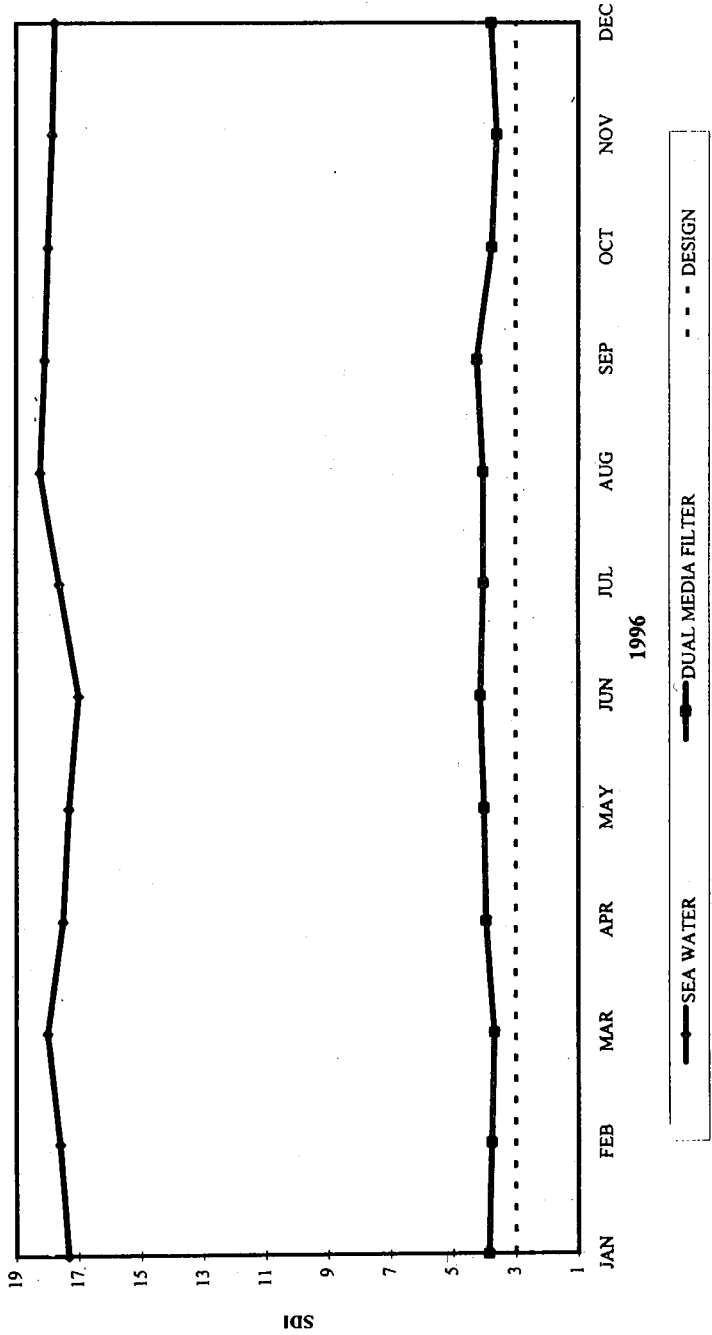
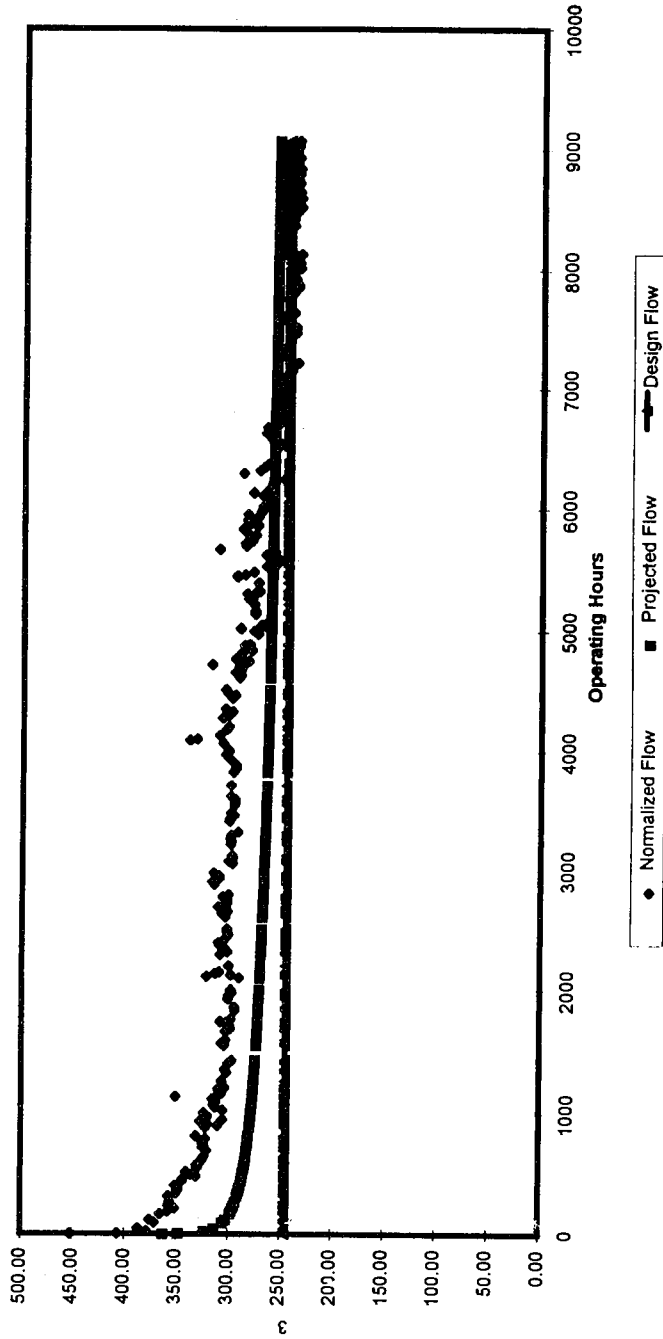


Figure IV

### Addur SWRO Desalination Plant - Bahrain PRE - TREATMENT SDI VALUES



**Figure V**  
**Addur SWRO Desalination Plant - Bahrain**  
**NORMALIZED PRODUCT FLOW - TRAIN A**



**Figure VI**  
**Addur SWRO Desalination Plant - Bahrain**  
**NORMALIZED PRODUCT TDS - TRAIN A**

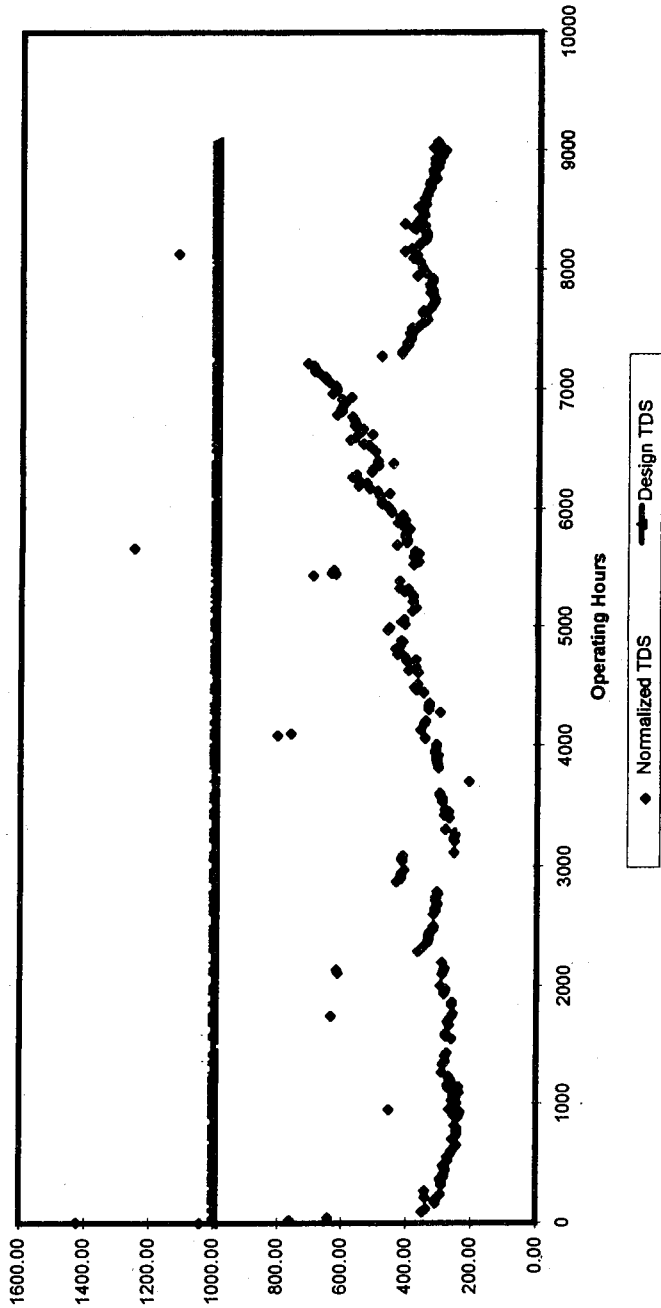
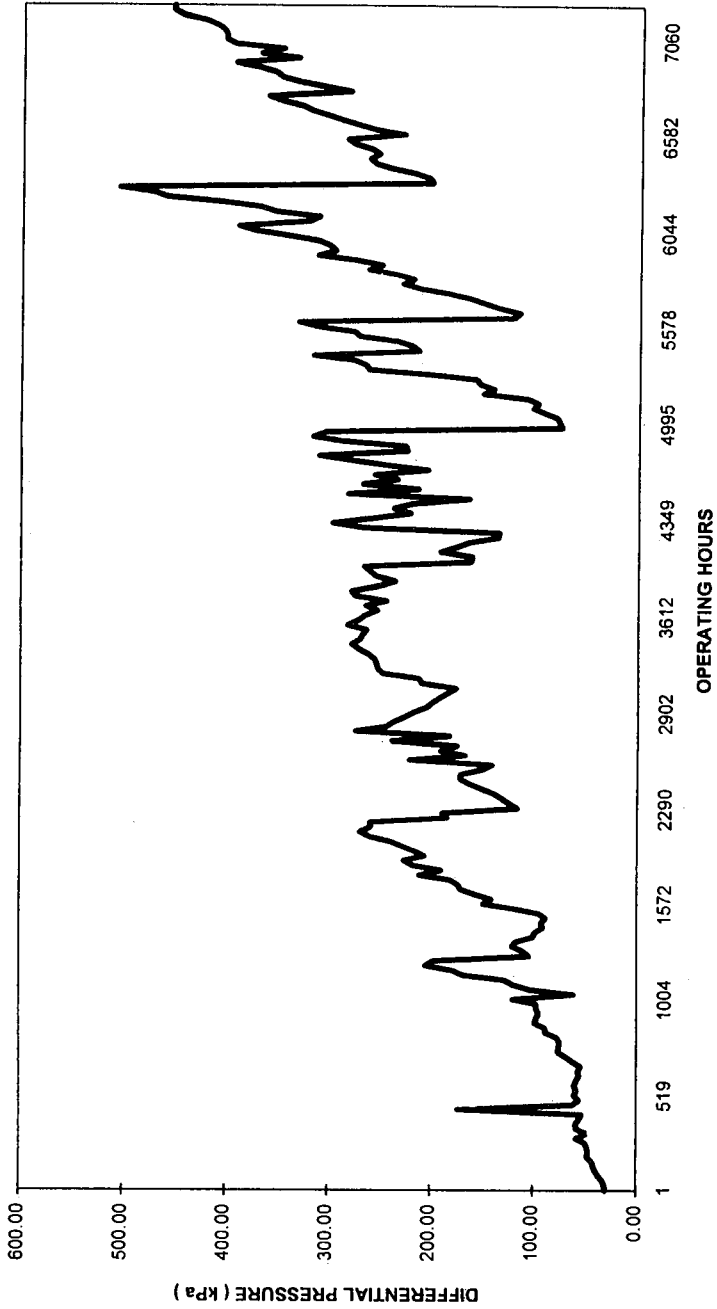


**Figure VII**  
**Addur SWRO Desalination Plant - Bahrain**  
**AVERAGE DIFFERENTIAL PRESSURE - TRAIN A**



# **Predictions of Performance of RO Desalination Plants**

*Ibrahim S. Al-Mutaz and Bander A. Al-Sultan*

# **PREDICTION OF PERFORMANCE OF RO DESALINATION PLANTS**

**Ibrahim S. Al-Mutaz and Bander A. Al-Sultan**

Chemical Engineering Dept., College of Engineering  
King Sand University, Saudi Arabia

## **ABSTRACT**

The present work will describe how complete mixing model can be used to predict the RO plant performance. Operating data for Manfouha RO plants were used to check on the validity of the obtained values from the proposed model. Good agreement were obtained. Discussions of the field data for Manfouha RO plant will be presented.

## **INTRODUCTION**

Better operation of reverse osmosis, RO, desalination plants can be obtained when maintaining good plant performance. Product quantity and quality may vary during operation due to feed variations and/or unexpected operating conditions. If simple check procedure is available, operator can easily accommodate these variations. Complete mixing model of RO module offer direct non-linear equations representing the flow and mass balances. The simultaneous solution of these equations yields accurate values for plant productivity (ratio of product flow to feed flow) and product concentration.

Detailed description of the complete mixing model will be presented in the subsequent sections. The application of this model in predicting the performance of reverse osmosis plant will be also considered.

### **Manfouha RO Plant: Process Description**

There are six water treatment plants in Riyadh area which produce potable water. They account for about 40% of Riyadh water supply. Five of these plants have reverse osmosis installation. Figure 1 shows the location of these plants[1].

Manfouha water treatment and reverse osmosis plant consists of two sections, Manfouha-I and Manfouha-II. They were scheduled to start in 1978. Manfouha-II was commissioned in November 1984 while Manfouha-I started in December 1985 [2].

The membranes used in Manfouha plant are B-9 hollow fine fiber, HFF, membrane made of aromatic polyamide with 80 micron outside diameter and a 40 micron inside diameter. These membranes are assembled in Permasep modules of model type 0840-150 and manufactured by DuPont.

The modules are arranged in three stages in taper array 4:2:1 so called "reject series". In this arrangement, the reject of the first stage modules is supplied to the second stage modules and the rejects from module of the second stage are fed into the third stage modules. The rejects of the third stage are sent to the reject disposal system. An intermediate pumping is not required since the module reject is under pressure. The number of modules of the same type mounted on the second stage is less than the number of modules on the first stage and so on. Figure 2 shows the module arrangement in a single pack.

The aim of this layout is to increase the overall conversion rate of the plant



while maintaining high sweep speeds, to improve the quality of the water produced and to minimize the precipitation and clogging risks.

The raw water pumped from deep wells is cooled to a temperature lower than 35°C. Sodium aluminate is then added to reduce the silica content. Ferric chloride as a coagulant is also added. Then water is treated in the lime-soda precipitators. Double filtration has been utilized to eliminate the suspended matter. The softened and filtered water in the water treatment plant is stored in a filtered water tank so called buffer tank. In this tank, water is treated with sulphuric acid in order to reduce the bicarbonates content and avoid CaCO<sub>3</sub> precipitation. The pH is in the range 5.9 to 6.4. Polyphosphate is also added to avoid salts precipitation, mainly CaSO<sub>4</sub> precipitation. Typical flow rates and chemical characteristics of the various streams are displayed on tables 1 and 2. The simplified plant flow diagram are given in figure 3.

Table 1: Typical Flow in Manfouha RO Plant

Flow	M <sup>3</sup> /h	
	Manf-I	Manf-II
Raw water input after cooling	1200	1800
Osmosed water output	750	1050
Clarified raw water output (blending).	250	350
Total production output	1000	1400
Reverse Osmosis reject output	120	176

Table 2: Chemical Characteristics of Manfouha RO Flows

Item	Feed	Product	Blending	Water	Reject
	mg/L CaCO <sub>3</sub>	mg/L CaCO <sub>3</sub>	ppm CaCO <sub>3</sub>	ppm	mg/L
Cations:					
ca <sup>++</sup>	190	3.8	144.66	57.87	160
mg <sup>++</sup>	200	22.5	81.66	19.85	468
Na <sup>++</sup>	763.3	127	244.10	112.29	3511
Total Cations:	1003.3	154	470.42	190.01	4139
Anions:					
HCO <sub>3</sub> <sup>-</sup>	6	7.5	58.32	71.15	73
C2 <sup>-</sup>	442.5	97	205.5	145.9	3141
SO <sub>4</sub> <sup>-</sup>	554.8	49.5	206.6	198.34	5368
Total Anions:	1003.3154	470.42	415.39	8582	
TDS, mg/l	1270	200	605.4	605.4	12721

Water is then pumped by five low-pressure centrifugal electric pump sets with a capacity of 500 m<sup>3</sup>/hr each. It is conveyed to ten 5 micron-mesh cartridge filters. Each of the lines is fitted with one differential pressure indicator to eliminate the colloidal matter. The filtered water, passed through the cartridge filter, can be directed either towards the RO pumping set or back to the softened and filtered water tank by means of an automatic valve.

The water is then pumped through five high pressure centrifugal pumps with a capacity of 424 m<sup>3</sup>/hr each. It is conveyed to the reverse osmosis modules at a pressure of about 25.6 bar on average. Membrane specifications should not be exceeded to avoid membrane deterioration. These include a pH of 5.9 to 6.4 and a maximum silica and aluminum content of 18 mg/l and 0.05 mg/l, respectively. Fouling index should be below 3 and temperature is maintained in the range 35 to 40°C. Membrane should be cleaned if the pressure drop across the module is increased 1 bar above the initial pressure drop, the salt passage is about 1.5 times the initial values or the product flow drop by 10%.

The osmosed water is directed to the mixing chamber. It has low salinity, less than 200 mg/l. During startup, the back pressure on the osmosed water side must not exceed 3.5 bar and the conversion level must always be adjusted in an increasing way. This is accomplished by opening the reject valve and then gradually closing it. In the mixing chamber, permeate water is mixed with the flocculated and filtered blending stream to achieve a final water with maximum concentration of about 500 mg/l.

The Manfouha II reverse osmosis plant is composed of four reverse osmosis lines, each line is composed of two packs. Each pack includes three stages of modules. The first stage has four racks. The second stage gets two racks. There is one rack only in the third stage. Each rack in any stage can receive up to twenty modules. Manfouha-I consists of three reverse osmosis lines of identical arrangement as found in Manfouha-II. At commissioning the number of permeators necessary to achieve the contractual flow was 546 and 768 for Manfouha I and II respectively compared with 589 and 782 foreseen at the contract time[2].

To each pack is associated one pack monitoring cabinet. Feed water flow, temperature and pH are recorded. Flow rates of product are measured for each rack. Pressure of the feedline, product line and reject stream are obtained. Conductivity is measured by portable meters for the pretreated water, product of each rack, overall product and reject streams. Figure 4 illustrates the data collection points.

## Complete Mixing Model

Flow patterns inside the reverse osmosis module have significant effect on the product and reject flow and concentration. Plug flow and complete mixing are among the suggested flow models in reverse osmosis modules. In plug flow model, no mixing in the shell side of the hollow fine fiber bundle is assumed. This creates a concentration gradient in the shell side. While in complete mixing model, there is no concentration gradient in the shell due to mixing. The shell concentration is essentially equal to the reject concentration.

Soltanieh and Gill gave the necessary assumptions for complete mixing [3]. They stated the following assumptions:

- a. The shell side concentration ( $c_1$ ) is uniform throughout the shell and is equal to the concentrate (reject) concentration ( $c_r$ ).
- b. The pressure drop in the shell is small. So the pressure in the shell is approximately equal to the feed pressure. A better approximation would be to take an average between the feed pressure and the reject pressure. The maximum error introduced by this averaging will be about 5 %, which occurs at the highest flow rate and the lowest pressure operation. For higher pressures (say above 400 psi) and medium flow rates, the error is about 1-2%.
- c. Due to the assumptions a and b above, all fibers within the bundle are exposed to the same concentration of solution and to the same pressure. Consequently, the permeate (product) concentration ( $C_3$ ) does not vary in the radial direction. However,  $C_3$  varies in the axial direction because the effective pressure drop (across the fiber) varies along the fiber. For simplicity, an average value of  $C_3$  is assumed and this average is set equal to the permeate (product) concentration,  $c_p$ .
- d. The pressure drop in the fiber bore plays an important role in the productivity of the unit. By using an appropriate expression for the permeation velocity ( $v_w$ ), for example from the solution-diffusion model, the average pressure ( $p_3$ ) then can be obtained.
- e. The permeation velocity varies along the fibers. The average permeation velocity ( $v_w$ ) is defined by substituting the average  $P_3$  and  $C_3$  in an appropriate membrane model.
- f. Concentration polarization is neglected.

g. The osmotic pressure difference is assumed to be proportional to the concentration difference across the membrane.

The complete mixing model can be presented by the following equations [4]:

$$I = (1 - \Delta)CR + \Delta C_P \quad (1)$$

$$V_w C_P = \Phi (C_R - C_P) \quad (2)$$

$$V_w = \beta [1 - \gamma (C_R - C_P)] \quad (3)$$

$$\Delta = \frac{(R_o^2 - 1) \Phi V_w}{2} \quad (4)$$

Where:

$\Delta$  is the dimensionless productivity, =  $F_p / F_f$ , with  $F_p$  as the product flow in  $m^3/hr$  and  $F_f$  is the feed flow in  $m^3/hr$ .

$C_R$  is the dimensionless reject concentration, =  $c_r / c_f$ , with  $c_r$  as the reject concentration and  $c_f$  is the feed concentration in gm solute/gm solvent.

$C_P$  is the dimensionless product concentration, =  $c_p / c_f$ , with  $c_p$  as the product concentration.

$V_w$  is the wall permeation velocity in dimensionless form. It is given by

$V_w = v_w / v_{w0}$ . Where

$$v_w = -A \left[ p_f - p_3 - \frac{\pi_f (c_1 - c_3)}{c_f} \right]$$

$$v_{sw} = -A (p_f - p_{atm})$$

In these equations,  $v_w$  is the wall permeation velocity and  $v_{w0}$  is the wall permeation velocity for pure water, cm/sec.  $A$  is the membrane permeability,  $cm^2 \text{ sec/gm}$ .  $P_1$  is the shell side pressure,  $gm/cm \text{ sec}^2$ .  $P_3$  is the fiber side pressure,  $gm/cm \text{ sec}^2$ .  $C_3$  is the shell side concentration, gm solute/gm solvent.  $C_f$  is the fiber side concentration, gm solute/gm solvent.  $p_f$  is the feed pressure,  $gm/cm \text{ sec}^2$ .  $p_{atm}$  is the atmospheric pressure,  $gm/cm \text{ sec}^2$ .  $\pi_f$  is the feed osmotic pressure,  $gm/cm \text{ sec}^2$ .

The constants  $\Phi$ ,  $\beta$ ,  $\gamma$ ,  $\Phi_1$  and  $\eta_f$  the complete mixing model equations depend on the membrane physical properties. They are given by the following equations:

$$\theta = -\frac{k}{v_{sw}}$$

$$\beta = \frac{1 - \Phi_2 \Phi_3 / 15}{1 - 0.4 \Phi_2 \Phi_3 - \Phi_2 \Phi_3 L_s (1 - \Phi_2 \Phi_3 / 15)}$$

$$\gamma = \frac{\pi_f}{(p_f - p_{atm})}$$

$$R_o = \frac{\bar{r}_o}{\bar{r}_i}$$

$$\Phi_1 = \frac{2(1 - \epsilon)v_w \bar{r}_i}{r_o v_f}$$

Values of  $\Phi$ ,  $\beta$ ,  $\gamma$ ,  $R_o$  and  $\Phi_1$  and can be found if the following data are defined for a specific membrane. The necessary data should include the following parameters which are defined as:

- $l_s$  is the seal length, cm
- $l$  is the active length of fiber, cm.
- $r_o$  is the outside fiber radius, cm.
- $r_i$  is the inside fiber radius, cm
- $v_f$  is the radial feed velocity, cm/sec.
- $r_s$  is the fiber bundle radius, cm.
- $r_i$  is the central feeder radius, cm.
- $R_o$  is dimensionless quantity, ( $r_o/r_i$  E= is porosity of fiber bundle.)

Values of  $\Phi_2$ ,  $\Phi_3$ , and  $L_s$  are given by:

$$\Phi_2 = \frac{2r_o l v_{sw}}{r_i^2 v_f}$$

$$\Phi_3 = \frac{8\mu l V_f}{r_i^2 (p_f - p_{atm})}$$

$$L_s = \frac{l_s}{l}$$

Table 3 shows values of the physical constants of 8B9 model 0840 hollow fine fiber manufactured by DuPont. A FORTRAN program was written utilizing ZSPOW IMSL library subroutine to solve the obtained nonlinear equations of the complete mixing model.

Table 3: Physical Properties of 8B-9 HHF Membrane

Items	symbol	Units	8B-9 HHF
Permeability of membrane	A	Cm <sup>2</sup> sec/gm.	7.39E-12
Diffusion constant	k	cm/sec.	1.8E-6
Porosity of fiber bundle	$\epsilon$ .		0.45
Outside fiber radius	$r_o$	cm.	-0.0042
Inside fiber radius	$r_i$	cm.	0.0021
Central Feeder radius	$cr_j$	cm.	1,905
Inside bundle radius	$fr_o$	cm.	7.62
Active length of fiber	l	cm.	76.2
Seal length	$l_s$	cm.	5.94
Specific area of fiber, $s_o = 2/r_o$	$S_o$	cm <sup>2</sup> /cm <sup>3</sup>	$(s_o = 2/r_o)$
Total mem. surface area		cm <sup>2</sup>	6131600
Total shell volume		cm <sup>3</sup>	28,000
Total number of fibers			up to 2MM
Fiber orientation constant	$K_o$		30

## Results and Discussions

Figures 5 and 6 show the plot of the RO plant productivity,  $F_p/F_i$ , versus time in months for the period 1414 to 1415 AH. The actual operating data, field data, and the model predicted values of the productivity for Manfouha-I and Manfouha-II RO plants are shown on these figures. Good agreement was obtained between the observed and the model prediction values.

The productivity values on the field data are rather constant with average values of and 0.856 for Manfouha-I and Manfouha-II RO plants, respectively. It shows little decline with time. Average values of the predicted productivity are 0.795 and 0.810 for Manfouha-I and Manfouha-II RO plants, respectively. It shows a slight increase with time opposite to the field data. This may be attributed to the constant membrane properties which were taken the proposed model.

Flux decline with time due to fouling is a serious operating problem in RO plants. There are number of important factors that contribute to fouling situation, such as membrane properties, solute properties and processing parameters [5,6]. Membrane permeability constant is one of the important membrane properties. Its values vary with time [7,8].

Operating data reflect the flux decline phenomena clearly. In the proposed model, the use of constant permeability of the membrane may be responsible

for the unexpected little rise in the flux. Membrane characteristics are rather changed during operation.

## ACKNOWLEDGMENT

The authors are grateful to the Riyadh Region Water and Sewage Authority who provided the operating data of Manfouha plant. Thanks to Mr. Hermann W. Pohland and Prof. M.A. Soliman for their great help and useful discussions. Our special thanks to Dr. A.I. Abdula'aly, the director of KACST General Directorate of Research Grant Program who made his laboratory available to us to calibrate the conductivity TDS data of the plant samples.

## REFERENCES

- 1- A. Ghulaigah and B. Ericsson. "Riyadh's Reverse Osmosis Water Treatment Plants- The Largest Demineralization Complex in the World", *Desalination* 30, 301, 1979.
- 2- L.M. Rovel and L. Daniel, 'Start-up of RO Models After a Very Long Storage Time: A Case lestory", *Desalination* 65, 373, 1983.
- 3- M. Soltaniegh and W.N. Gill, "Analysis and Design of Hollow Fiber Reverse Osmosis System", *Chem. Erg. Commun.* 18, 311, 1982.
- 4- A. E. S Al-Zahrani, "Simulation of Hollow Fine Fiber Modules in Reverse Osmosis Desalination Plants", M. S. Thesis in Chemical Engineering, King Sand University, Riyadh, 1991.
- 5- E. Mattiasson and B. Sivik, "Concentration Polarization and Fouling", *Desalination* 35, 59, 1980.
- 6- J.C. Schippers, J.H. Hanemaayer, C.A. Smolders and A. Kostense, "Predicting Flux Decline of Reverse Osmosis Membrane", *Proceedings of the International Congress on Desalination and Water Re-use, Manama, State of Bahrain, Nov. 29- Dec. 3, 1981.*
- 7- O.A. Hamed, A. Moet, T.M. Abdelrahman and A. Zaman-dri, "Performance Analysis of Sea Water Reverse Osmosis Plants", *Proceedings of IDA World Congress On Desalination and Water Sciences, Abu Dhabi, UAE, Nov. 18-24, 1995.*
- 8- M. Wilf and K. Klinko, "Performance of Commercial Seawater Membranes", *Proceedings of the IDA and VMC World Congress On Desalination and Water Treatment, Yokohama, Japan, Nov. 3-6, 1993.*

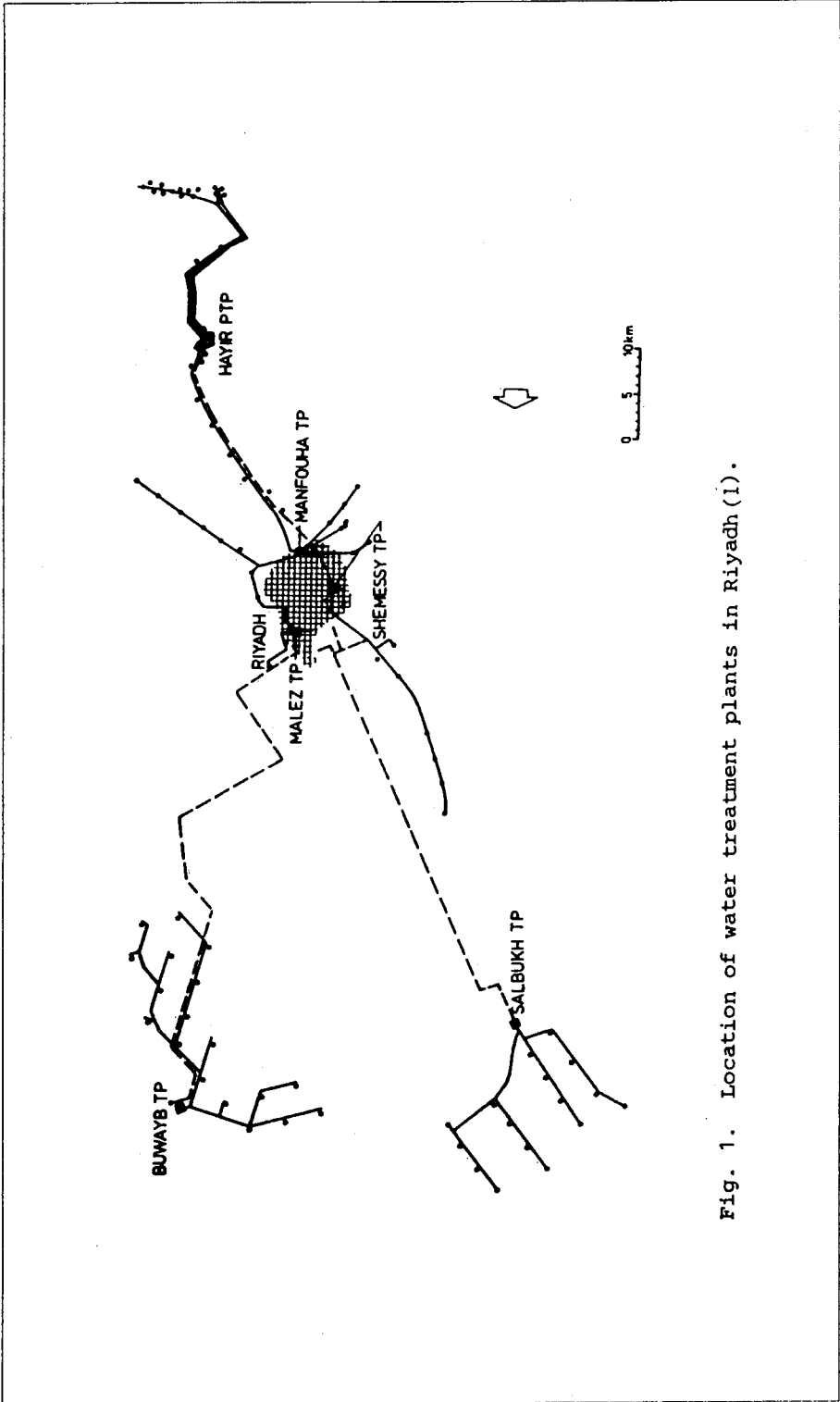


Fig. 1. Location of water treatment plants in Riyadh (1).



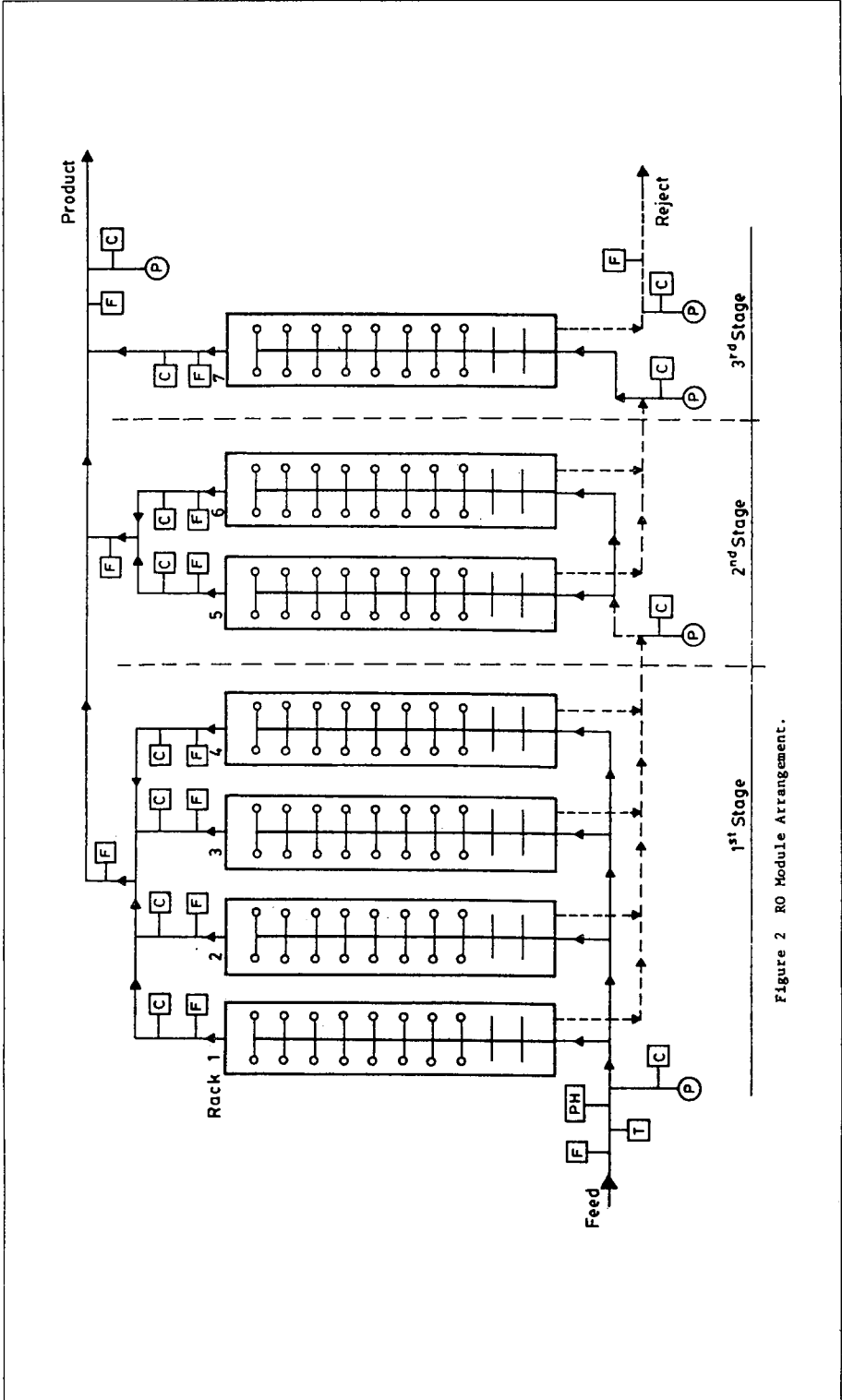


Figure 2 RO Module Arrangement.

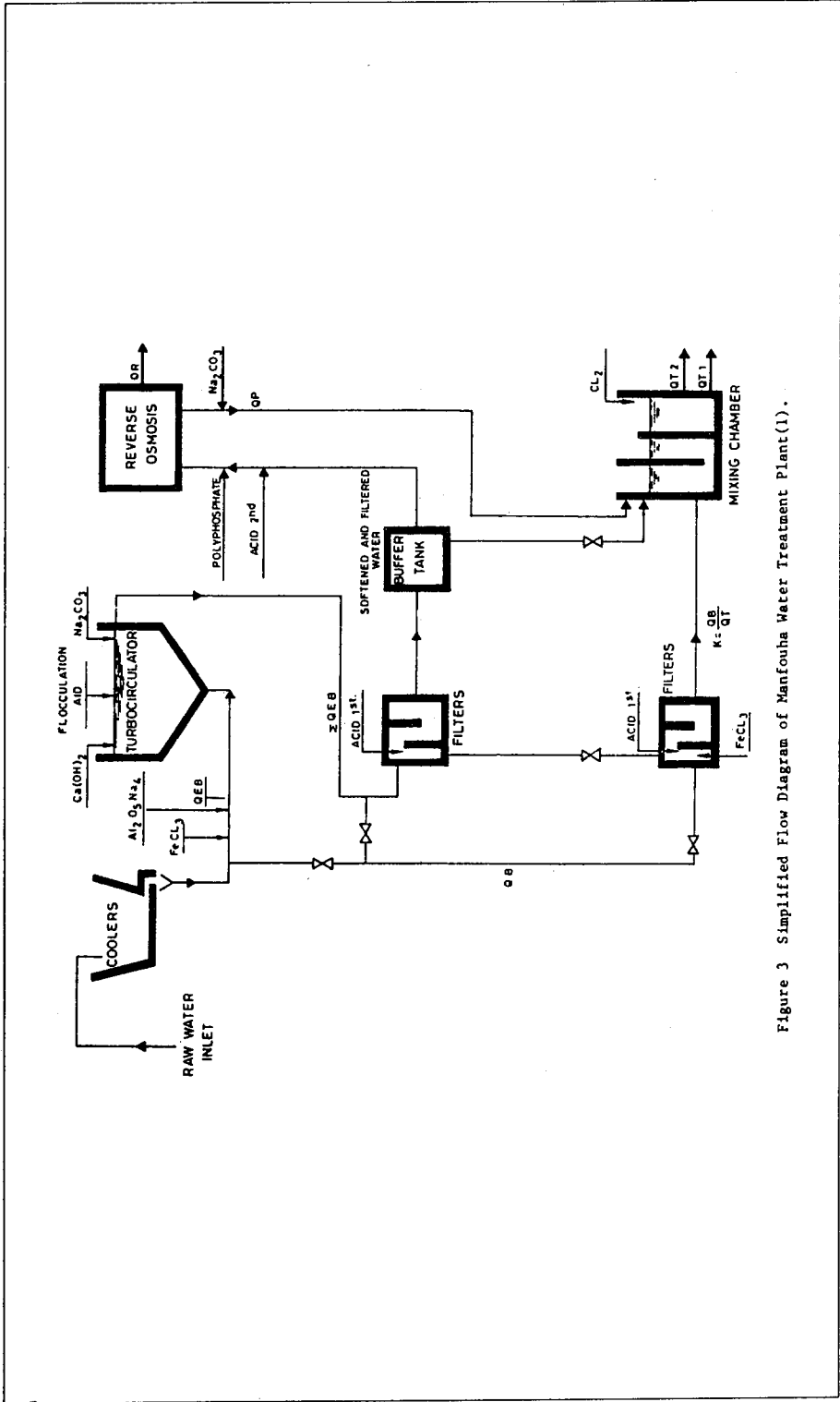


Figure 3 Simplified Flow Diagram of Manfouha Water Treatment Plant(1).

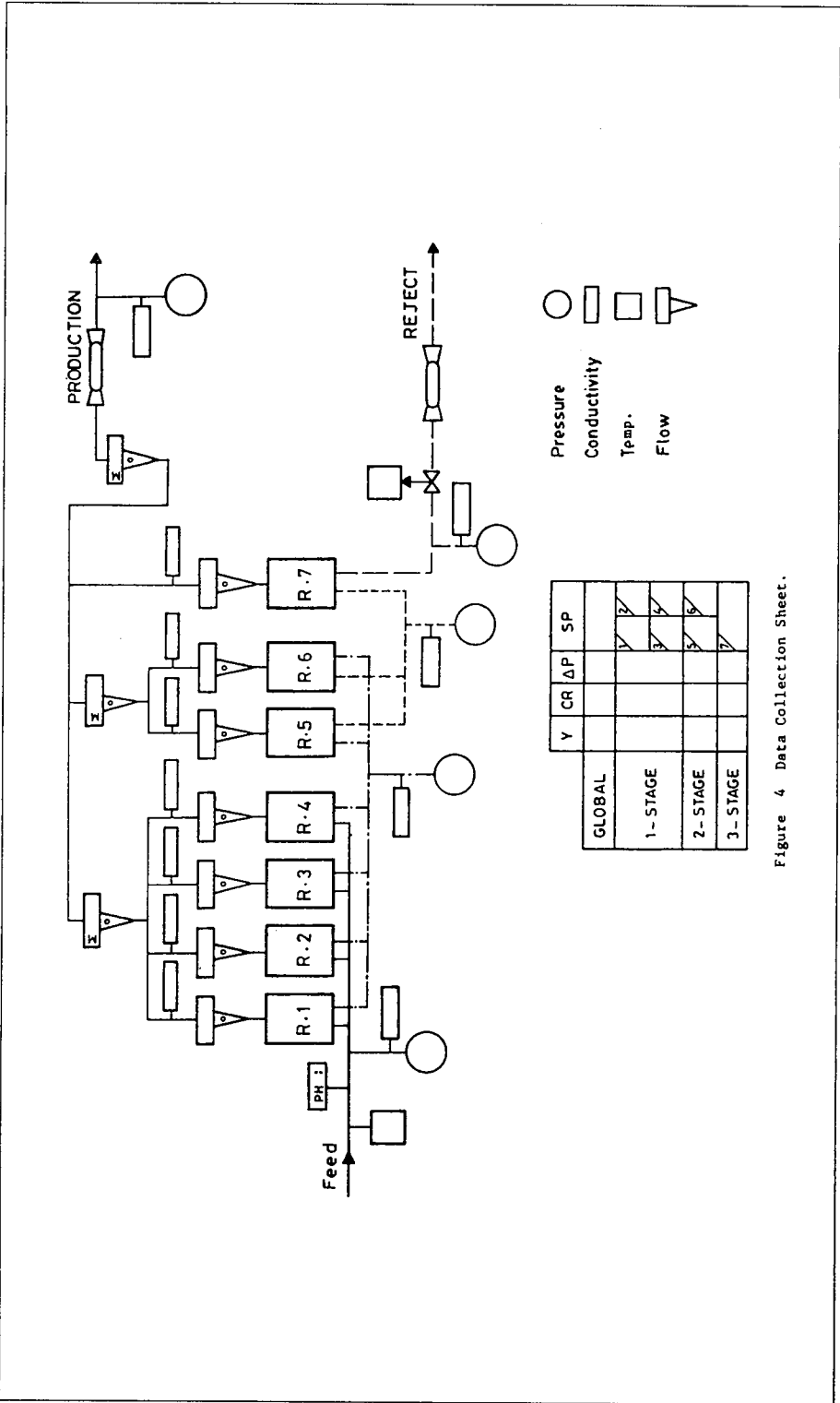


Figure 4 Data Collection Sheet.

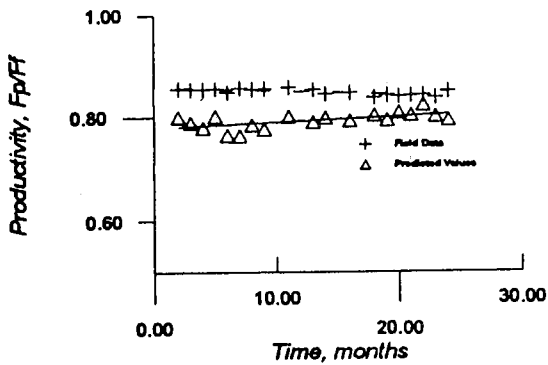


Figure 5 Plot of Productivity vs. Time for MF-I RO Plant

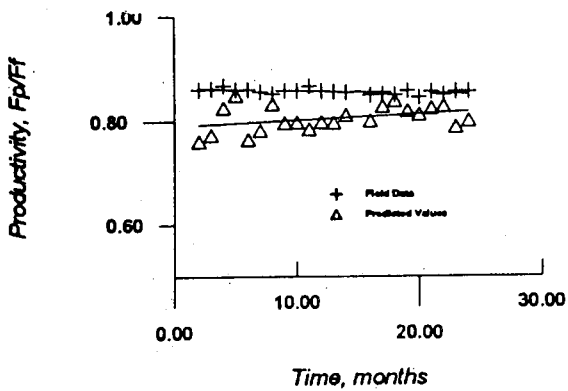


Figure 6 Plot of Productivity vs. Time for MF-II RO Plant

# **A Computer-Aided Design Program for Water Network Analysis**

*L. Khezzar, S. Harous, M. Benayoune,  
K. Al-Asmi and TMA Sajwani*

# **A COMPUTER-AIDED DESIGN PROGRAM FOR WATER NETWORK ANALYSIS**

**L Khezzar, S Harous, M Benayoune, K Al-Asmi &  
T M A Sajwani(\*)**

Sultan Qaboos University, Muscat, Sultanate of Oman.

(\*)Ministry of Electricity and Water, Muscat, Sultanate of Oman.

## **ABSTRACT**

The present paper presents a software designed and developed at Sultan Qaboos University in an effort to acquire and develop know-how in the area of simulation of steady state behaviour of a water distribution network. The program incorporates the efficient and reliable Newton loop and the linear theory methods. The usual Darcy-Weisbach and Williams pressure-flow correlations are included. In addition to pipelines the program can accommodate elements such as pumps and valves. The software provides a graphical user interface (GUI) which currently runs with MS Windows. Details of the GUI are explained as well as the general strategy adopted in the solution algorithm. Finally, sample results of simulations are presented and compared.

**Keywords:** Networks, GUI, Flows, Distribution, Pipelines

## INTRODUCTION

Steady state analysis of flow in pipe networks is of great practical significance in areas such as water or gas distribution systems, airconditioning, water firing and compressed air systems.

Efficient use of water resources in geographical areas such as the Gulf calls for well planned design of pipe networks for transmission and distribution, which requires among other things steady state analysis of flow and pressure. The size of such problems involves usually lengthy and tedious calculations, which can only be performed using a computer.

Network analysis received a great deal of attention in the sixties and seventies. Many of the algorithms proposed were later developed into commercial codes. However, there remains a need for a more robust and comprehensive system which combines the power and accuracy of calculation with flexibility and ease of use which leads to more optimal solutions. With the increase in power of computers over the past decade, and the advances made in the area of software development tools, it has now become feasible to develop much more sophisticated network design tools based on the advanced theories which were more difficult to implement few years ago because of lack of computer power and the lack of availability of good software design tools. The present paper reports on an endeavour which aims to develop a network design system which combines the most reliable solution methods with the latest software design tools to give the user the power and the flexibility to tackle any network design problem of any size or complexity. This endeavour is carried out by Sultan Qaboos University in collaboration with the Ministry of Electricity and Water in the Sultanate of Oman.

The first analysis method suited for hand calculation was developed by Cross in 1934 (Cross, 1934). His method is suitable for hand calculations and can be easily programmed on a computer, but may experience convergence problems. With the advent of digital computers, the nineteen sixties saw the development of automatic programs dedicated to the analysis of networks. Thus, McCormick and Bellamy (1968) developed a FORTRAN program which was run on the CDC 3200 and IBM 7040 and PDP-6 computers. The running time was of the order of 3 minutes! with more than half used for compilation and read-in of the program as compared to 3 to 5 days if done manually and that was considered to be an achievement!

In 1970 Epp and Fowler (1970) published a calculation method based on Newton's algorithm to obtain the solution to pipe network problems. Wood and Charles (1972), after noting that both Newton-Raphson and Hardy-Cross methods required

initial guesses for flow distributions and that very bad estimates of these values can lead to slow convergence and sometimes even impedes it, proposed the linear method. In this method the entire set of hydraulic equations are solved simultaneously for closed loop systems after linearising the energy equations. Excellent convergence was shown and the method obviates the need to estimate initial flow rates.

It is now recognised, see Wood and Funk (1992) that, if possible the Newton loop or the linear method should be employed for pipe network analysis and that convergence is assured if reasonable data is employed. The linear method is generally found to have slightly better convergence characteristics and does not require a balanced initial set of flows. The simultaneous path method requires the solution of significantly fewer equations, which will be an advantage if full matrix methods are employed. If sparse matrix techniques are used then this advantage is offset and the linear method is more efficient in terms of computing time.

Graph theory is now widely used in the mathematical description of water networks. There are basically three aspects of graph theory directly relevant to networks in general. When using Newton's loop method it is necessary to generate the independent set of fundamental loops in the graph, find the minimum spanning tree necessary to implement an initial set of flows and the shortest path algorithm used for the generation of pseudo-loops.

The present work reports on a computer-aided design program and methodology for steady state water network analysis called "Oman Water Network" or simply "OWN". The software is designed to operate under Microsoft-Windows environment and makes use of the latest tools for designing a user friendly software. Emphasis is put on the Graphical User Interface development. The present steady state version forms part of an ongoing research program aiming, in the long term, at developing a general purpose software for steady and unsteady analysis of networks. The next section describes the graph algorithms used and the underlying theoretical approach, followed by a description of the main features of the software and its graphical user interface. In Section 4 sample results from an example are presented followed by some conclusions in Section 5.



## **THEORETICAL CONSIDERATIONS**

### **The Problem and Characteristics of Networks**

The problem of simulating a distribution network in steady state is that of computing the values of node pressures and the values of flows in the individual pipes for known values of source pressures and fluid consumption in the nodes. The problem is non-linear and calls for proper treatment.

A pipe network is a collection of elements such as pipes, pumps, valves, tanks and reservoir connected together in a specific way. In general, the analysis of a network will be governed by three factors. The topology of the network which reveals its structure (are the pipes organised in series, branched with multiple tanks or looped?). The characteristics of the elements such as pipes, pumps and valves need to be carefully quantified. Finally, the mathematical methodology for the solution which highlights the solution strategy adopted. In the present version of the program, two methods of solution are incorporated, Newton and the linear theory methods.

### **Topology and Graph Theory**

A major requirement in Newton's loop method is the automatic generation of the fundamental set of loops of the network. There are many methods available in the literature to find the fundamental loops in a graph. The method by Travers (1967) generates the least number of interconnections (giving thus the most sparse Jacobi matrix) and is hence used here.

An additional requirement in the Newton loop method is an initial set of flows in the pipes. This is obtained from the known load values. If a minimum resistance tree is generated, then the load flows are assigned to the tree branches and in the remaining arcs of the graph, a zero flow is prescribed. A well known algorithm to find a minimum spanning tree is the one due to Prim (1957) and is used here.

In water networks if more than one fixed head node exist a pseudo loop needs to be added to the natural set of loops. The pseudo-loop is best chosen as a minimum path connecting two fixed grade nodes. In order to generate the pseudo loops, an algorithm to find the minimum path connecting two given nodes is needed. Several algorithms to find the shortest path between two nodes of a graph have been developed, Dijkstra's (1959) algorithm is used in this instance.

## Mathematical Model

### Pressure Drop Relationships

The flow inside the pipes is assumed steady, incompressible and fully developed so that end effects are ignored and can be laminar or turbulent.

The pressure drop in a pipe is modelled by the Darcy equation, which is also known as the Darcy-Weisbach equation:

$$\Delta P = 3.242.C_f \cdot \rho \cdot \frac{L}{D} Q^2 \quad (1)$$

Where  $C_f$  is the friction factor,  $L$  the length of the pipe,  $D$  its diameter,  $Q$  the flow rate and  $\rho$  the fluid density.

For laminar flow, the friction factor is given by the explicit relation:

$$C_f = \frac{16}{Re} \quad (2)$$

In turbulent flow several expressions have been proposed, the most famous and most used one is the Colebrook-White (1939) formula which fits the experimental values and is asymptotic to the smooth and rough pipe curves.

$$\frac{1}{\sqrt{C_f}} = -4 \cdot \log_{10} \left( \frac{k/D}{3.71} + \frac{1.26}{Re \sqrt{C_f}} \right) \quad (3)$$

Equation (3) is transcendental, and an iterative solution scheme is needed to solve it. A single iteration will produce a result within 1% if the initial estimate is calculated from equation (4).

Note that equation (3) is not explicit in  $C_f$ , but explicit relations approximating those obtained from the Colebrook-White equation have been formulated at a reasonable loss of accuracy, such as:

Swamee and Jain (1976):

$$C_f = 0.0625 \left[ \log_{10} \left( \frac{k/D}{3.71} + \frac{5.74}{Re^{0.9}} \right) \right]^{-2} \quad (4)$$

Yet another expression which allows explicit calculation pressure drop is the Hazen-Williams equation:

where  $C_{HW}$  is the Hazen-Williams coefficient which is dependent on roughness only.

In general the pipe flow equations described above can be expressed in a condensed form. For any pipe  $k$ , the pipe flow equation from node  $i$  to node  $j$  can be written as:

$$F(Q_k) K_k(Q^a)_k \quad (6)$$

where:  $F(Q_k)$  : the flow relation for the pipe  $k$   
 $K_k$  : the pipe constant for pipe  $k$   
 $(Q)_k$  : the flow rate in pipe  $k$   
 $a$  : the exponent = 2 for the Colebrook-White formula  
= 1.852 for the Hazen-Williams formula

The methodology of loop formulation is based upon Kirchhoff's second law which states that the pressure drop around a circuit is zero. Applying this law to the set of fundamental circuits in the network, we obtain the loop equations which can be written in matrix form as:

$$[B] [\Delta P] = 0 \quad (7)$$

where:  $[\Delta P]$  is the pressure drop vector in the branches, of dimension  $m$ .  
 $[B]$  is the branch-loop incidence matrix, which can be constructed from the result of the loop finding algorithm.

Using Equation (6) in (7) results in:

$$[B] [F(Q)] = 0 \quad (8)$$

In the loop formulation the non-linear system of equations (8) is solved for the loop flows and consequently for the pipe flows.

### Newton-Loop and Linear Theory Methods

The Newton multi-dimensional method can be summarised as follows, see Epp & Fowler (1972):

1. Determine an initial set of flow rates which satisfy continuity at all junctions.
2. Compute a flow adjustment for each circuit which tends to satisfy the energy equations by forcing continuity
3. Using the improved values of flow rates, repeat step 2 until convergence is achieved

In the solution, an initial approximate set of balanced branch flows at each node is made. These branch flows are approximations to their true values and hence a loop correction is added to the branch flows to yield better approximations. Convergence may be assumed if the sum of the pressure-drops around the loops attains a specified tolerance.

The essence of the Linear Theory Method is to linearise the pressure drop equation, thus

$$\Delta P_k = K_k Q_k \quad (9)$$

where :

$$K_k = K_k Q_k^{a-1} \quad (10)$$

Putting this form into the loop equations (8), a linear set of equations is obtained which can be solved by the usual means such as LU decomposition. Note however that  $K_k$  depends on  $Q_k$  and hence will be estimated from flow rates. Wood and Charles (1972) suggests that the initial flow rates need not be estimated and that  $K_k$  may be made directly equal to  $K_k$ . The linear method is known to converge more rapidly than the Newton method, see Wood and Funk (1992).

## SOFTWARE AND GRAPHICAL USER INTERFACE DESCRIPTION

The theoretical concepts described above are incorporated in the OWN package. The program consists of an engine driver to execute the calculations and a Graphical User Interface (GUI). The engine calls several routines to find the fundamental set of loops to form the branched-loop incidence matrix, determine the minimum resistance tree to fix the initial flows and eventually determine the minimum path between two fixed grade nodes if they exist. This information is passed to the flow calculation routine to compute the set of flows and pressure drops.

OWN exploits the latest software tools available for designing a user-friendly interface. The graphical user interface (GUI) is based on the Microsoft Windows tools which comprise, among many other control objects, windows with toolbars, icons, pull-down menus, push button, etc. For better user acceptability of the system, the GUI design is integrated with the body of calculation software, so that the user can see instantaneously the results of any action.

The interface aims to give the package flexibility by accommodating several options, invisible technology by stressing on functionality of the system and above all robustness. The package is designed to be easy to learn for the novice and be sufficiently efficient to use for the expert, see Snell (1995).

The first version of the package has been developed to run under Microsoft Windows on a personal computer (PC). The package can be used on any PC capable of running MS Windows. Typically this would be a 486 or a Pentium-based PC. The interface is developed using MS Visual Basic Version 4.0 Professional Edition, see Microsoft (1995).

### **The Main Window**

The OWN interface is made up of several forms (or windows). The Main window, which comes up when the user launches the system, contains the overall commands in the form of pull-down menus and a toolbar. The Main window gives the user access to the global commands of the system such as starting a new network, opening an existing one, saving and closing networks.

The Main window is a multiple document interface (MDI) type window with all the other windows as its children. This feature allows the system to manipulate several networks at the same time which means that the user can have several versions of the same network open, or two or more networks open at the same time.

The Main window provides seven menus to cover all the various tasks supported by the system. These include:

- \* File: to open, save and close a network
- \* Edit: for the various editing tasks such as cut, copy and paste.
- \* View: for the various viewing options, such as hiding and viewing the toolbar, or hiding the results.
- \* Calculations: for the various calculations options.
- \* Results: for displaying and printing the results.
- \* Windows: to view or organise the windows currently open.
- \* Help: for the various help options

## **The Draw window**

The next most important window is the Draw window, which is a child of the Main window. As its name indicate, this window is used to draw the network. Fig. 1 shows the Draw window open within the Main window.

The Draw window, which is opened for every network, allows the user to draw the topology of the network by simply clicking on the item to be drawn, then clicking on the draw area where it is to be placed. A serial number is automatically given to the item drawn. A pipe can be drawn between any two items simply by clicking on the pipe button then on the start and end nodes, Pipes are also given an automatic serial number as shown in Fig. 1.

An edit button (between the Pipe and the Print buttons on the toolbar) is available for the user to toggle between the draw mode and data entry mode. In draw mode the user can add items or pipes to the network. In data entry mode the user can double click on an item to bring up the data entry form to enter or modify its data. The user can also double click on the pipe number to bring up the data entry form for the pipe.

The Draw form is also used to display some results, such as flow rates and pressures, next to the nodes and pipes once the calculations have been done.

### **Data entry forms for the nodes**

The package supports only one general data entry form for the nodes. However, during data entry the system shows only the relevant data items for the type of item being considered, all the other data items are hidden. The data items shown are re-organised to make the form look better. Fig. 2 shows the data entry form for the node as an example.

### **Data entry form for the pipes**

The data entry form for the pipes is shown in Fig. 3. The data items included in it are self explanatory.

### **Calculations and control data**

When the user has entered all the relevant data he can run the package by pressing the calculation button or choosing calculate from the pull-down menu. In either case the package brings up a control data entry form through which the user can enter the information necessary to calculate all the flow rates, pressures etc. in the network.

## **Viewing results**

Once the calculations are performed, the results can be viewed in three formats: on the Draw area, either as bars or numbers (as shown in Fig. 1), on a separate graph or on a table form. A toggle button permits to switch between looking at either flow rates or pressures.

## **RESULTS**

The above calculation method was applied to several networks and for the sake of presentation purposes only the results relevant to the network shown in Fig. 1 are presented. This network was considered by Charles and Wood (1972). The pipeline data is given in Table 1 and the node loads are given in Table 2. The calculations were performed using the Newton's loop algorithm and the Hazen Williams relation given by equation (6) was used to model the pressure drop.

The volumetric flow rate results are presented in the last column of Table 1 and in Fig. I in l/s (negative flow values simply indicate the flow is in the opposite direction to the one assumed). Convergence was assumed when the sum of the loop pressure drops attained 0.002 and this was achieved after 5 iterations.

It can be seen that the results are in very good agreement with those obtained by Wood and Charles (1972). Although Wood & Charles (1972) achieved convergence with the Loop Method after 24 iterations no indication was given on the initial flow rate estimates and the criterion for convergence. The discrepancy in the number of iterations can be explained in terms of different initial flow distributions.

## **CONCLUSION**

A user friendly and efficient computer program for the analysis of steady state water distribution systems was developed using the latest software building tools. The program combines the power and accuracy of calculation with flexibility and ease of use. Non-expert users can use the system without much difficulty. After obtaining an initial solution, the user can run various scenarios of the type "what-if" by simply varying the different parameters of the network. Because the system runs in an event-driven mode it responds instantaneously to any changes in the network. This feature allows the user to obtain much more optimal networks. The system is being enhanced on

several fronts. The first extension includes novel algorithms not tried so far in any package. The second extension includes dynamic and extended time simulation capabilities.

Table 1 Data and Results

Pipe	Diameter (m)	Length (m)	Roughness CHW	Flow rates (l/s)
1	0.305	457.2	130	60.66
2	0.203	304.8	130	44.15
3	0.203	365.8	120	17.15
4	0.203	609.6	120	-9.83
5	0.203	853.4	120	-8.84
6	0.203	335.3	120	12.11
7	0.203	304.8	120	13.54
8	0.203	762.0	120	8.17
9	0.203	243.8	100	43.44
10	0.152	396.2	100	-2.59
11	0.152	304.8	100	8.55
12	0.254	335.3	130	-7.17
13	0.254	304.8	130	-16.03
14	0.152	548.6	120	5.37
15	0.152	335.3	120	16.51
16	0.152	548.6	120	-1.44
17	0.254	365.9	130	27.00
18	0.152	548.6	120	4.29
19	0.152	396.2	120	-4.56

Table 2: Node loads

Node No.	Demand (m <sup>3</sup> /s)
1	0.1041
4	-0.03155
5	0.0347
6	-0.02524
9	-0.03785
11	-0.04416



## REFERENCES

- Colebrook, C. F., "Turbulent Flow in Pipes With Particular Reference to the Transition Region Between the Smooth and Rough Pipes Laws", *J Inst. C. E.*, (1938-39), 133.
- Cross, H., "Analysis of flow In Networks of Conduits or Conductors," Bulletin No. 286, Univ. of Illinois Engr. Experiment Station, 1934.
- Dijkstra, E. W., "A note on Two problems in Connexion with Graphs", *Numerische Math.*, vol. 1, 269-271, 1959.
- Epp, R. and Fowler, A.G., "Efficient Code for Steady State Flows in Networks", *J. of the Hydraulics Division*, vol. 96 HY 1, January 1970.
- McCormick, M. & Bellamy, C. J., "A computer Program for the Analysis of networks of pipes and pumps", *The journal of the institution of engineers, Australia*, March 1968.
- Microsoft Corporation, "MS Visual Basic: Programming System for Windows Version 4.0, Professional Edition", 1995.
- Nielsen, H. B., "Methods for Analysing Pipe Networks", *Journal of Hydraulic Engineering*, vol. I 1 5, 2, p139, 1989.
- Paton, K., "An Algorithm for Finding a Fundamental Set of Cycles of a Graph", *Communications of the ACM*, vol. 12, no 9 September, 1969.
- Prim, R. C., "Shortest Connection Networks and Some Generalizations" *Bay I Sys. Tech. J.*, vol. 3 6, 1389-1401, 1957.
- Snell, M., "Visual Development tools", *Computer*, Vol. 28, 3 pp. 8-10, March 1995.
- Swamee, P. K., and A. K. Jain., "Explicit Equations for Pipe-Flow Problems", *Journal of the Hydraulics Division of the ASCE*, 102, no. FIYS, 1976.
- Travers, K., "The Mesh Method in Gas Network Analysis", *Gas Journal*, November 1, 1967.
- Wood, D. & Charles, C. A.O., "Hydraulic Network Analysis Using Linear Theory", *Journal of the Hydraulics Division*, vol. 98, July 1972.

Wood, D. and Funk, J.E., "*Hydraulic Analysis of Water Distribution Systems*", in "*Water Supply Systems, State of The Art and Future Trends*", Ed. by Carbrera, E. and Martinez, F., Computational Mechanics Publications, Southampton, Boston, 1992.

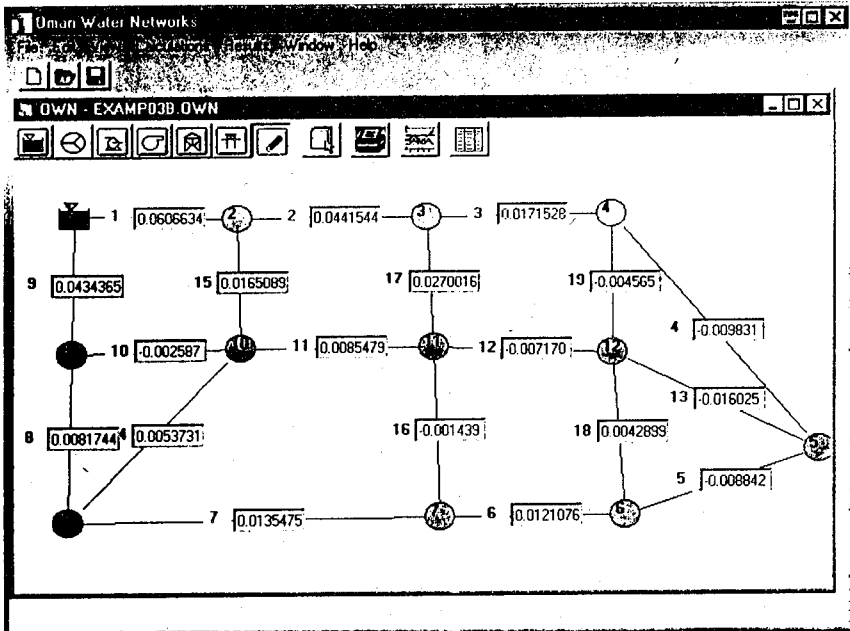


Figure 1: The Draw window open within the main window.

Structural data			
Node ID	R05	Node type	node
Node Seq. No.	2	Zone Identifier	Z2
Grid Coordinate X (m)	2610	Grid Coordinate Y (m)	1185
Variable data			
Elevation (m)	275	Demand (l/s)	450
Minimum head loss (m)	0.5		

Figure 2: The data entry form customised for the reservoir.

**Pipe Data**

**Structural data**

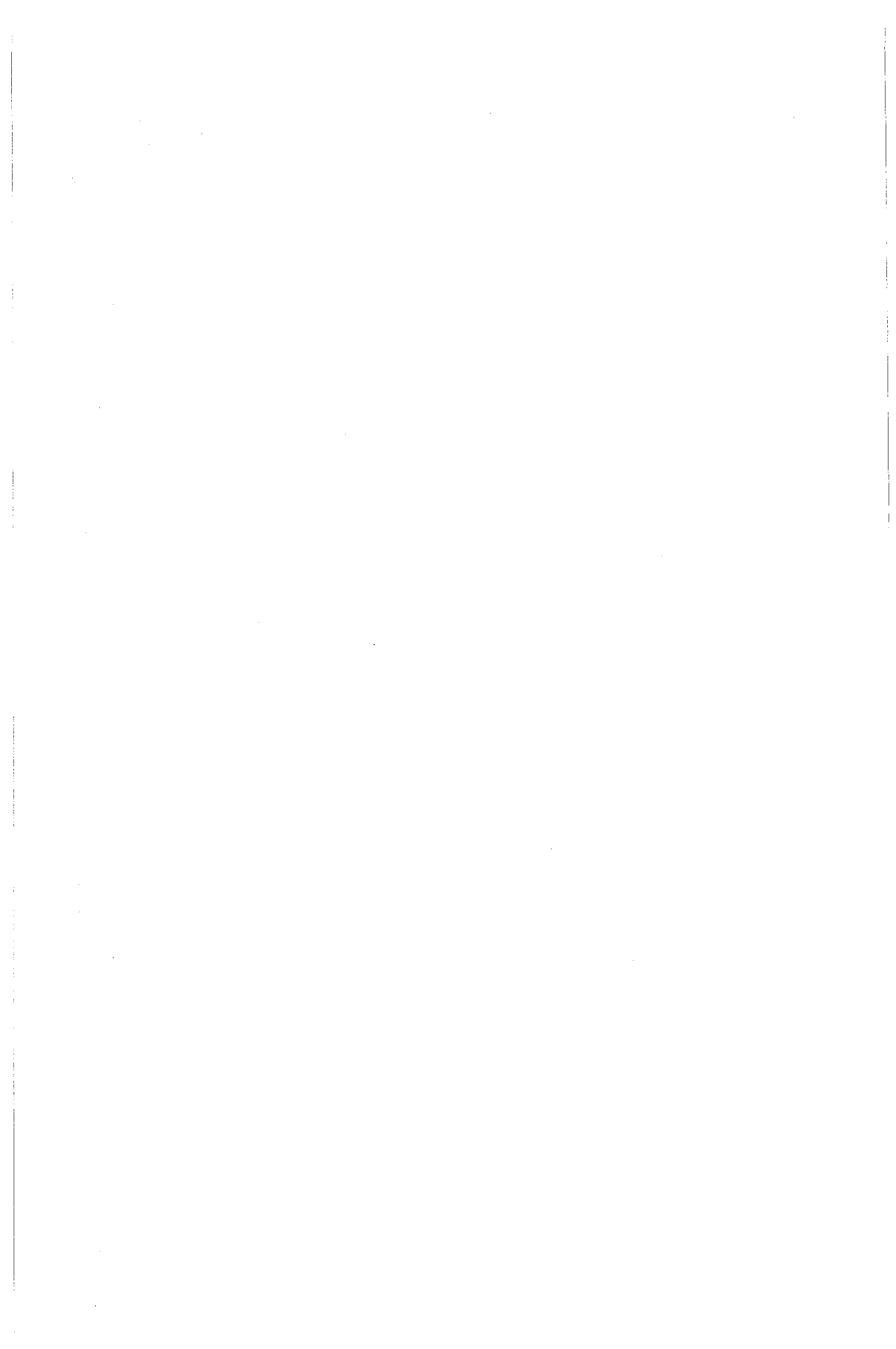
Pipe ID:  Start node:  End node:

**Variable data**

Length (m):  Roughness size (m):

Internal diameter (m):  Local Pressure loss (Pa):

Figure 3: Data entry form for pipes



# **Conceptual Cost Estimate System for Domestic Water Supply Projects**

*Al-Asfoor, Mashhoor Dawood*

# **CONCEPTUAL COST ESTIMATING SYSTEM FOR DOMESTIC WATER SUPPLY PROJECTS**

**Al-Asfoor, Mashhoor Dawood**  
Mashhoor Engineering Consultancy  
Muscat, Oman

## **ABSTRACT**

Large funds are expended on domestic water supply projects; however, lack of appropriate conceptual cost estimating techniques causes difficulties such as project delays and cost overruns. This presents a structured and systematic procedure for the implementation of a Conceptual Cost Estimating System (CCES) for Domestic Water Supply Projects. CCES has been designed to produce cost estimates at the conceptual stage when only a little information is available about the project.

The research began with the identification of the factors influencing the costs of pipeline, reservoir, and pumping station projects, yet, this paper is limited to the pipeline cost only. Next, historical cost data of commissioned projects were gathered from tender documents and subsequent regression analysis was carried out. The regression analysis was computer-based which facilitated a "what-if" analysis during the model creation course and helped examine the adequacy of the cost factors. Moreover, the adequacies of the cost models were checked and found to comply with the standards of the American Society of Cost Engineers.

This study demonstrated that a well thought-out integration among the science of cost estimation, statistical analysis, and computer technology enhances the practices of cost estimating. Although the research focused on the Sultanate of Oman as a case study, the methodology set forth is relevant to the construction and water industries in general, particularly in the Arabian Gulf countries.

## **INTRODUCTION**

### **Conceptual Cost Estimating**

Conceptual Cost Estimating is a vital tool for construction developers. It is necessary for planning, budgeting, funding, and construction management. The purpose of conceptual estimates is to produce as accurate an estimate as possible with very limited information. No detailed drawings or specifications are required for conceptual estimates; instead, a general conception of the project's characteristics such as size and location. In fact, conceptual cost estimating system facilitates early decision-making and judgment within the project development cycle.

### **Description of the Problem and Research Scope**

Billions of dollars are expended in the Arabian Gulf countries on water related projects. However, lack of appropriate conceptual cost estimating techniques causes project delays and cost overruns. This research focused on the problem in the Sultanate of Oman as a case study; however, the profile of this study should be relevant to the neighboring countries of the Gulf.

The researcher developed a Conceptual Cost Estimating System (CCES) based on statistical analysis of historical cost data. The CCES was constructed to estimate the costs of urban water supply projects within an acceptable range of accuracy. Moreover, it was designed to produce estimates when only little information is available about the project during the conceptual phase.

This research focused on Domestic Water Supply Projects in the Sultanate of Oman as a case study and addressed the MEW cost estimating function. The research work covered the estimating models of the Pipelines, Reservoirs, and Pumping Stations. However, this paper is limited to the pipeline cost estimate model.

## **REVIEW OF RELATED LITERATURE**

### **Construction Cost Estimating**

Until the nineteenth century, rough cost forecasting satisfied the society's needs fairly adequately. However, upon the significant economical advancement caused by the Industrial Revolution, construction industry began to appreciate



the importance of cost estimating. This appreciation resulted when those people realized the importance of optimizing the use of the scarce resources [Ferry and Brandon, 1991].

Construction cost estimates are distinct in nature from others in the sense that each construction project is unique in its characteristics; thus, an inherent uncertainty exists in any cost estimate whatsoever [Akeel, 1989]. An estimate is, by definition, a forecast of future events, and because of the uncertainties of the future, construction estimating will never be totally scientific. Instead, the preparation of accurate construction estimate is partly a science and partly an art [Adrian, 1982].

### **Types of Construction Cost Estimates**

Construction cost is the cost incurred by the construction activities only. The American Association of Cost Engineers (AACE) classified the various capital cost estimates into three categories: order of magnitude estimate, preliminary estimate, and definitive estimate. Order of magnitude estimate is used by owners after the mental definition of the project has been clarified. All it requires is the general conception of the project in terms of size, materials, construction method, and quality [Collier 1984]. According to the AACE, the following is applicable to this type of estimate:

Accuracy range	* (-30% to +30%)
Required information	* Capacity
	* Location
	* Utility requirements
	* Service requirements
	* Building Requirements
	* Raw materials and storage requirements
	* Finished product and its storage requirements

The proposed CCES falls in this category.

Preliminary estimate is executed based on the availability of information as the project evolves during the design stage. On the other hand, definitive estimate, also called 'bid estimate', is used by the contractors to produce a proper bid estimate based on complete project documents [Collier, 1984].

### **Cost Estimating Relationship (CER)**

CER is a relationship represented in the form of charts or formulas relating costs for complete projects "units" to single or multiple cost parameters,

based on collected data of previous projects. Relevant CERS are adjusted to a specific base date and place for consistency to account for inflation and possible impacts of various locations. This research work adopted the multiple CER because it accounts for multiple parameters which have influence on the cost of the project. Multiple CER is a technique for estimating costs from the physical and/or performance characteristics of the subject under consideration, regardless of the magnitude of the aggregated systems involved. Moreover, this method was practically introduced to the construction industry by mid 1970's and was characterized by the intensive use of regression analysis. [Manzancra, 1991]. It involves collecting and organizing historical cost data about the cost driving parameters and relating this cost data, through mathematical techniques, to the cost of the project being estimated. The general form of the compound CER model is as follows:

$$\text{Cost} = C + (B1*V1) + (B2*V2) + (B3*V3)..... + (Bn*Vn)$$

where,

C: Constant which represents a cost measure of the project.

Vn: Variable number 'n' which is influencing the cost of such as the material quality of a pipeline,

Bn: Associated constant of variable 'n' [Raftery, 1987].

### Statistical Background

The cost function used in this paper was derived empirically using statistical methods. In normal cases, the actual data shows a certain degree of scatter (lack of fitness) about the fitted cost function. It is particularly important that obvious uncertainties are expressed in an objective and unambiguous manner, and this can only be done in statistical language. It is suggested to refer to any statistics text book to understand the meanings of the statistical terms and nomenclature used in this manuscript.

### Modeling

Cost Estimating Models have different levels; for instance, suppose a model is required to estimate the capital cost of a pipeline project. At the simplest level, the model might simply relate the total cost to the population to be served. Such a "global" model could only be expected to give a rough estimate, satisfying the need for broad planning purposes. Alternatively, the model might consist of a collection of sub-models or "building bricks", each predicting the cost of separate processes or components within the works. Therefore, the model would be of interest to planners at design or contracting level,

whereas its greater detail might be irrelevant to the regional or national planner. The ultimate objective of this thesis is to develop cost models to be used as order of magnitude estimates at the conceptual stage of the project where hardly any detailed information is available.

### **Identification of Cost Determinant Factors**

The cost of any construction project is a function of several factors (cost drivers) as previously discussed in the literature review. In this step, tender documents for the completed water projects under consideration were analyzed and reviewed with the objective of determining those influencing factors. In addition, a close consultation was carried out with the Project Engineering Department of the MEW and the main MEW's consultants such as Mott McDonald International Ltd. Also, the literature of international studies was reviewed and taken into consideration when identifying those factors.

### **Common Factors**

There are some cost determinant factors which are common to all types of construction projects and are often related to the cost incurred by the general preparation and preliminaries (mobilization & demobilization) and site subsoil condition rather than the specific characteristics of the project. The following factors were found to be common and thought to have certain impacts upon the cost of any project:

#### **A) LOCATION OF THE PROJECT:**

When the project is located in remote areas, its cost tends to increase. This factor was measured by KILOMETERS representing the distance between the contractor's base and the project's location.

#### **B) DURATION OF THE PROJECT:**

When a project involves a longer duration, it implies that the project is large and/or less urgent causing the unit price to become lower. The magnitude of this factor is expressed in MONTHS.

#### **C) EXPECTED LIFE OF THE PROJECT:**

Long-lasting projects cost more than those of shorter life. This factor was excluded from the study because the data sample experiences no variation.

#### **D) MARKET ENVIRONMENT:**

During flourishing periods in the economy, demand for services, including construction, increases; this demand drops when the economy undergoes a

recession. This factor was excluded from the study because no data was readily available to measure its magnitude.

**E) GRADE OF CONTRACTOR:**

Generally, higher grade contractors provide better construction services and, consequently, cost more than those with lower grades who maintain inferior construction standards. In our case this factor was excluded because all projects constructed for the MEW are limited to the better grade contractors.

**F) GENERAL VICINITY OF SITE:**

The vicinity of the site affects the project's cost associated with accessibility and site restriction. This factor was measured with the WRC findings.

**G) GROUND CONDITION:**

Excavation of harder soils cost more than softer ones. WRC findings were adopted to measure this factor.

**H) SPECIAL FEATURES:**

Projects with special features such as remote control devices cost more than those with conventional arrangements. This was excluded because the sample experiences no variation.

**PIPELINE COST FACTORS**

The following cost determinant factors are applicable to pipeline projects only:

**A) DIAMETER:**

Cost of the pipeline is directly proportional to its diameter. This factor was measured by (mm).

**B) MATERIAL OF PIPES:**

Different pipe materials have different costs.

**C) TRENCHLESS CROSSING:**

It is required by Omani municipalities to use a pipe jacking technique (thrust boring) when laying the pipeline across the road. Trenchless crossing costs more than average pipe laying as it requires special equipment, special supervision, and consumes more time.

**D) WADI PROTECTION:**

The wadi (valley) protection is achieved by embedding the pipeline section

into a concrete rectangular casing across the width of the Wadi. Obviously, this arrangement costs more than the average pipe laying, which needs to be accounted for.

**E) TERRAIN:**

Laying a pipeline in a hilly area increases the complexity of the scheme, hence, increases the cost of the project.

**F) DIAMETER RANGE:**

Diversity of diameters indicates an increase in complexity of the scheme; hence, increases the cost of the project.

**G) TYPE OF SCHEME:**

The distribution system is more complex than the transmission system in terms of branching and junctions, thus, more expensive [Steel and McGhee, 1977].

**H) PRESSURE RATING:**

Pipes which could sustain higher working pressures cost more than those built for lower working pressure. However, this factor was excluded from our pipeline model because all pipes in Oman are standard in term of pressure rating.

**I) ENVIRONMENTAL CONSIDERATION:**

Pipelines laid in an aggressive environment need special protection. However, this factor was excluded from our pipeline model because all pipes in Oman are similar in term of environmental protection standard.

**Data Collection and Normalization**

Originally, final account costs rather than tender figures were to be used in this study. However, the researcher decided to use successful tender figures, instead, because the final account costs were unavailable.

- 1) In most cases, the final account is within  $\pm 5\%$  of the tender price.
- 2) Final costs would often be more difficult to relate to a specific date for inflation adjustment than would tender costs.

The collected historical cost data was produced in the period from 1979 up to 1992, during which costs nearly doubled through inflation and other factors. The purpose of normalizing the data for the effect of escalation is to relate the costs of all sampled projects to a common time reference and adjust the costs of all projects as if they were tendered at that time. All cost data were

discounted to January 1993 using the Average Annual Escalation Rates shown in Table 3.1.

Table 3.1 Average Annual Escalation Rates (AAER) in Oman

ITEM	ANNUAL ESCALATION FACTOR	SOURCE
Pipes, Fittings, Valves, and Equipment	5%	Development Council Petroleum Development - Oman Almuttawah Trading Company Amianttet Oman
Pipeline Installation	1.5%	Examination of Tender Documents. Interviews with Consultants and Contractors.
General Construction	1.5%	Development Council

### Development of Cost Models

Developing a regression model for a real problem is never a simple process. For a defined dependent variable, it is necessary to develop a long list of potential independent variables that thought to have an impact on the dependent variable. Then a certain amount of creativity is essential in order to reduce the long list of independent variables to a shorter list by various means. The functional form of the regression model will gradually be decided upon in conjunction with the development of the short list and the parameters of the model will be estimated using the collected data.

Initially all of the variables in Table 3.2 were entered in the model; the results of which are depicted by the computer output shown in figure 3.1. The combined effect of those variables is considered satisfactory (Adjusted  $R^2=0.9635$ ); however, many of those variables do not explain much about the model (Significance level  $> 0.05$ ), so the first step was to remove those



Leaving the following variables in the model:

- 1) Diameter
- 2) Proportion of DI pipes
- 3) Duration of the project
- 4) Wadi crossing

Correlation matrix for coefficient estimates

	CONSTANT	PIPE.DIA	PIPE.DI	PIPE.DUR
CONSTANT	1.0000			
PIPE.DIA	.1384	1.0000		
PIPE.DI	-.0796	-.2245	1.0000	
PIPE.DUR	-.0697	-.0374	.1960	1.0000
PIPE.DISTANCE	.2225	.6140	-.1832	.1693
PIPE.FLAT	-.5932	.1206	.1091	.2280
PIPE.SEMI_HILY	-.6397	-.0302	-.0380	.1767
PIPE.NO_CNGSTN	-.9097	-.2953	.0244	-.2000
PIPE.MID_CNGSTN	-.9377	-.2857	.0211	-.1513
PIPE.TRANS	-.1290	-.5646	-.3138	.2430
PIPE.ROAD_XING	-.3150	-.1612	.1060	-.0236
PIPE.WADI_XING	-.6490	-.6026	.0564	-.3342

Figure 3.2 Pipeline Correlation Matrix

When this initial model was created, concern was voiced at the absence of those variables felt to be important, even though could not demonstrate a statistical importance. Nevertheless, practical experience indicates that scheme costs are radically affected by variations in factors of this sort. At that point a practical treatment was used by introducing an Over - Under (O<sub>2</sub>) factor adopted from the research study conducted by the Water Research Center (WRC) [Water Research Center, 1977]. The scores of the O-U factor were adopted, because they measure relative rather than absolute levels and they were developed based upon the engineering characteristics of the projects. Table 3.3 exhibits the weights of those variables. The sum of the 7 scores for a contract constitutes the O-U factor, and is an attempt to summarize how easy or difficult the project is, and hence whether it is likely to be cheaper or more expensive than the average.

In spite of the explanation power of the diameter factor (DIAMETER), it is believed from practical experience that the cost of a pipeline is proportional to its cross sectional area or the squared diameter (DIA - SQR). When the O-U factor and the DIA-SQR were introduced into the model, the computer



output in figure 3.4 was generated.

Clearly, the Adjusted  $R^2$ , Standard Error of Estimate (SE)<sup>2</sup>, the Mean Absolute Error (MAE), the Durbin-Watson statistic have improved. In addition, the significance level of the individual explanatory variables have substantially improved by going below 0.05. Even though the significance level of the O-U factor is above 0.05, it is well below the significance level of its constituent variables when considered individually. Then it was decided to re evaluate the O-U factor by eliminating its significant variables which were determined to be the ground condition and the construction method. New values for the O-U were calculated and inserted into the model to produce the computer output shown in figure 3.5.

Clearly, the predictability of the model has increased ( $R^2 = 0.9906$ , whereas a value above 0.8 is considered satisfactory when modeling a real problem [Albright, 1987]). Moreover, all other statistics are kept within acceptable ranges. The analysis of variance (ANOVA) table, shown in figure 3.6, confirms the adequacy of the pipeline cost model by reporting a model significance well below 0.05. At that point it was decided to accept this model as a conceptual cost estimating tool for water pipeline projects in the Sultanate of Oman.

TABLE 3.3 Weights of Variables Considered in the O-U Factor

CONTRIBUTORY FACTOR	RANGE	WEIGHTING	COMMENTS
1. Depth range (m)	As per the specifications	Score 1 point for every depth range featured in contract	Diversity of depths might indicate an increase in the complexity of the scheme, and necessitate a variety of excavation and pipe-handling techniques.
2. Diameter range (mm)	$\leq 100$ $100 \leq 200$ $200 \leq 300$ $300 \leq 600$ $600 \leq 900$ $900 \leq 1200$	Score 1 point for every depth range featured in contract	Diversity of diameters might indicate an increase in the complexity of the scheme, and necessitate a variety of excavation and pipe-handling techniques.
3. General vicinity of site.	Easy/Rural Moderate/Suburban Difficult / Urban	1 3 8	The vicinity of the site will affect costs associated with : i) Site access; ii) Restrictions on site. operations.
4. Ground conditions	Normal Soil Rock	1 8	The inclusion of the ground type is necessary as excavation cost is known to depend upon soil conditions.
5. Scheme type	Transmission main Distribution Feeder	1 3	Distribution projects are more difficult to handle due to branching
6. Construction method	Trenching Pipe jacking	1 7	Trenchless crossing (pipe jacking) needs a special thrust boring equipment and technique which in turn has a proportional impact upon the cost.
7. Distance (km)	$< 40$ $\leq 250$ $> 250$	1 3 8	Remote sites costs more than locals due to the added transportation costs.

Model fitting results for: PIPE.RATE

Independent variable	coefficient	std. error	t-value	sig.level
CONSTANT	21.333335	5.883099	3.6262	0.0012
PIPE.DIA_SQR	0.000244	0.00001	24.0847	0.0000
PIPE.DI	9.406574	3.27079	2.8759	0.0078
PIPE.DUR	-1.331667	0.4625	-2.8793	0.0077
PIPE.O_U	-0.10564	0.373148	-0.2831	0.7793
PIPE.WADI_XING	0.008538	0.002361	3.6168	0.0012

R-SQ. (ADJ.) = 0.9893 SE= 7.154548 MAE= 5.012954 DurWat= 1.991  
 Previously: 0.9635 13.189326 7.543226 1.749  
 3 observations fitted, forecast(s) computed for 0 missing val. of dep. var.

Figure 3.4 Pipeline Model Fitting Results when O-U and DIA-SQR Factors were Introduced

Finally, the cost model of a pipeline project is represented by the following mathematical equation:

$$\text{Unit Rate (RO/m)} = 11.553358 + 0.000256 * \text{DIA\_SQR} + 9.593977 * \text{DI} - 1.322521 * \text{DUR} + 0.005603 * \text{WADI\_XING} + 0.919127 * \text{O\_U}$$

Where:

- DIA\_SQR : Square of average diameter (mm)
- DI : Percent of Ductile Iron material in the pipeline system divided by 100
- DUR : Duration of the project (month)
- WADI\_XING : Length of pipeline section requires wadi crossing protection (m).
- O\_U : Over\_Under factor; add up all corresponding scores for the factors in table 3.4 except Ground Condition and Construction Method.

Model fitting results for: PIPE.RATE

Independent variable	coefficient	std. error	t-value	sig.level
CONSTANT	11.553358	5.420003	2.1316	0.0423
PIPE.DIA_SQR	0.000256	0.000011	23.0037	0.0000
PIPE.DI	9.593977	2.907271	3.3000	0.0027
PIPE.DUR	-1.322521	0.432032	-3.0612	0.0049
PIPE.O_U MDFD	0.919127	0.458208	2.0059	0.0550
PIPE.WADI_XING	0.005603	0.00234	2.3940	0.0239

R-SQ. (ADJ.) = 0.9906 SE= 6.684376 MAE= 4.582459 DurWat= 2.016  
 Previously: 0.9893 7.154548 5.012954 1.991  
 33 observations fitted, forecast(s) computed for 0 missing val. of dep. var.

Figure 3.5 Second Modification of the Pipeline Model After Modifying O-U factor to O-U-MDFD



- 3) The cost determinant factors, discussed earlier, exert different impacts upon their cost model. However, the diameter of a pipeline is a dominant factor influencing the cost models.
- 4) Since the accuracy of any regression model depends considerably on the set of independent variables that are used to predict the dependent variable, a new variable, which was called Over-Under (O-U) factor, was introduced into the analysis in order to assess the likelihood of a project to be difficult or easy. The O-U factor was introduced after the failure of its underlying factors to show significance upon the predictability of the model when considered individually. The introduction of this independent variable has proven to be of significant aid in improving the prediction accuracy of the pipeline cost model.
- 5) This thesis demonstrated that a well thought-out integration among the science of cost estimation, statistical analysis, and computer technology can, effectively, enhance practices of cost estimating.

## **RECOMMENDATIONS**

- 1) Although CCES has been developed for the MEW's use in Oman, its techniques and principles remain relevant to the development of a conceptual estimating system in any domain, particularly in the Arabian Gulf countries. Hence, Water Industry practitioners in neighboring countries are advised to follow the profile set forth in this study to tailor their cost estimating systems.
- 2) The Directorate General of Water (DGW) in Oman is advised to use CCES as a reliable tool to estimate the construction cost of the domestic water supply projects considered in this study.
- 3) Collection of cost data in the DGW should be practiced as an integrated routine task within the current project management systems. Moreover, DGW is advised to store the collected data in a computerized database to facilitate easy retrieval and statistical analysis.
- 4) DGW is advised to build its own cost indices for the various projects, work items, and the frequently used materials.
- 5) When frequent model-updating becomes necessary, CCES can be linked with any appropriate statistical package supported with a data base management system to facilitate self updating of cost models.

- 6) It is quite likely that, with a larger sample of data, additional explanatory variables will become significant and some of the existing explanatory variables will become insignificant. Thus, intelligent selection rules can be linked to CCES for selecting the set of variables to be included in the regression models. This way, CCES will have the power to eventually discard any independent variable currently in the model if it becomes insignificant in the future, and select another independent variable, such as the presence of rock, if it proves to be more significant.

## REFERENCES

1. Adrian, J.J.; **Construction Estimating: An Accounting Approach**; Englewood Cliffs: Prentice Hall, Inc.; 1982.
2. Akeel, N.F.; **A Database Tool for statistically Based Construction Estimate**; Ann Arbor: UMI; 1989.
3. Albright, S. Christian; **Statistics for Business and Economics**, New York: Macmillan; 1987.
4. Collier; K.; **Estimating Construction Cost: A Conceptual Approach**; Reston: Prentice Hall Company; 1984.
5. Ferry, Douglas J, and Petter S. Brandon; **Cost Planning of Buildings**; Oxford: BSP Professional Books; 1991.
6. Manzanera, Ignacio; **Cost Estimating** Saudi ARAMCO publication: Dhahran; 1991.
7. Raftery; J.; "The State of Cost Price Modelling in the UK Construction Industry: A Multicriteria Approach"; **Building Cost Modelling and Computers** by P.S. Brandon; E. & F.N. Spon; London; 1987.
8. Steel, E.W., and Terence J. McGhee; **Water Supply and Sewerage**; New York: McGraw Hill Co., Inc.; 1979.
9. Water Research Center (WRC); **Cost Information for Water Supply and Sewage Information**; Medmenham: WRC; 1977.

# **Computer Analysis of Muscat Pipe Network**

*A. El-Zawahry*

# COMPUTER ANALYSIS OF MUSCAT PIPE NETWORK

**A. El-Zawahry**

Civil Engineering Department  
College of Engineering  
Sultan Qaboos University  
Oman

## ABSTRACT

This paper focuses on the analysis of an existing pipe network (Muscat Water Pipe Network). Muscat water pipe network was constructed in the seventies to serve the capital areas. The water supply system is comprised of around 625 km of transmission and distribution mains and service connections serving a community of 46,000 consumers. One of the well known and recognized method to solve and analyze pipe networks is Hardy Cross Method. A computer program called Micro Hardy Cross (MHC) is used to analyze the pipe network under investigation. Five different but interrelated types of analysis were carried out: the effect of friction formulas on the network pressure; the effect of demand on the pressure; the effect of roughness coefficients on the pressure (age of pipe); the effect of introducing elevated tanks and; the effect of adding pump stations. The results of the analysis showed that the network can afford 25% increase in the demand without having any significant drop in the nodes pressure. Up to 50% increase in the demand, minor modifications are needed by adding pumps and/or elevated tanks. More than 50% increase, more complicated and expensive solutions are required.

## INTRODUCTION

Water distribution system is one of the most vital and complicated infrastructures. To obtain an efficient and economical system satisfying the present and future needs, necessitates a lot of information, data collection and design. The source of water for Muscat Area Water System, at present, is about 25 percent from groundwater and 75 percent from desalinated water from the sea. The operational concept is to blend ground water. The blended water is treated, stored at Ghubrah and pumped through a primary pipeline transmission system to 9 storage reservoirs. Five of these reservoirs are at elevations such that they serve distribution system by gravity flow. The other reservoirs serve as storage from which secondary transmission systems transfer water to reservoirs which serve the main distribution systems. In addition one "in-line" pump station transfers water directly from the primary transmission pipeline system to a reservoir serving a distribution system by gravity flow. The question which is frequently asked whether the existing networks can stand additional demand and to what percentage of increase. To answer this question part of the Muscat pipe network has been selected for detailed analysis. The old Muscat area is highly populated, characterized by high water demand and can be separated easily from the entire network.

Several methods are used to analyze pipe network using finite element method [1], uncontrolled trial and error method, Freeman graphical method, method of section, and electric network analyzer method. Various techniques for solution on computer are used, Newton Raphson method, hydraulic model method, graph theoretic models method, linear theory method, method of characteristics "MOC", Central Method and Hardy Cross Method are discussed in [2-4]. In addition, two iterative procedures for solving network satisfying the node and loop equilibrium are discussed in [5].

In the present work, three alternative formulations of the governing equation in which pipe flows, junction heads or corrective loop flows were used to analyze the existing network and to predict the network performance due to further increase in demand. Several solutions (designs) were also investigated to improve the efficiency of the network. The network was tested and analyzed, regarding the effect of demand, pipe roughness introducing elevated tanks and/or pump stations. The effect of the friction formulas on the network pressure was also analyzed.

## WATER DISTRIBUTION SYSTEM IN MUSCAT

Two desalination facilities in the Muscat area produce potable water for the



# GULF OF OMAN

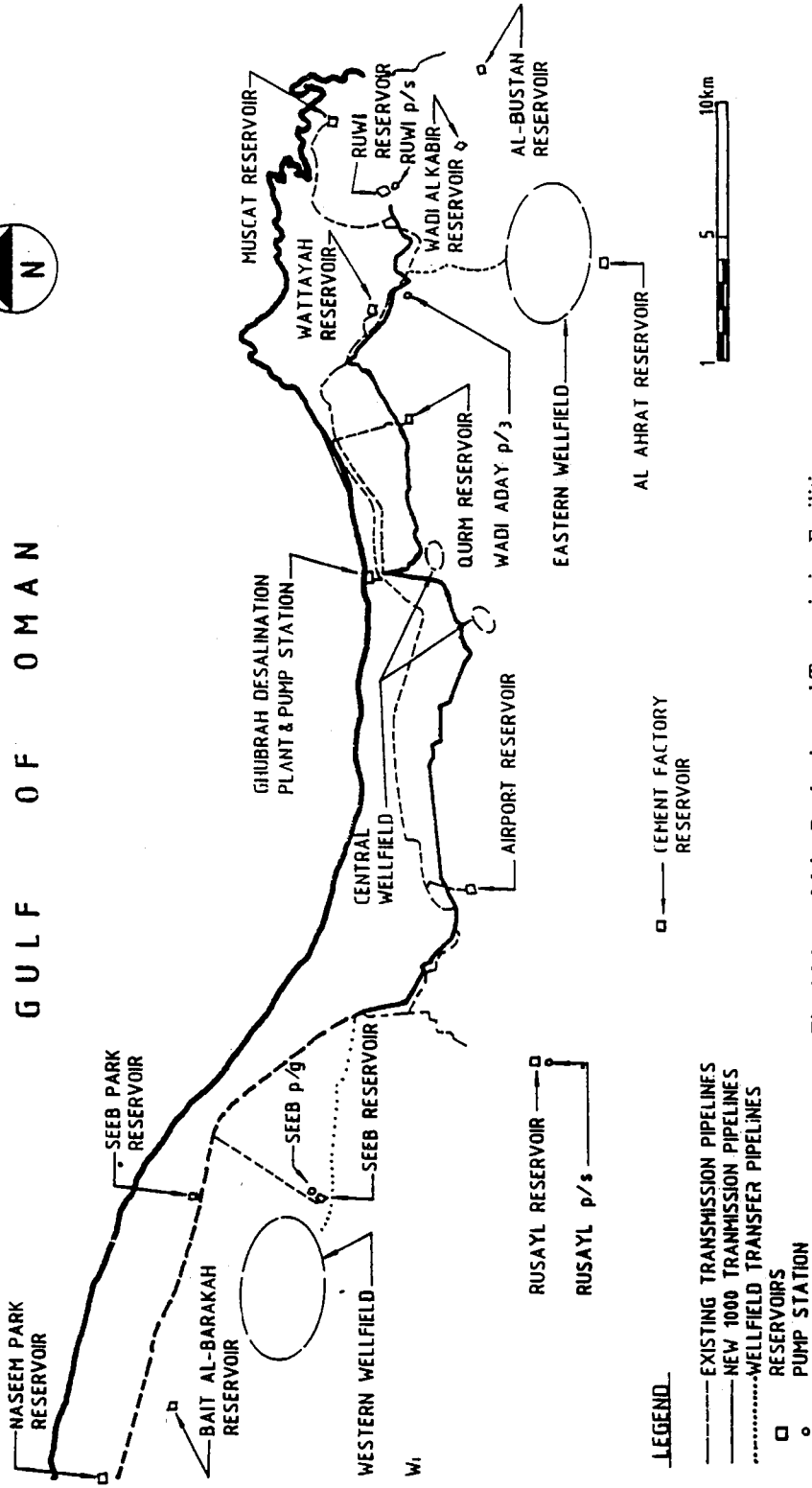


Fig. 1 Muscat Major Production and Transmission Facilities

Ministry of Electricity and Water supply system. The principal facility is at Ghubrah. The second facility is a small sea water desalination plant operated by the Oman Refinery Company (ORC) at Mina Al-Fahal. This desalination plant contains two 1,500m<sup>3</sup>/day multistage flash (MSF) units. The refinery distillers provide the refinery with processed water. Excess water in monthly quantity of water from ORC entering the system varies between 1,200 and 1,700 m<sup>3</sup>/day. The location of the Ghubrah desalination, treatment, storage, and pumping facility, the well fields, the complexes for transmitting water and the distribution reservoirs are shown on Figure 1;

The transmission pipeline system generally consists of a combination of 1000 mm and 600 mm diameter pipelines running east and west of the Ghubrah Complex and connecting the pump stations within Ghubrah to the primary distribution storage reservoirs which serve the different areas of the network. All reservoirs have separate inlets and outlets and generally serve individual distribution networks, except for the four distribution networks to the east of Ghubrah which have some interconnecting pipes. Ductile iron, asbestos cement and unplasticized polyethylene UPVC pipe have been used in the distribution systems. Service connections are mostly galvanized iron pipe [6]. Water supplied to consumers, both private and government is metered. In addition to the pipeline distribution network, portions of the system are supplied by tanker trucks which deliver water to individual users located in presently unserved areas. Currently there are 9 main tanker supply points. Muscat Reservoir, as shown in Fig. 1, is a twin compartment, 18,000 m<sup>3</sup> capacity, ground storage reservoir which serves the Muscat distribution area. The reservoir is float controlled with the high water level sea at elevation 70.5 m and the low water level set at 65.5 m. The inflow pipe consists of a 600 mm header pipe which branches into a series of 300 mm inlet pipes. The outflow piping arrangements consist of a series of 600 mm pipelines which connect into a 600 mm diameter outflow main.

The data used to solve and analyze the Muscat Water Pipe network has been collected from the maps of the Muscat water loss reduction program (Phase IV), [6]. The maps include the main connections, pipe type, ground elevation, topography and existing and expected population. To run MHC (Micro Hardy Cross) program on Muscat pipe network, tremendous amount of data is required. To facilitate the transfer of data from 1:2000 maps of Muscat area to MHC an effort had to be done. To generate a combined map combining all small maps, a computer program called Earth Resources Data Analysis System (ERDAS) has been used. The program was used to digitize all the small maps, using one frame of reference. The ground elevation of all the nodes, nodes coordinates, distance between nodes, lengths of pipes are also generated by

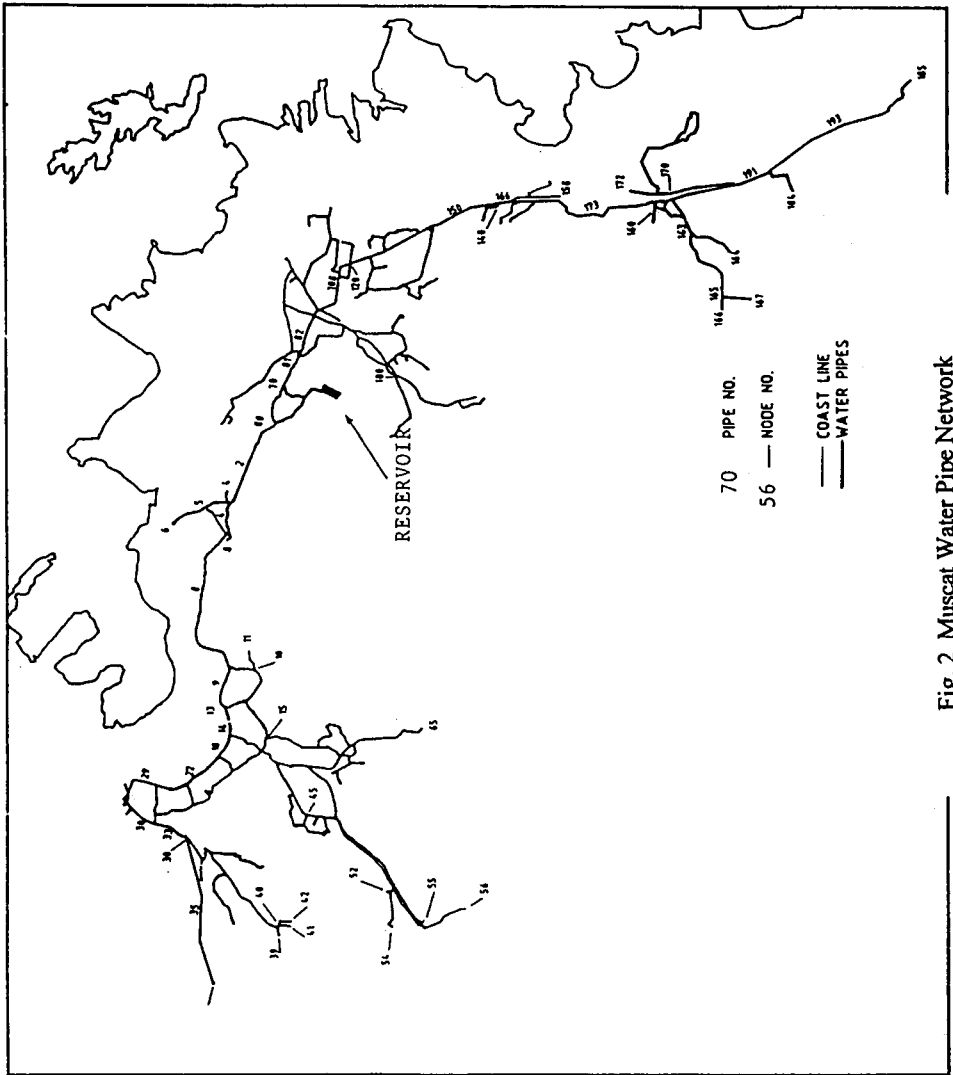


Fig. 2 Muscat Water Pipe Network

this program. The combined pipe network map of Muscat area is shown in the attached map, Fig (2). The system consists of 187 nodes, 216 pipes, and 20 loops and many dead end (branched) pipes. The total length of the pipes of the network was found to be nearly 42 km.

## MICRO HARDY CROSS PACKAGE

Micro Hardy Cross performs the flow analysis and pressure distributions in a water system, using the Hardy Cross method [7]. The program can be used to study an existing water system, to assess the impact of proposed expansions to the system, or to test the effectiveness of proposed alterations to the water system. Pressurized sewer lines and lift stations can also be modeled using Micro Hardy Cross. The analysis given by Hardy Cross method is mainly based on, the law of conservation of mass, and the law of conservation of energy.

The Hardy Cross Method is a controlled “trial and error” procedure. Corrections are applied to the assumed flow rates in a manner that leads to a hydraulically balanced system. The balanced system is one in which the computed flows and head losses match-up at the pipe junctions of the network. The total flow into any junction must equal to the total flow out of the junction. The Corrections applied to the assured flows are determined from the following formula.

$$\Delta Q = \Sigma HL / (C\Sigma - (HL/Q)) \quad (1)$$

where  $\Delta Q$  = the flow correction  
 $Q$  = assumed discharge in each pipe.  
 $HL$  = sum of the head losses for a loop using the appropriate sign (+ ve if the pipe flow clockwise).  
 $C$  = a coefficient

The value of the coefficient  $C$  and the Calculation of  $HL$  are based on the velocity or friction loss formula used. Three different friction formulas are used to analyze networks by MHC. These formulas are Hazen-Williams, Darcy Weisbach, and Manning. The three equations used are:

### Hazen-Williams:

$$V = 0.85 C_{HW} R_h^{.63} S^{.54} \quad (2)$$

**Manning:**

$$V = 1/n R_h^{2/3} S^5 \quad (3)$$

**Darcy - Weisbach:**

$$\begin{aligned} h_f &= f (L/D) v^2/2g \\ f &= 64/NR \text{ for } NR < 2000 \\ f &= f (e/D) \text{ for } NR > 2000 \\ &\text{(Moody Diagram)} \end{aligned} \quad (4)$$

where

$$\begin{aligned} v &= \text{pipe velocity (m/s)} \\ D &= \text{pipe diameter (m)} \\ R_h &= \text{hydraulic radius of pipe (m)} \\ S &= \text{slope of the total energy gradient line} \\ &= h_f/L \\ h_f &= \text{friction losses head between two arbitrary points (m)} \\ L &= \text{length of pipe between the two arbitrary points (m)} \\ e &= \text{pipe roughness height (m)} \\ C_H &= \text{Hazen-Williams coefficient} \\ NR &= \text{Reynold's Number} = \rho v D / \mu = \text{Fluid density (kg/m}^3\text{)} \\ \rho &= \text{Fluid viscosity (N.s/m}^2\text{)} \\ n &= \text{Manning's Coefficient} \end{aligned}$$

The pipe network is presented by MHC in a form of pipes and junctions (nodes). The model defines the node as a junction of two or more pipes or the end of dead end pipe segment. A reservoir or any water source is considered to be a node. Water withdrawal from the system are allowed only at the nodes. The nodes are classified as either fixed demand or fixed head. The pipes are defined as a conduit or device connecting two nodes (heat exchanger, filter and flow restriction). Loops may be classified into three types: closed, pseudo and open. In a closed loop, the last pipe is connected to the first. Pseudo loop contains series of pipes that are not closed, but whose starting and ending nodes have fixed hydraulic grade line elevations. A common example would be a loop connecting two reservoirs. The pump is treated as a pipe which gains head instead of losing head as water flows through it. A pump station is introduced by defining the pump head curve and the number of pumps that use this curve. The initial flows are computed by MHC using a sub-network of the total network called the spanning tree as shown in Fig. (3). A spanning tree of a pipe network contains only enough pipes to connect the fixed demand nodes to the fixed head nodes. There are no closed loops in

the spanning Tree. More details of Hardy Cross method are given in [8]. The package can handle up to 4000 pipes, 3000 nodes, 2000 loops, 200 pumps and 200 valves in the network. It can also handle, elevated tanks (fixed head nodes), pump stations, valves and groundwater wells. The ground elevation can also be included in the computer model.

## APPLICATION OF MHC

The old Muscat area data was fed to MHC. The data included, nodes coordinates, elevations, pipes diameter, length, roughness, formation and type of loops, location and elevation of elevated tanks, pump station location and curves. The detailed network is shown in Fig. (2). Many runs were carried out to achieve the previously mentioned types of analysis. The runs are summarized in Table 1.

TABLE I MHC COMPUTER RUNS.

Run No.	Formula	D.F.	Roughness	El. Tank	Pump	Remark
1	A	1	CHw=140	NO	NO	Reservoir
2	B	1	e=.0128	NO	NO	Reservoir
3	c	1	n=.009	NO	NO	Reservoir
4	A	1.25	CHw=140	NO	NO	Reservoir
5	A	1.5	CHw=140	NO	NO	Reservoir
6	A	2	CHw=140	NO	NO	Reservoir
7	A	1	CHw=100	YES	NO	Dead Ends
8	A	1	CHw=140	YES	NO	Dead Ends
9	A	1	CHw=60	YES	NO	Dead Ends
10	A	1.5	CHw=140	NO	YES	Node 58
11	A	1.5	CHw=140	YES	NO	Node 56
12	A	2	CHw=140	YES	NO	Some Dead Ends
13	A	2	CHw=140	NO	YES	5 Pumps

A = Hazen-Williams

B = Darcy-Weisbach

C = Manning

D.F. = Demand Factor

El.T. = Elevated Tanks

e = roughness height (mm)

n = Manning's Coefficient CHw = Hazen-William's Coefficient

Column 3 of Table I shows the demand factor (D.F.) values used in the analysis. A demand factor of 1.25 indicates an increase of 25% of the current demand. Columns 4 and 5 indicate the addition of elevated tanks and/or pumps to the system to increase the pressure head. Column 7 shows the locations of

adding elevated tanks and/or pumps in addition to Muscat reservoir.

There is no accurate measurements available regarding the water consumption. The demand calculation in Muscat area was based on the assumption that each person consumes about 125 liter/day, number of people living in a house is 8 on average, this leads to 1 m<sup>3</sup>/day consumption per family. The number of houses and families obtained from the maps, and the demand at each node was computed. The total consumption compared reasonably well with the groundwater and Ghubra desalination inflows to the network. In all the simulated cases, the solution was obtained after 16 iterations with insignificant error. Table 2 and Figure 4 summarize the iterations and the convergence graph. The convergence plot is a graphical display of the convergence trends of the analysis. The correction applied to each loop is plotted as a function of the iteration number on logarithmic scale (Figure 4).

### **Effect of friction formula on the Network Pressure**

Figure 5 presents the pressure at selected nodes for the three previously mentioned formulas. In the three methods the same constant demand was adopted. The distribution system consists of a combination of 1000 mm and 600 mm diameter pipelines made of ductile iron, asbestos cement and unplasticized polyethylene UPVC. The values of  $C_{HW} = 140$ ,  $n = 0.009$ , and  $e = 0.0128$  were approximately assumed and used. The three formulas were found to be reliable and the difference between them is insignificant, in order of (5%). In general for a large network and using trial and error method (MHC), the application of any of the three formulas is reliable with minor differences.

### **Effect of Roughness Coefficient on the Nodes Pressure Head**

To study the effect of the pipe material and/or age of pipe, several values representing different materials/age of pipe were tested. The analysis was carried out using Hazen William's method for  $C_{HW} = 60, 100$  and 140. Figure 6 shows the change in the pressure head at four selected nodes due to the change in CHW. Increasing CHW would reduce the resistance to the flow (smooth/ new pipe) and reduce the friction losses along the entire network. The pressure drop between the nodes is reduced and higher pressure values are maintained at the nodes. The pressure at close nodes to the source did not significantly change (node 90). The remote nodes pressure (node 45), changed significantly, reductions of 29% and 57% in  $C_{HW}$  would reduce the nodes pressure to about 15% to 59% of its original value, respectively. At node 68 the pressure attained a negative value for  $C_{HW} = 60$ , which is equivalent to a cast-iron pipe 40 years old.

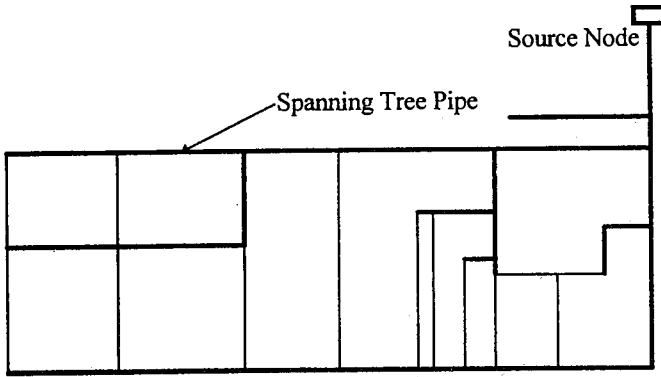


Fig. 3 MHC Spanning Tree Pipe (the bold line)

Table 2 Iteration Summary

Iteration	Largest Error (m <sup>3</sup> /h)	Worst Loop
1	326.3	2
2	111.6	1
3	26.8	11
4	13.4	19
5	11.2	19
6	1.4	19
7	0.7	5
8	0.4	5
9	0.3	4
10	0.2	4
11	0.1	3
12	0.1	6
13	0.0	5
14	0.0	4
15	0.0	3

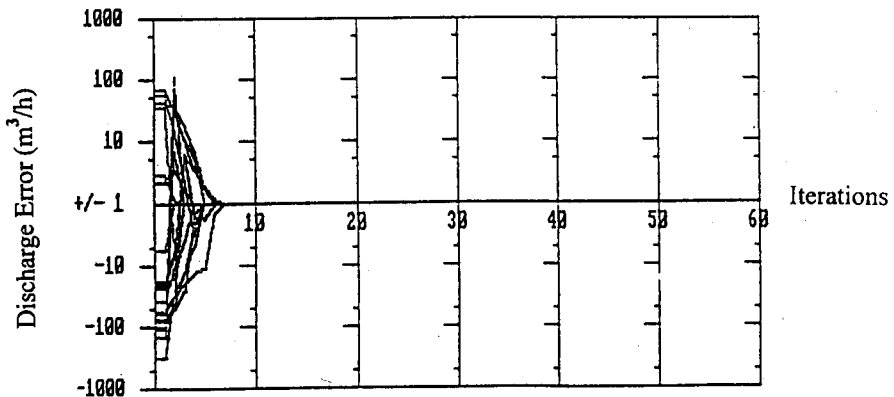


Fig. 4 Convergence Graph



## **Effect of Demand and Leakage on the Network Pressure**

To investigate the effect of increasing the water consumption and the leakage through the entire network, the outflow to each node is increased by multiplying the original flow by a factor greater than one, called the demand factor (D.F.). Three demand factors were used in the analysis (1.25, 1.5 and 2). Figure 7 shows the results of the analysis for some selected nodes. For a demand factor of 1.25, no pressure head at any node dropped below 14m of water (minimum design pressure). Increasing the demand factor to 1.5 caused a reduction in the nodes pressure at one node only (node 56) below 14m of water. Node 56 is the most remote node from the source. A demand factor of 2 caused pressure failure in twelve nodes below 14m of water. Moreover, in some nodes the pressure attained negative values, (node 56).

## **Effect of Introducing Elevated Tanks**

To overcome the problem of the pressure drop below the standard value, elevated tanks equipped with pumps are introduced to the network. The elevated tank guarantees a constant pressure head at the nodes where the tank is constructed. It redistributes the pressure at the surrounding nodes and equalizes the flows. In the case of a demand factor of 1.5 an elevated tank with constant head of 20 m was introduced at node 56. The results showed that the pressure was maintained above the standard, but the flow was reversed in some surrounding pipes and reduced. For a demand factor of 2, six elevated tanks with constant head of 30m were introduced to the network, at nodes 27, 31, 41, 56, 65, and 68. Figure 8 shows the results of the analysis. The pressure increased above 14 m of water in most of the twelve nodes, but in four nodes (39, 40, 41 and 56), the pressure remained below the standard. The solution would necessitate the construction of more elevated tanks with the same height or increase the height of the selected 6 tanks above 30 m of water which in both cases tends to be an expensive solution.

## **Effect of Adding Pump Stations**

A second alternative was to add several pump stations to the network to boost the network with the required pressure. The pressure generated by the pump is a function of the discharge required and following the pump rating curve. In the case of a demand factor of 1.5, one pump was placed at pipe 58 to increase the pressure at node 56. The maximum discharge of the pump was 25 m<sup>3</sup>/hr, while the maximum pressure head was 37 m of water. For a demand factor of 2, five pumps were placed at pipes 36, 43, 56, 66 and 72.

The results in Figure 8 showed that the pressure in all nodes maintained values much greater than 14 m of water.

## CONCLUSION

Micro Hardy Cross (MHC) proved to be a powerful software to handle large networks. The three methods of calculations used by MHC, Hazen-Williams, Manning and Darcy Weisbach are reliable and the difference between them in a large network is insignificant. The age of the pipe and / or the pipe material effect on the nodes pressure are highly significant (a reduction of about 60% in the pressure corresponding to the reduction of 57% of  $C_{HW}$ ). The existing network can withstand an increase of 25% in the demand on a form of increased consumption or leakage without having pressure in any node less than the standard (14 m of water). A demand factor of 1.5 requires placing an elevated tank or pump at one node to keep the required minimum pressure. Increasing the demand factor up to 2 (i.e. 100% increase) necessitates the use of several elevated tanks or pump stations. The solution of pump stations gives higher pressure in the affected nodes.

## REFERENCES

1. Abdel Magid, Hago, A., and Abdel Magid I., "Analysis of Pipe Networks by the Finite Element Method", *Water International*, 16 (1991), pp. 96 - 101.
2. Lain, C. F., and Wolla, M.L., "Computer Analysis of Water Distribution System, Part I-Formulation of Equations", *Journal of the Hydraulics Division, Proceedings of the American Society of Civil Engineers*, Vol. 98, No. HY2, 1972., pp. 335-344.
3. Lam C.F. and Wolla, M.L., "Computer Analysis of Water Distribution Systems", Part II-Numerical Solution", *Journal of the Hydraulics Division, Proceedings of the American Society of Civil Engineers*, Vol. 98, No. HY3, 1972, pp. 447-460.
4. Wood, D.J. and Charles, C.O., "Hydraulic Network Analysis Using Linear Theory", *Journal of the Hydraulics Division Proceedings of the American Society of Civil Engineers*, Vol. 98, No. HY7, 1972, pp. 1157-1170.
5. Collins, A.G., and Johnson, R.L., "Finite Element Method for Water Distribution Networks", *Journal of American Water Works Association*, Vol. 67, No. 7, pp. 385-389.
6. Study Report (Phase 1) "Muscat Water Loss Reduction Program (Phase IV)", Ministry of Electricity and Water Directorate General of Water, 1992.
7. Micro Hardy Cross, CECOMP, 17127 Bircher St., Granada Hills, CA 91344 U.S.A, 1988.
8. Hardy Cross, "Analysis of Flow in Network Conduits or Conductors", *Univ. Illinois Eng. Expt., Sta. Bull*, 286, 1936.

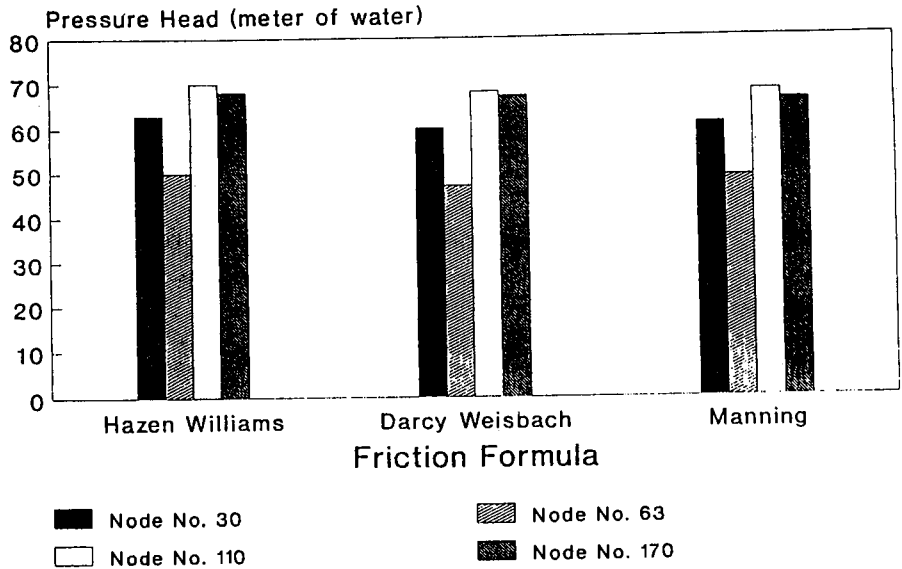


Fig. 5 Effect of Friction Formula on Nodes Pressure

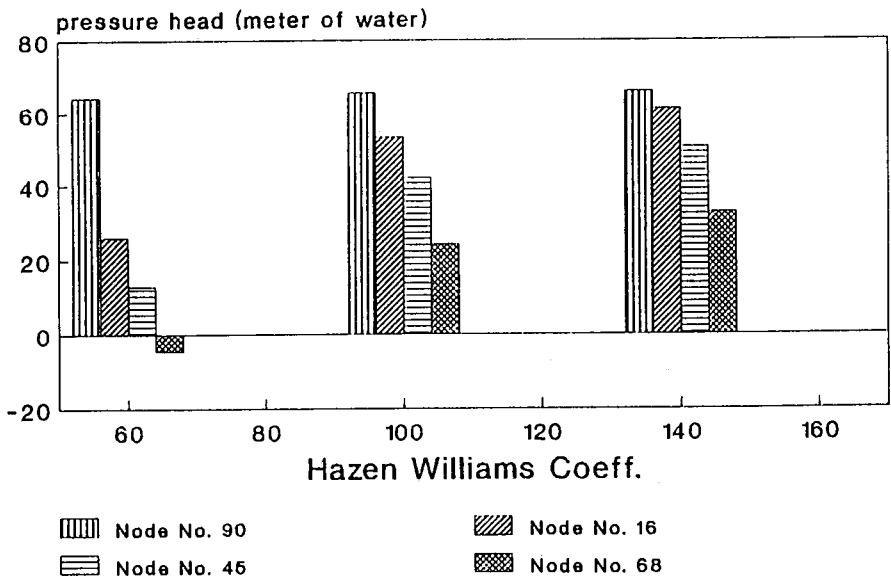


Fig. 6 Effect of Roughness on Nodes Pressure

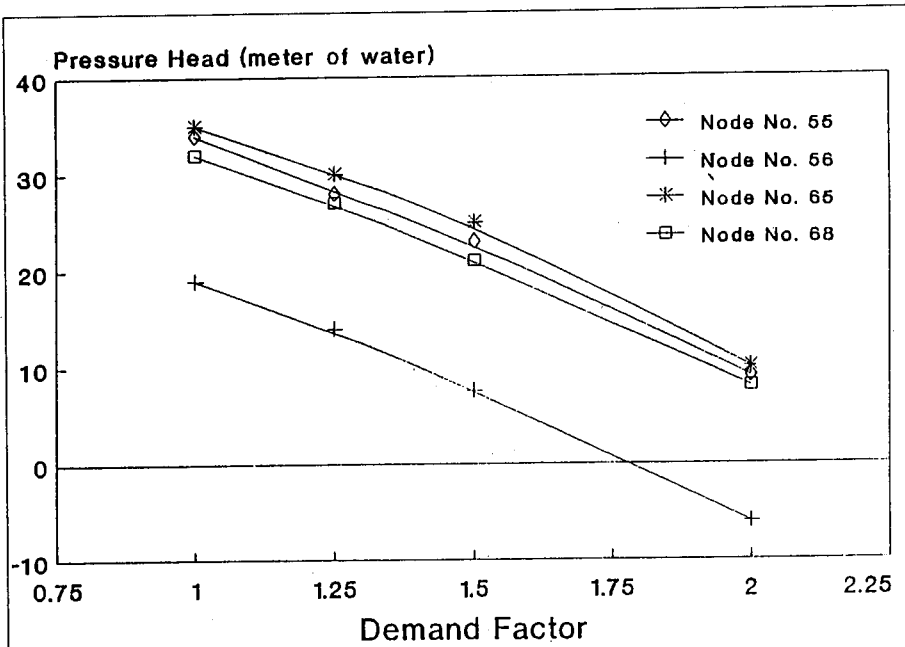


Fig. 7 Effect of Demand/Leakage on Nodes Pressure

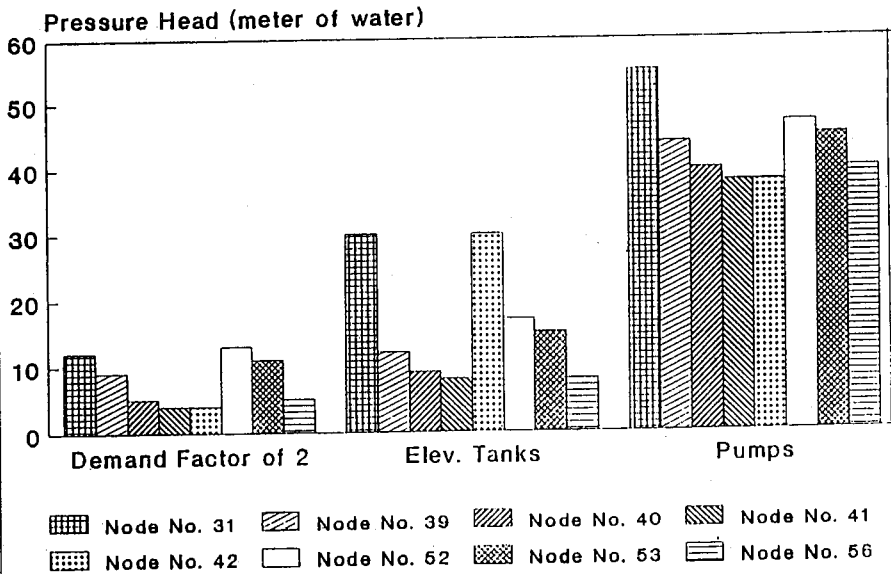


Fig. 8 Effect of Elevated Tanks/Pump Stations on Nodes Pressure

# **Water Transportation by Ductile Iron Piping Problems and Prospects**

*N.J. Paul, Murad Seleiman, Abdul Jalil Khoory  
and Adel El Masri*

# **WATER TRANSPORTATION BY DUCTILE IRON PIPING PROBLEMS AND PROSPECTS**

**N.J. Paul, Murad Suleiman, Abdul Jalil Khoory and Adel El Masri**  
Water and Electricity Department  
Abu Dhabi, U.A.E.

## **ABSTRACT**

Ductile iron piping has been successfully used for decades for the transportation of municipal water. One of the advantages is the ease of installation and the trouble free performance thereafter. The thick wall takes care of all corrosion losses and withstands all mechanical stresses and load of the urban traffic. It has an additional advantage in its immutability to attack by small doses of chlorine and other disinfectants normally used in potable water systems. In the recent years, the location where urban transport involving DC traction and other electrical groundings exist, or at locations where the high tension A.C. transmission cables are at close proximity, there are cases of failure in the form of deep pit and puncture.

In the Middle East, pipelines have failed in the past for unknown reasons and case studies of investigation show interesting results.

**Keywords:** spheroidal, subkha soil, static load, A.C. induced corrosion

## **INTRODUCTION**

Ductile cast iron pipes have been used in water transportation for about 15 years even in the third world countries. It is because ductile iron pipes are cheaper, and easier to install (requiring no welding or bolting) and the extra wall thickness offered as corrosion allowance is considered sufficient to take care of any mechanical and chemical problem for several decades without any need for maintenance or monitoring. Statistically, the percentage of failure in these lines either by unit time interval or by unit length in any installation is much lower as compared to normal carbon steel or alloy steel piping (1). However, the recent failure in critical locations has caused some anxiety to management (2). Whereas carbon steel has alternative protective measures such as coating and wrapping and cathodic protection, the DCI, piping were buried in the past either bare or with organic coating only. In view of the failures described below, the recent installations for water mains or even for the rarely used fire fighting lines which are buried in coastal areas or subkha soil, it was recommended to use additional protection measures such as galvanizing, coating and wrapping followed by cathodic protection. The question then raised was, "why less expensive carbon steel could not be used in place of the DCI if these protective measures are also involved?". Although literature is abound(3-6) with statistical and technical information about the failure of gray and ductile cast iron, it is still a matter of contention about the supremacy of one over the other. Besides, the efficiency of the coating made both inside and outside the pipeline, for the sake of offering protection, is also debatable in certain cases. From several history sheets of failure three case studies have been selected in order to find out,

- 1. why and how the failures have occurred.**
- 2. an estimate of the corrosion damage and the cost of replacement.**
- 3. the unit cost of an alternative material to DCI.**

### **CASE STUDY 1**

The distillate lines in one of the power stations has DCI piping made of centrifugally cast ductile iron material and conforming to ISO 2531 (1979) and provided with push-on or flanged joints in accordance with ISO4633. The pipes were of nominal wall thickness 150-900mm belonging to class K9. The pipe joints were designed for test pressure of 15-32 bar. They were cement lined inside as per ANSI/AWWA and on the outside they had 20-60 micron zinc spray and coated with tropical bituminous varnish of 70-100 micron, thickness. In some locations the pipes and fittings were covered with loose polyethylene sleeves.

These lines were buried, connecting two lots of water storage tanks at a distance of about 1000 meters and passing through a soil which was always wet and muddy because of the lawn on the ground surface. Besides, there were also buried high tension cables crossing at right angles to the piping at certain locations close to the power control room. In addition to these, there is a dormant old oil pipe line along with its oil inside lying abandoned close to the DCI lines. Recently leaks began to develop in these DCI water lines and as a temporary measure they were clamped (7) at those locations and covered up again. Understandably, the cause for the perforation had not been identified at that time.

### Case Study 2

In the town water supply system laid inside the city, one large main having a diameter of about 1600 mm had a failure at a location close to the chemical dosing plant and not far away from the pumping station. It was a fracture extending to several meters in length. This line had been in service for about fifteen years and the mode of failure became a matter of discussion. Was it a poor quality of material or was there some defect in the laying?

### Case Study 3

Inside one of the power stations, DCI pipes of large diameters are used for the supply of sea water to the distillers. A portion of the DCI lines connect the supply pumps and the carbon steel delivery lines. The carbon steel pipes are lined inside with Cu Ni and protected externally by coating and cathodic protection. These portions of DCI lines are coated inside with cement mortar or organic coating and installed above ground level. In the recent times, small failures have occurred in the lining material of the DCI at the bend. Though the damage was not severe small repairs had to be made very often. Is the failure due to erosion caused by turbulence or is it a galvanic coupling failure due to imbalance in cathodic protection or is it a failure due to the ageing of the coating material? A major concern was to find out the extent to which the DCI material was affected so that these high pressure lines would not burst as in the past cases.

## **FAILURE ANALYSIS**

Strangely, few references are available in literature about the *failure pattern* of DCI pipes although there are some statistics regarding DCI vs gray cast iron are reported(3). Apart from microscopy and metallographic examination no acceptable electrochemical technique is cited for the identification of any



conclusive mechanism of failure. Just because DCI is not very much used in critical installations like refineries or oil-fields but mainly for water transport, failures of this type cannot be considered as casual. In situations as mentioned in the case studies, it is not only the product loss that matters, but also the locations of the buried lines are critical as these are inside a power station where high tension buried cables and DCI pipelines are in close proximity. The other critical locations are in the heart of the city where lines are buried under or across main roads which are busy with traffic or at construction sites where building activities are in progress. A damage to one of these water mains can cause unlimited liabilities by way of indirect losses and therefore every care for preventive measure must be taken both for existing lines as well as for those planned for the future.

Secondly, in the case of DCI, failure based on graphitization does not hold good because of the introduction of spheroidal graphite in the cast and thus the defect was supposed to be circumvented. With the introduction of centrifugal casting facilities, the corrosion resistance also is said to be dramatically increased. Thus safety, extra capacity, service life and economy were claimed in the introduction of DCI. However comparative studies made in Calgary seemed to present a different view. Technically speaking, the spheroidal structures allow the material some amount of ductility, for tensile, elongation, notch and bending stresses. The modulus of elasticity of DCI is  $1.7 \times 10^5$  N/mm<sup>2</sup> which is the same as steel and is about twice as much higher than for gray cast iron. and the resistance capacity for a bending load is 30 to 100% higher than for normal carbon steel. Therefore if DCI fails it should be in the form of holes than fractures unless otherwise there is a tremendous sudden impact or an unusual static load.

That is why a satisfactory explanation is lacking for the crack failure of the town water main which had a longitudinal tear for a length of about three meters. In such a case what must have caused the "static" load on that section of the line that was in operation for over a decade without any symptoms of failure? It was verified that at the time of failure no new Ingh nse structures or road constructions took place over the pipe or in the near vicinity so as to cause undue mechanical vibrations or loads.

The second alternative is, to expect a cause or factor at the water side to initiate the possibility for a failure in the form of a longitudinal crack and a rupture. The safety factor assumed for the bursting pressure of such a large diameter pipelines is 4-6 times higher than the normal pumping pressure and this limit is seldom exceeded even in case of a blockage. Besides such a failure if occurred should be preferably close to a joint and not at the mid of a pipe length unless otherwise a material defect also existed at such a location. Therefore this type of failure is not due to a *mechanical stress* alone but a combination of factors. For the

water mains to fail there could be several causes such as:

1. Material failure
2. Mechanical aspects
3. Causes of corrosion
4. External and internal forces.

of which the first two are ruled out in this case. Most of the reports suggest the rare chances of a material failure in DCI (detected by microscopy) and more useful information could be obtained from a macro-examination and by a site inspection of the failure,(3) to arrive at a conclusive opinion.

## **CAUSES OF CORROSION**

### **Chemical attack soil side:**

In the early years, when the municipal water supply systems were installed, the soil and surroundings were not as aggressive as they are nowadays. In the present times, the municipal water lines are criss-crossed by foreign lines which carry corrosive chemicals, gases and fluids and their frequent failures spread the spillages to neighbouring DCI and cast iron lines thereby introducing sites of corrosion. Also the soil through which these lines pass are partially taken up for industrial and residential allocations and part of them for parking and agriculture (8). In the Middle East where these kind of changes are taking place at an accelerated phase, the buried lines have been forced to accept a rude “cultural shock”. The fertilizers and strong chemicals that are dosed to such a soil, and flooding it with water could help the vegetation but harmful for the pipeline getting soaked without limit. Some of the top soil must have been modified to suit the vegetation and the compactness of the soil around pipeline would have been affected significantly. Also an arid area called “subkha” land which looks like a salt pan in summer and a pool of water in winter (low lying areas with proximity to sea and which was always inundated with such salt water during high “tide” and winter seasons) suddenly gets transformed into golf club with palm trees and watered lawn, and a buried pipe line in that location is susceptible to short and long chain corrosion reaction. All these changes are done with good intentions of improving the socio-economic condition of the society but with no consideration for the compatibility of the old buried pipelines installed twenty years ago.

Such variation in soil nature and structure could set up differences in wetness/dryness properties, water retainability properties, porosity etc., affecting the available oxygen around the line in particular. Pockets of cavity in soil have been found beneath a pipe line suddenly created either due to soil erosion or

unknown causes in certain locations. All these variations in soil condition can cause both soil side corrosion and are also responsible for mechanical failures. From the foregoing reasons for failure, we tried to explain the three case studies mentioned above.

In case of the town water supply mains(case study 2) the crack was longitudinal extending to a length of three meters and the crack was in a staggered pattern. It was suspected as a material failure. But on both physical and laboratory microscopic examination, it was found that the material was nodular DCI and graphitisation was not the cause. The sheared surface indicated that a mechanical force was the final stroke for failure but the cracks have been connected by pitted locations. What caused the deep pits to be formed? The pits were in a string formation at the bottom of the pipe at 6'0 clock position not far away from the chemical dosing point. That explains the situation that a low pH at that location due to the HOCl could have initiated the coating failure and corrosion pits formation. A mechanical stress induced by an internal or external factor added to this, has resulted in the failure. Apart from this stray case the normal failure in the town water mains is only due to soil side corrosion, and leaky joints. Although about 55 leaks/replacements are reported each month, most of these are accounted to normal wear and ageing, misalignments, re-routing etc. which are not to be accounted to manufacturing or material failure. A heap of such material are shown in fig 1, which may indicate the burden on inventory. But considering the changes that take place in urbanisation, these failures are not to be attributed to a defect in material or in a system. Although carbon steel in a similar situation could have been rehabilitated at some cost by cutting, welding, coating and cathodic protection DCI does not offer any such possibilities at all.



**Fig. 1.** A heap of worn out DCI material

The *water side corrosion* was also responsible for the failure of the potable water pipeline inside the power station which was also rehabilitated recently. It not only failed due to HOCl at the chlorine injection point, but also due to AC induced corrosion at a portion of the line about 50 meters away from a HT cable crossing. The injection point was rehabilitated with new joints and placed inside a concrete pit (Fig. 2) to prevent it from soil side corrosion due to the irrigation waters (grass lawns above it). The leak was stopped off by a clamp, with a future plan to install a galvanic magnesium anode (9) at the hot spot as neither the pipeline nor the AC high tension cable cannot be re-routed. This is a unique case where several factors were at play.



**Fig. 2.** The injection point with new spools inside a concrete pit

### **WORN OUT VALVES RECOVERED**

Worn out valves recovered from town water supply are shown in Fig. 3. They vary in size from 4" to 36" dia and have been badly corroded externally and internally. In most cases the perforation has taken from soil side to the waterside and therefore the soil is to be blamed (split Tee 4" and the 4" valve) most of the units have shown poor or defective protective measures used 15 years ago. In future better coating compound will be used such as GRE so as to withstand erosion and chemical corrosion problems.

There is another case where the internal failure in a spool, was due to close knit tubercles concretions. *The biological corrosion* is said to be more prolific

at a temperature of 30 to 40 degrees and at pH of 5.5 and 8.5 and in the presence of minerals like sulphate, phosphate and ferrous ions. Such a condition is very common in water supply line.

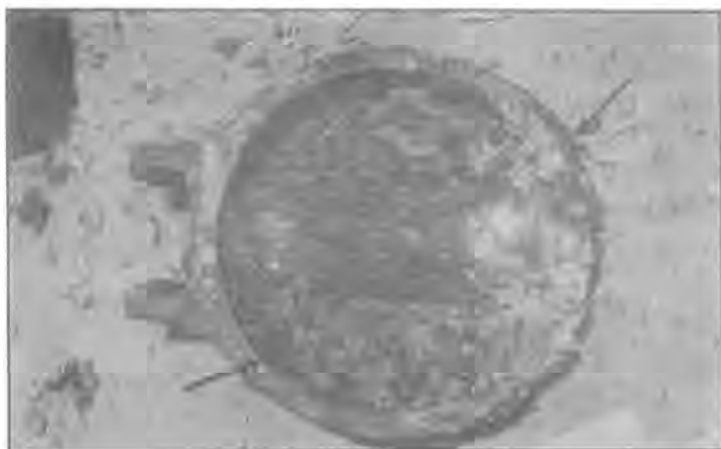


**Fig. 3.** Worn out valve corroded inside and outside.

### **Ductile iron under stagnant water conditions**

Fire fighting lines installed about 15 years ago pass through various soil and surface conditions such as, wet lawn, trenches, subka soil, underneath concrete pavement, road crossings etc. Recently a refurbishment project costing around 0.5 million dollars involved the repair and reconditioning of valves and piping which indicated that only part of the old valves could pass the hydrostatic test after welding, repair and re-coating. This indicates that *rehabilitation of DCI components also is not a fully guaranteed possibility.* The cause for failure in the lines are due to the fact that the fire water is stored in huge tanks and they are seldom replenished or consumed. It is a known fact that even in potable water under long stagnant condition the onset of bio fouling is an inevitable process. The ductile iron piping which contain stagnant water unused for long periods should be dosed with biocide or re-circulated and used for irrigation and replenished once in a month to avoid pitting/tubercle formation. Fire fighting systems are also susceptible to galvanic corrosion particularly as some of the fittings and the valves are made of brass or copper alloy. The pipes are not provided with cathodic protection either. However in the recent installation in one of the power stations, all these problems are averted at the design stage using external galvanising, coating and wrapping and internal rubber lining with appropriate fittings. In addition to this cathodic protection is also installed linking individual pipe units. This has come up also as a requirement as the pipeline is expected to have interference with foreign cathodic protected line and lies in the proximity of

its anode bed field.

## **CATHODIC PROTECTION**

It is still a debated subject as far as DCI is concerned. Except for cement weight coated submarine lines with galvanic anodes, and those under exceptional conditions as above, cathodic protection is considered redundant particularly for thick walled and coated lines. But in the case of a town water line inside the plant which had no other cause to fail yet ruptured, the only plausible explanation that could be offered is its intersection with a buried high tension cable close to it. In this case the installation of a grounding anode for that particular section of the line could have saved all the trouble.

## **CONCLUSION**

Considering all the aforesaid cases except in the town water supply lines the percentage of failure is considerably very low compared to carbon steel or bonna or other material.

In the case of failure more than one cause could be at play.

Metallographic analysis is useful only if quality of material is a suspect.

Macro- examination and site inspection at failure can give helpful information.

Water side corrosion can be eliminated by proper flow regulation and improved dosing methods.

Installation of galvanic anodes could help prevent both chemical and AC induced corrosion at the soil side.

With better type of coating and care at installation, it should be possible to achieve better performance in the years to come.

## REFERENCES

1. Melvin Romanoff- Performance of DCI pipes in soils MP 1987
2. Paul N.J, Adel Masri - Town Water main failure analysis-VVTD Int. report 1994
3. Mikhael N Gimelfarb - Corrosion prediction for underground pipeline MP. February 1990.
4. Jacobs J.A., and J.W Hewes - underground corrosion of water pipes in Calgary Canada. MP.
5. Kottmann A. - Material problems in underground Pressure pipes - GWF 1971
6. Gumniow R.W - The corrosion of municipal iron water mains. MP. 1984 p 39-42
7. Zaman Zadeh et al - Analysis of failure in water mains- MP. August 90 p 50
8. C.D. Rooke - A scientific assessment of the corrosion of iron mains in potable water supply. Corrosion management - April 1996 p 4.
9. Brian Green et al- In situ cathodic protection of existing ductile iron pipes MP. March 1992 p 32.

**Problems of Operation and Maintenance of  
Aged Deep Wells**

*Ibrahim M. Abo'Abat, Hasan Thabith Mohamed  
and Sulaiman Mubarak Abu Alaiwi*



# **PROBLEMS OF OPERATION AND MAINTENANCE OF AGED DEEP WELLS**

**Ibrahim M. Abo'abat, Hasan Thabith Mohamed & Sulaiman  
Mubarak Abu Alaiwi**

Riyadh Water O&M  
Riyadh, Saudi Arabia

## **ABSTRACT**

Riyadh Water Operation and Maintenance Programme operates and maintains about 161 different deep wells for treatment and distribution of potable water as per international applications. This study sums up the problems and our experience in solving them. There are also some recommendations to be followed in similar cases. In fact, this study is a real experience recorded for many years. As the wells are of different depth and water quality there are also different types of pumps used in them. The pumps are selected and installed as per the Saudi Ministry of Agriculture recommendations besides taking into account pump characteristics i.e. Total head, H.P., (Powl Power) - hydraulic thrust etc.

Our experience showed that these are the technical problems we faced:

- a) Damages of the basic structure, which occurs mainly due to the old age of the well. The chemical reactions and the water salts cause corrosion in the casing pipes and as a result the cement structure falls.
- b) The above also causes sand appearance in the pumped water.
- c) Hot deep wells water level decreases as such deep wells naturally do not receive any rain fall.
- d) Bending: due to geological reasons which were not known at the time of designing the well, but such bending has an allowed limit.
- e) Pollution: due to close sewage lines or use of types of cement which can not resist sulphur.
- f) Installation problems:  
Mainly for the equipment inside the well or the casing pipes due to salts or stain or water leakages.

## RECOMMENDATIONS

1. Filter and casing pipes should conform to the international specifications.
2. Cement should be poured at a time between the well hole and the casing pipes by using pressure.
3. A specialized company should test the casing and installations.
4. The cement drying period of 72 hours should be adhered to. No operation before this time.
5. Four sealant "O" Rings should be used to insulate the threads in all connections/couplings.
6. Non-return valves should be used whenever recommended.
7. For water level drops submersible pumps can be used.
8. Pumping should be discontinued if sand appears in the pumped water.
9. The deep well straightness should always be taken care of. Submersible pumps can solve the problems if the well is not straight, instead of drilling a new well.
10. The liner material and valves used at the layer of water should all be S. S. (Stainless Steel) and the openings should be as per specifications.
11. Well positions should be as far away as possible from sewer and sewer plants. If pollution occurs the well should be filled up and replaced by a new one.
12. Pipes to be painted as per specifications.
13. Care should be taken when installing the equipment, not to remove the paint.
14. S. S. Pipes should be used where steel bacteria is available.
15. All equipments should be painted as specified.
16. Suitable diameter pipes should be used for water flow to stop corrosion.
17. Packings and bushes used should be of specified materials.
18. A Plan to be followed for replacement of all equipment as per specifications to avoid sudden failure or major problems.
19. Periodical and Regular maintenance should be adhered to.

# MICROBIOLOGICAL QUALITY OF BOTTLED WATER SOLD IN KUWAIT

**Al-Nashi, B. and Anderson, J.G.**

Department of Bioscience and Biotechnology, Royal College Building,  
University of Strathclyde, Glasgow G1 1XW, UK.

## ABSTRACT

Sales of bottled mineral water in Kuwait and the other Gulf States, continue to increase as consumers search for an alternative to tap water. In 1995 the Kuwaiti mineral water bottler (Rawdatain) sold more than 33 million litres of mineral water (2.2 million K.Dinars). This has been prompted by the growing public concern and awareness about the safety of tap water, by offensive tastes, odours or colour of municipal water supplies, and by bottled water being seen as healthy, pure, and a better alternative to sugary soft and ordinary drinking water.

The purpose of this paper is to investigate the bacteriological quality of a variety of brands of bottled water sold in Kuwait, with particular reference to total viable counts, microflora identification, and the extent to which these products meet the local standards and regulations.

Consequently, the bacteriological quality of still bottled mineral water sold in Kuwait was examined. A total of 26 brands (1 domestic, 16 from Gulf States (GCC), and 9 imported from other countries) were analysed for total viable count (TVC), coliforms, *E. coli* and *Ps. aeruginosa*.

Ten brands exhibited no growth of heterotrophic bacteria, all of them from the Gulf States where the law permits sterilisation treatment prebottling. High and variable total bacterial counts were found in the other 16 brands and no coliform, *E. coli* or *Ps. aeruginosa* were recovered from any sample. The effect of storage temperature was studied and a slightly slower bacterial growth was observed in samples stored at 4°C than at 25°C.

The Vitek AutoMicrobic System was used for the identification of representative isolates. Among the 237 strains studied, *Pseudomonas spp.* was found most frequently but other organisms isolated included *Acinetobacter*, *Vibrio* and *Flavobacterium*.

**Keywords:** Natural mineral water, Bottled water, Microbiology, identification.

## INTRODUCTION

The Romans may have started the consumption of natural mineral waters two thousand years ago in the belief that they are beneficial to health, but the French have now taken over. They are the driving force, the impetus promoting mineral water throughout the world (Green, 1985).

The shift in drinking away from sugary soft drinks and strong spirits to bottled water is worldwide. In the United States of America, bottled water is actually the fastest growing beverage. Sales of bottled waters within the UK have tripled within the last five years (Hunter, 1993). France, the most important exporter, sells 1.3 billion litres of mineral water per year. In 1982, the production of natural mineral water in Europe almost reached 23 billion litres; four European countries have exceeded the 100 litres consumption per capita with Italy ahead of all (Fortuna, 1993).

The successful marketing of mineral waters as a fashionable, natural product associated with a healthy life-style, the dislike of the taste and concern over such problems as lead, nitrates and aluminium in tap water, and the realisation that in some areas water has been recycled many times through sewage treatment and water purification plants before it reaches the consumer's tap, have all contributed to the recent success of the bottled natural mineral water industry (Stickler, 1989).

The desert climates of the Middle East and the Gulf States, where temperatures soar (130°F) in summer, make countries such as Kuwait and GCC States natural for mineral water. Copious drinking is essential; daily intake may be between 6 litres in the hottest months, so that demand for bottled water and soft drink is enormous.

In Kuwait, a small country in the Gulf area, there is one mineral water brand produced and bottled locally. Rawdatain Natural Mineral Water bottling company, was set-up in November 1980 on a 50-square kilometre mineral water field, 100 kilometres north of Kuwait City with an operational production capacity of 44 million litres a year. Production and sales of Rawdatain natural mineral water is increasing every year, the latest annual report shows that in 1995 the company produced 33 million litres of mineral water and the sales income was 4.5 million sterling pounds approximately (Rawdatain 1995) Fig. 1. There are many other brands of numeral water imported from all over the world and sold in the local markets, many of them imported from other Gulf states where more bottled water companies are likely to be established possibly in response to the expansion in the demand for easy to carry, cooled and pure water.

However, with the increased geographical distribution and growth in bottled-water sales, an increasing proportion of the population is exposed to a potable water source of uncertain bacteriological quality. The need for systematic bottled-water quality surveillance is a growing concern to health authorities and many researchers (Geldreich, 1995).

So far, there is no published information on the microbiological status of mineral waters sold in Kuwait. This poster gives a general assessment of the current bacteriological status of mineral waters, and investigates the bacteriological quality of a variety of brands of bottled water purchased from retail outlets in Kuwait.

## DEFINITIONS

The term "natural mineral water" is by no means a scientific definition, as all waters of this earth are, more or less, mineralised (Fricke, 1993).

Natural mineral water is by definition and by Regulation, an untreated product extracted from a naturally-protected source. It differs fundamentally from bottled spring water and tap water, which rely upon treatment as a means of ensuring portability (MacGuire, F. 1992).

In Kuwait, the production and marketing of natural mineral water is governed by the Standards & Meteorology Department (Ministry of Commerce & Industry, 1990, which is very similar to the E.E.C Directive, 1980). These standards give comprehensive and authoritative definitions of many terms used in industry.

According to these standards, natural mineral water is clearly distinguishable from ordinary drinking water because: -

- it has a characteristic content and concentration of certain minerals and trace elements and other constituents.
- it is obtained from natural underground sources either by natural flow or a drilled bore.
- the stability of its composition, temperature and rate of flow are within the limits of natural fluctuation.
- it is bottled close to the point of emergence from the source and collected under hygienic conditions to preserve its original bacterial content.

The Kuwaiti legislation differs from the EEC Directive in the fact that it does not state clearly what type of treatments may be used for natural mineral water. This difference explains the use of ozone treatment to sterilise the Kuwaiti natural mineral water before bottling.

## THE MICROBIOLOGICAL STATUS OF MINERAL WATERS

Bottled mineral waters are characterised by their bacterial flora (Schwaker & Lorenz, 1981). Various studies have shown that bottled water may contain high densities of heterotrophic bacteria (e.g. Manaia, 1990). Occasionally, faecal pollution indicator bacteria (Geldreich et al, 1975) and *Ps. aeruginosa* (Rivilla & Gonzalez, 1988) are isolated. The presence and densities of bacteria in bottled water vary with brands, and also between sources (locations) (Geldreich et al, 1975).

Amongst the criteria prescribed in the Kuwaiti standards for mineral water are microbiological requirements which state that: -

1. Natural Mineral Water shall be free from parasites and pathogenic microorganisms at source bottling and during marketing.
2. At source
  - (i) the total colony count may not exceed 5 /ml at 37°C in 24 hours on Nutrient Agar and 20/ml at 20-22°C in 72 hours on Nutrient Agar.
  - (ii) should be free from micro-organisms caused by faecal contamination, and that includes: -
    - a. *Escherichia coli* and other *colifoms* and faecal Streptococci in any 250 ml sample examined.
    - b. Sporulated sulphite-reducing anaerobes in any 250 ml sample examined.
    - c. *Pseudomonas aeruginosa* in any 250 ml sample examined.
3. After bottling:  
these values should not exceed 100/ml at 20-22°C in 72 hours and 20/ml at 37°C in 24 hours. These values should be measured within the 12 hours following bottling and from bottles maintained at 4°C.
4. During marketing
  - (a) Natural water may not contain any of the micro-organisms referred to in Section 2(ii)
  - (b) The increase in the total colony count of a natural mineral water may only be that resulting from normal increase in the bacteria content which it had at source.

## INDIGENOUS AND CONTAMINATING MICROBIAL FLORA

Natural mineral water is not sterile, at source these waters will have a small population of starved bacteria. The situation can change dramatically as the water emerges from the underground source. The numbers of viable bacteria can increase to 10<sup>4</sup> - 10<sup>5</sup> cell/ml after 1-3 weeks storage. Most of the bacteria which are recoverable from these waters at source are Gram-

negative rods, typically belonging to genera such as *Achromobacter*, *Pseudomonas*, *Acinetobacter*, *Flavobacterium*, *Moraxella*, *Alcaligenes*, *Xanthomonas* and *Cytophaga*. Species identification of the autochthonous bacteria has proved to be difficult for most authors (Fleet & Mann, 1988).

Contamination rarely occurs at the water source as regulations require that the water source be well separated in distance from potential sources of sewage contamination (Leclerc, 1985). The most likely sources of contamination are equipment, bottles, caps, exposure of the water to air and contact with human and other animals during bottling.

Natural mineral water is an inhospitable environment for microbes. The likelihood is that many of the contaminating organisms with their requirement for organic materials to sustain survival and growth, will die off in the mineral water (Sticlder, 1989).

Contamination of mineral waters with the pathogenic species *Ps. aeruginosa* and *Ps. cepacia* has been of special concern since these species are oligocarphilic and have the potential to grow in the dilute environment of the water.

## **BACTERIOLOGICAL QUALITY OF SOME STILL BOTTLED WATERS SOLD IN KUWAIT**

### **Materials and Methods**

Twenty six different brands of non-carbonated natural mineral waters were purchased at retail outlets in Kuwait for microbial analyses. One was of Kuwaiti origin, 16 from Gulf States (GCC), 2 from Lebanon & Egypt, 2 from Iran and Turkey, and 5 from European countries. For each brand 10 bottles, of unknown age, mineral water (purchased from different locations) were examined.

### **Bacterial enumeration**

Total viable plate count (TVC) of water samples and decimal dilutions thereof were made in duplicate by the pour plate method on plate count agar (PCA) at 22°C for 96 h. and at 37°C for 48 h. (Anon, 1985).

### **Total coliform, *E. Coli* & *Ps. aeruginosa* detection**

Coliform bacteria were examined using a presence/absence test (Colilert IDEXX) where the dehydrated Colilert medium was added to 100 ml of the water contained in sterile plastic vessels without sodium thiosulphate and

this was incubated at 37°C. Samples were classified as presumptively total coliform and E coli positive on the basis of yellow colour production and long-wave fluorescence respectively (Fig . 3).

Samples of 250 ml were filtered in duplicate through (0.4 micro-metre pore size, 47 mm diameter) membrane filters and placed on Pseudomonas Agar with C-N supplement SR102 (Oxoid Ltd., Anon; 1985). Production of green or blue pigmented colonies indicated the presence of *Ps. aeruginosa*.

### **Effect of Storage Temperature**

The effect of storage temperature was monitored using six sterile glass bottles filled with water from brand (R) . Two bottles were stored at 4°C, another two at 35°C and the remainder at 40°C. To monitor bacterial population levels, enumerations of total viable counts on (PCA) incubated at 22°C were repeated after 2, 4, 10 and 20 days.

### **Bacterial Identification Using The Vitek AutoMicrobic System**

From each brand of mineral water 0.1 ml volumes were spread-plated in duplicate on PCA and PCA/10 plates and then incubated at 22°C and 37°C for 4 days and 2 days respectively. Representatives of the different colony types were taken from each plate, isolated, purified, screened by Gram stain, oxidase test and identified with the The Vitek System, using GNI (Gram Negative Identification cards, and NFC (Non-Fermenter identification Cards) according to the manufacturer's instructions. (Fig. 4).

## **RESULTS**

### **Total viable counts of still waters**

The bacterial densities of bottled water purchased from retail outlets were highly variable. Table (1) shows the average colony counts on PCA incubated at 22° and 37°C for 26 brands.

Ten brands (A, C, D, F, G, H, J, K, N, Q) from the Gulf States exhibited no recoverable heterotrophic bacteria at both 22° and 37°C, three of them (A, K, Q) were clearly labelled that their water was sterilised by ozone (Fig.2.); all other brands gave TVC ranging from (38,200) to (630) colony forming unit (cfu/ml) at 22° and (24,300) to (120) cfu/ml at 37°C.

At 22°C, one brand (O) gave T.V.C > 30,000. three brands (S, Y, M) > 20,000,



six brands (X, B, T, W, U, I) > 10,000; five brands (P, Z, E, V, R) > 1000; and one brand (L) less than 1000 cfu/ml. At 37°C, one brand (O) > 20,000, five brands (S, M, B, T, X) > 10,000; eight brands (U, I, V, P, E, V, W, Z) > 1000, and two brands (R, L) less than 1000 cfu/ml.

### **Total coliforms, *E. coli* & *Ps. aeruginosa***

Table (1) also shows that coliforms and *E.coli* were not detected in 100 ml of any of the 26 brands when examined according to the procedures in Figure (4). *Ps.aeruginosa* was not recovered from any 250 ml sample.

### **Effect of Storage - Temperature**

Results from the six samples stored at 4°C, 25°C and 40°C showed that the bacterial flora attained in the 4°C stored samples were slightly lower than that attained in the 25°C stored samples. On the other hand, bacterial enumeration was significantly decreasing in the samples stored at 40°C. (Fig 2).

### **Identification of strains from N.M Waters**

A total of 237 isolates were purified from the TVC populations of 15 brands. Table (2) shows the composition and frequency of isolated determined by (Vitek's AutoMicrobic System) - the photometric analysis of biochemical changes (Fig. 4).

Among the 237 isolates studied, a total of 147 strains could be identified at species level whereas 90 could not be identified. The 147 strains isolated were all Gram negative with exception of two strain (no further attempts were made to identify the two Gram positive strains), most were oxidase positive.

Species of *Pseudomonas* were predominant among the isolates (49 of the total of 147 ). This group included *Ps. vesiculariic*, *Ps. fluorescens*, *Ps. paucimobilis*, *Ps. stutzeri*.

Other main species isolated were, *Vibrio* (19 isolates), *Acinetobeter* (22 isolates). Among the other Gram-negative bacteria isolated were *Xanthomonas maltophilia*, *Eikenella corrodens*, *Alcaligenes tylosoxidans*, *Agrobacterium tumefaciens*, and *Ochromobactrum anthropi*. Usually several species were found in each brand of water.

## CONCLUSION

This study has presented for the first time, information on the microbiological status of some bottled still natural mineral waters sold in Kuwait.

The bacteriological quality of bottled natural mineral water appears to be variable from brand to brand and from sample to sample within the same brand. Most of the bottled natural mineral water produced in Kuwait or imported from Gulf States had no recoverable heterotrophic bacteria. Of the 17 brands of bottled water examined in this study, 10 brands were sterilised and their sterility were maintained during shelf life. This is due to the use of one or more methods of treatment for controlling the levels of microorganisms in bottled water in these countries.

There was no significant difference between the total viable counts in bottled natural mineral waters from the Gulf area and the imported brands. High total viable counts (TVC) were found in most samples after incubation at 22°C and 37°C. The multiplication of bacteria after bottling of a mineral water of extremely low nutrient level is an entirely normal biological process (Shmidt - Loronz, 1976).

The absence of indicator organisms namely coliforms, *E. coli* and *Ps. aeruginosa* in all samples suggests that these waters are free from pollution and comply with the Kuwaiti legislations.

Storage of bottled water at 4°C (Refrigeration) did not stop bacterial multiplication, but reduced it slightly. This effect supports other studies (Geldreich et al, 1975) in their recommendations to advise bottlers, retailers, and consumers to keep bottled water refrigerated.

Most of the organisms that are recoverable from the bottled water are Gram negative rods, belonging to genera such as *Pseudomonas*, *Flavobacterium*, *Acinetobacter*, *Vibrio*. The identification results clearly show that *Pseudomonas* species were numerically predominant in the aerobic heterotrophic microflora from natural mineral waters, followed by *Pasteurella* then *Acinetobacter*. There was no apparent difference in the genera growing on PCA/10 and PCA media. It was found that the Vitek System using GNI and NFC cards were useful for identifying strains isolated from mineral waters. It provides printed test results, often the same day, with a minimum of preparation and handling by lab staff.

## DISCUSSION

The type of treatment used for the production of bottled water in the Gulf Area was variable. Information collected from personal contacts, visits and from statements present on brand labels show that a combination of treatment steps including ion exchange, filtration and disinfection was used. Ozonation which has been shown to sterilise the product (Scheider and Rump 1983), or ultraviolet irradiation was most frequently used as the final disinfecting step before bottling.

Some concern has however been expressed following suggestions that the high numbers of bacteria found in unsterilised bottled water are above those specified in the Regulation, and may lead to stomach upsets (MacGuire and Ball 1992) and the possible decrease in sensitivity of the coliform test (Geldreich et al, 1975). However, there is no scientific evidence that these naturally occurring bacteria can cause stomach upset or are of any clinical significance and the Regulation sets limits which apply to the period within 12 h. of bottling beyond which normal growth in numbers is expected.

In view of the widespread production, importation and consumption of bottled waters sold in Kuwait and the potential microbiological risks associated with it, further investigation by sampling a larger number of samples including carbonated water is required.

## REFERENCES

- Anonymous. (1982) *The Bacteriological Examination of Drinking Water Supplies*. Reports on Public Health and Medical Subjects No.71. London, HMSO.
- Department of Standards & Metrology. (1989). *Kuwaiti Standards for Bottled Natural Mineral Waters*.
- Edberg, S. (1990). *Technical Assessment of the Microbiological Health Effects of Bottled Water*.
- Fleet G.H., and Mann, F. (1986). "Microbiology of natural mineral water: an overview with data on Australian waters." *Food Technology in Australia*. 38(3): 106-110.
- Fortuna, E. (1993). "Unrivalled growth for natural mineral waters." *Soft Drinks Management International*. (Sept.): 25-26.
- Frike, M. (1993). *Natural mineral waters, curative-medical waters and their protection*. *Environmental Geology* 22: 153-161.

Geldreich, E., Nash, H., Reasoner D., Taylor R. (1975). "The Necessity of Controlling Bacterial Potable Waters-Bottled Water and Emergency Water Supplies." *Journal of American Water Works Association*. 67: 117-124.

Green, M. and Timothy. (1985). *The good water guide*. London, Rosendale Press.

Hendricks, C.W. & Morrison, S.M. (1940). "Multiplication and growth of selected enteric in clear mountain strewn water." *Water Research*. 1:567.

Hunter, P.R. (1993). "The microbiology of bottled natural mineral waters." *J. App. Bacteriology*. 74: 345-452.

Leclerc, H., Mossel, D. and Savage, C. (1985). "Monitoring non-carbonated (still) mineral waters for aerobic colonisation." *International Journal of Food Microbiology*. 2 (341-347):

MacGuire, F.A.S. and D.J. Ball. (1992). *Microbiological aspects of bottled natural mineral water*. (Report) Environment Risk Assessment Unit, UK.

Mania, C., Nunes, O., Morais, P. and Costa, M. (1990). "Heterotrophic plate counts and the isolation of bacteria from mineral waters on selective and enrichment media." *Journal Applied Bacteriology*. 69: 871-876.

Rawdatain, Water Bottling Company. (1995). *Annual Report*, Kuwait.

Rivilla, R. and Gonzalez, C. (1988). "Simplified methods for the microbiological evaluation of bottled natural mineral waters." *Journal of Applied Bacteriology*. 64: 273-278.

Schmidt-Lorenz, W (1976) *Microbiological characteristics of natural mineral water*. *Annali dell istituto Superiore Sanita* 12, 93-112.

Schneider, W and Rump, H.H. (1 983). "Use of ozone in the technology of bottled water." 5: 95-101.

Schwaller, P. and Schmidt-Lorenz, W (1980.). "Flore microbienne de quatre eaux minerales non-gazeifikes etmises en bouteilles." *Zbi. Bakt. Hyg. I. Abt Orig.* : 330-47.

Stickler, D.J. (1989). "The microbiology of bottled natural mineral waters." *Journal of the Royal Society of Health*. 4: 118-124.

**Table (1) Colony counts in still bottled water sold in Kuwait**

Brand - country of origin	ph	Colony counts of bacteria (cfu/ml)				
		TC&E	Ps.aeu.	TVC (Average count of 10 samples)		
				22°C	37°C	
A. Rawdatain-Kuwait	7.80	-	-	0	0	
B. Gulfa-UAE	8.10	-	-	15889	11307	
C. Emirates-UAE	8.10	-	-	0	0	
D. Masafi-UAE	8.25	-	-	0	0	
E. Al-Grain- UAE	7.50	-	-	4800	2450	
F. Al-Shailal-UAE	8.25	-	-	0	0	
G. Oriental-UAE	8.25	-	-	0	0	
H. Hatta-UAE	8.05	-	-	0	0	
I. Jabal Akhdr- Oman	7.90	-	-	8972	5859	
J. Salsabeel-Oman	7.90	-	-	0	0	
K. Tanuf-Oman	7.80	-	-	0	0	
L. Assaha-Oman	7.90	-	-	630	120	
M. Bahrain-Bahrain	7.00	-	-	21800	16300	
N. Nada-Bahrin	7.20	-	-	0	0	
O. Alwadi-Saudi Arabia	7.20	-	-	38200	24300	
P. Alshifa-Saudi Arabia	7.20	-	-	7600	3700	
Q. Taiba-Saudi Arabia	7.40	-	-	0	0	
R. Sohat-Lebanon	7.90	-	-	2450	720	
S. Baraka-Egypte	6.90	-	-	28500	17900	
T. Safa-Iran	8.00	-	-	15400	11300	
U. Sultan-Turkey	6.75	-	-	10300	8100	
V. Evian-France	7.10	-	-	3710	2640	
W. Volvic-France	7.00	-	-	12500	3200	
X. Vittel-France	7.40	-	-	16300	10900	
Y. PierVal-France	8.00	-	-	26100	5800	
Z. Valvert-Belgium	7.70	-	-	6250	1150	

-, Represents zero count ; TC&E , total coliforms and E.coli;

Ps.aeu, Pseudomonas aeruginosa; TVC, total viable count

Table(2) Identification of bacterial strains isolated from bottled waters sold in Kuwait

Bacterial genus/species	Brand codes	No. of Isolates				Total
		PCA		PCA/10		
		22°C	37°C	22°C	37°C	
<b><i>Pseudomonas</i></b>						
<i>Ps. vesicularis</i>	B,E,M,R,V,W,X	15	8	1	3	27
<i>Ps. fluorescens</i>	W	1	-	-	-	1
<i>Ps. paucimobilis</i>	E,M,R,T,V	6	3	6	5	20
<i>Ps. stutzeri</i>	Y	-	-	1	-	1
<b><i>Xanthomonas maltophilia</i></b>	M,T	2	1	1	1	5
<b><i>Acinetobacter</i></b>						
<i>A. lwoffii</i>	E,O,P,R,T,V,W,X	18	-	2	1	21
<i>A. calcoaceticus</i>	L	1	-	-	-	1
<i>Eikenella corrodens</i>	X,Y	2	1	-	-	3
<i>Alcaligenes xylosoxidans</i>	V	1	-	-	-	1
<b><i>Flavobacterium</i></b>						
<i>F. meningosepticum</i>	B,R,U,X	1	-	1	2	4
<i>F. odoratum</i>	M	1	-	-	-	1
<i>F. indologenes</i>	U,X,Y	4	3	1	-	8
<i>Flavimonas oryzihabitans</i>	P	2	-	-	-	2
<i>Ochromobactrum anthropi</i>	M	1	-	-	-	1
<i>Agrobacterium tumefaciens</i>	Y	-	-	-	1	1
<i>Actinobacillus ureae</i>	L,O	-	4	-	-	4
<b><i>Vibrio</i></b>						
<i>V. alginolyticus</i>	M,R,W	4	-	-	-	4
<i>V. parahaemolyticus</i>	R,V,W,X,Y	6	5	1	1	13
<i>V. damsela</i>	B,M	-	1	-	1	1
<i>V. vulnificus</i>	X	1	-	-	-	1
<b>Provisional Pasteurella/ ( Vitek Identification )</b>						
	I,L,M,P,R,T,U,V,X,Y	11	10	5	1	27
<b>Unidentified</b>	B,L,M,O,R,T,U,V,W,X,Y	45	30	6	9	90
<b>Total</b>						<b>237</b>

year	volume (M liters)	value (\$ M dollar)	value ( Mdinar)
90	12.6	2.6	0.8
92	19.4	3.9	1.2
93	26.8	5.3	1.6
94	31.2	6.3	1.9
95	33.4	7.3	2.2

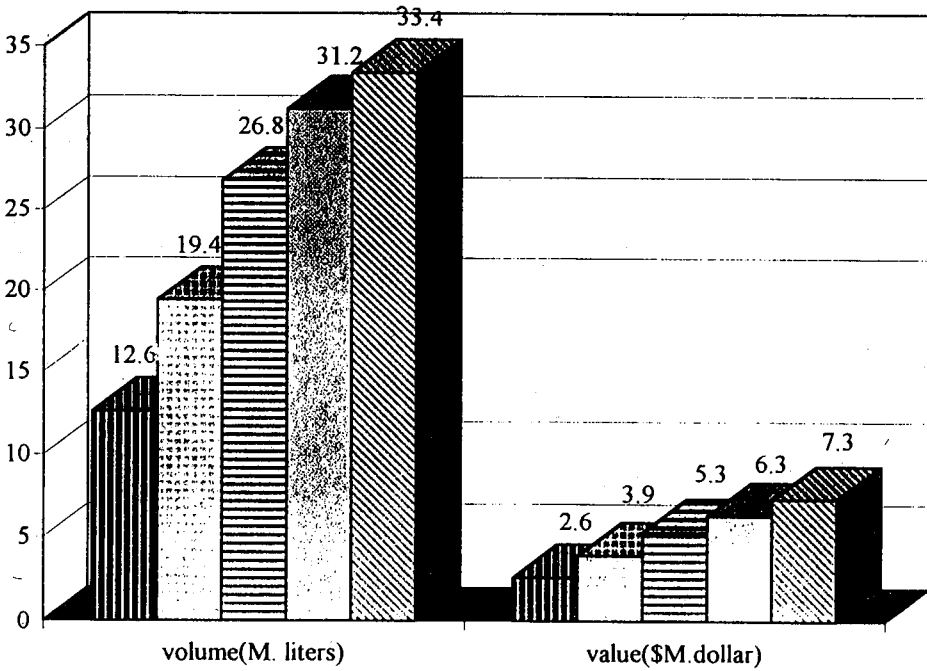


Fig.1. Sales of the Kuwaiti natural mineral water ( Rawdatain ) .

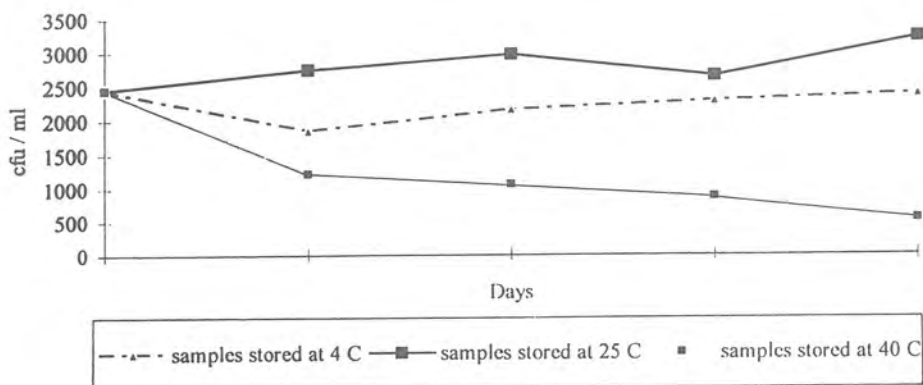


Fig.2. Effect of storage temperature on total viable count of bacterial flora in bottled water .

- 1 Add reagent to water
- 2 Incubate  
35°±.5°C for 24 hours
- 3 Read Results



Clear:  
Negative  
for total  
coliforms  
and  
*E. coli*



Yellow:  
Positive  
for total  
coliforms



Fluores-  
cent:<sup>b</sup>  
Positive  
for *E. coli*

<sup>b</sup>Use longwave 366nm UV lamp



#### Presence/Absence Format

Ideal for compliance with new Safe Drinking Water Regulations or wherever yes/no answers are desired. Reagent is unit dosed for addition to water samples of 100 ml. each. If quantitation is desired, the 100 ml. sample/reagent mixture can be transferred to five 20 ml. or ten 10 ml. tubes for MPN analysis.

Cat. No. WP020 20 unit doses  
Cat. No. WP200 200 unit doses

Fig.3. Colilert presence/ absence system was used for detecting total coliforms & *E. coli* in 100 ml samples of bottled water .



WORK FLOW for SINGLE-INLET TEST CARDS

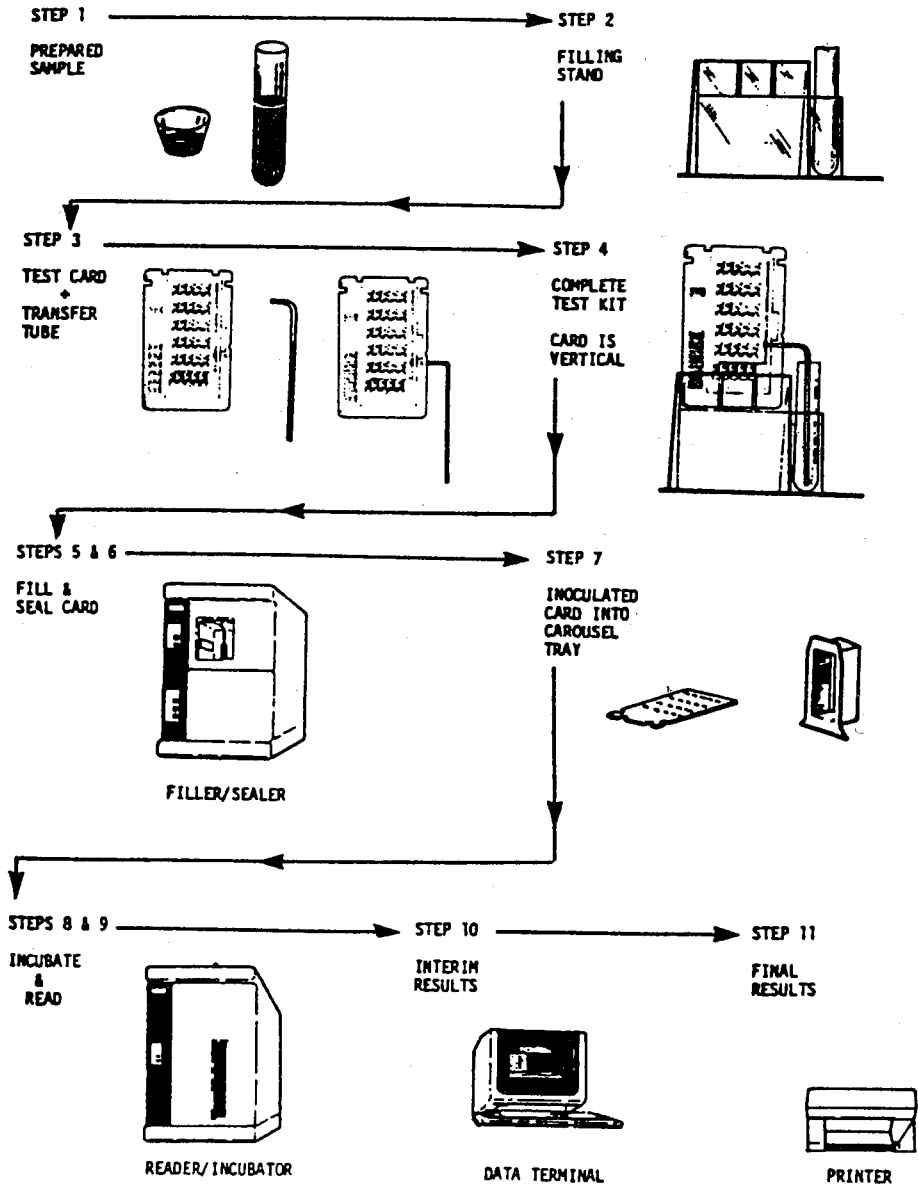


Fig.4. Vitek system work flow ; two types of card GNI & NFC ( industrial ) were used for identification of the bottled water isolates .

**Experimental Evaluation of Hardness  
Removal from Buraydah Groundwater Supplies**

*Abdulrahman I. Alabdula'Aly*

# EXPERIMENTAL EVALUATION OF HARDNESS REMOVAL FROM BURAYDAH GROUNDWATER SUPPLIES

**Abdulrahman I. Alabdula'aly**

King Abdulaziz City For Science and Technology

Riyadh, Saudi Arabia

## ABSTRACT

Groundwater is treated for the removal of hardness using chemical precipitation in treatment plants located in major cities of the central region of Saudi Arabia. Softening chemicals (lime, soda ash and caustic soda) and precipitation aids (sodium aluminate, ferric chloride and polymer) are used with varying dosages in those plants. The water production cost based on softening chemicals in the major 9 plants of the region is in the range of SR 0.12 to 1.35/m<sup>3</sup>. Experimental investigation on the raw water of Buraydah plant indicate that the optimum soda ash and caustic soda dosages needed to reduce total hardness from 250 to 120 mg/L as CaCO<sub>3</sub> are 140 and 60 mg/L, respectively. The expected water production cost associated with chemicals only would be SR 0.11 and 0.09/m<sup>3</sup> for soda ash and caustic soda, respectively.

**Keywords:** Groundwater softening, water treatment, Buraydah, Saudi Arabia.

## INTRODUCTION

Hardness in groundwater is predominantly due to calcium and magnesium ions although strontium, ferrous iron and manganous ions also contribute to some extent. Hardness levels vary from location to another but depend largely on the geologic formation of the aquifer. The hardness ions are capable of reacting with soap to form precipitates and hence form scale. Water is considered hard when its total hardness is in the range of 150-300 mg/L as  $\text{CaCO}_3$ , and the acceptable range is 60-120 mg/l, as  $\text{CaCO}_3$  [1]. Removal of hardness is accomplished by many ways of which chemical precipitation and ion exchange are the most common. Depending on the hardness type and concentration, chemicals such as calcium hydroxide (lime), sodium carbonate (soda ash) and sodium hydroxide (caustic soda) are added to precipitate hardness causing ions. Soluble calcium and magnesium compounds are nearly converted into insoluble compounds that are flocculated, settled and filtered. Other chemicals like sodium aluminate, ferric chloride, aluminum sulfate and polymers are used in the process to aid the precipitation. In general, lime is used to remove carbonate hardness, soda ash for the removal of non carbonate hardness and caustic soda to remove both types of hardness.

The groundwater in the central region of Saudi Arabia contains appreciable levels of hardness reaching in some locations to 900 mg/L as  $\text{CaCO}_3$  [2]. For drinking purposes, groundwater is treated in major cities and towns of the region. The treatment processes are aimed at reducing total dissolved solids (TDS), hardness and other major water contaminants. The region plants use cooling, softening, filtration, reverse osmosis and post treatment (pH adjustment and chlorination) processes. The softening process is considered as a pretreatment step to reduce both hardness and silica before passing the water through the RO membranes. The major plants are located in Riyadh, Buraydah, Unayzah, AlRass, Alzulfi, AlMajmaah and AlQuwaiyah, with water production capacities ranging from  $6.7 \times 10^3$  to  $21 \times 10^4$  m<sup>3</sup>/d. Six plants are located in Riyadh providing about 35% of the total city water supply. Chemical softening is used in Riyadh, Unayzah, AlRass and AlMajmaah plants. All plants (Except Alwasia in Riyadh, Buraydah and AlQuwaiyah) have RO treatment. Buraydah plant has neither chemical softening nor RO treatment whereas AlQuwaiyah plant incorporates cooling, filtration, electro dialysis and chlorination processes.

The objective of this paper is to present and discuss the results of a study conducted on Buraydah plant raw water for the removal of hardness using chemical softening on laboratory as well as pilot plant scales.

## GROUNDWATER SOFTENING IN THE CENTRAL REGION OF SAUDI ARABIA

There are 9 major treatment plants in the central region of Saudi Arabia that have softening processes, six in Riyadh and one each in Unayzah, AlRass and AlMajmaah. The plants production capacities, raw and product water TDS and total hardness are presented in Table 1. Softening in Riyadh, AlRass and AlMajmaah plants is carried out in turbocirculators (upflow clarifiers) whereas in Unayzah plant is carried out in sand pellet reactors which involves seeding with sand grains of sizes 0.2-0.40 mm and a dosing of caustic soda. In addition to the hardness reducing chemicals (lime, soda ash and caustic soda), precipitation aids are used in all plants except Unayzah. The chemicals used in the softening process and their dosages are presented in Table 2.

Information on water production cost concerning used chemicals is scarce. Based on available data, the cost varies from plant to another. The softening chemicals cost in Riyadh plants amounts to SR 41 million in 1993 giving an average unit cost of SR 0.33/m<sup>3</sup> [7]. For Unayzah and AlRass plants the cost is SR 0.12/m<sup>3</sup> and SR 0.26/m<sup>3</sup>, respectively, whereas that of AlMajmaah plant is SR 1.35 and 0.21/m<sup>3</sup> for new and old plants, respectively [2,5].

Table 1 Major groundwater treatment plants in the central region of Saudi Arabia where chemical softening is practiced [3-6].

Plant	Maximum production capacity (m <sup>3</sup> /d)	Raw water		Product water	
		TDS (mg/L)	Total hardness (mg/L)*	TDS (mg/L)	Total hardness (mg/L)*
Riyadh					
-Alwasia	210000	1172	612	1148	556
-Manfouha I&II	84400	1674	832	294	72
-Buwaib	66000	1720	816	324	60
-Salboukh	6672	1502	700	288	56
-Shemessy	57600	1178	592	498	208
-Malaz	288000	1426	652	292	76
Unayzah	51000	638	304	570	150
AlRass	51000	1350	536	368	87
AlMajmaah	8400	2045	733	524	188

\*as CaCO<sub>3</sub>

Table 2 Chemicals used for water softening with dosages in major groundwater treatment plants of the central region of Saudi Arabia [2,5 -7].

Plant	Used chemicals and dosages (mg/L)					
	Lime	Soda ash	Caustic Soda	Sodium Aluminate	Ferric Chloride	Polymer
Riyadh						
-Alwasia	100	70	-	-		0.25
-Manfouha I&II	110	326	-	10	-	0.06
-Buwaib	110	350	-	12	1.5	-
-Salboukh	125	235	-	24	-	0.20
-Shetnessy	110	220	-	9		0.10
-Malaz	129	239	-	12		0.20
Unayzah	-	-	100			
AlRass	-	271	87	20	10	
AlMajmaah	175	170	45	-	-	0.40

## REMOVAL OF HARDNESS FROM BURAYDAH WATER TREATMENT PLANT

### Buraydah Plant

The Buraydah water treatment plant supplies drinking water to the city of Buraydah, the second largest in the central region of Saudi Arabia. The plant was constructed in 1985 with a maximum production capacity of 96000 m<sup>3</sup>/d for the purpose of removing iron and manganese from groundwater supplies. The average daily production in 1993 was 67267 m<sup>3</sup>/d. The plant is supplied by water from 21 nearby deep wells [8]. The treatment processes include aeration, filtration and chlorination. Aeration is accomplished in two towers equipped with air diffusers where iron and manganese are oxidized in addition to the cooling of water and removal of gases. The filtration process consists of 20 upflow and downflow gravity filters with a surface area of 19.7 m<sup>2</sup> and 39.3m<sup>2</sup> each, respectively. The chlorinated water is stored in two reservoirs of 8000 m<sup>3</sup> capacity each.

### Experimental Procedure

Evaluation of hardness removal from Buraydah plant raw water using lime, soda ash and caustic soda was carried out on laboratory (jar test) and field (pilot plant) scale. The jar test experiments were conducted in order to obtain basic data that were necessary for designing and planning the field study. One hundred liters of Buraydah plant aerated water was collected and kept in

the laboratory until its temperature reached about 20°C. The used dosages of lime and soda ash were in the range of 0-400 mg/L and that of caustic soda was 0-150 mg/L. The chemicals were mixed with the raw water at 250 rpm for 2 min (fast mixing) followed by 30 min slow mixing at 70 rpm.

The pilot plant (Figure 1) was installed in Buraydah plant and supplied by raw water from the influent water to the actual plant. It consists of an aeration tower, precipitator, filters, chemical tanks, softened water collection tank and backwashing system. The aeration tower is 30 cm in diameter and 200 cm high, made of plexiglas, and equipped with air diffusers at the bottom providing air flow of about 1 m<sup>3</sup>/m<sup>3</sup> of water which is similar to what is being used in the actual plant. The precipitation unit is a square plexiglas tank, 90x90 cm, tapered at the bottom with a height of 240 cm and has fast mixing, slow mixing and precipitation chambers. The rapid mixing chamber is made of plexiglas, cylindrical in shape with diameter of 10 cm and a height of 200 cm, closed at the bottom where raw water and chemicals are introduced and is equipped with a mixer providing 100rpm mixing intensity. The slow mixing chamber is located around the fast mixing chamber, opened at both ends and is of a square cone shape, 18 cm at top and 41 cm at the bottom with height of 210 cm. The water flows from top to bottom where the precipitation chamber is located. The sludge is withdrawn by a pump from the bottom section of the precipitator. The softened water is collected in a channel around the upper part of the precipitator and flows into a collection tank. The precipitator provides a detention time of 2 hrs at 3 gpm water flow rate. The softened water pH is adjusted automatically in the softened water collection tank to about 6.5 using dilute HCl then pumped to the filters. There are three identical cylindrical glass columns with a diameter of 15 cm and height of 181 cm each. The media depth in each column is 75 cm supported on graded gravel 30 cm deep. Two columns contain silica sand of size 0.6-0.84 mm of local and imported origin whereas the third column contains green sand. The water flow rate was kept constant at 1 gpm (5.3 gpm/ft<sup>2</sup>). A total of 12 experimental runs were carried out, divided into 3 groups, based on chemicals used. The chemical dosages were selected so that the softened water has a pH of near 8, 9, 10 and 11. The filter run length varied from 6-12 hrs based on chemical dosages. Samples were collected every 1 to 3 hours based on the run length from raw, softened and filtered waters. At the end of each run, filters were backwashed for 20 min by pumping air and water (alternate or combined).

The samples temperature and pH were measured in the field at the time of collection whereas total hardness, alkalinity, Ca, Mg, Fe and Mn were determined in the laboratory following the methods specified in Standard Methods for the Examination of Water and Wastewater [9].

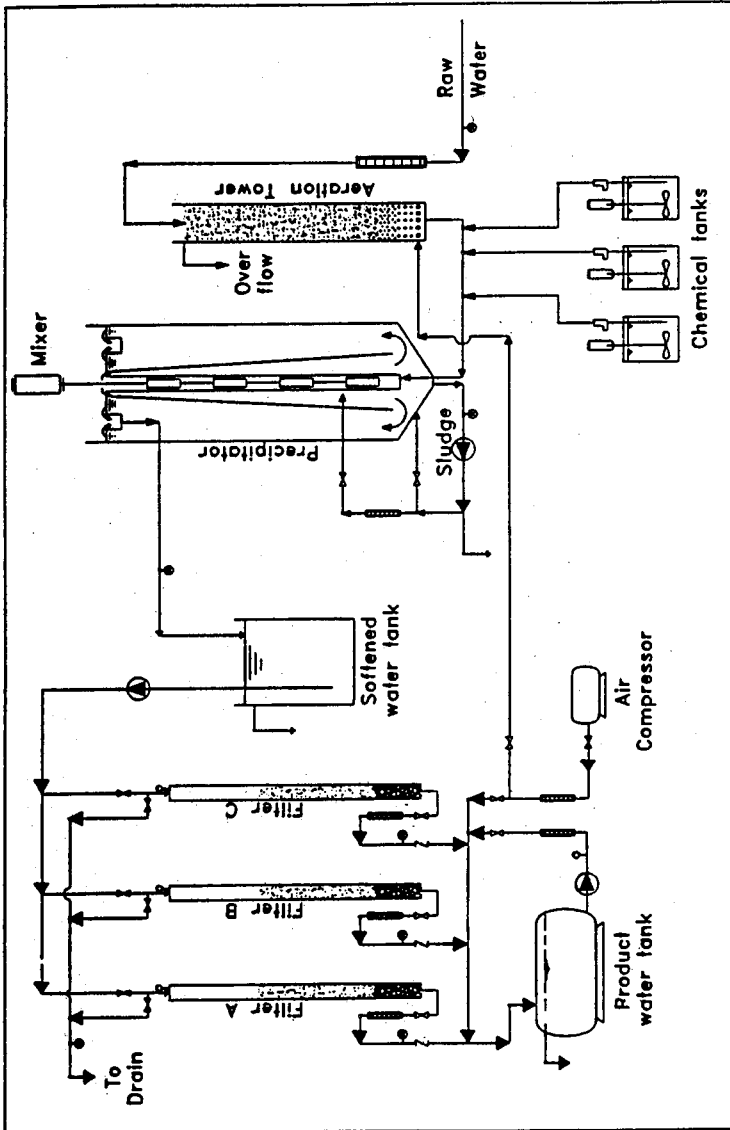


Figure 1. Schematics of Pilot Plant Setup



## RESULTS AND DISCUSSION

The average Buraydah plant raw water temperature, pH, TDS, total alkalinity, total hardness, Ca, Mg, Fe, Mn, Cl and  $\text{SO}_4$  during the experimental work were 37.9°C, 7.6, 728 mg/L, 118.6 mg/L As  $\text{CaCO}_3$ , 237.2 mg/L  $\text{CaCO}_3$ , 168 mg/L  $\text{CaCO}_3$ , 69.2 mg/L  $\text{CaCO}_3$ , 1.38 mg/L, 0.42 mg/L, 275 mg/L and 150 mg/L, respectively.

The results of jar test experiments for hardness using lime, soda ash and caustic soda are shown in Figure 2. Table 3 presents the results of Ca, Mg, Fe and Mn. The maximum hardness removal (40.7%) occurred at a lime dosage of 200 mg/L and above this dose the hardness started increasing. Dosing with soda ash or caustic soda resulted in an increase in hardness removal, reaching 63 and 100 mg/L as  $\text{CaCO}_3$  for dosages of 500 and 150 mg/L of the two chemicals, respectively. The maximum reduction in Ca when using lime was at 200 mg/L. Magnesium was observed to decrease with increasing lime dosage reaching about 4.1 mg/L as  $\text{CaCO}_3$  with the highest lime dosage of 400 mg/L. Soda ash had pronounced effect on Ca reduction with the increase in dosage whereas Mg was not significantly affected. Caustic soda caused slight decrease in Mg reduction with the increase in dosage. Total dissolved solids reduced by about 11% with 400 mg/L lime dose, increased by 46% with 500 mg/L soda ash dose but no significant change was observed when caustic soda was used. The increase in TDS is mainly due to the increase in Na levels in water when using soda ash and caustic soda.

The pilot plant results indicate that the three types of filters gave similar water quality and therefore the results presented are limited to those obtained for the column containing local media. The hardness results for the three used chemicals are shown in Figure 3 whereas the results for Ca, Mg, Fe and Mn are presented in Table 4. With lime it was possible to reduce hardness to 143 mg/L as  $\text{CaCO}_3$  (39% reduction) using a dosage of 200 mg/L which is very close to the results obtained in the jar test. Dosing of 200 mg/L of soda ash resulted in about 63% hardness removal which is better than what has been obtained in the jar test. Increasing the soda ash dosage does not significantly improve hardness removal. Caustic soda dosing gave a very good hardness removal at 75 mg/L as compared to the results obtained in the jar test. It was possible to reduce hardness level to 57 mg/L as  $\text{CaCO}_3$  at that dosage with no improvement with higher dosages. The chemicals effect on both Ca and Mg content followed the same trend as in the jar test for lime and soda ash but for caustic soda a noticeable reduction of both parameters was observed at 75 mg/L dosage. The differences in hardness removal for the same chemical dosage between the jar test and the pilot plant are attributed to factors such as mode of operation and water quality changes.

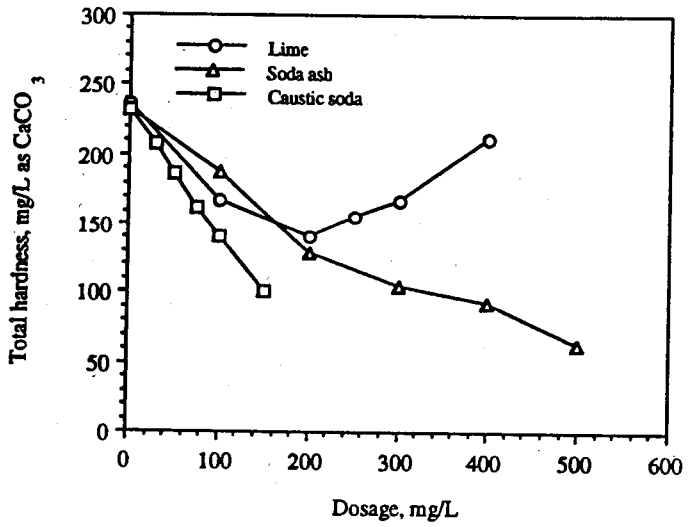


Figure 2. Results of jar test experiments for hardness .

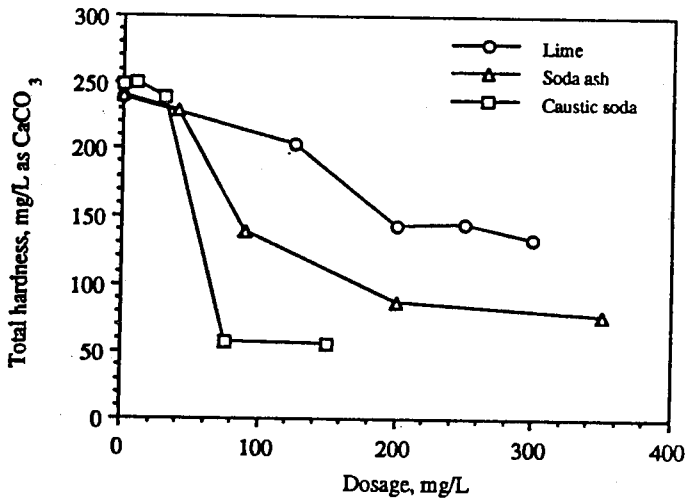


Figure 3. Results of pilot plant for hardness

Table 3. Jar test results for, Ca, Mg, Fe and Mn.

Chemical	Dosage (mg/L)	pH	Concentration, mg/L				
			TDS	Ca*	Mg	Fe	Mn
Lime	0	7.45	722	183.7	51.8	0.07	0.1
	100	8.90	662	107.8	60.1	0.06	0.1
	200	10.25	606	95.8	44.0	0.03	0.1
	250	10.75	654	127.8	28.0	0.05	0.1
	300	10.95	644	159.8	7.8	0.11	0.0
	400	11.15	644	207.7	4.1	0.04	0.0
Soda ash	0	7.60	728	163.8	67.9	0.05	0.2
	100	9.05	722	143.8	44.0	0.03	0.1
	200	9.35	736	79.9	48.1	0.04	0.0
	300	9.60	818	63.9	39.9	0.04	0.0
	400	9.80	906	55.9	36.2	0.04	0.0
	500	9.95	1064	26.9	36.2	0.03	0.0
Caustic soda	0	7.85	732	191.7	39.9	0.08	0.2
	30	9.15	730	151.8	56.0	0.04	0.1
	50	9.50	718	127.8	58.0	0.04	0.1
	75	9.80	724	103.8	58.0	0.04	0.1
	100	10.15	718	87.8	51.8	0.04	0.1
	150	10.70	768	63.9	36.2	0.04	0.0

\*as CaCO<sub>3</sub>

## CONCLUSIONS

Groundwater of the central region of Saudi Arabia contains appreciable amounts of hardness that require its reduction to the acceptable levels. Water softening in the major water treatment plants of the region is accomplished by lime, soda ash, caustic soda and precipitation aids. The cost of water production due to softening chemicals only varies from SR 0.12 to 1.35/m<sup>3</sup>. The results of pilot plant experiments (Figure 3) on Buraydah plant raw water reveal that the optimum soda ash or caustic soda dosages needed to reduce the raw water hardness to about 120 mg/L as CaCO<sub>3</sub> were about 140 and 60 mg/L, respectively. For lime, the 120 mg/L hardness level can not be achieved with the used dosages. Based on the current chemical costs (soda ash, SR 727/ton and caustic soda, SR 730/ ton), the water production cost when using the optimum dosages of soda ash and caustic soda would be expected to be SR 0.11/m<sup>3</sup> and 0.09/m<sup>3</sup>, respectively. The cost calculations assume 10% impurities in the soda ash (solid) and the caustic soda is in liquid form with 49%

concentration. It is recommended that further studies be carried out especially using a combination of softening chemicals and precipitation aids.

Table 4. Pilot plant results for Ca, Mg, Fe and Mn

Chemical	Dosage (mg/L)	Softened Water pH	Concentration, mg/L			
			Ca*	Mg*	Fe	Mn
Lime	0	7.61	155.1	82.7	1.47	0.42
	125	8.06	126.1	77.0	0.02	0.08
	200	8.88	83.1	59.7	0.01	0.08
	250	9.79	72.1	72.4	0.05	0.10
	300	11.00	85.3	47.3	0.03	0.10
Soda ash	0	7.63	159.3	81.1	1.44	0.44
	40	8.28	141.0	88.1	0.06	0.10
	90	8.76	66.9	72.4	0.04	0.10
	200	10.07	9.9	77.4	0.05	0.08
	350	10.67	1.7	75.7	0.03	0.10
Caustic soda	0	7.67	155.8	92.6	1.15	0.45
	10	7.95	158.0	91.4	0.20	0.10
	30	8.10	160.8	77.0	0.03	0.10
	75	10.47	14.4	42.8	0.01	0.01
	150	10.83	16.4	39.1	0.01	0.00

\*as CaCO<sub>3</sub>

#### ACKNOWLEDGMENT

The work reported has been financially supported by King Abdulaziz City For Science and Technology, Riyadh, Saudi Arabia. The author appreciates the cooperation of the Ministry of Water and Agriculture and the assistance received during the course of this research.

## REFERENCES

- [1] Sanks, R.L, Water Treatment Plant Design for the Practicing Engineer, Butterworth Publishers, Ann Arbor, MI, 1978.
- [2] Alabdula'aly, A.I. and Chammem, AA., Groundwater Treatment in Central Region of Saudi Arabia, Desalination, 96, p 203-214, 1994.
- [3] Alabdula'aly, A.I., Groundwater Quality and Treatment in Riyadh, Saudi Arabia Proceedings of the International Desalination Association Conference, Abu Dhabi, UAE, November, 1995, Vol. VI, p 43-57.
- [4] Al-Saati, A.J. and Alabdula'aly, A.I., Water softening Using Sand Pellet Reactors, Proceedings of the Second WSTA Gulf Water Conference, Manama, Bahrain, November, 1994, p 55-65.
- [5] Alabdula'aly, A.I., Design and Operation of A 51 ML/Day RO Desalination Plant in the Central Region of Saudi Arabia, Proceedings of the International Desalination Association Conference, Abu Dhabi, UAE, November, 1995, Vol. V, p 17-26
- [6] Alabdula'aly, A.I., Membrane Process Application in the Central Region of Saudi Arabia, Proceedings of the American Water Works Association Membrane Technology Conference, Reno, NV, USA, August, 1995, p 389-408.
- [7] El-Rehaili, A.M.; Alabdula'aly, A.I. and Al-Mutaz, I.S., Evaluation of the Chemical Treatment at Riyadh Water treatment Plants, Proceedings of the fourth Saudi Engineering Conference, Jeddah, Saudi Arabia, November, 1995, Vol. IV, p 59-69 (in Arabic).
- [8] Alabdula'aly, A.I.; Al-Saati, A.J. and Rapati, F.I., Recycling Filters Backwash Water In Drinking Water treatment Plants, Proceedings of the Second WSTA Gulf Water Conference, Manama, Bahrain, November, 1994, p 456-466.
- [9] Standard Methods for The Examination of Water and Wastewater, 17th Ed., APHA AWWA-WPCF, 1989.

**Trace Metals in Groundwater Treatment Plant's  
Product Water of the Central Region of Saudi Arabia**

*Abdulrahman Alabdula'Aly*

# **TRACE METALS IN GROUNDWATER AND TREATMENT PLANT'S PRODUCT WATER OF THE CENTRAL REGION OF SAUDI ARABIA**

**Abdulrahman Alabdul'aly**

King Abdulaziz City for Science and Technology

Riyadh, Saudi Arabia

## **ABSTRACT**

Trace metals were assessed in the raw and product waters of 8 water treatment plants in Riyadh, Buraydah and Unayzah (Saudi Arabia). Samples were analyzed for 12 trace metals by Inductively Coupled Plasma Spectrophotometer (ICP). All the detected metals were within the permissible limits of WHO. Cadmium, Ni and Se were absent in all plants waters. It was found that concentrations of metals like As, Fe and Mn decreased after various treatment processes compared to their levels in raw water. Aluminum increased in all product waters of the plants that use chemicals in the softening process. The increase in the Al levels is observed to take place after the softening process where sodium aluminate is used. However most of the Al is removed by sand filtration. Zinc and Cu levels in the product water have increased in many cases which may be attributed to the pipings. The removal of trace metals by reverse osmosis was in the range of 78.8-100%. Assessment of trace metals in the water distribution network is recommended.

**Keywords:** Groundwater, water treatment, trace metals, softening chemicals.

## INTRODUCTION

Metals can occur in water supply and their presence may be due to raw water, treatment process chemicals and leaching from the pipes used in the distribution network. Raw groundwater contains traces of metals and their concentration is related primarily to geologic formation of the aquifer. The use of chemicals especially in coagulation and softening processes result in an increase in certain elements in the plants final product water. The most commonly used chemicals in water softening and coagulation include calcium hydroxide (lime), sodium carbonate (soda ash), sodium hydroxide (caustic soda), aluminum sulfate (alum), sodium aluminate, ferric chloride and polymers. The concentrations of trace elements in the product water depend on the chemicals used, their purity and the treatment processes effectiveness in their removal. For example, the use of alum in coagulating surface waters to enhance the removal of particulate material cause an increase in the aluminum content of the plants finished water [1,2]. A survey of 80 surface water treatment plants in the USA that use alum as the primary coagulant indicate that 95% of the plants have aluminum content in their raw water of 0.40 mg/L or less as compared to 1.50 mg/L in the product water [2]. The American Water Works Association (AWWA) standards for water treatment chemicals specifies that chemicals must not contain soluble mineral or organic substances in quantities capable of producing deleterious or injurious effects on the health of those consuming a water that has been properly treated with the chemical. Moreover the recommended maximum allowable impurity limit should not be more than 10 percent of a contaminant or maximum contaminant level value contributed by a given impurity in a water treatment chemical.

Cities, towns and villages of the Central Region of Saudi Arabia rely almost entirely on groundwater for all water uses. Riyadh city relies on both treated groundwater and desalinated sea water. The groundwater used for drinking purposes is supplied from deep unconfined aquifers. Treatment plants have been constructed in major cities of the region for the purpose of TDS, hardness and other substances reduction. In general, the treatment processes include cooling, chemical softening, filtration, reverse osmosis and post treatment (pH adjustment and chlorination). The chemicals used in the softening process include hardness reduction chemicals (lime, soda ash and caustic soda) and precipitation aids (sodium aluminate, ferric chloride and polymers). In 1993, the Riyadh six groundwater treatment plants used 14234, 22114, 978, 150 and 24 tons of lime, soda ash, sodium aluminate, ferric chloride and polymer, respectively [3].



The objective of this paper is to assess trace metals levels in raw and product waters of 8 treatment plants in the Central Region of Saudi Arabia as well as the removal or increase of their levels due to the adopted treatment processes.

## **MATERIALS AND METHODS**

### **Study area**

The study covers 8 groundwater treatment plants in Riyadh, Buraydah and Unayzah (Figure 1). The plants production capacities, used processes and chemicals are presented in Table 1. The Riyadh six plants contribute about 35% to the city's total water supply and the remaining 65% is supplied by desalinated sea water. Buraydah plant whose treatment processes include aeration, filtration and chlorination supplies drinking water to Buraydah, the second largest city in the Central Region, about 350 km northwest of Riyadh. Unayzah plant meets the partial water requirement of Unayzah located about 20 km south of Buraydah. The Riyadh plants are supplied by 161 wells (136 deep and 25 shallow), Buraydah plant is supplied with water from 21 deep wells whereas Unayzah plant is supplied with water from 10 deep wells.

### **Samples collection and analysis**

Samples were collected once from the influent and final product waters of the Riyadh plants and 5 times from Buraydah and Unayzah plants. In addition, samples were collected seven times from 7 points within Buwaib plant in Riyadh to assess the changes in trace elements concentration due to different treatment processes. Samples were collected in 300 ml acid washed polyethylene bottles. The samples were acidified at the time of collection with spectroscopy grade nitric acid until the pH was less than 2, brought to the laboratory in ice boxes and stored at 4°C until analyzed.

Samples were analyzed for Al, As, Ba, Cd, Cr, Cu, Fe, Pb, Mn, Ni, Se and Zn using Perkin Elmer Model 1000 Inductively Coupled Plasma (ICP) spectrophotometer equipped with an Ultrasonic Nubilizer Model Cetac U5000 AT. The use of ultrasonic nubilizer result in 5 to 50 fold improvement in detection limits and a 10 fold signal enhancement to provide better reproducibility on trace level determinations. The ICP was calibrated with certified standards from Perkin Elmer and one standard with one set of samples was analysed routinely. Analysis was carried out in triplicate and the average values are reported. Assessment of the results precision and

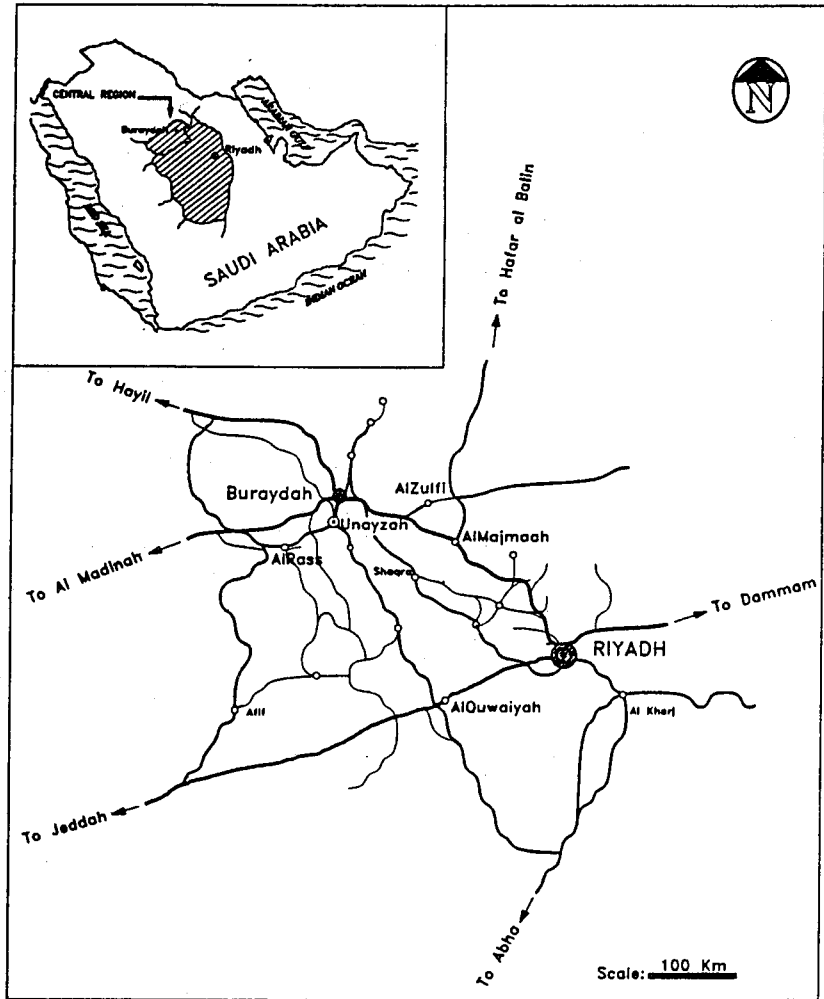


Figure 1. Central Region of Saudi Arabia

accuracy was carried out by replicate analysis of blank, standard and sample.

## RESULTS AND DISCUSSION

The trace metal concentrations in the influent and product waters of the eight groundwater treatment plants have been presented in Table 2 along with the ICP detection limits and the World Health Organization (WHO) standards for drinking water [7]. Cadmium, Ni and Se were not detected in raw or product waters of the 8 plants whereas As was not detected in Riyadh treatment plants raw and product waters but was detected in small amounts in Buraydah and Unayzah plants waters. Chromium was detected only in Unayzah raw and product water. None of the measured elements in the plants product waters exceeded the WHO MCL for trace elements.

Table 1 Studied plants production capacities, used processes and softening chemicals [4-6].

Plant	Maximum Production Capacity (m <sup>3</sup> /d)	Treatment Processes*	Used chemicals					
			Lime	Soda ash	Caustic Soda	Sodium Aluminate	Ferric Chloride	Polymer
Riyadh								
Alwasia	210000	C,S,F,P	x	x	-	-	-	x
Manfouha I&II	86400	C,S,F,R,P	x	x	-	x	-	x
Buwaib	66000	C,S,F,R,P	x	x	-	x	x	-
Salboukh	66720	C,S,F,R,P	x	x	-	x	-	x
Shemessy	57600	C,S,F,R,P	x	x	-	x	-	x
Malaz	28800	C,S,F,R,P	x	x	-	x	-	x
Buraydah	96000	A,F,L	-	-	-	-	-	-
Unayzah	51000	S,F,R,P	-	-	x	-	-	-

\*A= aeration; C= cooling; F= filtration; L= chlorination; P= post treatment (pH adjustment and chlorination); R= reverse osmosis and S= softening.

Considering the removal of different metals in the treatment processes, As, Fe and Mn were reduced in the range of 38.6-41.3%, 8.2-97.2% and 29-94.9%, respectively. Barium is noticed to increase in 2 plants (Alwasia and Shemessy) and was reduced in the other plants in the range of 2.8 to 77.9%. The low removal of Fe (8.21%) occurred in Shemessy plant where its product water is blended with raw water from Nesah wells. The water from Nesah

wells receives only chlorination, hence the Fe levels increase in Shemessy plant product water.

The increase in Al and Zn varied from one plant to another but the highest increase in Al was observed in Riyadh plants where sodium aluminate is used. In Buraydah plant where no chemical treatment is carried out, Al was removed completely and increased by only 30% to 5.2 µ/L in Unayzah plant which uses only caustic soda in the softening process. The product waters from all treatment plants (except Unayzah) had higher Zn levels than in the raw water which could be the result of piping used in the treatment plants as well as impurities in the chemicals used in the treatment. The increase in Zn levels was in the range of 13.3 to 5785 %.

The trace elements levels in Buwaib plant after different treatment processes are presented in Table 3. Only Fe and Mn were removed significantly by cascade cooling process and with softening and filtration the two parameters were further reduced. Aluminum increased to 273.2 µg/L in the softened water due to the use of sodium aluminate and with filtration its level dropped to 39.2 µg/L which shows that most of the aluminum was in the suspended form. The Zn levels were reduced from 4.8 µg/L in the raw water to 2.7 µg/l in the filtered water but increased to 35 µg/L in the plant product water which could be the result of piping used. Copper was not detected in

Table 2 Trace elements levels in raw and product water of the studied treatment plants

Element*		Concentration, µg/L							ICP Detection Limit µg/l**	WHO Standard	
		Abwaib	Manfooha	Buraydah	Salkhah	Shemessy	Maha	Buraydah			Unayzah
Al	RW	5.6	7.7	6.5	6.5	15.7	10.4	2.1	4.0	0.4	200
	PW	10.3	21.8	13.3	12.5	22.9	38.7	-	5.2		
As	RW	-	-	-	-	-	-	6.3	4.4	2.5	50
	PW	-	-	-	-	-	-	3.7	2.7		
Ba	RW	36.8	35.7	42.3	40.5	11.4	33.2	103	57.1	0.0012	-
	PW	38.3	7.9	16.7	15.8	23.9	8.2	100	55.5		
Cr	RW	-	-	-	-	-	-	-	12.1	0.08	50
	PW	-	-	-	-	-	-	-	11.0		
Cu	RW	-	-	-	-	-	-	1.6	-	0.16	1000
	PW	-	3.4	12	-	-	-	0.8	-		
Fe	RW	237	494	662	832	81.7	772	1864	23.3	0.08	300 *
	PW	40	59	106	85	75	105	52	1.0		
Pb	RW	-	-	-	-	-	-	1.0	6.4	1.0	50
	PW	-	5.6	-	-	-	-	2.0	1.8		
Mn	RW	18.9	10	299	154	18.1	235	235	16.8	0.02	100
	PW	2.0	7.1	20	16.1	1.0	12	12	11.4		
Zn	RW	37.6	2.6	4.8	1.6	11.3	21	21	108.8	0.04	5000
	PW	42.6	153	35	1.4	37.7	57	57	68.1		

\*RW : Raw water, PW: product water

\*\* The detection limits are based on the manufacture values using the U5000 AT Ultrasonic Nubilizer.

the plant raw water but reached a level of 12 µg/l in the product water. The increase in copper concentrations may again be attributed to pipes used in the treatment plant. Other elements (As, Cr, Pb and Se) were only detected in the RO reject water and were below the ICP detection limit in the raw water. Removal of trace elements by the RO varied from complete removal (Fe, Mn and Zn) to 87% for Al and 78.8% for Ba.

## CONCLUSIONS

The results show that trace metals levels in raw and product water of 8 different treatment plants of the central region of Saudi Arabia are well within the permissible limits of WHO for drinking water. Cadmium, Ni and Se were not detected in all treatment plants waters, As was detected in small amounts in two plants, whereas Cr was detected in only one plant.

Table 3 Trace elements levels in different locations in Buwaib plant

Sample	Concentration, µ/L									
Location	Al	As	Ba	Cr	Cu	Fe	Pb	Mn	Se	Zn
Raw	6.5	-	42.3	-	-	662	-	300	-	4.8
Cooled	6.1	.	34.9	-	-	442	-	239	-	3.1
Softened	273	-	24.5	-	-	145	-	12.5	-	2.7
Filtered	39.2	-	15.6	.	-	53.8	-	4.3	-	2.7
RO Permeate	5.1	-	3.3	.	-	-	-	-	-	
RO Reject	182	23.2	68	4.5	-	65.5	5.2	22.6	7.7	10.8
Final Product	13.3	-	16.7	-	1 2	106		20	-	35

Some elements (As, Fe and Mn) were consistently removed with varying degrees and others (Ba) was reduced in 6 plants and increased in the remaining two.

Aluminum was observed to increase tremendously in the plants product waters that use sodium aluminate. The Zn levels were observed to increase in seven plants due to possible release from the pipes. Copper was not detected in the raw water but was detected in 3 plants product water. The removal of trace elements in Buwaib plant was observed to be accomplished mostly by the RO. Iron, Mn and Zn were removed completely by the RO whereas the removal of Al and Ba were 87% and 79%, respectively. Elements that were not detected in the raw water were observed in the RO reject water.

In general it could be concluded that the use of chemicals and the type of pipes used in treatment plants affect slightly the levels of trace metals but not to a degree that will cause them to exceed the limits set by regulatory agencies. Assessment of trace elements in the distribution systems is required due to a number of factors that could have impact on their levels.

## ACKNOWLEDGMENT

The work reported has been financially supported by King Abdulaziz City For Science and Technology, Riyadh, Saudi Arabia.

## REFERENCES

- [1] Letterman, R. D. and Driscoll, C. T., Survey of Residual Al in Filtered Water, Jour. AWWA 80:4:154-158, April 1988.
- [2] Reiber, S.; Kukull, W. and Standish-Lee, P., Drinking Water Aluminum and Bioavailability, Jour. AWWA 87:5:86-99, May 1995.
- [3] El-Rehaili, A.; Alabdula'aly, A. and Al-Mutaz, I., Evaluation of the Chemical Treatment of Riyadh Drinking Water Treatment Plants, Proceedings of the Fourth Saudi Engineering Conference, Jeddah, Saudi Arabia, November, 1995, Vol. IV, p 59-69 (in Arabic)
- [4] Alabdula'aly, A., Groundwater Quality and Treatment in Riyadh, Saudi Arabia Proceedings of the International Desalination Association Conference, Abu Dhabi, November, Vol. VI 1995, p 4357.
- [5] Alabdula'aly, A.; Al-Saati, A. and Rapati, F., Recycling Filters Backwash Water in Drinking Water treatment Plants, Proceedings of the Second WSTA Gulf Water Conference, Manama, Bahrain, November, 1994, p 456-466.
- [6] Al-Saati, A. and Alabdula'aly, Water Softening Using sand Pellet Reactors in Saudi Arabia, Proceedings of the Second WSTA Gulf water Conference, Manama, Bahrain, November, 1994, p 55-65.
- [7] World Health Organization (WHO), Guidelines for Drinking Water Quality, Recommendations, Vol. 1, Geneva, 1984.

